Characterizing the Link Between Tau Aggregation and its Toxicity in Novel Gene-Transfer Based Rat Models of Pure Tauopathy

Marie d'Orange d'Orange

NNT : 2016SACLS339

THESE DE DOCTORAT
DE
L'UNIVERSITE PARIS-SACLAY
PREPAREE A
L'UNIVERSITE PARIS-SUD

ÉCOLE DOCTORALE N°568
Signalisation et réseaux intégratifs en biologie (Biosigne)

Spécialité de doctorat :
Sciences de la vie et de la santé

Par

Mme Marie d'Orange

Characterizing the link between Tau aggregation and its toxicity in novel gene-transfer based rat models of pure tauopathy

Thèse présentée et soutenue à Fontenay-aux-Roses, le 28 octobre 2016 :

Composition du Jury :

Dr. Serge Laroche Président du Jury	*Directeur de Recherche, Université Paris-Saclay, CNRS*
Pr. Nicole Déglon Rapportrice	*Professeur, Lausanne University Hospital*
Pr. Mike Stewart Rapporteur	*Professeur, The Open University*
Dr. Santiago Rivera Examinateur	*Directeur de Recherche, Université Aix-Marseille, CNRS*
Dr. Philippe Hantraye Directeur de thèse	*Directeur de Recherche, Université Paris-Saclay, CEA, CNRS*
Dr. Karine Cambon Encadrante de thèse	*Chargée de Recherche, Université Paris-Saclay, CEA, CNRS*

« *Celui qui s'imagine avoir seul la sagesse, l'éloquence, la force s'expose au ridicule. L'intelligence permet de se contredire.* »

Jean Cocteau

ACKNOWLEDGEMENT/REMERCIEMENTS

Tout d'abord, je souhaite remercier les membres du jury pour avoir accepté d'évaluer mon travail de thèse. Merci à Mike Stewart et Nicole Déglon pour leur lecture attentive du manuscrit et leurs nombreux commentaires très pertinents qui m'ont permis de prendre du recul sur nos résultats. Merci aussi à Serge Laroche et Santiago Rivera pour avoir accepté de participer au jury de thèse. J'ai beaucoup apprécié l'échange scientifique que nous avons eu grâce à vos questions lors de la soutenance.

Je tiens à remercier mon directeur de thèse, Philippe Hantraye, pour m'avoir donné l'opportunité de mener à bien ce projet tout d'abord lors de mon stage de M2 puis en me permettant de poursuivre en thèse. Merci de nous avoir accordé votre pleine confiance à Karine et à moi pour gérer ce projet en toute liberté. Merci aussi pour vos conseils judicieux quant à la poursuite du projet, votre hauteur de vue nous aura été extrêmement utile dans les moments critiques.

Un grand merci à toi, Karine Cambon, directrice de thèse officieuse mais réelle encadrante, pour m'avoir appris tous les aspects du métier de chercheur et pour m'avoir guidée dans ce projet. J'ai appris beaucoup de nos discussions scientifiques mais aussi juste en te regardant gérer tes journées de chercheuse/encadrante/chef de plateforme. Tu m'as montré qu'il était possible de mener à bien un projet de recherche très complet tout en étant au service des autres, ce que je trouve très inspirant. Merci aussi de m'avoir permis d'explorer de nombreuses approches différentes et de m'avoir fait confiance pour en mettre en place. Je garderai notamment un souvenir heureux des séances de travaux manuels dans l'animalerie. Merci enfin de m'avoir donné la chance de présenter notre travail lors de nombreux congrès, et notamment de m'avoir fait confiance quand je t'ai demandé de faire mes débuts face à la communauté scientifique avec un oral à la SfN. J'ai conscience qu'en tant que ta première thésarde, j'ai été autant un challenge pour toi que la thèse l'a été pour moi. Merci pour ta patience. Je pense qu'on peut regarder ce qu'on a accompli et dire avec fierté : On l'a fait !

Un grand merci aussi à Gwenaëlle Auregan pour son aide précieuse durant ces trois ans. Merci d'avoir été là à chaque étape, toujours pleine d'énergie et de motivation. Il aurait été difficile de gérer un projet d'une telle ampleur sans ta capacité impressionnante à mener de front ce qui prendrait à la plupart des gens (moi comprise) plusieurs journées. Merci aussi pour ta patience et ta pédagogie quand il s'agit de former les étudiants. Ta curiosité et ton envie de transmettre font que je sors de la thèse en ayant découvert un grand nombre de techniques. J'ai beaucoup appris en travaillant à tes côtés, la première leçon étant que, quand on a l'amour du travail bien fait, on réalise de grandes choses !

Cette thèse n'aurait pu se dérouler sans l'apport de nombreuses personnes :

Merci à Servier pour son implication dans le projet, et en particulier à Chantal Bourrier pour l'analyse transcriptomique, ainsi qu'à Elsa, Mylène et Dimitri pour toute l'aide qu'ils nous ont apportée, notamment durant la dernière année. Merci particulièrement d'avoir accepté, toujours avec bonne humeur, de participer à nos longues journées/semaines d'injections, même si celles-ci pouvaient parfois être un peu frustrantes. Merci enfin pour vos conseils et suggestions sur les différents aspects du projet, ce qui nous a permis de l'emmener encore plus loin.

Merci aussi aux membres de l'équipe BM pour leur aide, leurs conseils et pour avoir, par leur bonne humeur, donné aux réunions d'équipe un air de joyeuse réunion de famille. Merci Alexis pour tes précieux conseils tout au long du projet et pour m'avoir guidée avec bienveillance dans mes errements de biochimiste en herbe. Merci Marie-Claude pour ta gentillesse et pour m'avoir initiée aux joies des clonages et de la biologie moléculaire. Merci Charlène et Noëlle pour votre dynamisme, votre joie de

vivre, votre humour et pour avoir accepté toujours avec le sourire nos commandes de virus à la dernière seconde. Merci Julie pour tes sourires et ta bonne humeur qui égayeraient même la pire des journées. Merci Che pour tes conseils et pour m'avoir fait découvrir le monde merveilleux de la virologie. Merci Audrey et Séverine pour nos échanges entre thésardes souvent agrémentés de bons gâteaux maison. Merci enfin à Aijia pour avoir contribué à lancer les premières manips du projet astrocytes, repris maintenant par Anastasie qui, j'en suis sûre, va faire de belles choses.

Merci aux membres (et ex-membres) de la plateforme d'expérimentation animale, Martine, Sueva et Diane pour leur aide lors des nombreuses séances d'injections. Merci notamment à Martine pour sa patience quand il s'agit d'initier les jeunes thésards à l'art délicat de la stéréotaxie. Merci aussi de transmettre jour après jour avec tellement de conviction le principe que l'éthique doit primer avant tout.

Merci aussi à Jean-Marie et aux animaliers d'avoir toujours à cœur de prendre soin de nos petites bêtes. Merci notamment à Julien M, super-héros du A1 et du A2, pour sa gentillesse et pour avoir accompagné avec beaucoup de bienveillance mes premiers pas dans le monde du comportement.

Merci aux membres des plateformes d'imagerie pour m'avoir fait découvrir ce domaine complètement inconnu (et encore un peu obscur pour moi). Nadja, merci pour ta gentillesse et pour avoir pris le temps de m'expliquer encore et encore les principes de la TEP. Merci à Yann pour les multiples synthèses et pour nos discussions scientifiques toujours très enrichissantes. Merci à Julien F pour m'avoir appris les principes de l'IRM et à Léopold et Martine pour avoir rendu les quelques journées passées à l'IRM des moments très drôles. J'ai bon espoir que la « malédiction Rat Tau » parte avec moi.

Merci aux membres de la plateforme d'histologie, Caroline, Fanny et Pauline pour leur précieux conseils et de faire souffler un vent de bonne humeur sur les labos d'histologie. Merci aussi d'avoir la volonté de développer toujours plus de techniques afin de les mettre à disposition de la communauté et merci notamment à Fanny pour avoir passé autant de temps à mettre en place le Gallyas.

Merci à Carole et Maria, responsables de la plateforme de biochimie, pour leur disponibilité et pour leurs conseils sur les western blots. Merci à Lev pour le temps passé à nous guider dans le brouillard de VIS et pour avoir mis au point de magnifiques analyses de marquages histologiques. Merci à Caroline et Anne-Sophie pour avoir accepté avec bonne humeur nos demandes les plus incongrues (jusqu'à scanner du blanc sur blanc !). Merci à Emmanuel, Gilles, Carole, Marc, Géraldine, Sonia et Frédérique pour m'avoir permis, par leurs conseils et leurs remarques très constructives, notamment lors des lab meeting, de poser un regard neuf sur le projet. Merci enfin à Marie-Laure, Marie-Christine, Didier, Laurent, Aude et Kristell dont le travail permet de faire tourner MIRCen au jour le jour, ainsi qu'à Laurent Surdi, secrétaire de l'ED Biosigne, pour son dévouement, facilitant ainsi la vie de tous les doctorants.

Merci enfin aux collaborateurs dont les différents domaines d'expertise nous ont permis de construire un beau projet. Merci à Luc Buée, Morvane Colin et Raphaëlle Caillierez pour avoir partagé avec nous leur grande expertise de la biochimie de Tau. Merci notamment à Raphaëlle pour avoir donné de son temps pour me former au fractionnement et pour avoir répondu avec gentillesse et précision à mes nombreuses questions. Merci à Luc et Morvane pour leurs conseils très avisés sur le projet et à Morvane tout particulièrement pour avoir accepté de me suivre en tant que tuteur le long de ces trois ans. Merci également à Christoph Schmitz, Beate Aschauer et Maren Kiessling pour avoir apporté leur expertise de la stéréologie. Merci notamment à Beate pour les nombreuses journées passées pour nous au confocal et à Maren pour m'avoir appris, avec énormément de patience et de gentillesse, toutes les subtilités du comptage. Merci à Guy Schoen, Benoit Gallet et Christine Moriscot pour la microscopie électronique.

Merci aussi aux étudiants, techniciens, ingénieurs, post-docs et chercheurs pour avoir fait de MIRCen un environnement aussi dynamique et convivial :

Merci aux anciens, Lucile, Laetitia, Juliette, Chloé, Charlotte M, Matthias, Romain, Mickael, Marie-Anne et Benoit G, mais aussi à mes anciennes colocs du « bureau de passage » Déborah et Lucie G, pour avoir initié le mouvement, notamment grâce aux apéros post journal club. Merci notamment à Juliette, Lucile et Laetitia pour leur accueil lors de mon arrivée et pour avoir partagé avec les plus jeunes leur expérience « d'anciennes ». Avec des étudiantes aussi douées comme modèle, la thèse ne pouvait que bien démarrer. Un grand merci à Benoit G pour avoir, avec la patience d'un grand frère, conseillé et soutenu la jeune thésarde un peu perdue que j'étais. Merci pour ton amitié sans faille, ta franchise et tes analyses toujours très fines qui rendent tes conseils d'autant plus précieux ! Avec ton énergie, ta rigueur et ton intelligence, je n'ai pas de doute, tu vas faire des merveilles.

Merci à mes collègues de promo, Brice, Nam, Charlotte, Noémie, Yaël et Romain. C'était très agréable de faire cette thèse à vos côtés. Merci Brice d'avoir importé à MIRCen tes coutumes étranges de canadien, contribuant ainsi à animer tout le labo. Tu laisses en héritage un certain nombre de traditions qui sont parties pour durer. Merci aussi de nous avoir montré le chemin du PMU et merci à Jean-Marc d'avoir accueilli avec bienveillance et gentillesse nos réunions de thésards anonymes.

Merci aux autres étudiants et collègues, Audrey, Laurène, Lucie D, Sandro, Marco, Benoit S, Clément G, Clément B, Anastasie et Clémence D pour avoir peuplé de vos rires et de votre bonne humeur les labos, les pauses café et les soirées. Merci à Aurélie, Charlène, Noëlle, Ioanna et Susannah pour leur grain de folie et à Nad et Jérémy pour leur extrême gentillesse. Merci au colocs successifs du bureau 210C, Marianne, Pierrick et Juliette, pour avoir accompagné de leur présence les longues journées de stéréologie et pour avoir supporté sans se plaindre ma tendance extrême à la ponctuation. Merci notamment à Marianne pour sa bonne humeur et sa gentillesse, c'était très agréable de travailler à tes côtés. Merci aussi aux jeunes « 3ème années », Séverine pour ton optimisme indestructible très inspirant, Kelly pour ta gentillesse (et pour ta complicité forcée de mes emprunts de café à Noémie) et Clémence L d'animer joyeusement tout ce petit monde. Je regrette d'avoir découvert trop tard ta grande intelligence et ton extrême gentillesse. Bon courage à vous trois, ainsi qu'à Jérémy et Zhenzhen, pour cette troisième année qui est la plus éprouvante mais aussi, vous allez voir, la plus enrichissante. J'ai une confiance aveugle en votre réussite future !

Un grand merci enfin à la joyeuse bande sans qui cette thèse n'aurait pas été aussi belle. Noémie, Charlotte, Yaël, merci les enfants d'avoir été une raison de plus de se lever le matin (et vous savez à quel point le réveil est difficile pour moi). Merci pour votre soutien sans faille même, et surtout, quand je ne l'avais pas demandé. Vous avez été des piliers mais avant tout des modèles.

Cha, à la fois mère poule et grande sœur cool, « merci pour tout » me parait insuffisant. Merci d'avoir toujours à cœur de prendre soin de tout le monde, que ce soit par l'écoute ou le meilleur des remèdes : un peu de vin, beaucoup de charcut' et une joie de vivre communicative ! Tu m'as appris que la première qualité d'un chercheur est de se remettre en question mais qu'il faut toujours se battre pour ce qu'on croit juste. Bref, je compte bien prendre exemple sur ta rigueur, ton courage et ta motivation.

No, la MacGyver de la science et de la vie, je ne le dirai jamais assez : quand je serai grande, je veux être toi ! Quand tu fais les choses, tu les fais en grand et toujours avec brio. J'aimerais un jour avoir ta force de caractère et ton sens aigu de l'analyse. Merci d'avoir partagé tous les moments de galère et permis de les relativiser grâce à ton humour. J'espère que dans le futur tu seras fière de ce que tes poussins auront accompli (et je me compte comme poussin), car tu y auras fortement contribué !

Ya, biquette, tout d'abord merci pour ta patience face à trois filles à l'humour pas toujours subtil. Merci aussi pour ta gentillesse, ta bienveillance et ton côté papa poule (même si tu cherches désespérément à le cacher). Tu as érigé la curiosité en principe de vie ce qui, allié à une grande finesse d'esprit, fait de toi un chercheur impressionnant ! J'aurais beaucoup appris en te côtoyant (jusqu'aux règles du foot US) et notamment que tout domaine d'étude inconnu est un domaine qui ne demande qu'à être exploré.

Tout ça pour vous dire, les enfants, que vous êtes de belles personnes, et de la classe des grands chercheurs (le pire, c'est que vous n'en avez pas conscience). Ça aura été un plaisir et un honneur de faire cette thèse à vos côtés. Bref, ces trois ans avec vous auront été « *Hallucinants… !* ».

Merci enfin à mes amis et ma famille pour tout leur soutien et pour avoir supporté pendant trois ans mes sautes d'humeur et mon indisponibilité chronique. Merci notamment à Marianne et Laetitia pour leur amitié de longue date et pour avoir écouté avec patience mes charabias scientifiques. Un énorme merci enfin à mes parents pour leur soutien de toujours. J'ai conscience que cette thèse a parfois été aussi difficile pour vous que pour moi. Merci de votre confiance absolue en mes capacités, qui m'a poussé jusqu'au bout. Cette thèse au fond c'est aussi un peu la vôtre.

OUTLINE

LIST OF FIGURES

LIST OF TABLES

ABBREVIATIONS LIST

AAV	Adeno-associated viruses
Aβ	Amyloid β
Aldh1l1	Aldehyde dehydrogenase 1 family, member L1
ALS	Autophagy-lysosome system
AMPK	5' adenosine monophosphate-activated protein kinase
APP	Amyloid precursor protein
α-syn	α-synucelin
AD	Alzheimer's disease
AGD	Argyrophylic grain dementia
bGHpA	Bovine growth hormone polyadenylation signal
CaMKII	Calcium/ calmodulin-dependent protein kinase II
CBA	Cytomegalovirus/chicken β-actin
CBD	Corticobasal degeneration
Cdk5	Cyclin-dependent kinase 5
CNS	Central nervous system
CSF	Cerebrospinal fluid
DG	Dentate gyrus
EC	Entorhinal cortex
eNFT	Extracellular NFT ("ghost tangle")
FTDP-17	Frontotemporal dementia with Parkinsonism linked to chromosome 17
FTD-s	Frontotemporal dementia spectrum
FTLD	Fronto-temporal lobe degeneration
GFP	Green fluorescent protein
GSK-3	Glycogen synthase kinase-3
GTOs	Granular Tau oligomers
HC	Hippocampus
HD	Huntington's disease
Hprt1	Hypoxanthine phosphoribosyltransferase 1
iNFT	Intracellular NFT
ITR	Inverted terminal repeats
KI	Knock-in
KO	Knock-out
LTD	Long-term depression
LTP	Long-term potentiation
MAPT	Microtubule associated protein Tau
MARK	Microtubule affinity-regulating kinases
MB	Methylene blue
MBD	Microtubule-binding domain
MEGF10	Multiple EGF-like-domains 10
MERTK	Myeloid-epithelial-reproductive Tyrosine Kinase
mHtt	Mutant Huntingtin
MoPrP	Murine prion promoter
MT	Microtubule
MVB	Multi-vesicular bodies

NFT	Neurofibrillary tangle
NT	Neuropil thread
PART	Primary age-related tauopathy
PD	Parkinson's disease
PET	Positon emission tomography
PHF	Paired helical filaments
pi	Post-injection
PKA	cyclic AMP-dependent protein kinase A
PP2A	Protein phosphatase 2A
Ppia	Peptidylprolyl isomerase A
PSP	Progressive supranuclear palsy
p-Tau	Phosphorylated Tau
SF	Straight filament
SP	Senile plaque
SSC	Saline-sodium citrate
TNFα	Tumor necrosis factor α
t-Tau	Total Tau
UPS	Ubiquitin-proteasome system
WPRE	Woodchuck hepatitis virus posttranscriptional regulatory element
WT	Wild-type

INTRODUCTION

INTRODUCTION

General introduction

Since the initial description that Alzheimer's disease (AD) progression is associated with the sequential propagation of Tau pathology along anatomically-connected brain regions (Braak and Braak, 1991; Delacourte et al., 1999), it was suggested that Tau may be a relevant target of disease-modifying therapies for AD. Later on, a number of pathologies, termed tauopathies, were described having in common the aggregation of Tau protein in given brain regions (Buée et al., 2000). This further supported the need for the development of Tau-targeting drugs that may be of use for the treatment of tauopathies as a whole.

As yet, no drug or treatment has proven efficacy to relieve these diseases despite significant efforts in the field. Among the many therapeutic strategies developed to target Tau-associated neurodegeneration, several are based on the inhibition of Tau aggregation (Holtzman et al., 2016). This can be done by targeting several steps of the process, from inhibiting the induction of aggregation (e.g. through inhibitors of Tau phosphorylation) to dissolution of long formed aggregates with the use of passive or active immunotherapy (Pedersen and Sigurdsson, 2015). Compounds designed to prevent aggregate elongation were also recently developed (Himmelstein et al., 2012). Most strategies already gave significant results in pre-clinical studies, allowing the reduction of Tau pathology and, in some cases, leading to cognitive improvement. Passive and active Tau-directed immunotherapies are at the very beginning of the clinical phase. For inhibitors of Tau aggregation, however, a few clinical data are already available. First results of a phase 3 clinical trial for methylene blue (MB), for example, were presented recently during the Alzheimer's Association International Conference, yielding quite disappointing results with no effect on the progression of cognitive decline and brain atrophy in AD patients. Although the primary end-point in developing therapies is the reduction of cognitive and functional decline, it is also necessary to address the question of therapeutic impact on Tau pathology.

To this respect, the availability of imaging and peripheral biomarkers of Tau pathology is of critical importance. Notably, one of the most readily accessible is the measure of Tau levels in the cerebrospinal fluid (CSF). It was suggested that CSF total Tau (t-Tau) reflects the extent of neuronal and axonal degeneration in the brain (Blennow et al., 2010). Indeed, transient increase in CSF Tau was observed in patients following stroke or brain trauma, the degree of increase being related to the extent of brain damage. High CSF t-Tau was also associated with progression from MCI to AD (Blom et al., 2009) and with stronger cognitive decline in patients with AD (Sämgård et al., 2010), suggesting that it may also be a good correlate of Tau pathology in the brain. In the case of other tauopathies, the relationship between CSF t-Tau and brain pathology may however be slightly different. Indeed, while CBD is also associated with increased CSF t-Tau (Mitani et al., 1998), it was recently shown that PSP patients present with CSF t-Tau even lower than control subjects (Wagshal et al., 2015). Differences in this peripheral marker may thus allow differential diagnosis of tauopathies. Elevated levels of phosphorylated Tau (p-Tau) in CSF were also described to be associated with AD (Blom et al., 2009; Sämgård et al., 2010) while no correlation between those and brain damages following stroke or brain trauma were described to date (Blennow et al., 2010), suggesting that it may be an even better correlate of Tau pathology. Although quantitation of CSF Tau may already prove useful for the follow up of therapeutic impact during clinical trials, the absence of standardized cut-off values of positivity precludes its immediate use as determinant

of clinical diagnosis for AD dementia (McKhann et al., 2011). Much effort remains also to be done to determine the usefulness of this marker for differential diagnosis of tauopathies.

Current developments in Tau imaging are focused on the identification of tracers allowing the visualisation of Tau aggregation by positon emission tomography (PET) imaging (Shah and Catafau, 2014). Most of those tracers are chemical derivatives of amyloid dyes, i.e. composites able to bind aggregates enriched in β-pleated sheets such as Tau and amyloid β (Aβ) proteins. Because of those origins, one of the main challenges in the field is to develop compounds that specifically bind to Tau aggregates compared to other amyloids. Other issues to be considered during the development of Tau-directed PET tracers include: 1) the necessity for the compound not only to enter the brain but also to pass through plasma membrane, as Tau aggregates are intracellular; 2) the ability of the tracer to recognize different Tau isoforms, as differences in this respect are observed between tauopathies; 3) the ability of the tracer to recognize Tau aggregates irrespective to the post-translational modifications, as Tau aggregation is associated with strong modification of the protein and 4) design compounds that recognize Tau aggregates irrespective of their localisation as those can be found in grey or white matter, depending on the tauopathy (Shah and Catafau, 2014). Differences were observed in the several families of Tau tracers with respect to fulfilling those different criteria, none of them being able to recapitulate all necessary features. Therefore, much effort still remains to be done to confirm the specific target of Tau-directed tracers and to assess their usefulness for differential diagnosis of tauopathies and for follow-up of Tau pathology.

Thus, developments in Tau-directed therapies and Tau-related biomarkers may gain from progressing concurrently and would probably benefit from a better understanding of Tau physiopathology. Indeed, further insight in the commonalities and differences of tauopathies may aid therapeutic development by determining if a common pathologic pathway can be targeted. Similarly, development of Tau imaging tracers and peripheral biomarkers would gain from a better understanding of the mechanistic commonalities and differences between tauopathies. The development of novel animal models will be required to address those different questions (Holtzman et al., 2016), notably by using tools allowing the concomitant development and direct comparison of models reproducing the specific pathology of each tauopathy. Assessment of the different biomarkers described above in those models would allow better translation of results obtained in animals to the clinics, given that identified pathological pathways may be first confirmed in post-mortem studies using samples from tauopathy patients.

In this introduction we will describe current advances in the understanding of Tau physiology and pathology, with a specific focus on the relation between Tau aggregation and neurodegeneration. A last part will comprise a description of the different approaches used to model Tau pathology in rodents, how those models may help gaining insight into the pathological processes common to tauopathies and their limitations with respect to the question addressed in our project. Indeed, the work of this PhD project was centred on the development of new rodent models of sporadic and genetic tauopathies to study whether those present commonalities in the mechanisms linking Tau aggregation and its toxicity. This necessitated an approach allowing the direct comparison of different models, which may be hindered in transgenic animals due to the phenotypic variability observed between models.

I – Tau in physiological conditions

1) Structure of Tau protein

a) Expression and alternative splicing of Tau

Human Tau gene and alternative splicing

Human Tau is encoded by a single microtubule-associated protein tau (MAPT) gene localized on chromosome 17q21 (Neve et al., 1986). Six main isoforms of the protein are present in the adult brain, arising from the alternative splicing of exons 2, 3 and 10 (**Figure 1**). Those differ depending on the number of 29 amino acids-long inserts localized in the N-terminal part of the protein (Goedert et al., 1989a; Lee et al., 1989), encoded respectively by exons 2 and 3, giving rise to isoforms with either zero, one or two inserts (respectively noted 0N, 1N and 2N). In addition, alternative splicing of exon 10 leads to the production of isoforms with either 3 or 4 repeats in the C-terminal domain (labelled respectively 3R and 4R; (Goedert et al., 1988, 1989b). In the peripheral nervous system, Tau is found in the form of a single "big Tau" isoform, corresponding to the 2N4R form with the addition of exon 4a (Mandelkow and Mandelkow, 2012). Human Tau sequence shows strong homology with that of other mammalian species, including cows (Himmler, 1989; Himmler et al., 1989), mice (Lee et al., 1988) and rats (Kosik et al., 1989a). Rodent Tau is 11 residues shorter N-terminal region and has a few substitutions along the entire sequence but shows, however, perfect homology with that of humans in the C-terminal part.

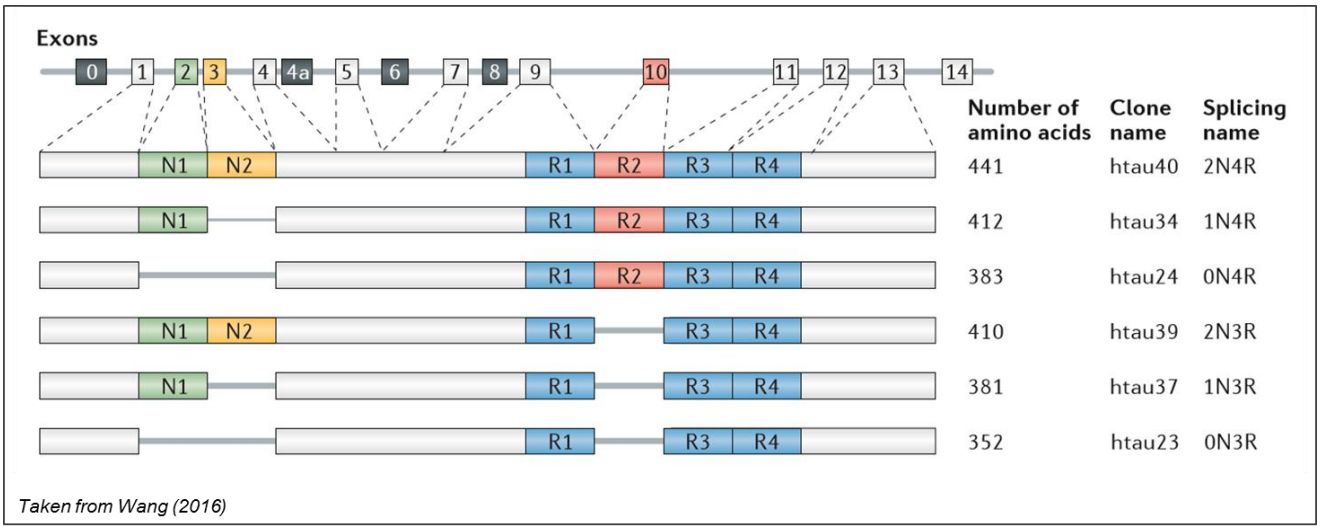

Figure 1: Isoforms of Tau protein arising from the alternative splicing of MAPT gene
4R isoforms present with 4 repeats in the C-terminal part of the protein while 3R isoform arise from the alternative splicing of exon 10 encoding the second repeat. This is done in combination with the alternative splicing of exon 2 or exons 2 and 3, giving rise to isoforms with zero (0N), one (1N) or two (2N) N-terminal repeats.

Developmentally regulated expression of Tau isoforms

Tau is present in the foetal brain in the form of a single isoform bearing 3 C-terminal repeats and zero N-terminal insert (0N3R, Goedert et al., 1989b). This expression of a single "foetal isoform" is again highly conserved between species and can also be observed in rodents. In both rodent and humans, there is a shift during post-natal development with the progressive increase in the expression of 4R isoforms (Drubin et al., 1984; Goedert et al., 1989a; Kosik et al., 1989a; Takuma et al., 2003). The relative expression of all 6 isoforms, however, differs between species (**Figure 2**). Indeed, while human adult brain shows similar expression of 3R and 4R isoforms, rodents present with an enrichment of 4R

isoforms this imbalance being even stronger in mice (Hanes et al., 2009; Takuma et al., 2003). With respect to the N-terminal region, species differences can also be observed with 2N isoforms being relatively less expressed in human(Goedert et al., 1989a; Takuma et al., 2003) and mice (Liu and Götz, 2013) while similar levels of all N-terminally spliced isoforms can be observed in the adult rat brain (Hanes et al., 2009).

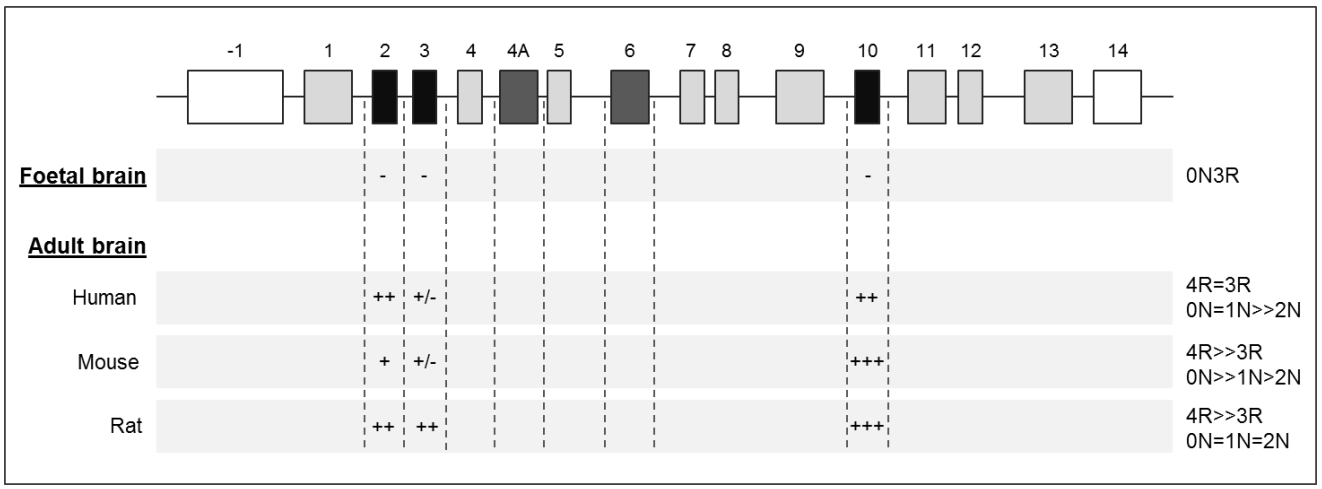

Figure 2: Relative expression of Tau isoforms in the developing and adult rodent or human brain
Exons present in all Tau isoforms are presented in light grey (1, 4, 5, 7-9 and 11-13), those outside of the coding sequence are shown in white (-1 and 14) while those present in other minor isoforms in dark grey (4a and 6). Lastly, exons subjected to alternative splicing to produce all six major isoforms are presented in black (2, 3 and 10).

b) Biochemical properties of Tau and 3-dimentional structure of the protein

Tau is a highly polarized protein with an overall neutral, slightly basic, character (Cleveland et al., 1977a, 1977b), the N-terminal part of the protein presenting a predominantly acidic composition while the last 40 C-terminal residues are roughly neutral (Himmler et al., 1989). This asymmetry of charges may play an important role for Tau interaction with its partners (Mandelkow and Mandelkow, 2012).

The protein is highly hydrophilic and heat-resistant which suggests that it may undertake a relatively loose conformation (Lee et al., 1989; Weingarten et al., 1975). This was confirmed using nuclear magnetic resonance, showing that Tau is natively unfolded (Mukrasch et al., 2009). Only few sites of secondary structures (α-helix, β-strand, poly-proline II helix) are observed along the protein (**Figure 3**) and appear relatively transient, conferring a high flexibility to Tau. Consistently, only two cysteine residues are present in the protein, localized in repeats 2 and 3 in the C-terminal domain, thus limiting intra-molecular disulphide linkage (Kosik et al., 1989a). Despite its relative low content in secondary structures, Tau protein can present with global folded conformations (Mukrasch et al., 2009), including a described paper-clip structure, formed by the folding of N-terminal and C-terminal ends over the repeated region (Jeganathan et al., 2006). Local changes in Tau conformation can be observed upon binding to the MT, notably around repeats 2 and 3 in the C-terminal domain (Kadavath et al., 2015a). Those form a local hairpin structure which may act as a hook, allowing the anchor of Tau at the interface of tubulin heterodimers (Kadavath et al., 2015b).

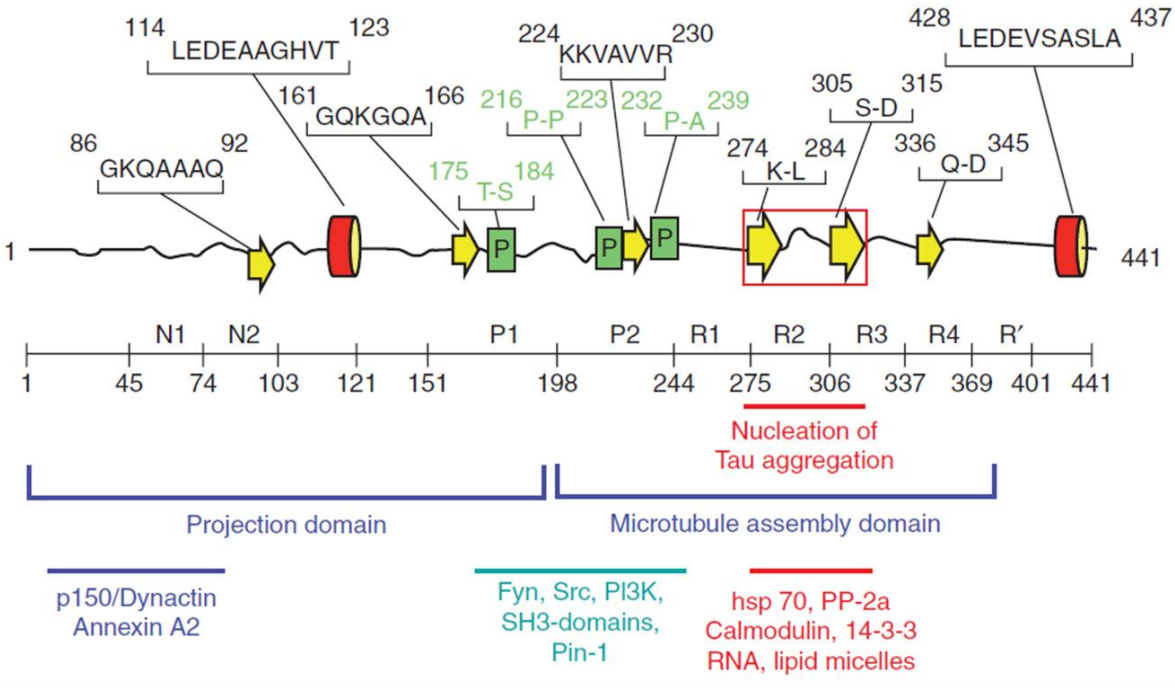

Taken from Mandelkow (2012)

Figure 3: Localisation of secondary structures observed along Tau protein
Most of the chain is highly unfolded, with shorts elements of secondary structures observed along the entire protein, including α-helix (red), β-strand (yellow) and poly-proline II helix (green).

c) Domains of Tau protein

Domains of Tau protein can be defined respective to their amino-acid composition as well as interaction with Tau binding partners (see **Figure 3** above). Hence, the C-terminal part of the protein was designated as the MT-assembly domain after the discovery that the C-terminal repeats correspond to microtubule-binding domains (MBD; Himmler, 1989; Lee et al., 1989). Similarly, the N-terminal domain, containing a Proline-rich region, was named projection domain because it was shown to present no interaction with the MT and to project from the MT surface (Hirokawa et al., 1988). This clear dissociation between domains with respect to biochemical properties and binding partners is thought to be associated with distinct functions of Tau.

Primary association of Tau to the MT thus occurs through the 3 to 4 repeated domains. Additional sites of interaction where however also observed in other parts of the C-terminal region (Mukrasch et al., 2009). Interestingly, the strength of MT-Tau interaction is dependent on the number of MBDs although one repeat is sufficient for the interaction to occur (Lee et al., 1989). This may be associated to Tau function in promoting MT assembly as 4R forms induce faster MT assembly than 3R forms (Goedert and Jakes, 1990). Additional Tau binding partners were later described to show interaction with the MT-binding region, including nucleic acids (Krylova et al., 2005), potentially mediating an additional role of Tau C-terminal domain, as well as several kinases and phosphatases, known to be involved in Tau post-translational modification (reviewed in Mandelkow and Mandelkow, 2012).

A large variety of Tau interactors were also found to bind to the N-terminal projection domain. For example, the amino-terminal part of Tau was found to interact with the motor protein dynactin (Magnani et al., 2007) as well as to bind to membranes, leading to Tau association to the plasma membrane

(Brandt et al., 1995) or to organelles such as the Golgi apparatus (Farah et al., 2006). Lastly, the Proline-rich region contains several motifs that serve as binding sites for proteins of the src family, such as the tyrosine kinase Fyn (Lee et al., 1998). Altogether, this suggests that, instead of being uniquely a MT-associated protein, Tau may play a large variety of functions into the cell.

2) Localisation of Tau expression

a) Expression of Tau protein in different brain regions

Tau protein is found strongly enriched in the central nervous system with an alternative “big Tau” isoform observed at the periphery (Mandelkow and Mandelkow, 2012). In humans, Tau mRNA is found in all brain structures with only few regional differences in expression (Goedert et al., 1988, 1989b). Slight differences in the pattern of expression of different N-terminal Tau isoforms were however described in rodents (Hanes et al., 2009; Liu and Götz, 2013), which may underlie functional differences.

b) Cellular and sub-cellular localization

In the brain, Tau is primarily observed in neurons (Binder et al., 1985; Goedert et al., 1989b; Kosik et al., 1989b) but is also expressed at low level in glial cells, notably oligodendrocytes (LoPresti et al., 1995). The pattern of isoforms expression may differ between neuronal populations. For example, while both 3R and 4R isoforms are present in pyramidal cells of the cortex and HC, granular cells of the dentate gyrus express only 3R Tau isoforms (Goedert et al., 1989b), again implying functional differences of Tau isoforms.

In adult neurons, Tau is found highly enriched in the axonal compartment (Binder et al., 1985; Dotti et al., 1987) where it binds to MTs, promoting their stabilization. Sorting of Tau occurs during post-natal development where there is a shift from its initial somatodendritic localization to specific enrichment in the axon (Litman et al., 1993). This occurs concurrently to the apparition of 4R isoforms (Drubin et al., 1984) and a strong reduction in the extent of Tau phosphorylation (Kanemaru et al., 1992). The actual mechanism governing Tau sorting remains poorly understood. This may involve direct transport of Tau to the axon, as Tau mRNA was also found in somas and dendrites (Kosik et al., 1989b). There is also enrichment of Tau mRNA in the axon itself. Indeed, a 3’ untranslated region was identified in MAPT gene that targets Tau mRNA at the axon. The observation of a co-localization between Tau mRNA and protein in the axon thus suggests that local translation may also occur (Aronov et al., 2001).Lastly, sorting may also be related to the presence of a barrier in the axon initial segment, preventing the retrograde transport specifically of MT-bound Tau to the somatic compartment (Li et al., 2011). Tau binding to the MT is regulated by its phosphorylation which may explain why fetal Tau, that shows strong phosphorylation, is located to the soma.

Small concentrations of Tau were also observed in other neuronal compartment, notably in dendrites (Ittner et al., 2010) and in the nucleus (Sultan et al., 2011). Interestingly, in rodents, the relative sub-cellular distribution differs between N-terminal isoforms. Hence, 1N isoforms are specifically enriched in the nucleus and in dendrites while 2N Tau shows robust cytoplasmic and axonal expression (Liu and Götz, 2013). This suggests again the implication of different isoforms in various Tau functions. Lastly, Tau was also recently found to be secreted into the interstitial fluid (Yamada et al., 2011). Tau release to the extracellular space may be done through transport in ectosomes (Dujardin et al., 2014a) and is stimulated by neuronal activity (Fá et al., 2016; Pooler et al., 2013) suggesting that it may be implicated in the modulation of synaptic activity.

3) Functions of Tau

a) Functions of MT-bound Tau

MT polymerization and regulation of MT dynamics

Initial in vitro studies reported a role of Tau in the induction of MT polymerization from free tubulin (Cleveland et al., 1977a, 1977b; Weingarten et al., 1975), suggesting that Tau is sufficient for both nucleation and elongation of MTs. This function of Tau in the induction of MT formation may be related to its ability to bind several tubulin heterodimers through its MT-binding domain region (Mukrasch et al., 2009), leading to a local increase in tubulin concentration and inducing polymerization. Consistent with the fact that Tau isoforms with 4 repeats present a stronger MT binding (Lee et al., 1989) , 4R isoforms induce faster MT assembly than 3R forms (Goedert and Jakes, 1990).

In addition to this effect on initial MT polymerization, Tau was later shown to also influence the dynamics of already formed MTs. Indeed, MTs are dynamic structures that constantly undergo polymerization-depolymerisation events, a phenomenon termed dynamic instability (Feinstein and Wilson, 2005). In this context, Tau was found to promote the rate of polymerization while decreasing the rate of depolymerisation. In addition, Tau is also able to decrease the frequency of “catastrophe” events (i.e. transitions from growth to shortening). Altogether, those results implicate Tau as a main actor in MT stabilisation. Interestingly, differences were observed between isoforms in their ability to control MT dynamics. Indeed, while 4R Tau influences shortening and growth events, 3R isoforms had no effect on dissociation rate (Panda et al., 2003).

Implications during development and at adult age

The differential ability of 3R and 4R isoform to stabilize MTs has several implications during development and at adult age. The observation that Tau in the foetal brain is present in the form of a single 0N3R isoform (Goedert et al., 1989b), and that the apparition of mature Tau isoforms correlates with the formation of stable MTs (Litman et al., 1993) suggests that this developmentally regulated switch in expression may be implicated in neuronal differentiation (**Figure 4**). Indeed, Tau has been found to play an important role in the formation and maintenance of the neurons polarity. Reduction of Tau levels using antisense oligonucleotides abolishes neurons polarity by inhibiting axonal formation (Caceres and Kosik, 1990) while primary neurons from Tau KO mice exhibit deficits in axon elongation (Dawson et al., 2001).

During post-natal development, Tau migrates from its initial somatodendritic localization (Litman et al., 1993) to the distal portion of the axon (Kempf et al., 1996) where it can play a role in the growth of the axon. The apparition of 4R isoforms (Drubin et al., 1984) then leads to a strong increase of MT stabilization, allowing the maintenance of the newly formed axon. At adult age, MT-bound Tau thus plays an important role in the conservation of this polarized architecture of the neuron. The expression of both 3R and 4R isoforms at adult age may, however, be necessary for the maintenance of some MT dynamics because over-stabilization of MTs may have deleterious impact on synaptic plasticity (Feinstein and Wilson, 2005).

Regulation of axonal transport

At adult age, MT-bound Tau in the axon presents an increasing concentration gradient from the initial segment to the distal part (Black et al., 1996), such that it is particularly concentrated around synaptic terminals (Kempf et al., 1996). This specific distribution along the axon has strong implication for axonal transport as MT-bound Tau was found to modulate the activity of motor proteins (**Figure 4**). Indeed, it was shown that kinesin motors, which are the proteins responsible for the transport of vesicles from the soma to the synapse, detach from the MT when encountering clusters of MT-bound Tau (Dixit et al., 2008). This effect of Tau on MT-kinesin interaction is concentration dependent, which is consistent with a role of Tau in regulating axonal transport. Indeed, lower Tau concentration at the soma would allow kinesin motors to bring vesicles to the synapse where high concentration of Tau would then permit the release of cargos. The effect of Tau on dynein-dynactin motors is less pronounced than on kinesin. Again, this is consistent with the maintenance of a normal axonal transport as dynein motor proteins are involved in the retrograde transport from the synapse to the soma. Tau can also act on other parameters to modulate transport along the axon. Indeed, it was also found to affect the association between motors and cargoes (Wang and Mandelkow, 2016). For example, it can compete with other cargoes for binding to kinesin or induce the release of cargoes from kinesin (Kanaan et al., 2011). This action of Tau would thus further potentiate the delivery of vesicles to the synapse.

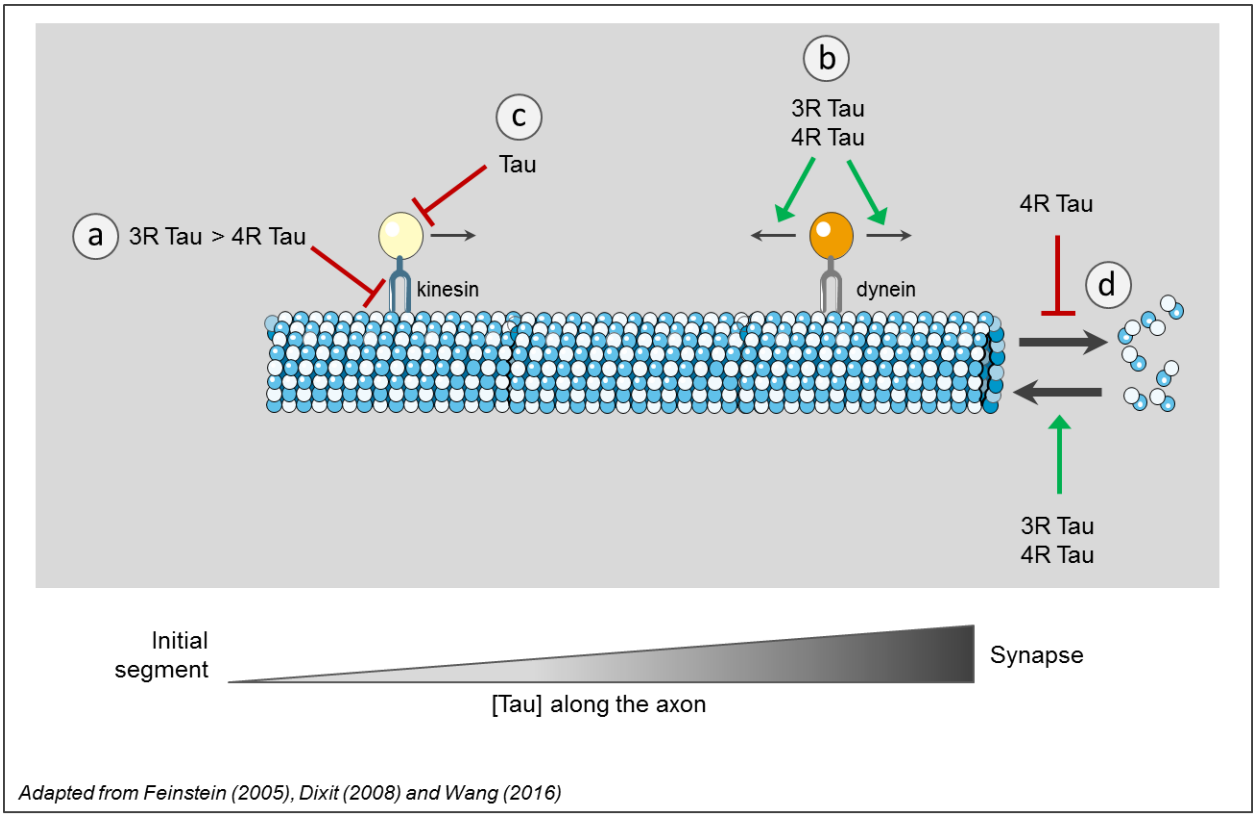

Figure 4 Functions of MT-bound Tau

MT-bound Tau regulates transport of cargoes along the axon in several ways: a) Tau and kinesin are in competition with each other for the binding to MTs, such that kinesin will detach upon encounter with MT-bound Tau. This may be necessary for the delivery of vesicles to the synapse as higher Tau concentrations are observed at synaptic terminals. b) In contrast, Tau does not induce dynein detachment. Conversely, dynein motors will either stop or reverse direction when encountering Tau. c) Tau also acts on the motor-cargo interaction either by competing with cargoes for binding to kinesin or by inducing cargo release. In addition, the developmental switch in isoforms expression plays a role in formation and maintenance of the polarized structure of the axon (d).

b) Additional functions of Tau

In addition to its known localisation in the axon, Tau was found to be also expressed in other neuronal compartments, suggesting additional roles of the protein. First, some Tau isoforms were found to be enriched in the nucleus (Liu and Götz, 2013) were they bind to DNA (Sultan et al., 2011). Tau localization to the nucleus is increased in conditions of oxidative or heat stress associated with an increase in its binding to DNA. In this context, Tau was found to promote DNA protection against stress-induced degradation, by modulating DNA repair processes (Violet et al., 2015).

Small quantities of Tau protein were also observed in dendrites although its functions at the post-synaptic terminal are still poorly understood. It was recently reported that synaptic Tau may have a role in mediating the interaction of NMDA subunit NR2b with PSD95 by allowing the targeting of Fyn kinase to the synapse (Ittner et al., 2010). This would allow the phosphorylation of NR2b by Fyn, this phosphorylation being known to enhance NR/PSD95 interaction. Similarly, Tau was recently found to be necessary for the induction of long-term depression (LTD; Kimura et al., 2014). In this study, induction of LTD was associated with strong phosphorylation of synaptic Tau, suggesting that it may be involved with synaptic plasticity occurring during LTD. Lastly, recent data also suggest a function of dendritic Tau in hippocampal adult neurogenesis (Pallas- Bazarra et al., 2016). Indeed, in mice showing a deficiency in Tau protein, new-born neurons exhibit pre- and post-synaptic morphological abnormalities associated with deficits in synaptic activity. In addition to its role at the synapse, Tau was recently reported to have additional roles in the modulation of synaptic activity through its extracellular pool. Indeed, release of Tau to the extracellular space was found to be stimulated by neuronal activity (Fá et al., 2016; Pooler et al., 2013). In addition, extracellular Tau is able to increase post-synaptic calcium entry through muscarinic receptors (Gómez-Ramos et al., 2008).

4) The role of phosphorylation in modulating Tau function

Tau is the substrate of many kinases and phosphatases that tightly regulate its phosphorylation state (Noble et al., 2013). Among the 85 putative phosphorylation sites on Tau protein (Martin et al., 2011), most of them cluster around the proline-rich region and are constituted of Thr-Pro or Ser-Pro motifs that are the target of proline-directed serine/threonine kinases (Wang and Mandelkow, 2016), such as glycogen synthase kinase-3 (GSK-3), cyclin-dependent kinase 5 (cdk5) and 5' adenosine monophosphate-activated protein kinase (AMPK). Additional phosphorylation sites are found in or around the MT-binding region and are targeted by non-proline-directed kinases, including among others microtubule affinity-regulating kinases (MARKs) cyclic AMP-dependent protein kinase A (PKA) and Calcium/ calmodulin-dependent protein kinase II (CaMKII). In addition, Tau is subjected to dephosphorylation through the action of several phosphatases, the most prominent being protein phosphatase 2A (PP2A), that is responsible for about 70% of Tau dephosphorylation (Iqbal et al., 2016). PP2A influences Tau phosphorylation status both by acting directly and through the regulation of Tau-directed kinases. Altogether, those processes thus allow a tight control of Tau phosphorylation suggesting that it may play an important role in the modulation of its functions.

Indeed, a large number of Tau phosphorylation sites were found to reduce Tau-MT interaction (Cho and Johnson, 2003, 2004; Fischer et al., 2009) with, as an effect, a reduction of MT stabilisation (Liu et al., 2007). This post-translational modification plays an important role during development, at a time where morphological plasticity is needed. Indeed, Tau is heavily phosphorylated in the foetal brain (Kanemaru et al., 1992), which probably allows the strong dynamics of MTs necessary for the development of polarity during neuronal differentiation. The apparition of 4R isoforms in adult brain is associated with a

strong reduction in Tau phosphorylation, allowing the stabilisation of the neuronal structure. Phosphorylation and dephosphorylation events still occur at adult age, however, permitting the fine tuning of Tau functions. Indeed, correct modulation of axonal transport, for example, may require equilibrium between MT-bound Tau and phosphorylated free Tau to govern the frequency of vesicle transport by motor proteins (**Figure 5**, Ballatore et al., 2007). In addition, phosphorylation likely modulates other functions of Tau as nuclear and extracellular Tau, for example, are found mainly in a dephosphorylated state (Dujardin et al., 2014b; Pooler et al., 2013; Sultan et al., 2011). Phosphorylation of Tau at the N-terminal end was also found to prevent its binding to membranes (Noble et al., 2013).

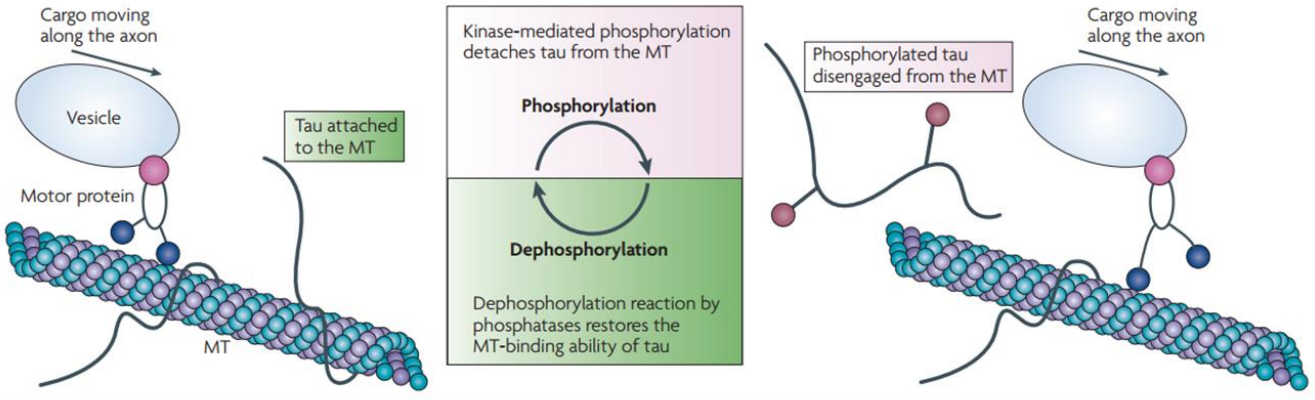

Taken from Ballatore (2007)

Figure 5: The effect of phosphorylation on Tau-mediated regulation of axonal transport
In the brain, there is a dynamic equilibrium between MT-bound and free phosphorylated Tau that may be involved in the regulation of axonal transport. Indeed, the binding of Tau to the MT prevents correct axonal transport by inducing the detachment of motor proteins. Phosphorylation of Tau induces its release from the MT allowing passage of motor proteins and delivery of cargo to the synaptic terminal.

To conclude, the multiple functions of Tau in neurons make the protein an important factor of neuronal survival and proper functioning. The tight modulation of different isoforms expression (Kosik et al., 1989a), Tau localization (Binder et al., 1985) as well as post-translational modifications of the protein (Kanemaru et al., 1992) is an important factor for Tau functions into the cell. This is of particular importance during development where Tau governs axonal polarity (Caceres and Kosik, 1990) but also at adult age through its impact on cell structure and axonal transport (Dixit et al., 2008). Dysregulation of either isoforms ratio (Hutton et al., 1998) or Tau phosphorylation (Grundke-Iqbal et al., 1986) thus have significant impact on neuronal survival. This is the case in a large family of diseases, termed tauopathies, were Tau dysfunctions are associated with neurodegeneration.

II – Tau protein in pathological conditions

1) Presentation of the different tauopathies

a) Neuropathological and clinical characterization of tauopathies

Tauopathies are neurodegenerative diseases characterized by the aggregation of hyperphosphorylated Tau in neurons and glial cells. The accumulation of those lesions is associated with neurodegeneration in specific brain regions, leading to cognitive impairments and ultimately dementia. Distinction can be made in those pathologies between amnesic dementias and pathologies of the frontotemporal dementia spectrum (FTD-s).

Amnesic dementias include Alzheimer's disease (AD), Down's syndrome, primary age-related tauopathy (PART) and Argyrophilic grain disease (AGD) and are characterized by the preferential involvement of medial temporal cortices as well as limbic structures (Buée et al., 2000). In FTD-s dementias, Pick's disease and frontotemporal dementia with Parkinsonism linked to chromosome 17 (FTDP-17) have in common the preferential involvement of frontotemporal cortices leading to either frontal disinhibition (Pick's disease) or impairment in executive functions (FTDP-17). Structures of the limbic and/or nigrostriatal pathways can also be involved in some cases of Pick's disease, leading to a large diversity of symptoms (Greenfield's Neuropathology - 8th edition, Weller, 2008). FTD-s include additionally two other disorders, progressive supranuclear palsy (PSP) and corticobasal degeneration (CBD) that are thought to be tightly related. PSP is associated with preferential neurodegeneration of basal ganglia, brainstem and cerebellum, leading primarily to subcortical motor disturbances. CBD, on the other hand, involves selective neurodegeneration of the parietal cortex leading to cortical motor disturbances and moderate dementia.

Overall, tauopathies are sometimes clinically difficult to distinguish as some may give rise to very similar symptoms. In addition, comorbidity is often found in the brain of demented patients rendering difficult a definite diagnosis. Lastly, it has been suggested that some of those tauopathies may exist as a disease spectrum (Dickson et al., 2011). PSP and CBD, for example, may be only distinguished by the relative burden of Tau lesions in specific brain regions. Between the pure PSP, characterized by only subcortical deposition, and pure CBD, where Tau deposits are found only in the cortex, the whole range of mixed histopathology can be observed. Other parameters may be necessaries for a differential diagnosis of tauopathies. Below are reviewed ways to distinguish them.

b) 3R vs 4R vs 3R+4R tauopathies

Tauopathies can be first distinguished by the ratio of Tau isoforms found enriched in aggregates which led to a classification of those pathologies into four categories (Sergeant et al., 2008). Indeed, hyperphosphorylated Tau is characterized by a shift in its apparent molecular weight observed by western blot, which led to the identification of a biochemical signature characteristic of different tauopathies (Mailliot et al., 1998).

In class I tauopathies, all six isoforms of Tau are present into the aggregates (**Figure 6**) and can be observed by SDS-PAGE as four separate bands, ranging from 60 (0N3R) to 74 kDa (2N4R). The hyperphosphorylation of Tau protein leads to an apparent shift of molecular weight such that 1N3R and 0N4R isoforms as well as 2N3R and 1N4R appear at the same size, respectively 64 and 69 kDa. This classical profile is characteristic of AD and other related tauopathies, including Down's syndrome, Niemman-Pick disease type C and some cases of frontotemporal dementia linked to chromosome 17

(FTDP-17; Sergeant et al., 2005). Class II tauopathies are characterized by the selective aggregation of 4R isoforms migrating as a triplet on SDS-PAGE (64, 69 and 74 kDa). This is the case for corticobasal degeneration (CBD), progressive supranuclear palsy (PSP), argyrophylic grain dementia (AGD) and most cases of FTDP-17 associated with mutations in the MAPT gene. Conversely, the isoforms mostly involved in class III tauopathies are those containing only 3 MBDs, giving a pattern of migration on SDS-PAGE ranging from 60 to 69 kDa. This category is mainly represented by Pick's disease as well as some familial cases of FTDP-17. Lastly, class IV includes one single tauopathy called myotonic dystrophy that is characterized by the aggregation of the foetal Tau isoform (0N3R) and strong downregulation of isoforms containing N-terminal repeats.

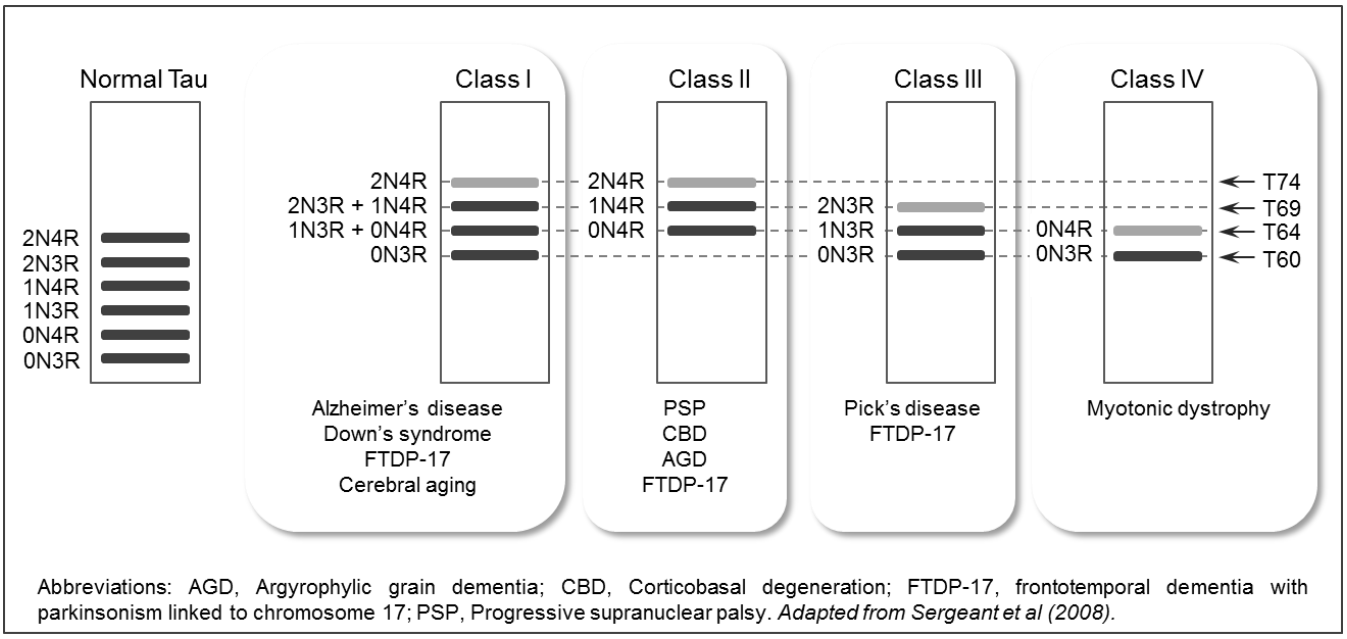

Abbreviations: AGD, Argyrophylic grain dementia; CBD, Corticobasal degeneration; FTDP-17, frontotemporal dementia with parkinsonism linked to chromosome 17; PSP, Progressive supranuclear palsy. *Adapted from Sergeant et al (2008).*

Figure 6: Biochemical signature of different tauopathies
Hyperphosphorylated pathological Tau protein presents an apparent shift in molecular weight when compared to normal dephosphorylated counterparts when resolved onto SDS-PAGE gels. Thus, tauopathies presenting with all 6 Tau isoforms in aggregates (Class I) are characterized by a triplet at 60, 64 and 69 kDa with an additional faint band at 74 kDa. Class II and class III tauopathies are characterized by the specific aggregation of 4R and 3R isoforms respectively, which can be identified as a doublet (at 64 and 69 kDa for 4R tauopathies and at 60 and 64 kDa for 3R tauopathies).

c) Sporadic vs genetic tauopathies

Tauopathies can be categorized into sporadic or genetic pathologies, depending on whether mutations on MAPT genes have been associated with the disease. To this respect, AD can be considered a sporadic tauopathy because, although familial mutations on APP or presenilin genes have been described (Blennow et al., 2006), no causative mutation appears on Tau gene in this disease. Most tauopathies are actually sporadic although some familial cases have been described, mainly in FTDP-17. In addition, several genetic risk factors have been described.

Causative mutations in familial tauopathies

Among tauopathies, FTDP-17 is the pathology presenting the largest genetic diversity. To date, more than 30 mutations have been associated with this disease (Sergeant et al., 2005), most of them in the microtubule-binding region. Those mutations have been observed to promote the aggregation of Tau (e.g. P301L, Hong et al., 1998) or decrease its affinity for the microtubule (e.g. R406W, Hutton et al., 1998). Others affect the alternative splicing of exon 10, either increasing (e.g. N279K) or decreasing

4R:3R ratio (e.g. ΔK280, Hong et al., 1998; Hutton et al., 1998; Swieten et al., 2007). Those mutations lead to a large variety of anatomo-pathological presentations, based on the type of cells affected, the composition and the morphology of aggregates. All give rise, however, to a single clinical phenotype, suggesting that different pathological processes may converge towards a common pathway. Conversely, a same mutation can be associated with the development of different tauopathies within a single family (Bugiani et al., 1999), suggesting that additional factors are involved in the development of Tau pathology.

Tau haplotypes and other genetic risk factors

Most genetic risk factors associated with the development of tauopathies seem to affect the regulation of Tau expression, leading to an increase in the production of the protein. One of the most studied genetic variations is the implication of Tau haplotypes. Indeed, hundreds of nucleotide differences have been observed on the MAPT gene, giving rise to two haplotypes (Caillet-Boudin et al., 2015). H1 haplotype has been associated with numerous tauopathies, including CBD, PSP (Cruchaga et al., 2009), AGD (Togo et al., 2002), tangle-predominant dementia (Santa-Maria et al., 2012) and AD (Myers et al., 2005). Interestingly, it has been shown that H1c sub-haplotype increases Tau expression and affects the splicing of exon 10, inducing an increase in the 4R:3R isoforms ratio (Myers et al., 2007).

Other variations in Tau gene have been associated with disease. For example, DNA hypomethylations, possibly inducing an increase in Tau expression, have been associated with sporadic AD and PSP (Barrachina and Ferrer, 2009; Iwata et al., 2014). Recently, a non-causative mutation has been associated with increased risk of developing AD and PSP (Coppola et al., 2012). Lastly, report of duplications of MAPT gene, alone or in combination with other genes from the same chromosomic region, was found to be associated with the development of fronto-temporal lobe degeneration (FTLD; Rovelet-Lecrux et al., 2010) or AD (Hooli et al., 2014). Taken together, those results suggest that, in absence of causative mutations, the overexpression of Tau itself may have a detrimental role (Rossi and Tagliavini, 2015). It remains that a direct genotype-phenotype correlation is often difficult rendering even more necessary the study of tauopathies as a whole to identify common pathological pathways.

d) Primary vs secondary tauopathies

Another way tauopathies can be distinguished from each other is on whether Tau pathology is associated with another proteinopathy. If it is the case, the disease is considered a secondary tauopathy in opposition to pathologies where Tau aggregates on its own (i.e. primary tauopathy). Most described tauopathies are thought to be primarily Tau-related with the exception of AD and Down's syndrome where, according to the amyloid cascade hypothesis, Tau aggregation is thought to be a consequence of Amyloid-β (Aβ) deposition (Hardy and Higgins, 1992).

More recently, it was suggested that both Parkinson's disease (PD), characterized by the accumulation of α-synuclein (α-syn), and Huntington's disease (HD), characterized by the aggregation of mutant huntingtin (mHtt), could be classified as secondary tauopathies. Although Tau pathology may not be the main driver of neurodegeneration in both pathologies, it has been implicated in modulating both α-syn and mHtt adverse effects. MAPT H1 haplotype has been associated with increased risk of developing PD (Ezquerra et al., 2011) and with increased aggregation of α-syn in dementia with Lewy bodies (Colom-Cadena et al., 2013). In addition, α-syn is a known Tau binding partner (Mandelkow and Mandelkow, 2012) and Tau is found enriched in Lewy bodies, the characteristic PD lesion. In the case of HD, MAPT H2 haplotype has been associated with the extent of cognitive decline in patients (Vuono et al., 2015)

while attenuation of motor disturbances was observed HD transgenic mice crossed with MAPT-/- mice (Fernández-Nogales et al., 2014). In addition, Tau inclusions were observed in the brain of HD patients, sometimes in the same neurons bearing aggregates of mHtt (Fernández-Nogales et al., 2014; Vuono et al., 2015).

Pathological trigger in secondary tauopathies: is Tau pathology really secondary?

Tau pathology in primary tauopathies is most probably the main driver of neurodegeneration, along with other external factors. In the case of secondary tauopathies, however, one question is whether both proteinopathies act synergically or if Tau pathology is found downstream in the pathological cascade. The most common hypothesis in the case of AD is the amyloid-cascade hypothesis that posits Tau as a downstream effector of Aβ-induced toxicity. Indeed, neuropathological studies have shown that the correlation between temporal lobe amyloid load and neuronal loss or cognitive deficits, disappeared when taking into account the number of NFTs in the region (Giannakopoulos et al., 2003). In addition, knocking-out Tau protein in animal models of AD leads to reduced Aβ-induced toxicity and preservation of cognitive function without affecting amyloid pathology (Roberson et al., 2007). However, evidence against the amyloid-cascade hypothesis has recently emerged. Indeed, Tau pathology can be found in healthy subjects long before the apparition of amyloid pathology (Braak and Del Tredici, 2011) and amyloid plaques develop at the axon terminal of tangle-bearing neurons (Schönheit et al., 2004). In addition, AD-like Tau deposition in the entorhinal cortex and hippocampus, associated with dementia, has been found in absence of Aβ deposition (Ikeda et al., 1999). Whether this represents a distinct disease known as primary age-related tauopathy (PART; Crary et al., 2014; Jellinger et al., 2015) or merely pre-clinical AD (Duyckaerts et al., 2015) remains a matter of debates. It remains that Aβ is not a prerequisite for Tau-associated neurodegeneration.

In the case of other secondary tauopathies, e.g. HD and PD, the question remains open as the potential implication of Tau to the pathological mechanisms has not been extensively studied. Current evidence points towards Tau pathology as being a secondary phenomenon, implicating Tau in worsening a pre-existing pathogenic event (Gratuze et al., 2016). Indeed, in the case of PD, α-synuclein has been shown to promote Tau fibrillization (Giasson et al., 2003), while in the case of HD, mHtt induces Tau hyperphosphorylation and relocalisation (Blum et al., 2015).

e) Morphology of Tau aggregates and affected cell-types

Definite diagnosis of a tauopathy is only available post-mortem by the observation of typical lesions in given cerebral regions. To this respect, tauopathies are again highly heterogeneous (**Figure 7**). Indeed, while Tau inclusions are mainly found in neurons in AD, PART and Pick's disease, severe Tau accumulation is found in astrocytes and oligodendrocytes for both PSP and CBD (Berry et al., 2001). In the case of FTDP-17, the relative involvement of neuronal and glial cells depends on the point mutation associated with the phenotype (Sergeant et al., 2005). Usually, the composition of glial inclusions is similar to that observed in neurons, with respect to isoform ratios and pathological Tau epitopes (Ferrer et al., 2014), suggesting that, among a given tauopathy, similar processes may occur in different cell-types. Alternatively, the formation of glial Tau inclusions may be associated with the transfer of aggregates from one cell to another. This could occur via either passive release of Tau aggregates into the extracellular space (Pooler et al., 2013) or active phagocytosis by glial cells (Chung et al., 2013). The origin of glial Tau inclusions has, however, never been fully addressed.

On the other hand, the morphology of Tau inclusions in a given cell-type can be strikingly different between tauopathies. For example, while AD is characterized by flame-shaped NFTs, neuronal inclusion in Pick's disease takes the form of small Pick's bodies (Yoshida, 2006). This may be associated with differences in the mechanism of Tau aggregation as in the former aggregates are composed of paired helical filaments (PHFs) while in the later they take the form of straight filaments (SF; Greenfield's Neuropathology - 8th edition, Weller, 2008).The difference in morphology of astrocytic lesions may be related to the involvement of different sub-class of astrocytes (Berry et al., 2001). This heterogeneity of morphology may also represent different steps of maturation of the lesion. Indeed, while Gallyas-negative astrocytic inclusions are found in distal processes, the Gallyas-positive aggregates are found in the soma and proximal processes of the astrocyte (Ikeda et al., 2015).

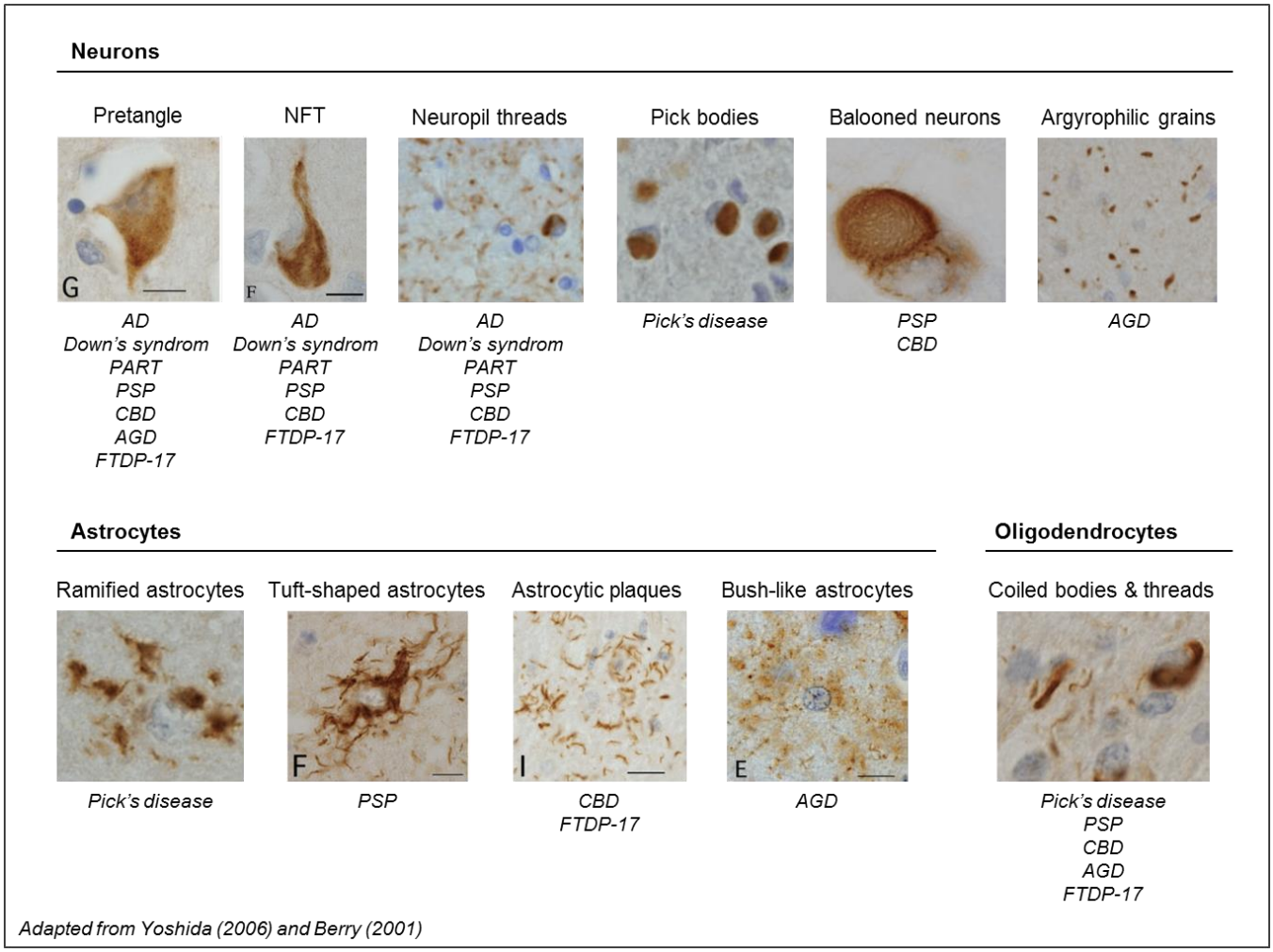

Figure 7: Morphology of Tau aggregates in different tauopathies

Anatomo-pathological study of the patients' brain using AT8 antibody allows a more precise description of the pathology and a definite diagnosis. More specifically, the relative burden of neuronal and glial Tau pathology may be a way to distinguish tauopathies. In addition, while some neuronal inclusions may be observed in numerous tauopathies (e.g. NFT, neuropil threads) some can be used as a signature of specific tauopathies (e.g. Pick bodies for Pick's disease, argyrophilic grains in AGD). Similarly, the morphology of astroglial pathology may be the only way to distinguish very similar tauopathies (e.g. tuft-shaped astrocytes in PSP versus astrocytic plaques in CBD).

Morphology of Tau filaments:

Lastly, tauopathies also differ by the morphology of Tau filamentous aggregates constituting those lesions. For example, AD and related tauopathies (i.e. Down's syndrome and PART) are characterized by the accumulation of paired-helical filaments (PHFs), presenting a double helical structure with a cross-over periodicity of 78 nm (Crowther and Wischik, 1985). Conversely, mostly straight filaments (SF) have been observed in Pick's disease (Rewcastle and Ball, 1968) and PSP (Tomonaga, 1977). In CBD, twisted filaments reminiscent of AD PHFs were observed (Ksiezak-Reding et al., 1994). However, they differed from PHFs by numerous morphological parameters. Indeed, twisted filaments in this pathology were larger, shorter in length and with a larger periodic twist of approximately 170 nm. In the case of FTDP-17, the morphology of Tau filaments seems governed by the properties of the mutation associated with Tau pathology (Barghorn et al., 2000; Crowther and Goedert, 2000). Indeed, while mutations affecting all 6 isoforms (e.g. V337M) produce fibrils with similar morphology than those observed in AD, intronic mutations affecting the splicing of exon 10 lead to filaments with a ribbon-like morphology and mutations affecting Tau aggregation (e.g. P301L) to the formation of PHFs and SFs.

In conclusion, tauopathies are characterized by the pathological aggregation of Tau protein into the soma of neuronal and glial cells, associated with neurodegeneration and leading to cognitive impairments. This class of pathologies, although presenting many commonalities, is phenotypically highly heterogeneous. This renders difficult to decipher what mechanisms may be responsible for Tau-associated neurodegeneration.

Indeed, while Tau pathology may only be a downstream effector of Aβ pathology in AD (Hardy and Higgins, 1992), the fact that familial FTDP-17 cases are associated with mutations in MAPT gene (Hong et al., 1998; Hutton et al., 1998; Swieten et al., 2007), suggests that Tau in itself plays an active role in degeneration. The large spectrum of clinical presentation observed in tauopathies raises the question of what mechanism underlies the involvement of specific brain regions and cell populations in different disorders. In addition, while the aggregation of specific isoforms can lead to strikingly different phenotypes (i.e. 3R opposed to 4R tauopathies), a high heterogeneity can also be found within the same disorder (i.e. FTDP-17 that can be associated with the aggregation of either 3R, 4R or all Tau isoforms, Sergeant et al., 2005). Lastly, while a single mutation can lead to several disorders (Bugiani et al., 1999), sporadic and familial cases are often clinically indistinguishable within a single tauopathy.

The use of versatile tools enabling the development of models recapitulating specific features of Tau pathology should help us resolve the question of the commonalities in the pathological processes underlying tauopathies but also allow us to determine what distinguishes them.

2) Mechanisms of Tau aggregation

a) Sequence of Tau aggregation

Conformation changes of soluble Tau are the trigger of its aggregation

The Tau protein is thought to be highly unfolded both in solution and when bound to the MT (Cleveland et al., 1977b; Mandelkow et al., 2007) . However, it is also able to take a partly folded conformation in solution, the C-terminal domain folding over the MBDs and the N-terminal domain coming in proximity of the C-terminus (Jeganathan et al., 2006). This paperclip conformation, however, seems relatively weak and probably transient. Interestingly, however, pseudo-phosphorylation at several pathological epitopes was found to induce a compaction of this paperclip conformation, associated with an increased rate of aggregation (Jeganathan et al., 2008). This suggests that hyperphosphorylation of Tau may induce a more stable secondary structure, that in turn makes the protein more prone to aggregate. Indeed, this compact conformation showed reactivity for conformational epitopes that are found at early stages of AD pathology (Jeganathan et al., 2008) and usually observed in Tau aggregates (Maeda et al., 2007).

Conformation changes may trigger Tau aggregation by rendering the MBDs more exposed. Indeed, it is now well known that the core of PHFs is composed of the repeated domains, the other parts of the protein forming a “fuzzy coat” around the filament axis (Wischik et al., 1988). In addition, two hexapeptides lying in this MT-binding region (i.e. PHF6 and PHF6*) have a strong tendency to form β structure, this being necessary for Tau aggregation (Bergen et al., 2000). Indeed, point mutations with known pro-aggregation properties (i.e. P301L and ΔK280) are associated with changes of local structure of those hexapeptides, leading to increased tendency to form β structure (von Bergen et al., 2001). Those results and the fact that cross-β structure is a known characteristic of PHFs (Berriman et al., 2003) suggest that the MBD region of Tau may play an important role in the process of aggregation. A change in conformation may thus affect the availability of those domains for interaction which subsequently may drive aggregation.

Sequence of Tau aggregation into PHFs

A strong body of evidence suggests that, from those initial conformational changes, Tau proteins are successively incorporated in aggregates of increasing size (**Figure 8**; Cowan and Mudher, 2013). This sequential process of aggregation starts with the assembly of Tau dimers and trimers (Sahara et al., 2007). Two types of dimers can be distinguished depending on whether they necessitate disulfide bounds to form (cysteine-dependent dimers) or arise from another unknown mechanism. Formation of both forms of dimers is dependent of the MBD region, and more specifically the PHF6 and PHF6* sequences (Bergen et al., 2000; Sahara et al., 2007). It was thus suggested that anti-parallel dimerization may occur by interaction of the MBD region (Patterson et al., 2011).

Dimers then give rise to higher-order oligomeric species (Patterson et al., 2011), cysteine-dependent dimers being more prone to oligomerization and the formation of higher order aggregates (Sahara et al., 2007). Those large oligomers seem to be a prerequisite to the formation of fibrillary aggregates as they are found *in vitro* before the apparition of fibrils (Sahara et al., 2007). In addition, immunostaining for Tau oligomers can be observed mostly in neurons presenting early Tau pathology and not in mature NFTs, suggesting that oligomerization precedes tangle formation (Patterson et al., 2011). Granular Tau oligomers (GTOs) were also observed in brain regions devoid of mature NFTs (Maeda et al., 2006) and, *in vitro*, before fibril formation, those GTOs being able to form in turn fibrils (Maeda et al., 2007). Taken together, those results suggest that oligomers may represent an intermediate between dimers and PHFs.

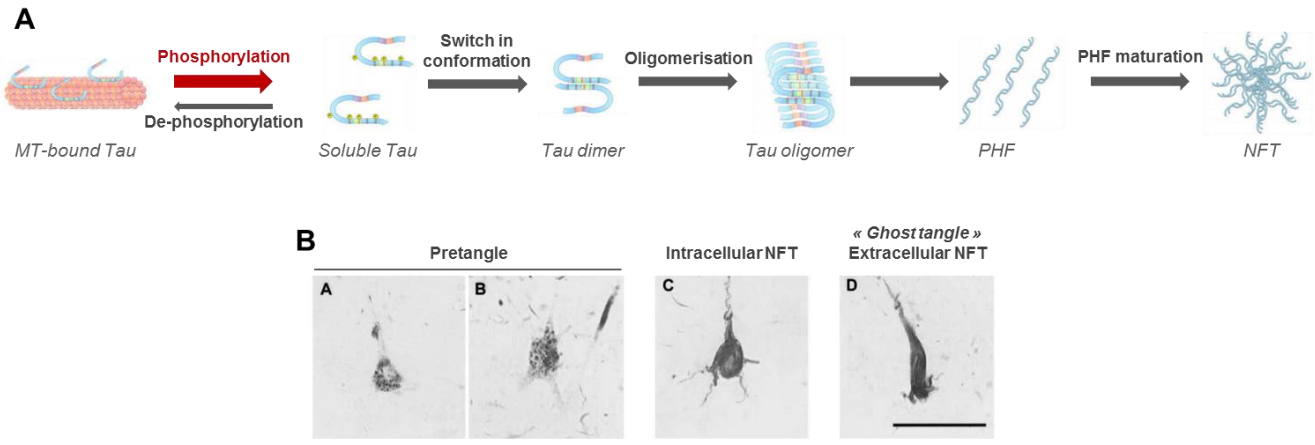

Figure 8: Sequence of Tau aggregation

A) After release from the MT, Tau protein starts to aggregate. An initial change in its conformation induces dimerization followed by the formation of oligomeric species. Large Tau oligomers then rearrange into PHFs that, when accumulating, lead to the apparition of NFTs. B) Maturation of PHFs into NFTs also follows a specific sequence starting with granular perinuclear and cytoplasmic inclusions in the pre-tangle stage. Then, during the intracellular NFT stage, large fibrillary aggregates accumulate in the soma. This is often associated with a displacement of the nucleus. Lastly, the extracellular NFT can be considered as the remains of a neuron that have died from PHF accumulation. It is characterized by the extracellular accumulation of fibrils in the form of a neuron in absence of a membrane or nucleus.

In a recent *in vitro* study, the kinetics of Tau aggregation was assessed and the effect of pro-aggregation point mutations (i.e. P301L and ΔK280) on the rate of aggregation determined (Shammas et al., 2015). In this study, the formation of oligomers peaked relatively rapidly (within 30min), while fibrils formation reached completion only after several hours. This suggests that, while the reaction of oligomerization is quite favourable, the process of fibril elongation may be quite long. This led to the suggestion that fibrils do not form directly from oligomers. Instead, oligomer may necessitate to undergo a shift in conformation before-hand, this conversion process rendering them competent for elongation. This could be associated with the observation that pre-tangle like structures, composed of hyperphosphorylated Tau, but not presenting Gallyas positivity, are present in subcortical nuclei from a very young age (Braak and Del Tredici, 2011). Nonetheless, experiments conducted in transgenic mice showed that NFTs can become positive for amyloid dyes, such as Thioflavin S, within 24h (de Calignon et al., 2010) , suggesting that this conversion process may occur fairly rapidly.

Maturation of Tau aggregates within neurons

It is now quite established that mature NFTs form from the accumulation of PHFs into the cell. Indeed, electron-microscopy studies showed that tangles in the brain of AD patients are composed of PHFs (Bancher et al., 1989). It was also shown *in vitro* that PHFs can rearrange over time to form clusters that present the same characteristics than AD brain-derived NFTs (Rankin et al., 2008). This follows a process of maturation (**Figure 8**) that can be observed using different antibodies and colorations (Augustinack et al., 2002; Bancher et al., 1989; Braak et al., 1994; Galván et al., 2001). In the first stage, named pre-tangle, diffuse or granular Tau aggregates are found around the nucleus and in the cytoplasm. Those are usually not positive for amyloid stains but are reactive for several phospho-epitopes. Then, in the intracellular NFT stage (iNFT), large fibrillar argyrophilic inclusions accumulate in the soma of neurons, to the point that nuclear displacement is often observed. During this stage, signs of neuritic deterioration can also be observed. The last stage of aggregation, named extracellular NFT

(eNFT) or “ghost tangle”, is characterized by extracellular fibrillar Tau deposits in the shape of neuronal cell bodies. In this stage, no nucleus can be observed and neurites often present morphological abnormalities, suggesting that the neuron has died. Interestingly, while this stage is highly positive for amyloid dyes (such as Thioflavin S staining and Gallyas silver impregnation), a loss of phospho-Tau immunoreactivity is often observed.

b) Tau post-translational modifications and their link to Tau aggregation

Tau hyperphosphorylation

Since the observation that Tau present in PHF preparations is abnormally phosphorylated (Grundke-Iqbal et al., 1986), it has been suggested that phosphorylation plays an important role in the process of aggregation. Indeed, with 85 putative sites, phosphorylation is the most prominent post-translational modification of Tau (**Figure 9**, Martin et al., 2011). Among those sites, many are phosphorylated in physiological conditions and become hyperphosphorylated during tauopathy, with phosphorylation also occurring at additional pathological sites. Hyperphosphorylation probably represents an early event in the pathological cascade as it can usually be observed in neuronal somas before the apparition of argyrophilic NFTs (Braak et al., 1994). One of the mechanisms by which it drives Tau aggregation is through the reduction of Tau-MT interaction. For example, pseudophosphorylation at Ser262 has been found to induce a change in the secondary structure of the first and second repeats in the MT-binding domain, associated with a strong reduction of Tau binding to MT (Fischer et al., 2009). Phosphorylation of Tau on Thr231 has also been described to induce a reduction of Tau binding to the microtubule (Cho and Johnson, 2003, 2004). This may increase the concentration of soluble unbound Tau that may in turn be more prone to aggregate.

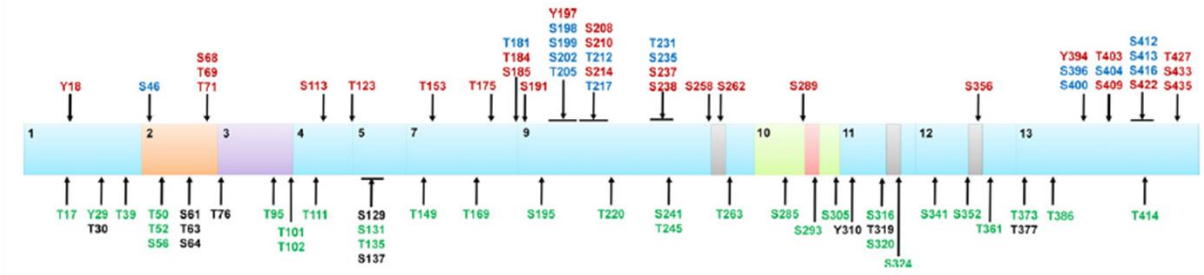

Martin (2011)

Figure 9: Different phosphorylation sites described on Tau protein
Some are found uniquely in physiological conditions (green), others are phosphorylated in AD brain (red). Hyperphosphorylation designates phosphorylation at those pathological sites and additional phosphorylation at physiological sites (blue).Putative phosphorylation sites that have not yet been observed are indicated in black.

Interestingly, however, phosphorylation at Ser262 that leads to the release of Tau from the MT also inhibits its aggregation (Schneider et al., 1999). The change in Tau conformation leading to detachment from the MT may in turn reduce the ability of the MBD to form intermolecular interactions (Fischer et al., 2009). Similarly, 9E18-phosphoTau KI mice, that present a reduction in MT-bound Tau proteins do not show any kind of Tau aggregate (Gilley et al., 2016), suggesting that hyperphosphorylation and liberation of Tau from the MT are not necessarily sufficient to induce aggregation. Further processes may thus be necessary to promote polymerization of Tau. This could include other post-translational modifications as well as further phosphorylation at additional sites. Indeed, several pathological phosphorylation sites were found to have no effect on MT binding (Cho and Johnson, 2003), or have even opposite effects (Liu et al., 2007), suggesting that those may act elsewhere in the pathological cascade leading to Tau aggregation.

Effect of phosphorylation on Tau aggregation

The presence of some epitopes associated mainly with pre-tangles indeed suggests that some phosphorylation sites may trigger association (Augustinack et al., 2002). This suggests that those epitopes may appear after detachment of Tau from the MT and may be implicated in the aggregation process, by promoting polymerization of Tau. More precisely, it is possible that sequential phosphorylation of Tau may occur concurrently to its sequential aggregation, driving successively processes of oligomerization and fibrillation. Indeed, some phospho-epitopes located in the MT-binding regions induce oligomerization of Tau but are not sufficient for fibril formation (Tepper et al., 2014). Conversely, oligomerization of Tau has been described to occur before phosphorylation at the AT8 epitope (Lasagna-Reeves et al., 2012a). Sequential phosphorylation at the AT8 (phospho-Ser202/Thr205) and AT100 (phospho-Thr212/Ser214) epitopes has been found to modify Tau conformation rendering the protein more prone to aggregate without affecting its ability to bind MT (Jeganathan et al., 2008). This suggests that additional conformational changes of Tau proteins may convert oligomers into a form prone to fibrillation. Lastly, phosphorylation at several pathological sites has been shown to be able to induce the clustering of preformed fibrils into NFT-like structures (Rankin et al., 2008). Polymerization can thus occur before phosphorylation and some specific phosphorylation sites may be involved in the formation of NFTs from PHFs. The localisation of phosphorylation sites on Tau protein may be determinant on its effect on aggregation. Indeed, while phosphorylation at the KXGS motif in the MBD does not have obvious effect on Tau aggregation (Khlistunova et al., 2006) phosphorylation of the C-terminal region strongly is a strong enhancer of Tau aggregation (Liu et al., 2007).

Effect of truncation on Tau aggregation

Among Tau post-translational modifications, the second most studied is truncation. Tau is the substrate of many proteases including caspases, calpains and aminopeptidases (Chesser et al., 2013). The temporal relationship between aggregation and truncation, however, remains a matter of debate. For example, Tau fragments produced by endogenous cleavage at Glu391 were found to be enriched in PHFs (Novak et al., 1993). Generation of this fragment likely occurs through stepwise proteolysis of Tau. Cleavage of by caspase-3, -7 or-8 generates a fragment truncated at Asp421 (de Calignon et al., 2010; Gamblin et al., 2003) that is then further processed to produce the 151-391 fragments found in PHFs (Guillozet-Bongaarts et al., 2005). Caspase cleavage seems to be an early event in NFT formation process, although after the apparition of Alz50 reactivity, a marker of misfolded Tau (Guillozet-Bongaarts et al., 2005). This could suggest that cleavage occurs after fibril formation.

Strong body of evidence, however, suggest that this cleaved form of Tau plays an important role in the process of aggregation. Indeed, caspase cleaved Tau is found in the brain of AD patients, both pre-tangles and mature NFTs (Guo et al., 2004). In a transgenic mouse model, caspase activation was found to precede tangle formation, suggesting that caspase cleavage may occur before fibril formation (de Calignon et al., 2010). Moreover, transgene suppression reduced caspase activation suggesting that soluble Tau species are responsible for caspase activation, further implicating caspases as early effectors of Tau pathology. Indeed, overexpression of the 151-391 fragments in transgenic rats was found to be sufficient to induce Tau aggregation, the aggregation process following the classical pattern observed in AD patients (Zilka et al., 2006). Caspase cleaved Tau is also able to induce the aggregation of endogenous murine protein, suggesting that Tau fragments are able to nucleate aggregation (de Calignon et al., 2010).

The way Tau truncation may promote Tau aggregation may be through the removal of inhibitory activity from the C-terminal domain. Indeed, recombinant Tau fragments composed uniquely of the MT-binding region are more prone to aggregation *in vitro* than full-length Tau (Barghorn et al., 2000). Similarly, caspase-cleaved Tau was also found to polymerize more rapidly than full-length Tau (Gamblin et al., 2003). Altogether those results suggest that N-terminal and C-terminal regions of Tau may inhibit aggregation and that truncation may promote fibrillation by exposing the repeated domains.

Other post-translational modifications

Other post-translational modifications of Tau have been described, including nitration, polyamination, acetylation and glycosylation (Martin et al., 2011). Those may also play important roles at different steps of Tau aggregation. For example, reduced O-GlcNAcylation of Tau was described in low glucose condition as well as in the brain of AD patients (Liu et al., 2004). O-GlcNAcylation reduces Tau phosphorylation at several pathological epitopes and reduced O-GlcNAcylation observed in patients is associated with increased hyperphosphorylation of Tau (Liu et al., 2009). This implicates O-GlcNAcylation early in the pathological process.

Acetylation may also occur early in the process of Tau aggregation. Indeed, acetylation of Tau inhibits its ubiquitination and targeting to the proteasome, thus impairing its degradation and leading to its accumulation *in vitro* (Min et al., 2010). Increased acetylation was observed in pathological conditions in vitro and in the brain of AD patients, preceding hyperphosphorylation and NFT formation. Interestingly, the effect of acetylation on Tau function and aggregation may depend on the region of the protein that is targeted, much alike what is observed with phosphorylation. Indeed, acetylation of Tau at Lys174 prevents its degradation but has no effect on aggregation (Min et al., 2015). Conversely, acetylation of Lys280 inhibits Tau function and promotes aggregation (Cohen et al., 2011) while targeting of the KXGS motif in the MT-binding region instead impairs Tau aggregation (Cook et al., 2014). This suggests that those post-translational modifications may occur as a response to pathological conditions and that, in turn, an imbalance in the post-translational processing of Tau may act as a trigger or enhancer of Tau aggregation.

Interplay between post-translational modifications and relation to aggregation

The way all those post-translational modifications interact to promote Tau aggregation is however still poorly understood (**Figure 10**). The primary alteration may be reduction in O-GlcNAcylation of Tau, triggering hyerphosphorylation and subsequent release of Tau from the MT. Acetylation may also be involved in the increase in Tau phosphorylation. The sequence of events afterwards and, more specifically, the temporal relationship between phosphorylation, aggregation and truncation remains a matter of debate. In both human and mouse brain, the number of NFT-like structures presenting with phosphorylated Tau exceeds that of structures positive for truncated or misfolded Tau (Mondragón-Rodríguez et al., 2008), which was described as evidence that phosphorylation precedes conformation changes and cleavage. Conversely, phosphorylation of caspase-truncated Tau has also been described, promoting its aggregation (Cho and Johnson, 2004). In addition, Tau cleavage as also been found to induce hyperphosphorylation and promote aggregation (Zhang et al., 2014) and stepwise cleavage of Tau fragments was described as a prerequisite for Tau aggregation *in vitro* (Wang et al., 2007). Thus, those two post-translational modifications probably act in synergy to promote aggregation. Conversely, those may also represent respective compensatory mechanisms to halt the aggregation process. Indeed, phosphorylation at Ser422 for example was found to precede caspase-cleavage of Tau and inhibit

truncation in vitro (Guillozet-Bongaarts et al., 2006). Conversely, truncation may be arising from an attempt to degrade soluble hyperphosphorylated Tau (Chesser et al., 2013).

To conclude, Tau aggregation seems to be tightly regulated through different post-translational modification. Some of the could be related to an attempt of slowing down the process, which may in turn become deleterious and further potentiate Tau polymerization. Targeting only one of those post-translational modifications may not be sufficient to counteract Tau aggregation when the process has already been triggered. However, targeting the earliest dysregulations, such as O-GlcNAcylation or Acetylation, may prevent the machinery being started.

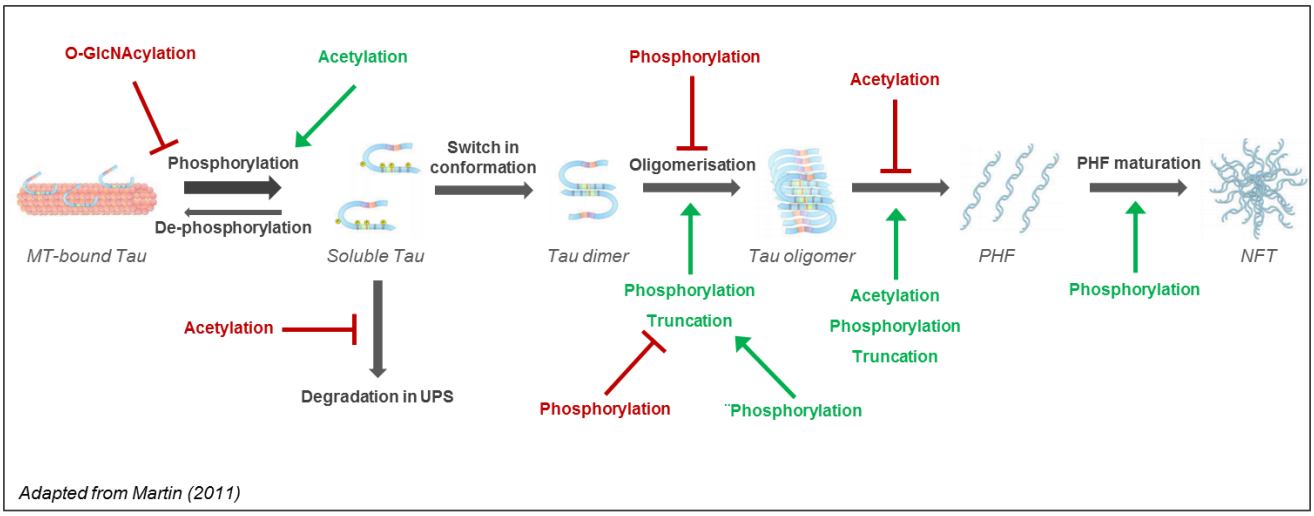

Figure 10: Interplay between post-translational modifications during Tau aggregation
The primary alteration may be reduction of O-GlcNAcylation that induces Tau hyperphosphorylation, leading to the detachment of Tau from the MT. Further phosphorylation, truncation and other post-translational modifications may then occur concurrently or sequentially to promote Tau polymerization. In addition, those may be inter-dependant with a first modification inhibiting or, on the contrary, priming Tau for subsequent post-translational processing (e.g. effect of phosphorylation on truncation). Lastly, a given modification may present with opposite effects depending on its location on the protein. Potentiating effects are represented with green arrows, inhibiting effects with red line breaks.

c) Prion-like spreading of Tau pathology

Anatomical connectivity

Evidences for the prion-like spreading of Tau pathology arise from the observation that anatomically connected regions become sequentially involved in AD (Braak and Braak, 1991; Delacourte et al., 1999, **Figure 11**). Tau pathology starts in the locus coeruleus and progressively spreads to the transentorhinal, entorhinal and hippocampal regions before reaching all neocortical regions starting with the temporal cortex (Braak and Del Tredici, 2011; Braak et al., 2011). Thus, the progression of Tau pathology from the locus coeruleus to other brain regions follows the known pattern of connectivity of this structure, which is consistent with the idea that Tau pathology spreads through anatomical connections. Indeed, neurons from the locus coeruleus send dense projections to the transentorhinal region. Then, the progression of Tau pathology in the parahippocampal-hippocampal circuit is first observed in the entorhinal subfields that directly project to the hippocampus (HC) and later in the regions from which outputs of the HC leave (Hyman et al., 1984; Lace et al., 2009). Lastly, all cortical regions that are progressively affected in AD are reciprocally connected, the pattern of Tau pathology being consistent with the distribution of those connections in cortical layers (Braak and Tredici, 2011, 2015).

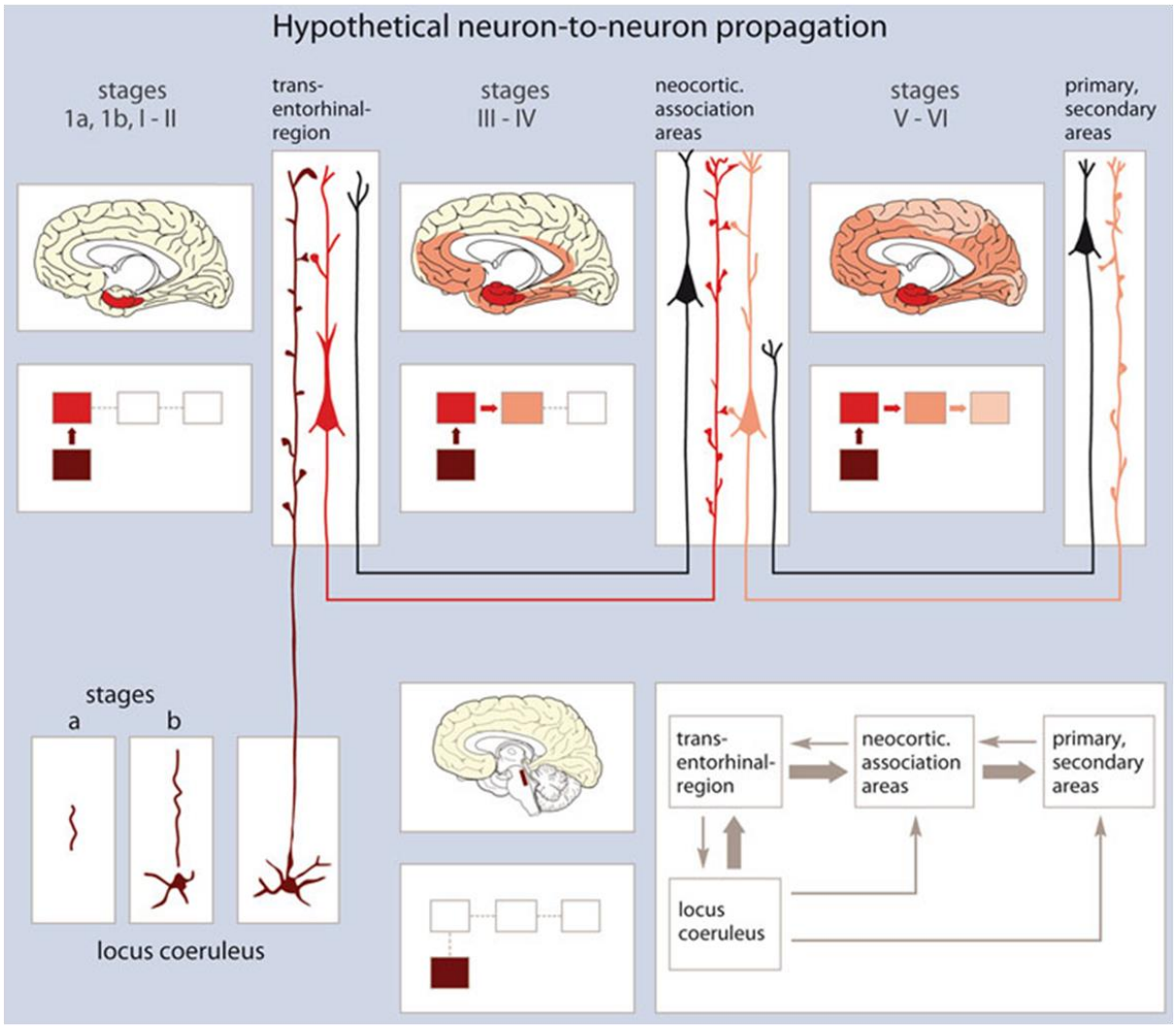

Braak and Del Tredici, (2011b)

Figure 11: Staging of AD Tau pathology and its relation to the hypothesis of trans-synaptic spreading
Subcortical stages (stages a-c) are characterized by the aggregation of Tau in the locus coeruleus and other subcortical nuclei. Neurons from the locus coeruleus send dense projections to the transentorhinal region, where Tau pathology is found to progress, first as pre-tangles (stages 1a and 1b) then as argyrophilic NFTs (Braak stages I-II). Then, pathology spreads to the hippocampal region (Braak stages III-IV) and finally to the entire isocortex, starting with the temporal lobe (Braak stages V-VI). Interestingly, all cortical regions that are affected in the progression of AD pathology are tightly connected. The circuit of sensory-motor information starts in the primary sensory cortex and travels through the association cortex before reaching the temporal limbic system. This pathway is made of reciprocal connections with the exception that on the "return" pathway, connections are more diffuse, synaptic contact being made in all cortical layers with the exception of layer IV. Interestingly, layer IV of the cortex is usually devoid of Tau pathology in AD patients.

Data from animal models of tauopathies also confirms the idea of a trans-synaptic spreading of Tau pathology. Indeed, injection of either human brain extracts (Clavaguera et al., 2009) or recombinant Tau fibrils (Sanders et al., 2014) in the brain of transgenic mice leads to the induction of Tau pathology. This pathology shows a time-dependent pattern with the sequential propagation to neighboring regions (anatomically connected to the injection site or to each other). In addition, in a transgenic mouse model where human Tau expression is restricted to the entorhinal cortex Tau is first found to aggregate in neurons from the entorhinal cortex before progressing to the HC (de Calignon et al., 2012). Those aggregates appear in neurons where no transgene expression can be found, suggesting that

pathological Tau is able to travel through anatomical connections and enter downstream neurons where it induces the aggregation of endogenous Tau.

It was suggested that this prion-like trans-synaptic spreading of Tau pathology may be responsible for the diversity of phenotypes observed in tauopathies. Indeed, when injected to specific brain regions, preformed Tau fibrils are able to propagate to connected areas (Peeraer et al., 2015) and thus impair the function of an entire network, leading to different patterns of behavioural deficits (Stancu et al., 2015).

Mechanisms of Tau transfer along anatomical connections

The question that remains, however, is whether this spreading of Tau through anatomical connections is due to the passive release of Tau from degenerating neurons or if it involves an active transfer of pathological species. Although spreading may occur from both mechanisms, the observation of Tau oligomers both at pre-synaptic and post-synaptic terminals may argue for an active transport mechanism (Tai et al., 2014). Indeed, it was shown *in vitro* that Tau protein is able to travel from the soma and axon of a primary neuron to a secondary neuron (Dujardin et al., 2014b) and that this transfer is potentiated when the two populations are able to form synaptic contacts (Calafate et al., 2015). Neuronal activity also seems to promote Tau propagation (Calafate et al., 2015; Pooler et al., 2013). This suggests that synaptic contact plays an important role in the propagation of Tau pathology and that Tau may be released via synaptic vesicle (Pooler et al., 2013). It is highly probable however that this is not the sole mechanism by which Tau can be transferred between neurons (Wang and Mandelkow, 2016).

Indeed, several *in vitro* and *in vivo* studies showed that Tau can be found in ectosomes and exosomes in both physiological and pathological conditions. However, the amount of Tau released through exosomes is higher in tauopathy models compared to control animals (Polanco et al., 2016) and Tau present in exosomes is found mainly in a pathological truncated form (Dujardin et al., 2014a). This suggests that, while Tau is physiologically excreted through ectosomes, accumulation of pathological Tau may induce autophagy mechanisms associated with Tau cleavage and integration into multi-vesicular bodies (MVBs). Spill-over of those MVBs in the form of Tau-containing exosomes would then occur, allowing for the spreading of Tau pathology. After release into the extracellular space, aggregates could then enter the downstream neuron by active endocytosis (Frost et al., 2009), mediated by Tau binding to heparin sulfate proteoglycans (Holmes et al., 2013), where they are able to induce the aggregation of endogenous Tau by a seeding and spreading mechanism.

Lastly, it has recently been suggested that reactive microglial cells, present at the site of neuro-degeneration, may be involved in the spreading of Tau. Indeed, transgenic mice expressing human Tau in a microglial fractalkine receptor (CX3CR1) knockout background present microglial activation before spreading of Tau pathology (Maphis et al., 2015). This suggests that the progression of neuro-inflammation may be a trigger for the spreading of Tau pathology along connected regions.

Seeding and spreading mechanism

Evidence for a seeding and spreading mechanism comes from the finding that human Tau is able to nucleate the aggregation of endogenous murine Tau in a wide variety of models (Clavaguera et al., 2009, 2013; de Calignon et al., 2012). In these studies, ggregates are usually composed of a mixture of endogenous and exogenous Tau, suggesting that human Tau aggregates act as a seed to convert the endogenous protein into a pathological form (Frost et al., 2009). Indeed, those induced aggregates are found in a fibrillary form, much alike the ones that seeded aggregation, suggesting transmission of a conformation. Those aggregates are usually also seeding-competent, i.e. able to transfer between cells

and to further induce aggregation. The stability of Tau aggregation through multiple generations, observed both *in vitro* and *in vivo*, thus confirms that Tau pathology acts through a seeding and spreading mechanism (Calafate et al., 2015; Frost et al., 2009; Sanders et al., 2014).

What is less clear, however, is which species of Tau may be responsible for this seeding and spreading mechanism. It was shown in several studies that most Tau species were able to enter cells (Michel et al., 2013; Mirbaha et al., 2015), although Tau aggregates are more readily taken up by cells in culture compared to monomeric Tau (Frost et al., 2009). However, only aggregated Tau could seed further aggregation (Falcon et al., 2015).

As for the step of aggregation necessary for Tau seeding, insoluble Tau aggregates seemed able to induce further aggregation (Clavaguera et al., 2009; Peeraer et al., 2015), but Tau oligomers seemed to be the most seeding-competent when injected into the brain of wild-type mice (Lasagna-Reeves et al., 2012b). Interestingly, transferred Tau species are mainly in a dephosphorylated state (Dujardin et al., 2014b; Pooler et al., 2013). Indeed, while Tau pathology in mice models is associated with strong phosphorylation of the protein at a number of pathological epitopes, the pattern of phosphorylation of exosomal Tau is different, with several epitopes being absent (Polanco et al., 2016). This suggests that seeding-competent and toxic Tau species may not necessarily be the same.

Inhibition of aggregation has been a main focus of study for the development of Tau-directed therapies in order to prevent tau-induced neurodegeneration. Indeed, several stages of this complex sequence of aggregation can either be targeted directly or through the modulation of post-translational modifications known to influence this process of aggregation. In addition, preventing Tau propagation may also represent a viable therapeutic approach.

However, several considerations have to be taken into account for an efficient therapeutic strategy using aggregation inhibitors. First, factors that influence Tau aggregation may act concurrently as enhancers and inhibitors of polymerization (e.g. acetylation, Cohen et al., 2011; Cook et al., 2014) probably depending on the stage of aggregation at which they intervene. Secondly, the finding that transferred Tau species present different post-translational processing than that present in cells (Polanco et al., 2016) suggest that seeding-competent and toxic Tau species may not necessarily be the same. It is also possible that in some additional factors may intervene to potentiate Tau aggregation, such as it has been suggested for Aβ (Osinde et al., 2008). In other words, little is known to date of the link between Tau aggregation and its toxicity. This matter will be addressed in following sections of this introduction, with a particular focus on which stage of Tau aggregation may represent the toxic species.

3) Which forms of Tau are toxic?

a) Classic view of NFTs as being toxic

Since the discovery that the spatial progression of Tau pathology is associated with increased severity of AD dementia (Braak and Braak, 1991), it has been suggested that NFT formation played an active role in neurodegeneration. Indeed, several studies have found a strong correlation between NFT number and neuronal loss as well as clinical score, suggesting that NFT-dependent neurodegeneration plays an important role in the cognitive decline found in demented patients (Dickson et al., 1995; Giannakopoulos et al., 2003). This is supported by the finding that reducing NFT formation correlates with a diminution of neurodegeneration (Noble et al., 2005). NFT-bearing neurons also present a strong decrease in several pre- and post-synaptic markers when compared to neighboring neurons, implying that synaptic transmission is impaired due to tangle formation (Callahan et al., 1999; Ginsberg et al., 2000).

b) Evidence against toxicity of NFTs

This classic view of NFTs as being the main species of Tau-induced toxicity is however now strongly questioned. Indeed, spatial dissociation between NFT formation and neurodegeneration was observed in the brain of AD patients (Vogt et al., 1998) as well as transgenic mouse models (Spires et al., 2006). In addition, not all atrophied neurons found in a given region of AD cases and transgenic mouse models present hyperphosphorylated Tau inclusions while Tau accumulation can be found in morphologically normal neurons (Andorfer et al., 2005; van de Nes et al., 2008; Rocher et al., 2010). In addition, although NFT number correlates with neurodegeneration, it has been shown that the amount of neuronal loss strongly exceeds the number of tangle-bearing neurons (Gómez-Isla et al., 1997; Vogt et al., 1998), suggesting that most neurons die from another mechanism. Thus, NFTs formation does not seem necessary nor sufficient for neuronal loss to occur. On the contrary, neurons seem to be able to live for decades after Tau started to aggregate in the soma (Morsch et al., 1999).

Recent evidence suggests that tangle-formation may actually be protective for the cell. In a transgenic mouse model exhibiting impairments in synaptic plasticity, both NFT-positive and NFT-negative neurons were able of synaptic potentiation, although to a lesser extent than observed in wild-type mice. Interestingly, tangle-bearing neurons seemed more able to react to environmental enrichment, suggesting not only that they were fully integrated in neural networks, but seemed more functional than those containing only soluble Tau (Fox et al., 2011).

In addition caspase activation, an indicator of apoptosis, is found to appear in neurons prior to tangle formation (de Calignon et al., 2010; Spires-Jones et al., 2008). All caspase-positive tangle-bearing neurons, however, displayed an intact nucleus, suggesting that those were not undertaking neurodegeneration. This process of caspase activation was triggered by soluble Tau species, as transgene suppression abolished caspase activation, and lead to Tau aggregation. Taken together, those results suggest that tangle formation arises from initial activation of apoptosis mediated by soluble Tau species and that Tau aggregation into PHFs allows neurons to escape acute neurodegeneration.

c) Soluble species are responsible for Tau-induced neurotoxicity

It was then suggested that soluble Tau species may be responsible for toxicity. Indeed, only soluble hyperphosphorylated Tau, but not PHF-Tau, is able to sequester the normal protein, leading to an inhibition of MT assembly (Alonso et al., 2006). In a model using AAV-mediated gene transfer of mutant Tau, strong neuronal loss was observed in the hippocampus in absence of large Tau aggregates or

ghost tangles (Jaworski et al., 2009). Reduction in synaptophysin transcript can also be observed in NFT-free neurons of AD patients compared to control subjects, suggesting that pathogenic mechanisms may be in place in those patients that could simultaneously induce synaptic defects and Tau aggregation into PHFs (Callahan et al., 1999).

Further evidence for the involvement of toxic soluble species of Tau comes from the study of inducible mouse models. Indeed, in the rTg4510 model, Tau transgene suppression is able to halt neurodegeneration, rescues impairment in synaptic plasticity (Fox et al., 2011), and leads to behavioural recovery while NFTs continue to form (SantaCruz et al., 2005). Interestingly, long transgene suppression led to an increase in NFT formation suggesting that tangles may represent a less harmful stable form, used by the cell to trap toxic soluble species. In a more recent study, although clearance of NFTs could be observed after long transgene suppression, shorter treatment were already able to reduce neuronal loss and halt synaptic degeneration without inducing dissolution of NFTs (Polydoro et al., 2013).

Work from a different team, using mice conditionally expressing mutant pro-aggregation forms of Tau, yielded similar results. Cognitive performance and synaptic markers recovered after transgene suppression, while large Gallyas-positive aggregates remained up to 4 months following doxycycline treatment (Sydow et al., 2011a). Interestingly, however, the composition of those aggregates seemed highly dynamic, as they were found to contain uniquely murine Tau after transgene suppression (Sydow et al., 2011b). This could serve as evidence that NFTs do indeed serve as a trap of soluble toxic species.

d) The aggregation of Tau is necessary for toxicity

The question that remains however is which form of soluble Tau may be responsible for toxicity. Aggregation of Tau still seems necessary for its toxicity. Indeed, in a cell model expressing either wild-type, pro-aggregation ΔK280 or anti-aggregation Tau fragments, toxicity was observed mostly in the condition where Tau was able to aggregate, i.e. in the pro-aggregation condition where Thioflavin S-positive Tau fibrils were observed (Khlistunova et al., 2006; Wang et al., 2007). Interestingly, toxicity was observed long before the apparition of PHFs, suggesting that lower order aggregates are the major contributors of Tau-induced toxicity. Similar results were obtained when those fragments were expressed in mice (Mocanu et al., 2008). Similarly, conditional expression of full-length human Tau bearing the pro-aggregation ΔK280 mutation led to cognitive impairment and synaptic defects associated with Tau aggregation, although no end-stage NFT was observed (Van der Jeugd et al., 2012). This led to the identification of soluble oligomers as potential candidates for the species responsible of toxicity.

e) Toxicity of Tau oligomers

First evidence for the toxicity of Tau oligomers came from anatomo-pathological studies in which Tau oligomers, composed of phosphorylated Tau, were observed in the brain of AD patients (Lasagna-Reeves et al., 2012a; Patterson et al., 2011). Tau oligomers were a component of most lesions (in pre-tangle neurons, in neurons bearing intracellular-NFT, threads, coiled bodies and neuritic plaques) but were interestingly mostly absent from ghost tangles. Those oligomers could be observed in the frontal cortex of AD patients, even at stages where NFTs are not already present in this region (Maeda et al., 2006). This suggests that Tau oligomers formation precedes the apparition of tangles, implicating them upstream in the pathological cascade. This is consistent with the recent finding that a non-causative MAPT mutation, that increases oligomer formation, is associated with increased risk of developing AD and PSP (Coppola et al., 2012).

Initial report of small multimeric Tau aggregates in rodent models was done in rTg4510 mice (Berger et al., 2007). In this study, authors were able to identify two multimers (respectively of 140 and 170 kDa) whose levels correlated tightly with cognitive performance of mice. Interestingly, 140kDa Tau was observed even before the apparition of cognitive deficits, suggesting that it had to accumulate before affecting neuronal function. This was supported by the finding that treatment with methylene blue, an inhibitor of Tau oligomerization, leads to the rescue of oligomer-mediated nucleic acid damage in mice subjected to hypothermia-stress (Violet et al., 2015). Following injection in wild-type mice, both recombinant and brain-derived Tau oligomers are the only species able to induce a large variety of cellular defects, including reduction of synaptic and mitochondrial markers, caspase activation and neuronal loss, leading to cognitive deficits (Lasagna-Reeves et al., 2011, 2012b)Those effects could be observed in another study prior to the apparition of tangles (Fá et al., 2016). This confirms that oligomers exert direct toxicity irrespective of the presence of NFTs. This was also observed *in vitro*. Indeed, when applied to cells, recombinant Tau producing the highest level of Tau oligomers is the one that induces most cell death and membrane leakage (Flach et al., 2012). In addition, the amount of membrane leakage was strongly correlated with the amount of oligomers, confirming that those represent the major toxic species. More specifically, Tau trimers were shown to exert particular toxicity when compared to monomers and dimers (Tian et al., 2013).

The case of granular Tau oligomers (GTOs)

GTOs are amorphous round-like aggregates composed of approximately 40 Tau proteins (Maeda et al., 2007). Those oligomers could be observed in the frontal cortex of AD patients, even at stages where NFTs are not already present in this region, suggesting that they represent an intermediary state of aggregation (Maeda et al., 2006). Few studies have been performed to unravel the contribution of GTOs to pathogenic mechanisms because of the many difficulties encountered when trying to isolate and visualize them. Indeed, although they are large insoluble aggregates of approximately 1800 kDa, they do not sediment in standard fractionation protocols (Maeda et al., 2007). In addition, their high resistance to several reducing conditions blocks them from entering standard SDS-PAGE gels and be detected (Cowan and Mudher, 2013). Two recent studies in *Drosophila*, however, identified GTOs as contributors of neuronal protection, potentially by trapping smaller toxic oligomers (Ali et al., 2012; Cowan et al., 2015). In the first study, chaperones were able to induce the aggregation of Tau soluble oligomers into larger aggregates reminiscent of human GTOs and this was associated with improvement of cognition and halted neurodegeneration (Ali et al., 2012). In the second study using GSK3-β inhibitors, the rescue of motor deficits and disrupted axonal transport was associated with the formation of GTO-like structures that presented morphological similarities compared to those observed in AD brain (Cowan et al., 2015).

f) Can the phenotypic variability observed in tauopathies be attributable to the formation of distinct prion-like strains?

It has been suggested that the diversity of phenotype observed in different tauopathies may be due to the nature of Tau aggregates. More specifically, one hypothesis is that Tau can be present in the form of several prion-like strains, characterized by specific conformations of the protein, each presenting various degrees of toxicity and inducing different phenotypes.

This is supported by several studies using animal models of tauopathies. Indeed, when brain homogenates from different tauopathies were injected into the brain of transgenic mice, they triggered the formation of Tau lesions that closely resembled those observed in human cases. More specifically, some gave rise mainly to neuronal Tau aggregation (AD and PART cases) while other also induced the formation of glial Tau aggregates in the form of tufted astrocytes (PSP cases) or astrocytic plaques (CBD

brain homogenates; Clavaguera et al., 2013). Tau pathology induced by those homogenates not only differed by the cell type but also by the reactivity of Tau aggregates to different pathological Tau epitopes, the stage of Tau aggregation, the pattern of spreading as well as the toxicity induced (Boluda et al., 2015). Those differences may be due to the very nature of Tau aggregates that may differ between tauopathies depending either on the involvement of specific isoforms, their conformation or both of those factors. Indeed, distinct strains of Tau aggregates can be produced *in vitro*, those presenting biochemical differences that lead to distinct phenotypes when inoculated into the brain of transgenic mice (Sanders et al., 2014).

Interestingly, very distinct patterns of Tau strains can be isolated from the brain of patients suffering from different tauopathies. This suggests that the specific association of different strains may represent a signature of each tauopathy and contribute to the specific phenotype observed in each disease (Sanders et al., 2014). For example, mutations in Tau gene may give rise to different prion-like strains that may explain phenotypic differences observed between sporadic and genetic tauopathies. Indeed, overexpression of mutant P301L Tau using lentiviral vectors is more toxic than overexpression of wild-type Tau (Caillierez et al., 2013). Those two constructs differ also in their spreading capacity, wild-type Tau spreading further than the mutant P301L protein (Dujardin et al., 2014b). Whether those differences are due to specific conformations of the protein, each having specific mechanisms of toxicity, or rely on the differential production of soluble versus highly aggregated Tau species remains to be studied. Interestingly, some tauopathies, such as AD, are associated with strains of fairly homogenous nature while others exhibit a high variability in the biochemical properties of Tau aggregates (Sanders et al., 2014). This is reminiscent of FTDP-17 cases where different mutations are associated with distinct phenotypes (Sergeant et al., 2005) and suggest that distinct prion-like strains may underlie Tau pathology even in a single disorder.

Although accumulating evidences point towards soluble oligomeric forms as the main contributors of Tau-induced toxicity, it remains that NFT formation may not be benign. The observation of "ghost-tangles" in the brain of patients (Bancher et al., 1989) suggests that somatic aggregation of Tau in the form of PHFs may still have adverse effects. Tangle-bearing neurons do indeed often present structural abnormalities (Andorfer et al., 2005). This suggested a novel model (Figure 12) in which soluble species would be responsible for acute toxicity. NFT formation would in this case represent a defence mechanism put in place by the cell to trap toxic soluble species. Accumulation of fibrillary material would then in turn have adverse effects, leading to slow neuronal death. In addition, recent data suggest that NFTs are not entirely inert but instead undergo fusion and fission events, and are in constant exchange with soluble aggregates (Guo et al., 2016). Long-term toxicity of those large species may thus be related to the continuous production of soluble toxic seeds.

The notion of prion-like strains has been recently developed in order to explain the phenotypical diversity observed in tauopathies. This theory suggests that differences in the conformation of Tau aggregates may underlie differences in the ability to trigger toxic mechanisms responsible for the specific phenotypes observed in tauopathies, notably the type of cell affected (Clavaguera et al., 2013; Sanders et al., 2014). Whether those differences may be due to different morphologies of Tau aggregates or are the consequence of a differential production of soluble versus insoluble species remains to be determined.

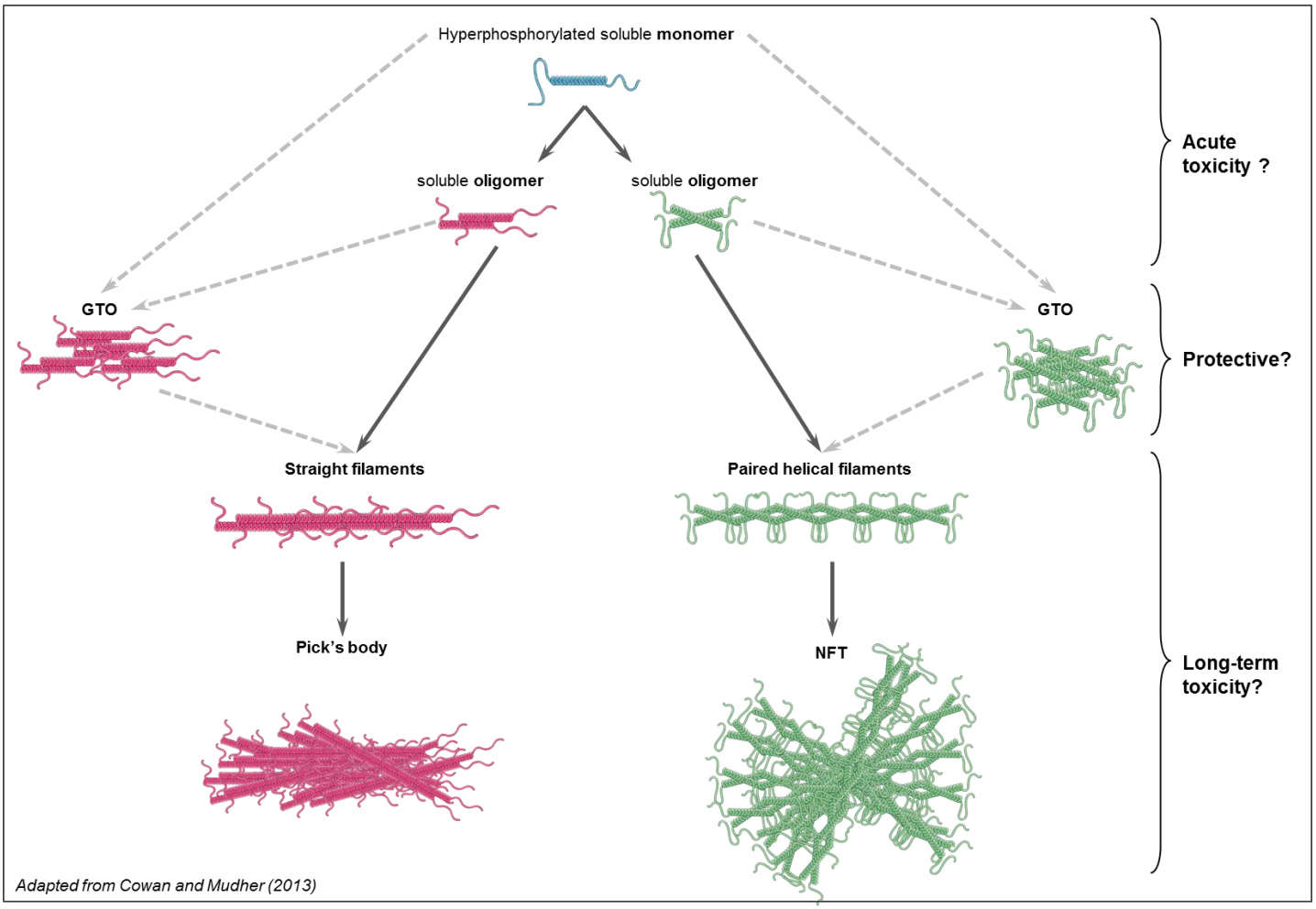

Figure 12: Model recapitulating the different potential toxic species of Tau in tauopathies

Small soluble species in the form of oligomers may be responsible for acute neuronal death. Formation of larger aggregates, such as GTOs or NFTs, may represent a defense mechanism put in place by the cell to trap those soluble toxic species. On the longer term, the accumulation of large insoluble aggregates may in turn affect neuronal integrity and lead to slow neurodegeneration. The differences in the morphology of Tau aggregates observed in tauopathies may be the consequence of specific pathological pathways leading to the formation of Tau conformers with different properties of toxicity. Another possibility is that tauopathies differ in the amount of oligomeric forms produced or in the ability of cells to convert those soluble toxic species into larger aggregates. The ability of different Tau proteins to aggregate to a certain stage may be governed by conformational and biochemical differences, which may be referred to as prion-like strains.

4) Mechanisms of Tau-induced toxicity in tauopathies

a) Toxic loss of function

It was suggested that one of the mechanisms by which Tau exerts its toxicity may be through a toxic loss of function. Although Tau depletion does not induce gross behavioural abnormality in rodents (Tucker et al., 2001), slight locomotor deficits (Ikegami et al., 2000) and memory impairments (Ahmed et al., 2014) were however observed in old Tau deficient mice. This suggests that, although compensatory mechanisms such as upregulation of other MT-associated proteins may limit the effect of Tau depletion, Tau deficiency may still be detrimental to neurons and, to a greater extent, to aging cells. This toxic loss of function probably involves reduced MT stabilization as hyperphosphorylated Tau shows impaired MT binding and polymerization (Fischer et al., 2009; Tepper et al., 2014). In addition, several mutations linked to FTDP-17 are associated with a reduction in Tau-MT interaction (Hong et al., 1998). Disruption of MT assembly would then lead to deficits in axonal transport as well as loss of neuronal structure and polarity which may, in the long run, cause neuronal death through deafferentation. Additional functions may also be affected by the trapping of Tau into aggregates. For example, heat stress was recently found to promote oligomerization of Tau and to prevent its translocation to the nucleus and binding to DNA. Thus, it impairs its protective function against oxidative nucleic acid damages (Violet et al., 2015).

b) Toxic gain of function

At the synapse

One of the earliest features of tauopathies is the relocalization of Tau from its initial axonal compartment to the soma and dendrites of neurons (Braak and Braak, 1991). Accumulation of aggregates in the somatodendritic compartment is thought to underlie Tau toxic gain of function. Indeed, synaptic impairment and degeneration are early pathological markers both in the brain of patients (Callahan et al., 1999; Ginsberg et al., 2000) and in a number of animal models (Eckermann et al., 2007; Polydoro et al., 2009; Schindowski et al., 2006).

The mechanisms of Tau-induced synaptotoxicity may be plural (Pooler et al., 2014). One of them is the impairment in kinesin transport of cargos along MTs. Indeed, one of the mechanism by which Tau regulates axonal transport is by inducing release of cargos from kinesin motor proteins, this function being mediated by a portion of its N-terminal domain (Kanaan et al., 2011). Under pathological conditions, there is an increase in the inhibitory action of Tau on anterograde transport. Associated to the relocalisation of Tau to the somatodendritic compartment, this will lead to an impairment of vesicular transport to the axonal terminal, preventing axons to receive the necessary supply in organelles such as mitochondria or synaptic vesicles (Reddy, 2011; Stamer et al., 2002). This impaired vesicular transport was also observed in dendrites. Indeed, increased Tau levels in synaptic terminals were shown to induce bundling of MT, leading to strong impairment in mitochondrial motility (Thies and Mandelkow, 2007). This was associated with a strong reduction of ATP supply leading ultimately to synaptic decay.

Tau may also lead to mitochondrial defects through additional direct toxic mechanisms. Indeed, overexpression of Tau *in vitro* was shown to affect mitochondrial function with reduced ATP production and increased susceptibility to oxidative stress (Schulz et al., 2012). Dysregulations of fission and fusion mechanisms were also observed leading to mitochondrial elongation and complex I defects (Li et al., 2016).

Synaptotoxicity of Tau was also observed to involve additional mechanisms. For example, hyperposphorylated Tau at the synapse was found to be associated in a transgenic mouse model with reduced expression and targeting to the membrane of NMDA and AMPA receptors (Hoover et al., 2010). Tau was also found to mediate the excitotoxicity of Aβ oligomers. Indeed, Aβ oligomers were found to induce accumulation of phosphorylated Tau at the synapse (Mairet-Coello et al., 2013; Zempel et al., 2010), leading to synaptic degeneration. This action of Tau may be associated to its involvement in targeting of fyn kinase to the synapse that increases NMDA/PSD95 coupling (Ittner et al., 2010). Lastly, extracellular Tau oligomers were also found to affect synaptic plasticity, inducing deficits in long-term potentiation (LTP) and memory impairment (Fá et al., 2016).

Most data to date implicate Tau oligomers as the main contributor of synaptic toxicity. Indeed, synaptic loss was observed both in mice expressing pro-aggregation ΔK280 that was rescued after transgene suppression (Eckermann et al., 2007; Van der Jeugd et al., 2012), suggesting that soluble Tau species instead of aggregates were responsible for synaptic decay. Consistently, electrophysiological changes in transgenic mice expressing P301L mutant Tau occur before the apparition of tangle-like lesions (Berger et al., 2007) and synaptic loss independently to NFT formation (Rocher et al., 2010). Lastly, reduction of Tau oligomers in mice overexpressing wild-type (WT) human Tau on a Tau KO background was found to rescue defects in NR2b trafficking (Ma et al., 2013). It remains that NFTs may on the longer term also have adverse effect by sequestering essential components (Wang and Mandelkow, 2016).

Impairment of proteasome & autophagy

Neurons must trigger degradation processes in order to counteract the progressive accumulation of toxic aggregates. To this respect, the finding that Tau in NFTs is ubiquitinated suggests that ubiquitin-proteasome system (UPS) may be activated in response to Tau aggregation (Perry et al., 1987). In addition, autophagy was also found to be involved in Tau degradation (Chesser et al., 2013). Accumulating evidence, however, suggest that both systems may be impaired in tauopathies hence contributing to Tau-mediated neurodegeneration. Indeed, the accumulation of Tau oligomers at the synapse in AD brain was found to be associated with a local increase in UPS components and ubiquitinated substrates, suggesting that the UPS at Tau-bearing synapses are unable to degrade substrates (Tai et al., 2012). This impairment of UPS activity seems mediated by direct interaction of oligomeric and fibrillary insoluble Tau aggregates with proteasome subunits (Myeku et al., 2016).

Similarly, impairment of the autophagy-lysosome pathway was also described in different studies. Indeed, accumulation of autophagic markers was found in the brain of patients suffering from different tauopathies (Piras et al., 2016). Those colocalized with phosphorylated Tau, suggesting that Tau aggregates may be responsible from those defects. Increase in lysosomal markers was also observed as diffuse cytoplasmic staining, which may be indicative of lysosomal membrane rupture. This would be consistent with another in vitro study that showed lysosomal membrane leakage induced by Tau aggregates (Wang et al., 2009). Lastly, knowing that both protein degradation pathways share common effectors, such as chaperone proteins p62 and Hsp70, it is possible that impairment in one of the pathways may trigger or potentiate defects in the other. Indeed, while proteasome inhibition has been found to promote autophagy, impairment in autophagic processes was found to induce dysfunctions in the UPS system, probably by causing accumulation of chaperones such as p62 (Chesser et al., 2013). Thus, there may be the setting of a vicious cycle where Tau aggregation induces impairment in degradation pathways thus leading to further Tau aggregation. Impaired UPS and autophagy would also induce accumulation of other non-degraded substrates or defective organelles, leading to neuronal distress.

c) Pathways implicated in Tau-induced neuronal death

The pathways involved in Tau-induced neurodegeneration have not yet been fully uncovered. Indeed, in transgenic mice, although caspase activation was found to precede the formation of NFTs, those tangle-bearing neurons were found to persist for days suggesting that they were able to escape acute apoptosis (Spires-Jones et al., 2011). Similarly, increased mitochondrial fusion, which was found in another model, is thought to represent a compensatory mechanism in order to make the cell more resistant to apoptosis (Li et al., 2016). This, however, led to synaptic defects suggesting that it may, in the longer term, be neurotoxic. Lastly, several mouse models showed Tau-associated neurodegeneration through the induction of cell-cycle markers (Andorfer et al., 2005; Jaworski et al., 2009), suggesting that cell-cycle re-entry may be part of a mechanism of Tau-induced neuronal death.

d) Implication of neuro-inflammation in the pathogenic events

In AD and other tauopathies, neuro-inflammation was found to accompany Tau pathology. Hence, activated astrocytes and microglial cells were observed surrounding tangles in AD brain (Sheng et al., 1997). Similarly, microglial activation was observed in PSP and CBD brain (Ishizawa and Dickson, 2001). In both cases, neuro-inflammation correlates with Tau pathology but whether it has a positive or deleterious effect, however, is still a matter of debate. Indeed, both astrocytes (Probst et al., 1982) and microglia (Cras et al., 1991) were found to infiltrate extracellular “ghost” tangles suggesting that they may be involved in the degradation of Tau aggregates. Conversely, strong microglial activation could be observed previous to tangle formation in the brain of transgenic mice (Yoshiyama et al., 2007). Interestingly, microgliosis occurred concurrently to synaptic loss and inhibition of neuro-inflammation in those mice ameliorated phenotype. Altogether, those results suggest that neuro-inflammation triggered by Tau pathology itself may act as a driver or potentiator of Tau-associated neurodegeneration (Zilka et al., 2012).

The mechanisms by which reactive glial cells may modulate Tau toxicity remain however poorly understood. One possible implication of microglial cells may be through the production of pro-inflammatory cytokines. Indeed, mutation in the microglial receptor Trem2 was recently found to be associated with increased risk of AD (Guerreiro et al., 2013). Studies in the peripheral system implicated Trem2 as a negative regulator of inflammatory cytokines. Thus, missense mutation in this gene may influence this function and promote AD pathology (Chung et al., 2015). Another potential implication of glial cells may be through their involvement in synaptic elimination. Indeed, clusterin (CLU), another recently identified risk variant for AD, implicates the complement cascade in AD neuropathology. This is consistent with finding that complement proteins colocalize with Tau pathology (Shen et al., 2001). Similarly, astrocytes were recently found to mediate synapse elimination during development and at adult age, mediated by the MEGF10 and MERTK pathways (Chung et al., 2013). This study showed also that synaptic pruning was dependent on neuronal activity and decreased with aging. One hypothesis would be that, in the aging brain, less effective synaptic elimination would lead to the maintenance of defective, long-lived, synapses that would then be more prone to defective activity and more sensitive to injury (Chung et al., 2015). Astrocytes also present with phagocytic activity in the context of neuronal injury and phagocytosis of degenerating neurons may prevent bystander cell death of neighbouring neurons (Lööv et al., 2012). Given that many tauopathies are associated with the formation of Tau lesions in astrocytes (Yoshida, 2006), one may wonder whether those arise from engulfment of Tau-positive neuronal debris or synapses. If this was proven to be the case, the questions that would next to be addressed is whether

the presence of those lesions underlie defects in elimination and what are the consequence of this accumulation of Tau on astrocytic function.

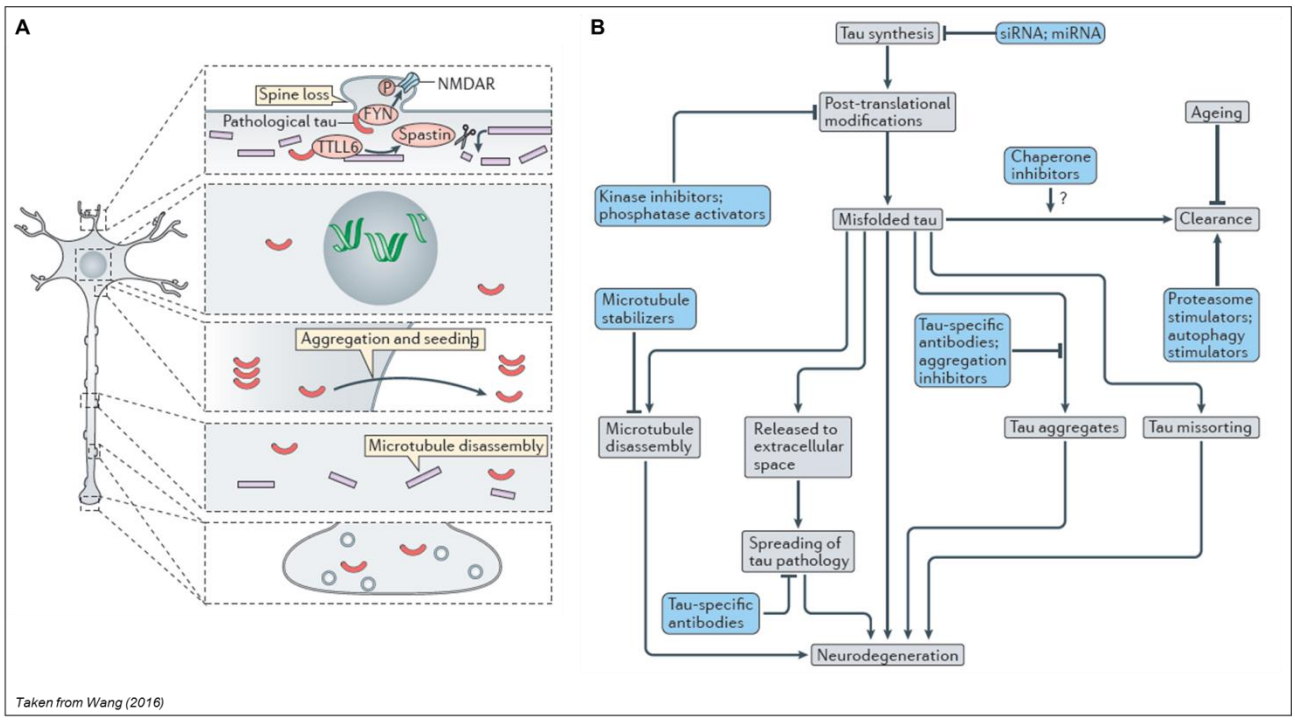

Figure 13: Mechanisms of Tau-induced toxicity and therapeutic targets
A) Tau may act through different pathological mechanisms, including MT disassembly due to toxic loss of function of hyperphosphorylated Tau, loss of nuclear protective function and synaptotoxicity including potentiation of Aβ-induced excitotoxicity. B) Disease-modifying therapies may target those different pathological pathways in addition to other targets, such as inhibition of Tau phosphorylation and aggregation as well as stimulation of Tau clearance.

Several pathways were suggested to be involved in Tau-induced toxicity (Figure 13), impairment of MT assembly and axonal transport, loss of nuclear protective effect, mitochondrial impairment and synaptotoxicity, each of those being a potential target of disease-modifying therapies. It remains to be determined, however, whether several of those processes occur in the same cell and, in that case, in which order they appear. This will be of crucial importance for efficient therapeutic intervention.

In addition, although similar processes were observed in models of sporadic and genetic tauopathies, such as neurodegeneration through cell-cycle re-entry (Andorfer et al., 2005; Jaworski et al., 2009), the finding that different Tau fragments are associated with either PSP or CBD (Arai et al., 2004), suggests that those may be implicated in the distinct pathological processes. Deciphering this issue will be necessary to determine if a same therapeutic approach can be applied to different tauopathies.

III – Rodent models of tauopathies

The aim of this section is not to give an exhaustive description of all existing animal models. Instead, the different approaches used to model tauopathy in rodents will be presented, along with their respective advantages and disadvantages with respect to the characteristics required for our study.

1) Transgenic rodent models

a) Transgenic mice

Tau knock-out (KO) mice

The toxicity of Tau in tauopathies is thought to act through both toxic gain of function of the pathogenic protein and toxic loss of function of normal, MT-bound, Tau. To test this later hypothesis, several models were developed in order to study the effect of deficiencies in Tau gene expression. Generation of a transgenic mouse lacking Tau protein (Tau KO) was indeed performed by inserting a transgene for green fluorescent protein (GFP) into exon 1 of Tau gene (Tucker et al., 2001), leading to the complete knocking-out of all 6 Tau isoforms. No gross behavioural or morphological abnormalities could be observed in this model. In another study, KO of MAPT gene did not lead to gross morphological abnormalities of the central nervous system (CNS), although those transgenic mice showed reduced MT stability and defects of MT organization in some small calibre axons (Harada et al., 1994). The authors interpreted the absence of gross detrimental effect of MAPT KO by the compensatory overexpression of other MT-associated proteins. This suggests that Tau loss of function may also be compensated in pathological conditions. Even in old mice (up to 21-22 months old) no gross memory deficit could be observed in either MAPT +/- or MAPT KO mice in several tasks, suggesting that Tau depletion does not affect memory even at a later age (Morris et al., 2013).

However, several studies did report behavioural and morphological effects associated with loss of Tau protein. Indeed, Tau KO mice have been found to exhibit deficits in motor coordination, hyperactivity and slight memory impairment (Ikegami et al., 2000). More recently, another study showed impaired memory in both contextual and cued fear conditioning in 6 months old Tau KO mice, associated with deficits in synaptic plasticity (Ahmed et al., 2014). Animals tested in this study did not present spatial memory impairment when tested in the Morris Water Maze. Tau depletion may thus induce subtle synaptic defects associated with the impairment of some but not all memory processes. Primary neurons from Tau KO mice exhibited deficits in axon elongation, suggesting that some deficits observed in KO mice may be related to developmental effects of Tau suppression (Dawson et al., 2001). Altogether, these results suggest that most of cognitive deficits observed in Tau KO mice may be related to the detrimental effect of Tau suppression during development. This does not rule out an effect of a toxic loss of function in the pathological processes associated with tauopathies but those may be partly compensated by over-expressing other MT-associated proteins. Toxic gain of function of aggregated Tau may thus also play a strong role in Tau-induced neurodegeneration.

Tau knock-in (KI) mice

Tau KI mice were developed by crossing transgenic mice overexpressing all 6 isoforms of the human wild-type Tau protein (Duff et al., 2000) with Tau KO transgenic (Tucker et al., 2001). This model, named hTau, displays somatic accumulation of hyperphosphorylated Tau from 3 month of age in the HC and neocortex (Andorfer et al., 2003). Abnormal conformation of the protein was observed from 9 months and extensive PHF1 positivity, a marker of tangle-like structures, from 12 months of age. Thioflavin S-positive

mature NFTs were observed from 15 months of age (Andorfer et al., 2005). Sarkosyl-insoluble Tau fibrils were extracted from those mice, accumulating from 2 months of age, bearing strong morphological similarity to those extracted from the brain of AD patients (Andorfer et al., 2003). Those mice reproduced the progression of Tau pathology observed in AD, this in absence of any Tau sur-expression or mutation of MAPT gene, thus successfully modelling an AD-like tauopathy. Significant neuronal loss was observed between 8 and 17 months of age, a significant number of degenerating neurons exhibiting signs of apoptosis (Andorfer et al., 2005). There was however no clear association between degeneration and accumulation of Tau fibrils, suggesting that most degenerating neurons did not die because of PHFs accumulation. Alternatively, clearance of Tau aggregates may have occurred after neurons had died. More recently, deficits in spatial memory and synaptic defects were described in this model at 12 months of age, thus preceding NFT formation (Polydoro et al., 2009). Altogether, results obtained on the hTau model confirm that expression of all 6 isoforms of wild-type human Tau is sufficient to induce the development of a tauopathy. Neurotoxicity of Tau was observed before and independently from the development of NFT-like lesions, confirming the important role of soluble pathogenic Tau species in Tau-related neurotoxicity.

Transgenic mice expressing mutant Tau protein

Aside from models described above, most of tauopathy models developed over the years had in common to rely on the overexpression of Tau mutants (**Figure 14**). Among them, many showed a development of Tau pathology in brainstem and spinal cord, in addition to cortical and limbic structures. This led in most cases to the apparition of strong locomotor impairment which interfered with cognitive testing, thus limiting the interest of those models for translational research. For example, in the JLNP3 model expressing mutant P301L Tau protein under control of the murine prion promotor (MoPrP), homozygote animals developed motor deficits from 4,5 months of age, consecutive to significant loss of motor neurons and associated to the development of neurofibrillary pathology in the spinal cord (Lewis et al., 2000). It was later assumed that the reason of this strong development of Tau pathology in spinal cord relied on the choice of promoter used to drive transgene expression. Indeed, those models had in common the use of either MoPrP (Lewis et al., 2000; Yoshiyama et al., 2007) or murine thy1 promoter (Allen et al., 2002; Terwel et al., 2005). Later, this drawback was overcome using a promoter more specific for forebrain regions, such as that of Calcium/calmodulin-dependent protein kinase II (CaMKII). In those later developed models, transgene expression was indeed found specifically in cortical and limbic regions, leading to the development of Tau pathology in structures relevant for the study of AD tauopathy (Tatebayashi et al., 2002).

When comparing the temporal relationship between phenotypic markers in these different models, it may seem difficult to draw a definite conclusion on the specific sequence of processes associating Tau aggregation to its toxicity. In most models, however, cognitive deficits and neuronal and synaptic impairment seem to occur before the apparition of argyrophylic tangle-like structures (Maurin et al., 2014; Oddo et al., 2003; Schindowski et al., 2006; Terwel et al., 2005) further implicating soluble species as toxic players in Tau-driven neurpathology. The differences observed between models in the age of onset may be related to the mutations used to induce Tau pathology. Indeed, those have been found to affect differently Tau function and aggregation. For example, the P301L mutation has pro-aggregation properties (Hong et al., 1998) which is consistent with the relatively early Tau aggregation observed in models overexpressing this mutant. Conversely, the R406W mutation is associated with a decreased affinity of Tau for the MT (Hutton et al., 1998) but may not have the same potentiating effect regarding its

aggregation. This is supported by the observation of a relatively late onset of Tau pathology in transgenic mice expressing this mutant (Tatebayashi et al., 2002).

Phenotypic differences between transgenic models expressing the same Tau mutant can also be observed (Lewis et al., 2000; Terwel et al., 2005). This is reminiscent of what found in human tauopathies where a single mutation can give rise to different clinical presentations (Bugiani et al., 1999). However, it may be difficult to directly compare phenotypes from different transgenic tauopathy models because of the variability arising from the location of transgene insertion. One striking example of this issue is the case of THY-Tau22 and THY-Tau30 transgenic models. Both models were generated concurrently by pronuclear injection of a cDNA containing G272V/P301S double mutant Tau driven by the murine thy1 promoter (Schindowski et al., 2006). Those two models however show strikingly different phenotypes caused by a variation in the location of transgene expression. Indeed, while THY-Tau22 mice showed Tau expression primarily in the forebrain, the transgene was also highly expressed in spinal cord in the case of THY-Tau30 mice. This led to strong locomotor impairment and significant muscular atrophy in THY-Tau30 (Leroy et al., 2007) that were not observed in THY-Tau22 model.

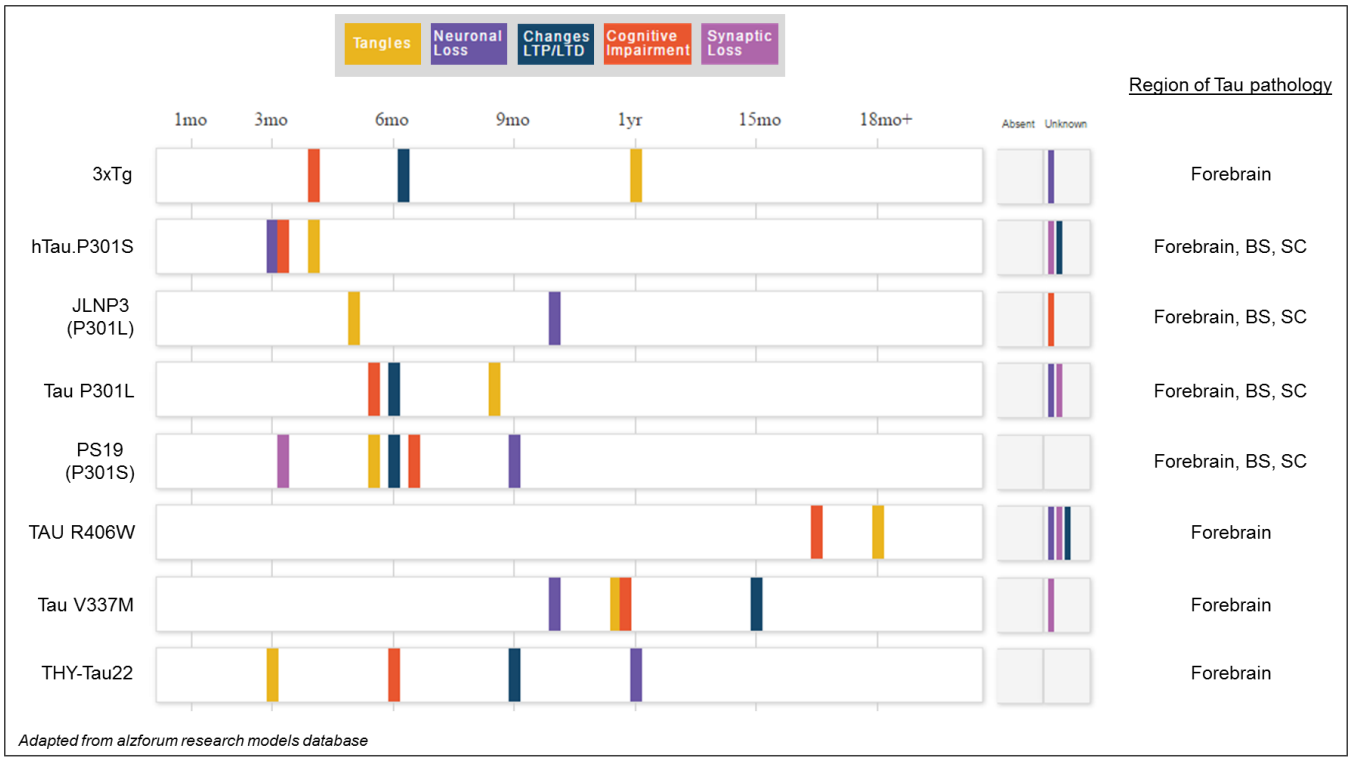

Figure 14: Comparative representation of the different phenotypes observed in transgenic mouse models
Time-course of the different phenotypic traits is presented for each model. Brain regions presenting Tau pathology are also indicated. BS, brainstem; SC, spinal cord.

Regulatable transgenic mice expressing mutant P301L Tau

To overcome the drawback of Tau expression in the spinal cord, an inducible model, named rTg4510, was developed using mutant P301L Tau controlled by the CamKII promoter, allowing transgene expression mainly in the forebrain, primarily in the HC and cortex (Ramsden et al., 2005). Tau abnormal conformation was observed at an early age, i.e. 2.5 months old, associated with Tau hyperphosphorylation, both increasing with age. Other pathological phospho-epitopes, markers of more mature tangle pathology, were then observed from 5 months of age, including AT8 and AT100. This

occurred before the apparition of extensive argyrophilic NFT-like pathology, first in the cortex. Significant neurodegeneration was also observed at 5 months and onward. Interestingly, memory impairment was observed as early as 2.5 months of age, thus before the occurrence of significant neuronal loss and the apparition of extensive NFT-like pathology, and worsened with age.

The possibility to control transgene expression in this model using doxycycline was used to study the reversibility of Tau pathology and Tau-induced neuropathological changes (SantaCruz et al., 2005). It was shown that short transgene suppression was able to halt Tau pathology, preventing the apparition of NFTs if administered before the development of argyrophilic lesions. Administered after the occurrence of NFTs, treatment was not able to inhibit further Tau aggregation. However, both treatments were able to stop neuronal death and restore cognitive function, despite a steady increase in NFT numbers and already significant neurodegeneration, representing a 50% loss of CA1 neurons. This suggests that neuronal dysfunction more than actual neurodegeneration is implicated in memory impairment. This also further supports the idea that expression of soluble toxic species, more than PHF accumulation, is responsible for Tau-induced toxicity. This is consistent with the finding that memory deficits in this rTg4510 model is inversely correlated with the amount of oligomeric species (Berger et al., 2007). Interestingly, long transgene suppression even increased the amount of NFT-like lesions, supporting the idea that Tau aggregation into NFTs may serve as a trap for soluble species.

More recently, a model named rTgEC was developed where the expression of the same transgene was restricted to the entorhinal cortex (de Calignon et al., 2012). Progressive accumulation of Tau aggregates was observed in the entorhinal cortex, leading to the formation of Gallyas-positive NFT-like lesions at 18 months of age. Propagation of Tau pathology was then observed at 24 months post-injection with the accumulation of hyperphosphorylated Tau in granular cells of the dentate gyrus, this appearing concurrently to the degeneration of cortical neurons. Transgene suppression in this model was found to reduce Tau pathology as well as its propagation to connected regions and prevent synaptic and neuronal loss (Polydoro et al., 2013). Interestingly, transgene suppression was also able to promote clearance of pre-existing NFT-like lesions suggesting that, even though those are highly insoluble, prolonged treatment can allow their clearance.

Regulatable transgenic mice expressing mutant ΔK280 Tau

Concurrently, Eva-Maria Mandelkow's team developed another inducible model using mutant ΔK280 human Tau (4R2N isoform; Eckermann et al., 2007). This mutation, found in a case of FTDP-17 (Rizzu et al., 1999), was found to exhibit strong pro-aggregation properties (Barghorn et al., 2000; von Bergen et al., 2001), thus rendering it suitable for the development of tauopathy models. Interestingly, in this model based on a tet-OFF system, doxycycline was administered during mating and 6 weeks after birth, thus avoiding any developmental effect of transgene expression. One key feature of this model is the relative low overexpression of human Tau, representing 3-fold the level of endogenous murine Tau. Although weakly overexpressed, transgene expression led to the aggregation of both human and murine Tau in the HC as early as 4 month of age. This was associated with missorting and abnormal conformation of both proteins as well as the apparition of many pathological phospho-epitopes. Only few Gallyas-positives NFT-like structures could be observed, however, and at a very late age (24 months old), this model thus representing more a pre-tangle pathology. This was associated with synaptic loss at 13 months of age, impairment of synaptic plasticity and memory deficits, but no obvious neuronal loss (Van der Jeugd et al., 2012). Interestingly, the same team developed another model based on the over-expression of the same mutant Tau isoform bearing in addition two proline substitutions (I277P/I308P)

that reduce the β-propensity of repeat-domains and thus have anti-aggregation properties. In this model, Tau pathology was also observed but to a lesser extent, with only weak phosphorylation of Tau protein, less somatic missorting and no conformational shift. This induced less synaptic defects while animals were cognitively spared. Altogether, those results led to the suggestion that Tau aggregation is a pre-requisite to its toxicity, leading to cognitive impairment.

Concurrently, the same team developed another model based on the overexpression of the same pro-aggregation and anti-aggregation mutants, this time using truncated Tau constructs containing only the 4 MT-binding repeated domains (Mocanu et al., 2008). Similar to what observed in the previous model, exogenous human pro-aggregation Tau was expressed at a low level (the human to mouse Tau ratio being around 0.75:1) but induced this time strong Tau pathology starting at 3 months of age. Tau aggregation was observed in the form of sarkosyl-insoluble Tau fibrils and Gallyas-positive NFT-like lesions. This was associated with both synaptic loss and neurodegeneration starting at 5 months of age. Impairment in synaptic plasticity and memory deficits were observed from 10 months of age (Sydow et al., 2011a, 2011b) which were related to morphological abnormalities of presynaptic terminals and reduction of Ca2+ influx (Decker et al., 2015). Interestingly, those effects were observed before the appearance of NFT-like lesions, suggesting that pre-tangle oligomeric species may be associated with those deficits. Again, mutant anti-aggregation produced much lower deficits in absence of Tau pathology but the fact that both mutant pro-aggregation models (expressing either full-length or truncated Tau) trigger similar deficits associated with different levels of Tau aggregation further support the idea of soluble oligomeric Tau species as being the key neurotoxic player.

In addition, much alike what was done with the rTg4510 model, those models were used to study the reversibility of Tau pathology and Tau-associated deficits. In all cases, doxycycline treatment was found to almost completely reduce aggregated human Tau while some aggregates composed purely of mouse Tau remained (Eckermann et al., 2007; Mocanu et al., 2008). In the case of truncated pro-aggregation mutant, however, mature Gallyas-positive NFTs persisted. Interestingly, transgene suppression was associated with the rescue of cognitive deficits and reversal of synaptic impairments (Sydow et al., 2011a; Van der Jeugd et al., 2012) even though aggregates of murine Tau were still present. Those results further suggested that it was the expression of aggregation-prone soluble species, rather than the formation of mature tangles, that caused Tau-induced neurotoxicity (**Figure 15**, Hochgräfe et al., 2013). The change in composition of Tau aggregates following transgene suppression thus point towards a role of large aggregates as an attractive pool trapping soluble toxic species. Indeed, following transgene suppression soluble mutant human Tau was probably slowly cleared while pathological murine Tau could seed further aggregation of the continuously produced endogenous protein. Those would then be integrated into new aggregates composed uniquely of murine Tau. Interestingly, this also suggests that those large aggregates are in constant exchange with the soluble pathological pool and that they are dynamic structures.

The maintenance of large aggregates in absence of transgene expression may be related to its slower degradation, this is in agreement with another study from the same team showing that aggregated Tau presented with a longer half-life than soluble Tau (Yamada et al., 2015). Interestingly, a recent study using those different models showed that preventive methylene-blue treatment, administered long before Tau aggregation was able to prevent the aggregation of mutant full-length Tau and reverse cognitive deficits (Hochgräfe et al., 2015), while short preventive and therapeutic treatments, occurring after the onset of Tau pathology had less effect. In the context of methylene-blue treatment aggregation is inhibited while transgene is still being expressed. New seeds can thus still be formed and interact with

already established large aggregates, which may explain why short preventive and therapeutic treatments are less effective. Those results point towards the necessity of diagnosing tauopathies before the onset of symptoms in order to administer treatments before extensive Tau pathology.

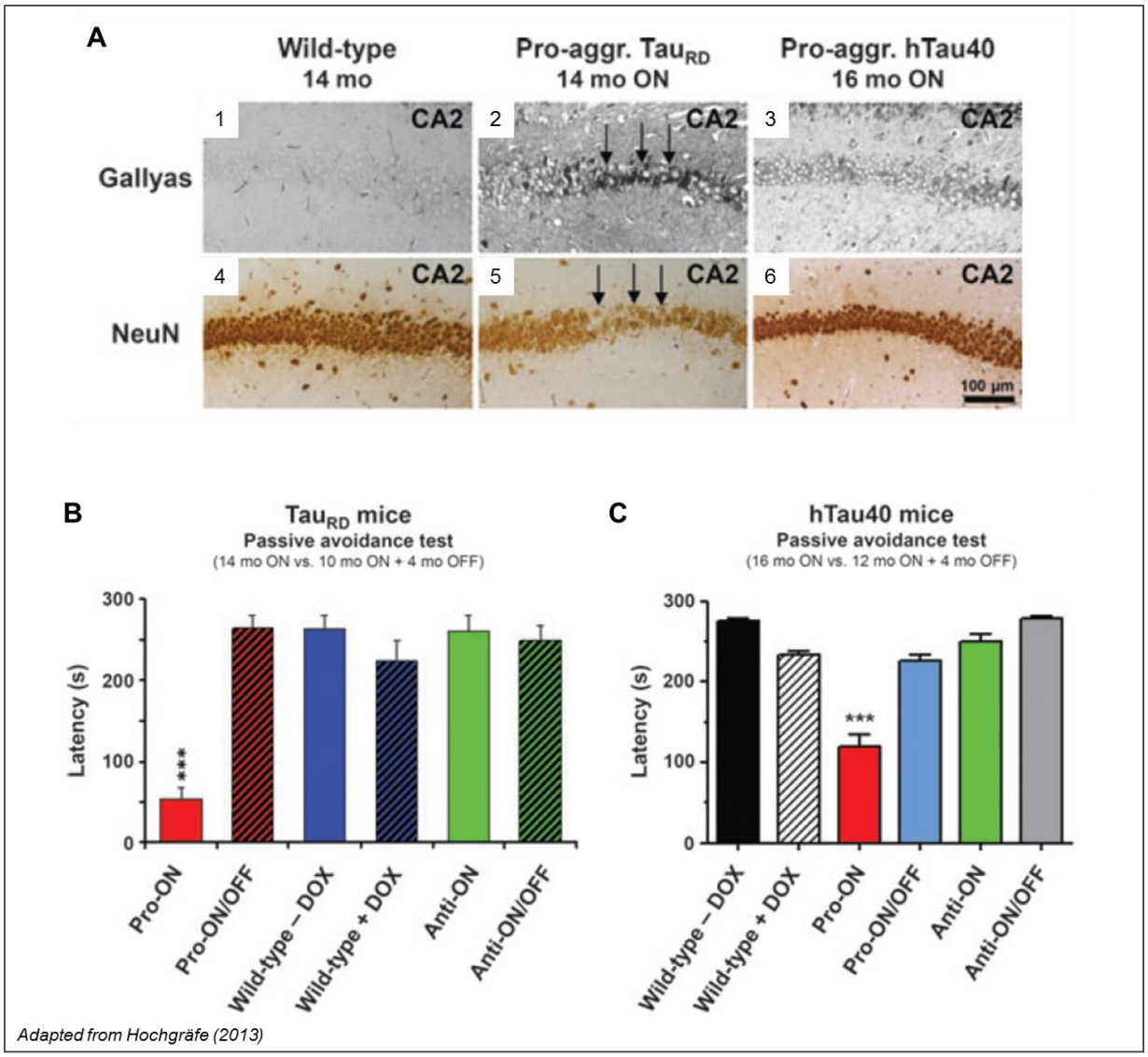

Figure 15: Cognitive deficits in mice expressing mutant ΔK280 are associated with the expression of aggregation-prone species rather than the formation of mature NFTs

A) Gallyas-positive NFT-like lesions were observed after 14 months of truncated ΔK280 mutant Tau expression while no tangle-like structure could be observed with ΔK280 mutant full-length Tau B) and C) Both models, however, displayed memory deficits observed in the passive avoidance test. hTau40 refers to full-length Tau bearing the same ΔK280 mutation in Tau (C) and presenting later onset than truncated Tau (B). In both cases, however, those deficits could be rescued after 4 months of transgene suppression. Pro-ON corresponds to the pro-aggregation group with continuous transgene expression, Pro-ON/OFF to the same group where transgene is expressed for 14 months and suppressed using doxycyline (DOX) for 4 monts. The same conditions are done on the anti-aggregation group that exhibit, in addition to ΔK280, two Pro substitutions inhibiting its aggregation.

b) Transgenic rats

Although significant insight into the pathogenesis of tauopathies was already obtained using transgenic mouse models, rats may be in some cases better suited for the modelization of neurodegenerative diseases. Indeed, in the context of tauopathies, adult rats present the advantage of expressing both 3R and 4R Tau isoforms (Hanes et al., 2009), similarly to humans, whereas expression in adult mice is mostly composed of 4R isoforms (Liu and Götz, 2013). This may render modelization of Tau aggregation in rats more relevant to that observed in human tauopathies. On a practical side, the large body size of rats allows the study of peripheral biomarkers (i.e. blood and CSF dosage) that are not readily accessible in mice (Do Carmo and Cuello, 2013). Similarly, their larger brain size makes possible the use of *in vivo* imaging techniques for the follow up of the pathology. The use of similar biomarkers in animal and human studies should permit a better translation of pre-clinical results to clinical developments.

Because of technical difficulties generally encountered in the development of transgenic rat models, there has been only few attempts to model Tau pathology in rats. Most of these attempts were made for the development of AD rat models and thus relied on the over-expression of mutant APP and PS1. In most cases, amyloidosis was observed with no or very mild development of Tau pathology (Do Carmo and Cuello, 2013). The only exception was that of a transgenic rat model developed by expressing mutant APP and preselin-1 on a Fischer 344 rat background (Cohen et al., 2013). In this model, the induction of an amyloidosis was accompanied by the development of a tauopathy, characterized by the accumulation of sarkosyl-insoluble fibrils from 6 months of age and the apparition of argyrophilic tangle-like structures at 16 months. In addition, significant cognitive impairment, in the form of hyperactivity and memory deficits, was observed from 6 months of age and worsened with time while significant hippocampal neuronal loss could be detected from 16 months, starting with the loss of 20% of neurons in the HC.

Transgenic rat models of pure tauopathy were even less described. In a recent study, expression of full-length mutant P301L Tau in the cortex and cerebellum was associated with an age-dependent increase of pathological phospho-epitopes (Korhonen et al., 2011). But no tangle, neuronal loss or cognitive deficit could be observed.

To date, the only successful attempt to develop a transgenic rat model of tauopathy was based on the observation that the core of PHFs is composed of Tau truncated at amino-acids 151-391 (Novak et al., 1993). It was thus suggested that those fragments may play an important role in neurodegenerative processes occurring during tauopathy. To study this question, the team of Michal Novak developed a transgenic model through the over-expression of the 151-391 truncated fragment from WT human 4R Tau isoform in a spontaneously hypertensive rat background (Zilka et al., 2006). Truncated Tau was found to be expressed primarily in the brain stem and spinal cord and led to the formation of numerous argyrophilic NFT-like structures composed of both human and murine Tau (**Figure 16**). Those developed through the known maturation process of NFT observed in humans, from AT8-positive pre-tangles to “ghost” tangles. The amount of Tau fibrils continuously increased from 3 months of age and negatively correlated with lifespan, confirming the toxic effect of truncated Tau. Tau pathology was also described to develop in the hippocampus of those rats (Hrnkova et al., 2007), starting at 4.5 months of age, and characterized by Tau hyperphosphorylation. Consistent with the location of transgene expression and the extent of Tau pathology, animals exhibited several cognitive alterations, including memory deficits from 4.5 months and impairment of locomotor abilities from 6 months of age. Later on, multi-test behavioural assessment showed general deficits in motor abilities in those rats starting at 3 months of age (Korenova

et al., 2009). Altogether, those results suggest that truncation in itself is able to promote Tau aggregation and trigger a tauopathy that is associated with cognitive deficits.

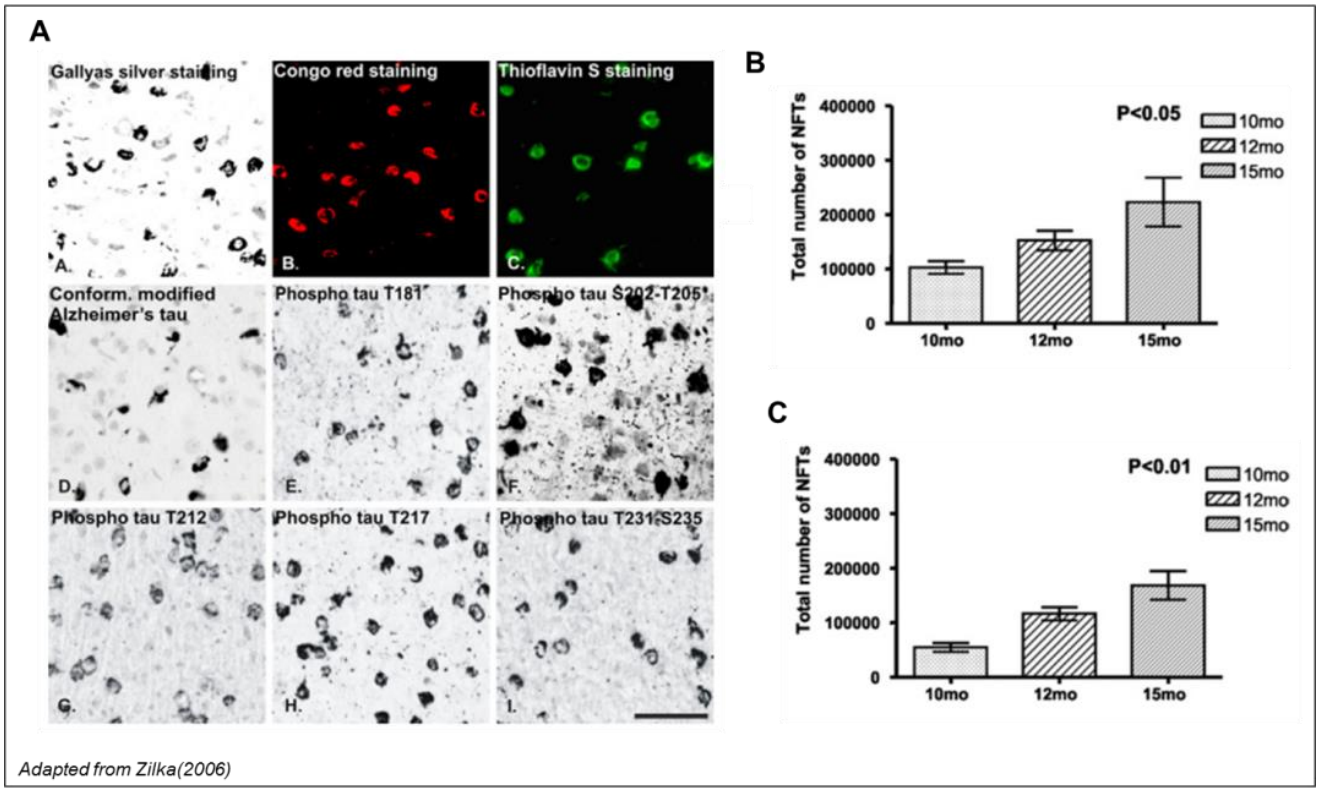

Figure 16: Extent of Tau pathology in transgenic rats expressing truncated 151-391 Tau
A) Tau aggregates in this model are positive for a number of pathological phospho-epitopes as well as several amyloid dyes (Gallyas, Congo Red and Thioflavin S) confirming their NFT-like nature. B) and C) stereological quantification of the number of NFT-like lesions on AT8 (B) and DC11 (C) staining showed and age-related increase in NFT number.

Later on, the comparison of two lines from this model presenting differences in the level of Tau expression was also performed (Koson et al., 2008). Interestingly, the effect of truncated Tau on lifespan was inversely correlated to the level of expression. The level of NFT load, however, was independent on the level of expression as similar Tau aggregation was observed in both lines. No obvious neuronal loss could be observed in those models but signs of axonal degeneration were described at 7 months of age, with axonal vacuolization and decreased myelin staining (Zilka et al., 2010). Interestingly, the amount of Tau fibrils was directly correlated to cognitive impairment with animals suffering from severe cognitive defects presenting 4 times more sarkosyl-insoluble Tau than mildly impaired animals. Longitudinal CSF sampling was also performed at mild and severe cognitive stages. Increase in CSF p-tau181 was observed along with worsening of cognition, and level of CSF Tau was found to correlate with the level of sarkosyl-insoluble Tau fibrils. Altogether, this suggest that CSF pTau levels may be a useful biomarker to follow disease progression, reflecting the accumulation of insoluble Tau aggregates in the brain and correlating with cognitive performance.

More recently, another line of rats was developed by the same team, allowing the expression of the 151-391 fragment this time bearing only 3 repeats (3R) in the MT-binding region (Filipcik et al., 2012). Much alike what was observed with the 4R fragment, transgene expression led to the development of extensive Tau pathology in the cortex, with the progressive formation of numerous argyrophilic NFT-like lesions up to 15 months old. Progressive accumulation of sarkosyl-insoluble Tau fibrils was also

observed with the progressive recruitment of endogenous Tau to aggregates, while no neuronal loss could be observed up to 15 months of age. This suggests that truncation of 3R or 4R isoforms may trigger similar pathological processes.

2) Models using gene transfer

a) General considerations

To date, there are only few studies that used viral vectors for the development of tauopathy models. Most of them had in common the study of specific questions that would have been difficult to address using other methods. Indeed, the main advantage of gene transfer is its versatility, allowing the direct comparison of several parameters in a given study. In addition, modelisation through gene-transfer allows the expression of pathogenic proteins in adult animals, thus avoiding developmental effects. This is of particular importance in the case of neurodegenerative diseases that usually occur at adult age. Below, will be presented the different models developed using gene transfer (**Table 1**) with a specific focus on their application for the study of a given question.

b) Gene transfer in mice

Initial studies using vector-mediated gene transfer of Tau in mice were performed in transgenic models of amyloidosis. Those were developed in order to study the impact of β-amyloid on the development of a tauopathy and its effect on neurodegeneration. Indeed, the amyloid cascade hypothesis posits Tau as a downstream effector of Aβ pathology (Hardy and Higgins, 1992) and knocking-out Tau has been found to reduce Aβ-induced toxicity (Roberson et al., 2007). The question that remained, however, was whether amyloidosis is able to trigger or worsen Tau pathology.

To answer this question, lentiviral vectors coding mutant P301S Tau were injected in the hippocampus of APP23 mice, a model of amyloidosis devoid of Tau pathology (Osinde et al., 2008). In both wild-type and transgenic mice hyperphosphorylated Tau was detected in the form of AT8-positive cell bodies. More pronounced hyperphosphorylation was observed in APP transgenic mice, which was associated with the development of argyrophilic NFT-like structures. This suggests that the pre-existence of an amyloidosis potentiated the development of a tauopathy. A similar study, using adeno-associated viruses (AAV) to express mutant P301L Tau in the hippocampus of APP751 transgenic mice, showed that the induction of a tauopathy in the context of an amyloidosis was associated with stronger neurodegeneration when compared to wild-type mice (Ubhi et al., 2009). This provided further evidence for Tau as the driver of neuronal loss and suggested that amyloidosis may potentiate directly or indirectly Tau aggregation. More recently, gene-transfer of human Tau in the entorhinal cortex of APP/PS1 mice was found to induce the hyperphosphorylation and aggregation of Tau associated with both neuronal loss and cognitive deficits (Dassie et al., 2013). This effect on neuronal integrity and behaviour was stronger with mutant proteins that tended to aggregate more, thus confirming that the neurotoxic effect of Tau depended on its propensity to aggregate.

However, the mechanisms of Tau-induced neurodegeneration may be plural and do not necessarily rely on the formation of large fibrillary aggregates (Andorfer et al., 2005). This was indeed the case in a model of pure tauopathy generated by injection of AAV vectors expressing either WT or mutant P301L Tau protein in the hippocampus of WT mice (Jaworski et al., 2009). Indeed, with both vectors, strong neurodegeneration was observed as early as 3 weeks post-injection, this occurring in absence of extensive Tau aggregation. Interestingly, this neurotoxic effect was dose-dependent, suggesting that the

level of soluble Tau species may be an important factor. In a second study from the same group, it was also suggested that the neurotoxicity of Tau constructs is associated with the induction of strong neuro-inflammation (Jaworski et al., 2011). Indeed, inflammation in this model was observed in close proximity of degenerating neuronal processes before the observation of neuronal loss, suggesting that glial cells may play a role in the process of neurodegeneration triggered by Tau pathology.

More recently, two other models of tauopathy were developed using AAV-mediated gene transfer, yielding quite different results. In the first study, injection in the entorhinal cortex led to the development of a tauopathy initially restricted to this region, characterized by hyperphosphorylated Tau followed by the formation of NFT-like lesions, associated with synaptic and neuronal degeneration (Siman et al., 2013). Human Tau protein then spread to granular cells of the dentate gyrus, although not in a pathological form. This propagation was later found to occur independently from the presence of endogenous murine Tau (Wegmann et al., 2015). In the latter study, intra-cerebroventricular injection of AAV vectors was performed in mouse pups, leading to widespread transgene expression of human Tau in both limbic and subcortical regions (Cook et al., 2015). Induction of a tauopathy was observed in those different regions, characterized by the hyperphosphorylation of Tau and the formation of argyrophilic lesions. This was associated with synaptic defects and memory impairment but in absence of neurodegeneration.

It is not well established what may be the reason for the discrepancy between the results of these different studies. The data suggest, however, that a key element of Tau-related neurotoxicity may be the kinetics of Tau aggregation. Indeed, acute neurodegeneration was observed in the model from Jaworski and colleagues after only 3 weeks of strong transgene expression (Jaworski et al., 2009). In the model where Tau expression was restricted to the entorhinal cortex, neuronal loss was observed before the formation of argyrophilic lesions (Siman et al., 2013). Those results thus confirmed those obtained using transgenic mouse models, suggesting that NFT formation may occur as a reaction to acute neurotoxicity.

c) Gene transfer in rats

Viral-vectors mediated gene transfer of Tau in the rat brain was used by two teams in the past years to model Tau pathology, interestingly with quite similar results .

The animal models developed by Klein and colleagues had in common the use of AAVs to overexpress either wild-type (WT) or mutant P301L human Tau under the control of the cytomegalovirus/chicken β-actin (CBA) promotor. Initial studies from this group involved injection of AAV-Tau into the substantia nigra pars compacta of adult Sprague-Dawley rats. Tauopathy was observed in these models as early as 3 weeks post-injection, characterized by hyperphophorylation of Tau, missorting to the dendro-somatic compartment and NFT-like pathology. This was associated with significant loss of TH-positive neurons and motor impairments (Klein et al., 2005). No significant difference in the extent of Tau pathology could be observed between WT and P301L mutant Tau constructs. Subsequent studies from the same group showed that toxicity of Tau on the neurons of the SNc was directly correlated to the level of Tau expression (Klein et al., 2008a) and that this toxicity was potentiated in old animals (Klein et al., 2010).

Interestingly, similar results were obtained when those vectors were injected in the entorhinal cortex (EC; Ramirez et al., 2011) or the hippocampus (HC; Mustroph et al., 2012). Indeed, overexpression of mutant P301L Tau in those regions led to the development of a tauopathy, with hyperphosphorylation and tangle-like pathology observed at 3 months post-injection. Behavioural impairment was observed in both studies although no obvious neuronal loss could be observed when vectors were injected in the EC. On the contrary to what was observed in the SNc, WT Tau overexpression in the HC did not lead to

significant neuronal loss or behavioural impairment (**Figure 17**), although Tau pathology was very similar to that induced by mutant P301L Tau (Dayton et al., 2012). This discrepancy in the toxicity of WT Tau may be explained by the absence in the vector of the woodchuck hepatitis virus posttranscriptional regulatory element (WPRE), a sequence known to promote transgene expression (Klein et al., 2002) and that was shown to enhance Tau pathology (Klein et al., 2004).

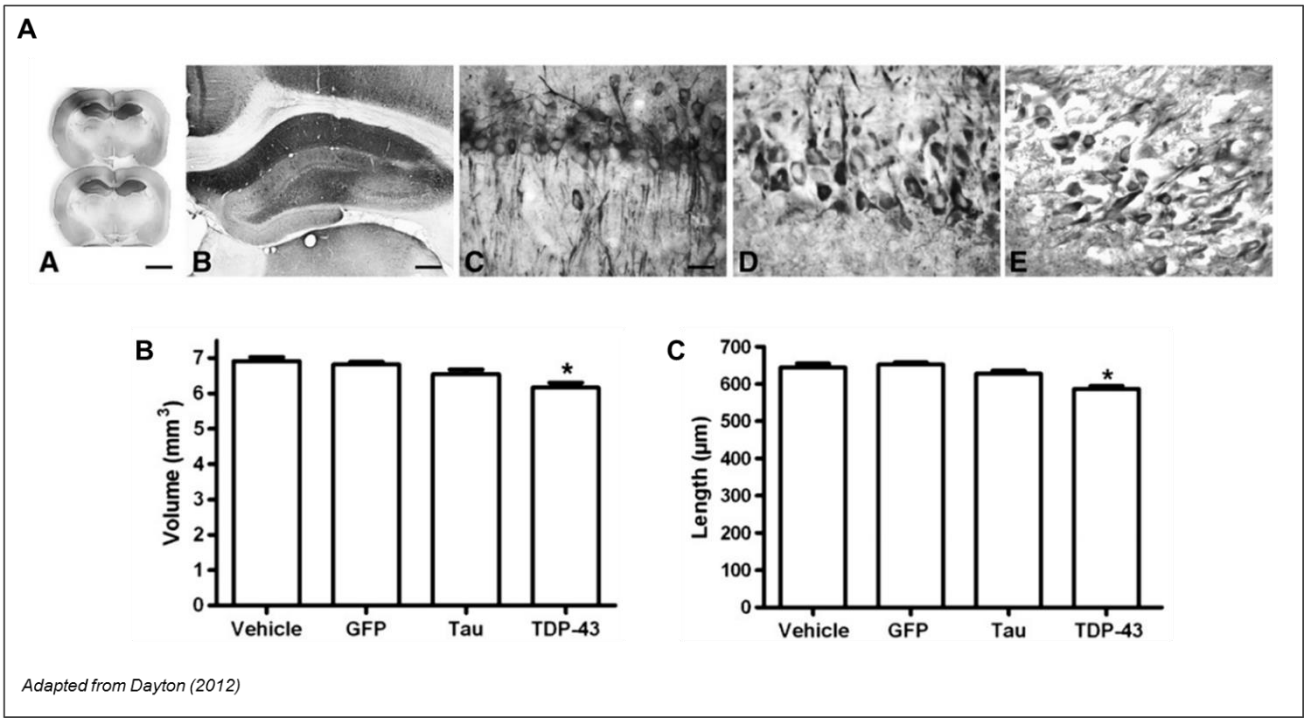

Figure 17: Tauopathy induced by AAV-mediated overexpression of wild-type Tau in rats HC do not lead to significant neuronal loss

A) Extent of Tau pathology: Human Tau (E1 antibody) was largely expressed in the dorsal HC (a) with extensive staining of neuronal processes (b). Hyperphosphorylation and missorting of Tau to the somato-dendritic compartment were observed using CP13 antibody(c, d). Staining with Ab39 antibody (e) showed the presence of mature NFTs. B) and C) Tau pathology in those animals was not associated with significant neuronal loss. No atrophy of the hippocampus (B) or reduction of the pyramidal layer (C).

Altogether, these different studies allowed a better understanding of the link between Tau pathology and cognitive symptoms. Indeed, they showed that the overexpression of Tau in different brain regions led to similar pathology, leading to behavioural impairment. This suggests that the differences observed in tauopathies may be associated to the location of Tau pathology and not necessarily to different processes. Similarly, the tauopathy induced by WT Tau bears strong resemblance to that induced by mutant P301L Tau, suggesting that sporadic and genetic tauopathies may occur through similar pathological processes. Those results may be taken with caution, however, because the fast development of pathology may hide differences that would have been unravelled with a slower time-course. Lastly, those studies confirmed that the level of Tau expression and aging may be factors modulating the extent of Tau pathology, consistent with clinical data. These conclusions were made possible by the fact that AAV-mediated gene transfer allows direct comparison of different studies, on the contrary to transgenic models where, for example, the location of transgene insertion strongly influences the phenotype obtained.

The model developed by the team of Luc Buée was conceived by lentivirus-mediated gene transfer of WT and mutant P301L Tau to the rat hippocampus (Caillierez et al., 2013). The use of lentiviruses allows a more spatially restricted expression of transgenes (de Backer et al., 2010), rendering this model more relevant to the study of spreading. In the initial description of this model (Caillierez et al., 2013), differences in the kinetics of Tau pathology could be observed between constructs. Indeed, overexpression of WT Tau led to strong hyperphosphorylation but only limited Tau aggregation up to 8 months post-injection. Conversely, Tau aggregates were observed following mutant P301L Tau expression, starting with neuritic aggregation at 4 months post-injection followed by tangle-like AT100-positive inclusions at 8 months post-injection. Interestingly, the apparition of tangle-like structures was concurrent with signs of neuronal distress (i.e. shrinkage of CA1/2 layer) and appeared more pronounced in rats expressing mutant Tau.

Along with this initial report of different phenotypes induced by WT and mutant Tau constructs, a later study from the same group showed that those constructs also differed in the extent of Tau spreading (Dujardin et al., 2014b). Indeed, WT Tau-expressing animals showed wider propagation of Tau protein to anatomically-connected regions compared to mutant P301L Tau-injected animals. This may be related to the differences previously observed in the extent of Tau aggregation and suggests that soluble species may be responsible for trans-synaptic Tau spreading. Again, this observation was made possible by the fact that gene transfer allows direct comparison of different constructs and by the spatially restricted transgene expression obtained with lentiviral vectors.

Table 1: Gene-transfer based rodent models of tauopathies

Gene-transfer based mouse models of tauopathy

Authors	Date	Genetic background	Vector	Injection site	Form of Tau	Behavioural test	Main results
Osinde, Clavaguera et al.	2008	WT mice APP23 tg mice	Lentivirus	HC	P301S (4R0N)	n.a.	Vector expression similar in both groups Increased pTau in APP mice, NFT uniquely in APP mice
Ubhi, Rockenstein et al.	2009	WT mice APP751 tg mice	AAV2	HC	P301L (4R1N)	n.a.	Tauopathy: Little pTau in WT mice, associated with small (n.s.) neuronal loss Tauopathy: High pTau level in APP mice, fbrillar somatic Tau by EM, associated with 50% loss in CA3 neurons
Jaworski, Dewachter et al	2009	WT mice	AAV1/2	HC	WT/P301L (4R2N)	n.a.	Dose and time-dependent neurodegeneration for both P301L and WT tau assoc with inflammation and microgliosis, NO NFT
Jaworski, Lechat et al.	2011	WT mice YFP and CX3CR1-GFP tg mice	AAV1/2	HC	P301L (4R2N)	n.a.	Axonal and dendritic degeneration, synaptic and neuronal loss Strong microgliosis and astrogliosis, permeability of the BBB and oxidative stress
Dassie, Andrews et al.	2013	WT mice APP/PS1 tg mice	AAV6	Entorhinal Cortex	WT/3PO (4R2N) P301S (4R0N)	Morris Water Maze	Tauopathy: pTau and Tau aggregates 3PO > P301S > WT Neuronal loss in 3PO>P301S>WT Tau in both EC and CA1, no effect on amyloid pathology. Memory impairment in the 3PO Tau group only
Siman, Lin et al.	2013	WT mice	AAV9	Entorhinal Cortex	P301l (4R2N)	n.a.	Tauopathy: pTau and NFT uniquely in the Entorhinal Cortex , spreading of human Tau (not pTau) to the dentate gyrus granular cells Significant neuronal loss in the Entorhinal Cortex and synaptic degeneration in the perforant pathway
Cook, Kang et al.	2015	WT mice (pups)	AAV1	ICV	P301L (n.a.)	Open-field, Plus-Maze, Fear conditioning	Widespread expression (limbic and subcortical areas), tauopathy: pTau, NFT No neuronal loss but degradation of PSD95 and dystrophic neurites associated with microgliosis and astrogliosis as well as behavioural and memory impairments
Wegmann, Maury et al.	2015	WT mice TauKO mice	AAV8	Entorhinal Cortex; HC	P301L-GFP (4R2N)	(n.a.)	Propagation of human Tau protein even in absence of endogenous murine Tau

Gene-transfer based rat models of tauopathy

Authors	Date	Genetic background	Vector	Injection site	Form of Tau	Behavioural test	Main results
Klein, Lin et al	2004	WT rats (Sprague-Dawley)	AAV2	Septum	P301L (4R2N)	n.a.	Tauopathy: pTau, NFT WPRE-induced increased transgene expression leads to stronger Tau pathology
Klein, Dayton et al.	2005	WT rats (Sprague-Dawley)	AAV2	SNc	WT/P301L (4R2N)	Rotational behaviour	Tauopathy: Ab39 positive NFT-like neurons observed in both WT and P301L groups. Behavioural impairment and loss of TH neurons
Klein, Dayton et al.	2006	WT rats (Sprague-Dawley)	AAV8	HC; SNc	P301L (4R2N)	n.a.	AAV8 : stronger and more widespread expression than other vectors: combine AAV5 widespread expression with AAV2 high intracellular expression
Klein, Dayton et al.	2008	WT rats (Sprague-Dawley)	AAV2, 8, 9, 10	SNc	P301L (4R2N)	Rotational behaviour	Toxicity is dependant on Tau expression level (related to the serotype used Loss of TH neurons, behavioural impairment
Klein, Dayton et al.	2010	WT rats (Sprague-Dawley)	AAV9	SNc	WT (4R2N)	Rotational behaviour	Tauopathy: observed in both young and old rats. Associated with loss of TH neurons and behavioural impairment. Both were higher in old rats compared to the young rats
Ramirez, Poulton et al.	2011	WT rats (Sprague-Dawley)	AAV2	Entorhinal Cortex	P301L (4R0N)	Y-maze	Tauopathy: ptau, NFT Impairment in spatial memory but no neuronal loss
Mustroph, King et al.	2012	WT rats (Sprague-Dawley)	AAV9	HC	P301L (4R2N)	Y-maze	Tauopathy: ptau; NFT Neuronal loss assoc. with gliosis and oxidative stress, impairment of spatial memory
Dayton, Wang et al.	2012	WT rats (Sprague-Dawley)	AAV9	HC	WT (4R2N)	Morris Water Maze	Tauopathy: Tau overexpression specifically in the neuropil; ptau; NFT No neuronal loss, no memory impairment
Caillierez, Bégard et al.	2013	WT rats (Wistar)	Lentivirus	HC	WT/P301L (4R1N)	n.a.	Tauopathy: pTau increases with time in both WT and Mut groups. NFTs in Mut > WT Neuronal loss in both groups
Dujardin, Lecolle et al	2014	WT rats (Wistar)	Lentivirus	HC	WT/P301L (4R1N)	n.a.	Transfer of Tau protein to distant connected regions. Wider spatial propagation was found with WT Tau compared to mutant P301L Tau.
Dujardin, Begard et al	2014	WT rats (Wistar)	Lentivirus	HC	WT (4R1N)	n.a.	Exosomal release of Tau is associated with Tau pathology

Abbreviations: AAV, adeno-associated viral vector; HC, Hippocampus; ICV, intracerebroventricular; n.a.; not available SNc,Substantia nigra pars compacta; WT, wild-type

3) <u>Induction and propagation of a tauopathy following injection of Tau fibrils</u>

Several studies have been performed using recombinant or brain-derived Tau aggregates, in order to determine the mechanisms underlying the induction and spreading of Tau pathology. The implications of those studies have already been described in part II – 2) – c) of this introduction. For this reason, those models will be described here with a focus on their technical advantages and disadvantages compared to gene-transfer based models.

a) <u>Whole brain-homogenates and brain-derived aggregates</u>

Initial studies involved the injection of whole human or murine brain homogenates in transgenic mice expressing WT or mutant forms of human Tau. For example, the injection of brain extracts from mutant P301S transgenic mice led to the induction of the pathology in a time-dependent pattern with a progressive increase in the number of aggregate as well as the sequential propagation to connected regions (Clavaguera et al., 2009). Similarly, brain homogenates from different tauopathies, injected into the brain of transgenic mice overexpressing human wild-type Tau, triggered the formation of Tau lesions that morphologically resembled those observed in human cases (**Figure 18**, Clavaguera et al., 2013). The possibility of studying the differential phenotypic induction produced by homogenates from different origins may allow the identification of the differences and communalities of several tauopathies. It may be quite difficult, however, to decipher the specific contribution of Tau aggregates using whole homogenates given that patient with tauopathies often present with additional comorbidities. In addition, this approach may not be well suited for the identification of the stage of Tau aggregation involved in neurodegeneration because of the unknown relative composition in aggregates of whole homogenates.

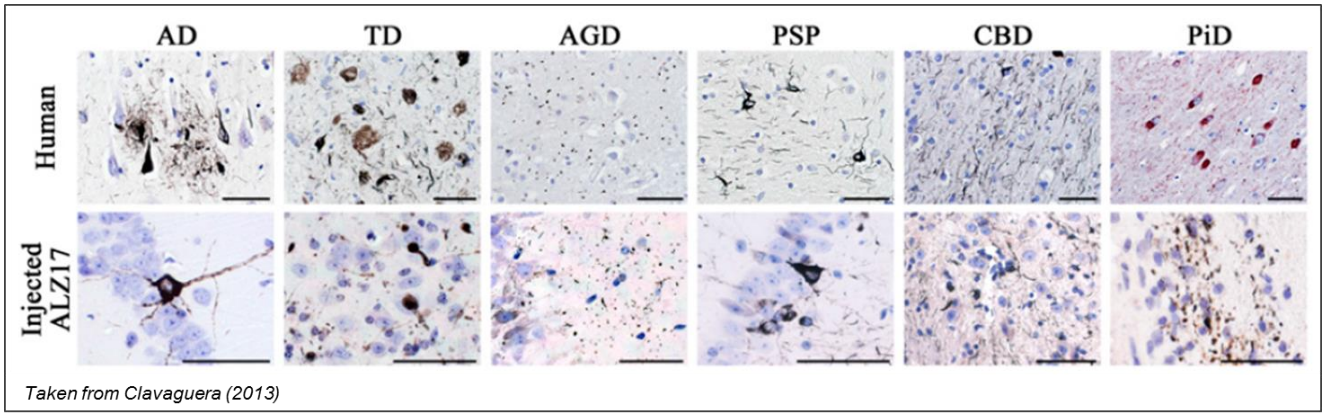

Figure 18: Different morphologies of neuronal Tau inclusions produced by different human Tau homogenates
Gallyas silver staining showed differences in the morphology of Tau aggregates produced by injection of brain homogenates in transgenic mice expressing wild-type human Tau (Alz17). NFTs were observed following injection of AD CBD and tangle-only dementia (TD) brain homogenates. AGD brain homogenates produced argyrophilic grains, PSP brain globose NFTs, while Pick's bodies were observed following injection of PiD homogenates.

An alternate approach thus consisted in the isolation of Tau aggregates from brain homogenates. For example, brain-derived Tau fibrils from AD and CBD cases were injected into the hippocampus of mutant P301S human Tau transgenic mice (Boluda et al., 2015). Tau pathology induced by those two homogenates differed by the cell type affected, the reactivity of Tau aggregates to different pathological Tau epitopes, the stage of Tau aggregation, the pattern of spreading as well as their level of toxicity, confirming the phenotypic diversity of tauopathies. Similarly, brain-derived oligomers but not fibrils were able to alter long-term potentiation in hippocampal slices and induce memory impairments when injected in mice (Lasagna-Reeves et al., 2012b). One drawback of this approach, however, is the relative

incertitude on the “purity” of Tau extracts. Indeed, aggregates in patients have been found to be highly heterogeneous, Tau trapping a number of other proteins during polymerization. One may question whether the effects observed using this approach do represent Tau-mediated toxicity.

b) Recombinant Tau aggregates

One way to bypass those limitations is to use synthetic Tau aggregates, which was done in several studies. For example, recombinant Tau fibrils were injected in several brain regions of transgenic mice expressing a mutant human Tau isoform (Peeraer et al., 2015). This led to the development of a tauopathy first in the region of injection before spreading to anatomically connected regions (Peeraer et al., 2015), leading to impairment in the associated function (Stancu et al., 2015). In a study from another team, recombinant Tau oligomers were found to be the only species able to induce cognitive deficits compared to Tau fibrils and monomers when injected to wild-type mice (**Figure 19**; Lasagna-Reeves et al., 2011). The use of synthetic Tau aggregates in these studies allowed the purification and isolation of several orders of Tau aggregates (i.e. monomers, oligomers and fibrils), giving further insight into the mechanism of Tau toxicity and spreading. One may question, however, to which degree those synthetic aggregates may behave similarly to those produced in a more complex environment.

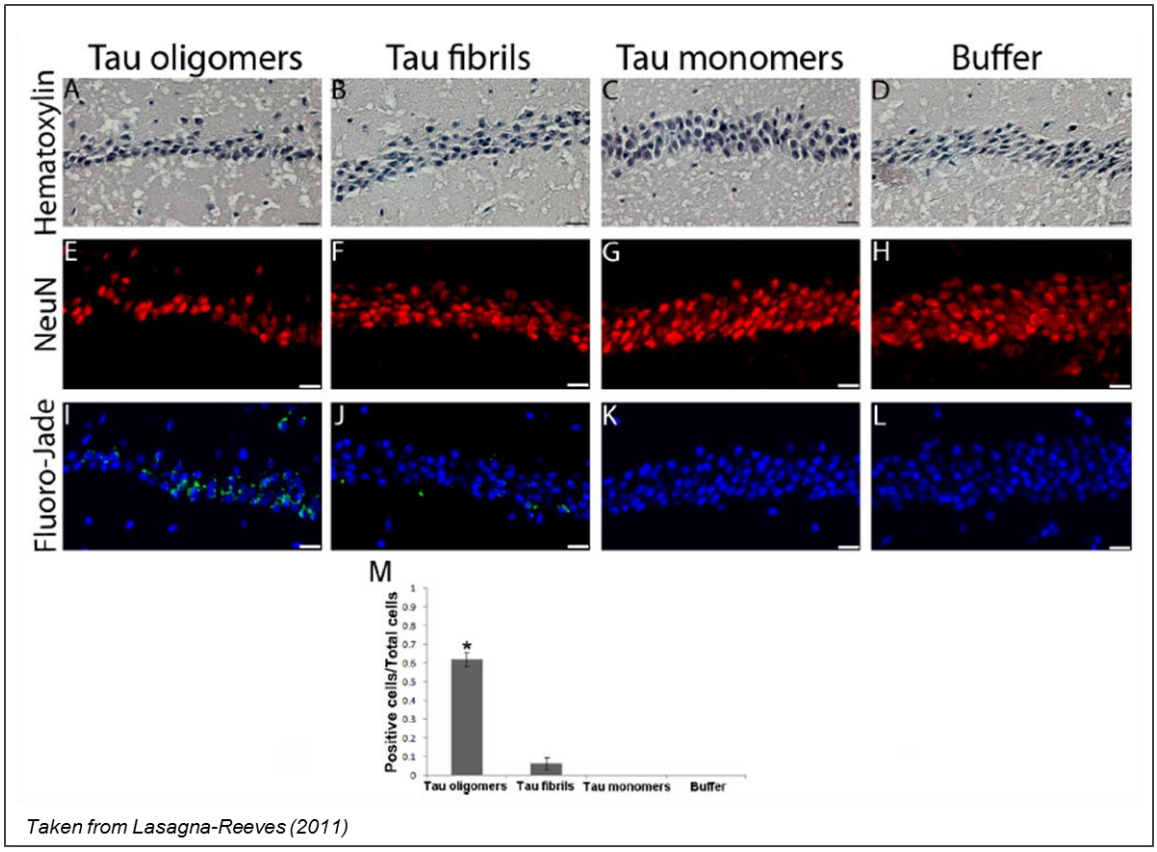

Taken from Lasagna-Reeves (2011)

Figure 19: Recombinant Tau oligomers but not fibrils or monomers induce neuronal loss
Significant loss of neurons could be observed on either hematoxylin or NeuN staining following injection of Tau oligomers (A) but not fibrils (B) or monomers (C) in wild-type mice. 63% of the cells in the animals injected with oligomers were positive for the marker of degenerating neurons fluoro-jade (M) while only 6.5% of the cells were positive for this marker in the group injected with Tau fibrils.

More generally, most of these studies were performed in transgenic animals expressing a mutant form of Tau, as the pathology induced in non-transgenic animals was usually quite sparse (Clavaguera et al., 2009). Although allowing the study of the mechanisms mediating the toxicity of mutant Tau, those models may not be as relevant for the study of sporadic tauopathies.

To date a large choice of rodent models of tauopathy are available to use, which have already allowed a better understanding of pathological mechanisms associated with Tau induced neurodegeneration. Each of them however present with its specific advantages and drawbacks and the use of a model in particular thus should be driven by the type of question to be answered. Hence, while "classical" constitutive transgenic models may be of great use for the study of long-term processes underlying Tau pathology, the more recent development of inducible models allowed a better understanding of the link between soluble Tau, toxicity and aggregation (Hochgräfe et al., 2013; SantaCruz et al., 2005). However, direct comparison of several transgenic models may be hindered by the phenotypic variability induced by the location of transgene insertion (Schindowski et al., 2006).

Alternative approaches have thus been developed over the years in order to study the commonalities and differences of tauopathies. For example, injection of brain-derived or recombinant Tau aggregates have been used to determine if those reproduced the phenotypic variability observed in tauopathy patients (Clavaguera et al., 2013). Similarly, injection of Tau aggregates of different orders supported the pathogenic role of soluble oligomers when compared to fibrillary species (Lasagna-Reeves et al., 2011). More recently, the development of vector-based tauopathy models also allowed the study of questions that would have been difficult to address using alternative approaches. Hence, the injection of vectors allowing the overexpression of human Tau in APP mutant mice (Osinde et al., 2008) allowed the study of the interaction of both proteinopathies. Similarly, injection of lentiviral vectors encoding either WT or mutant P301L Tau allowed direct comparison of the pathology in models of sporadic and genetic Tau pathology (Caillierez et al., 2013).

Lastly, one should take into account the translational benefit of a given model. Indeed, mouse models are more readily available given the technical difficulties encountered in the development of transgenic rat models. It remains that the larger body and brain size of rats allows the study of biomarkers that may be directly comparable to those measured in human. For example, in a transgenic rat model overexpressing a truncated form of Tau, increased CSF phosphorylated Tau was found to correlate with cognitive decline (Zilka et al., 2010), reminiscent of what observed in AD tauopathy. The practicality of the model should also be considered as transgenic models usually necessitate a long time before the appearance of a significant phenotype. Generating fast-developing models should thus prove useful for a use in preclinical research.

IV – Thesis objectives

Tauopathies are a large family of neurodegenerative diseases characterized by the aggregation of Tau protein inside the brain. Despite this common hallmark, tauopathies present with a large diversity, either of the type of cells affected or brain regions involved leading to specific cognitive deficits. Several mechanisms of Tau-induced toxicity were proposed which may be related to the large contribution of Tau to different neuronal functions. The identification of those different toxic effects of Tau was however mostly done in transgenic animals expressing mutant Tau protein. It remains to be established whether similar mechanisms also occur in sporadic tauopathies. Considering those issues, the development of Tau-directed disease modifying therapies would gain from the study of tauopathies as a whole and from the identification of pathological commonalities and differences underlying Tau-associated neurodegeneration. More specifically, one question that remains to be addressed is whether the mechanisms linking Tau aggregation to its toxicity are different in genetic and sporadic tauopathies. To this respect, the development of animal models allowing the direct comparison of Tau-associated deficits underlying various tauopathies would be of great use.

Hence, the first aim of this project was to develop rodent models of sporadic and genetic tauopathies using AAV-mediated gene transfer of the human Tau protein. The use of viral vectors-mediated expression of Tau, by its versatility, allowed this direct comparison. The development of those models in rats also permitted a multimodal approach with the study of peripheral biomarkers that are not readily accessible in mice, such as levels of Tau in CSF. The choice of rats was also driven by the possibility to perform *in vivo* PET imaging in the future, which could allow better characterization of the target of currently developed Tau-directed tracers. Such studies could be considered because of the rapid time-course often observed using vector-based models.

We also aimed to study the link between Tau aggregation and its toxicity and how those may relate to cognitive impairments. The use of different vectors to overexpress wild-type or mutant Tau in our models allowed us to address this later question. We chose to inject those different vectors in one common brain structure in order to determine how different types of Tau pathology may be associated with the impairment of a given function. In this respect, our models were thus not developed in an attempt to recapitulate the full disease spectrum of a given tauopathy, but to serve as tools for the differential study of the pathogenic effects of Tau aggregation underlying sporadic and genetic tauopathies in general.

MATERIAL & METHODS

MATERIAL & METHODS

I – Vectors construction and in vitro validation of the constructs

1) Vectors cloning

Expression vectors were cloned using Gateway 2 LR Clonase system (Invitrogen). This system is based on homologous recombination of att sequences inserted into the different vectors (**Figure 20, B**). Two types of vectors were used for cloning, a destination vector and entry vectors (**Figure 20, A**). The destination vector contained the single stranded rAAV2 backbone including inverted terminal repeats (ITRs). This destination vector also contained the woodchuck hepatitis virus posttranslational regulatory element (WPRE) inserted upstream of the bovine growth hormone polyadenylation signal (bGHpA). This WPRE sequence was used because of its known ability to enhance transgene expression in the context of AAV-mediated gene transfer (Loeb et al., 1999). A RFA sequence, that acts as a "suicide-cassette", inserted between the attR1 and attR2 recombination sequence served to negatively select plasmids that had not undergone recombination.

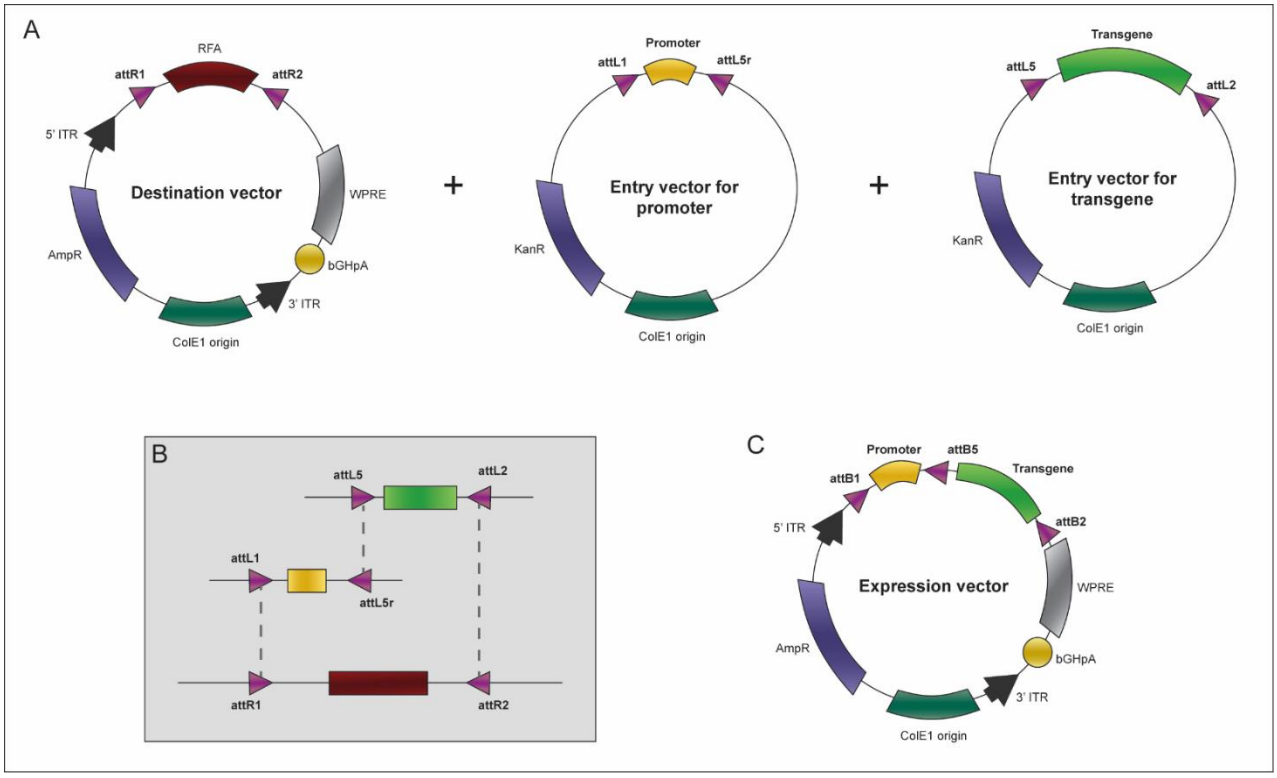

Figure 20: Schematic representation of the Gateway 2 LR cloning method used for vectors production
A) Entry vector (left) containing the rAAV2 backbone sequence including WPRE sequence and bGHpA inserted between ITRs. An ampicillin resistance gene (AmpR) served to positively select plasmids that contained the AAV backbone. The RFA sequence, used as a "suicide-cassette", served to negatively select plasmids that did not undergo recombination. Two entry vectors were used: one containing the promoter inserted between attL1 and attL5r sequences (middle) and one containing the transgene flanked by attL5 and attL2 sequences. Kanamycin resistance gene (KanR) is present in both entry vectors. B) Reaction of homologous recombination between att sequences of the destination vector and entry vectors are indicated by dashed lines. C) This leads to the replacement of the RFA "suicide-cassette" in the destination plasmid by promoter and transgene, leading to the production of expression vector that can be positively selected when cultured in a medium containing ampicillin.

Two entry vectors were then added, one containing the promoter flanked by attL1 and attL5r sequences. the other containing the transgene inserted between attL5 and attL2 sequences. Entry vectors used for the construction of hTAU^{WT} and hTAU^{P301L} vectors were a kind gift of L. Buée (Caillierez et al., 2013). The entry vector used for the hTAU^{ProAggr} transgene was synthetized by GeneART (ThermoFisher, Carlsbad, California, USA). LR cloning was then performed by homologous recombination of the att sequences (**Figure 20, B**) to produce the expression vector (**Figure 20, C**) containing the promoter and the transgene inserted into the AAV backbone. Selection of the expression vector was then done on a medium containing ampicillin to eliminate entry vectors that did not undergo recombination.

Four different constructs were used during the entire study (**Figure 21**). All were expressed under the control of the chimeric cytomegalovirus/chicken-β-actin (CBA) promoter. This hybrid promoter was chosen because of its known ability to drive strong transgene expression in pyramidal neurons when used for AAV2-mediated gene-transfer into the hippocampus (Klein et al., 2002). Three Tau constructs were cloned.

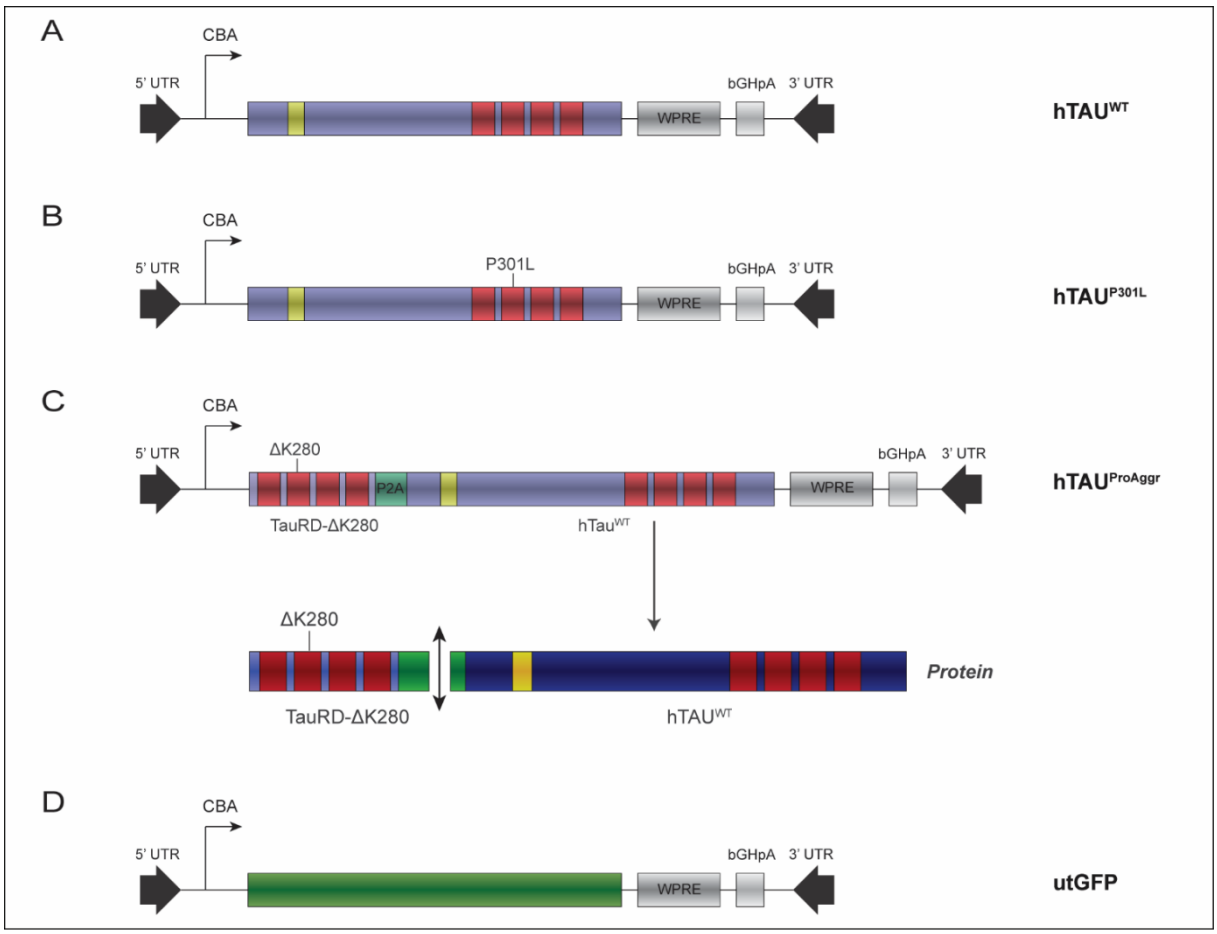

Figure 21: Schematic representation of the different vectors used in this study

All constructs were expressed under the CBA promoter and contained the WPRE expression-enhancing sequence as well as bGHpA tail. A) Construct expressing wild-type human 1N4R Tau isoform, termed hTAU^{WT}, containing only one N-terminal repeat (yellow) and four MBDs (red) B) Construct expressing P301L mutant 1N4R human Tau isoform, termed hTAU^{P301L}. C) Bi-cistronic construct, termed hTAU^{ProAggr} allowing the co-expression of hTAU^{WT} and a pro-aggregation peptide (TauRD-ΔK280) composed of the four repeated-domains of human Tau, bearing the ΔK280 pro-aggregation mutation. A single chimeric protein is produced into the cell that gives rise, after cleavage of the 2A peptide sequence, to a 1:1 expression ratio of hTAU^{WT} and TauRD-ΔK280. D) Construct, termed utGFP, where all ATG initiating codons are mutated allowing the expression of a GFP mRNA that is not translated into a protein.

The first one, named hTAU^{WT} (**Figure 21, A**), contained the wild-type 1N4R isoform of human Tau and served as a model of sporadic tauopathy. The second, named hTAU^{P301L} (**Figure 21, B**), contained the same isoform bearing the P301L mutation, found in cases of FTDP-17, and served as a model of genetic tauopathy. The third Tau vector was constructed in order to potentiate the aggregation of wild-type Tau. This construct, termed hTAU^{ProAggr} (**Figure 21, C**), expresses a chimeric protein constituted of human wild-type Tau (hTAU^{WT}) and a pro-aggregation peptide (TauRD-ΔK280) linked by a 2A peptide (P2A). The pro-aggregation peptide is constituted of the MT-binding region of 4R Tau bearing the ΔK280 mutation, a deletion initially described in a case of FTDP-17 (Rizzu et al., 1999) and presenting with strong pro-aggregation properties (Barghorn et al., 2000; von Bergen et al., 2001). This peptide was used because of its known ability to promote aggregation of endogenous murine Tau when expressed in transgenic mice models (Hochgräfe et al., 2013) and because it contains both hexapeptides PHF6 and PHF6* necessary to Tau assembly into PHFs (Bergen et al., 2000). This construct will be translated into a single chimeric protein into the transduced cell. Cleavage at the P2A sequence will then occur, releasing hTAU^{WT} and the pro-aggregation peptide in a 1:1 ratio. This 2A peptide is a sequence found in some members of the picornavirus family (Ryan et al., 1991) that has already been used successfully for bicistronic expression of transgenes after AAV-mediated gene transfer into the rat brain (Furler et al., 2001). A fourth construct, named utGFP (**Figure 21, D**), was used to express a GFP transgene where all ATG initiating codons were mutated. This resulted in the production of a GFP mRNA that would then not be translated into a protein. This construct was used in our study to overcome the described toxicity of GFP protein expression in some AAV-mediated models (Klein et al., 2006).

2) <u>HEK cells transfections with vectors plasmids</u>

For in vitro validation of Tau constructs, HEK-293T cells were transfected with the different plasmids. For this purpose, 750 000 cells were plated on 6 wells plaques. 200µl transfection mix, containing 5 µg of plasmids, 50µl of $CaCl_2$ and 100µ of HBS, was then prepared and left to precipitate for 15-20 min. The precipitate was then deposed onto cells and left to incubate for 4-5h at 37°C. The culture medium containing the transfection mix was then removed and fresh culture medium was added onto cells. Cells were then left to incubate at 37°C for 36-48h before lysis in a buffer containing 137 mM NaCl, 20 mM Tris pH8, 1% NP-40, 10% glycerol, 2 mM EDTA and protease inhibitors (Complete, Roche, Bâle, Switzerland). Lysed cells were then centrifugated at 13 000g for 30 min at 4°C and BCA dosage of proteins was performed on the supernanant before processing of the samples for western blot analysis.

3) <u>AAV vectors production</u>

All constructs were packaged into AAV2/8 capsids by the MIRCen viral production platform as described (Berger et al., 2015). Briefly, viral particles were produced by co-transfection of HEK-293T cells with (1) an adenovirus helper plasmid (pXX6-80), (2) an AAV packaging plasmid carrying the rep2 and cap8 genes and (3) the AAV2 expression vector containing the transgene. 72 hours following transfection, recombinant vectors were purified and concentrated from cell lysate and supernatant by ultracentrifugation on an iodixaniol density gradient followed by dialysis against PBSMK (0.5 mM $MgCl_2$ and 1.25 mM KCl in PBS). Concentration of the vector stocks was estimated by real-time-PCR following the method described by Aurnhammer et al. (2012) and expressed as viral genomes per ml of concentrated stocks (Vg/ml).

Rationale for the choice of AAV2/8 as transgene-carrying vector

The choice of the type of viral vector as well as of the caspid/promoter combination was governed by two pre-requisites: (1) Achieve widespread expression in most of the HC and uniquely in this region, in order to produce a phenotype strong enough to induce cognitive deficits, (2) drive transgene expression mainly in the neuronal population. To achieve widespread expression of the transgene, an AAV vector was chosen over lentivirus because of its larger diffusion, leading to more widespread transduction of a given structure (de Backer et al., 2010). Then, AAV2/8 pseudotype was chosen among the serotypes available at MIRCen because it fulfilled the two above mentioned criteria. Indeed, a study using AAV2/8 capsid and CBA promoter showed that this capsid allows both strong transgene expression (reminiscent of what was observed with AAV2) and widespread transduction area (similar to that observed with AAV5; Klein et al., 2006). This made AAV2/8 pseudotype the most promising capsid for the widespread expression of Tau transgene in the entire hippocampus. Others have already used this serotype/promoter combination in a study to drive Tau expression in the substantia nigra (Klein et al., 2006). AAV2/9 serotype was also found to induce widespread expression of Tau in this region (Klein et al., 2008a). However, this serotype was not selected for our study for several reasons. First, it was found to diffuse more to overlying cortex. Secondly, this serotype induces strong transgene expression at very early time-points, leading to acute neuronal loss (Klein et al., 2008a). In our context, AAV2/8 pseudotype was thus selected for its more progressive time-course of transgene expression.

There is controversy on the cell-type transduced by AAV2/8 vectors with studies showing almost uniquely neuronal transduction (Taymans et al., 2007) and others showing also strong transduction of astrocytes (Aschauer et al., 2013). Recent reports suggest, however, that the purification method of AAV particles may play an important role in the tropism of AAV2/8 vectors, iodixianol gradients allowing mostly neuronal transduction (Klein et al., 2008b). Indeed, in this study, AAV2/8-CBA-GFP construct, purified on iodixianol gradient, was found to produce efficient transduction of pyramidal neurons in the CA1 hippocampal subfield as well as granular cells in the dentate gyrus, with mostly neuronal transduction pattern (Klein et al., 2008b). Similarly, AAV2/8 capsid with CMV promoter, purified with the same method, leads to strong neuronal transgene expression and almost no transduced astrocytes (93% and 7% respectively) when injected in the striatum (Taymans et al., 2007). This was confirmed by observations made in the laboratory (data not shown) and led to the selection of AAV2/8 for efficient neuronal delivery of our different transgenes.

II – Stereotaxic injections

Animals were housed in a temperature-controlled room maintained on a 12 hr light/dark cycle. Food and water were available ad libitum. All animal studies were conducted according to the French regulation (EU Directive 86/609 – French Act Rural Code R 214-87 to 131). The animal facility was approved by veterinarian inspectors (authorization n°B 92-032-02) and complies with Standards for Humane Care and Use of Laboratory Animals of the Office of Laboratory Animal Welfare (OLAW – n°#A5826-01). All procedures received approval from the ethical committee. Adult male Wistar rats (250 g each; JANVIER, France) and male C57BL/6J mice (20g) were used for AAV infections.

Prior to stereotaxic surgery, anaesthesia was first induced by placing the animals in an induction chamber with 4% isoflurane until they were unconscious. Adult male wistar rats were then injected with an anaesthetic composed of a mixture of Kétamine (Imalgène 1000, 75mg/kg) and Medetomidine hydrochloride (Domitor, 0.5mg/kg), administered intraperitoneally. For mouse injections (male adult C57BL/6J mice), anaesthesia was performed using Kétamine (Imalgène 1000, 100mg/kg) and Xylazine

(10 mg/kg). For local anaesthesia, lidocaine (7mg/kg) was administered subcutaneously under the scalp skin 5 minutes before the beginning of surgery. To prevent corneal desiccation, ophthalmic ointment was regularly placed in the eyes. During the surgery, normal body temperature was monitored and maintained by using temperature- controlled electric heat pads.

AAV vectors were injected using a 34-gauge blunt-tip needle linked to a Hamilton syringe (Hamilton, Reno, NV) by a polyethylene catheter at the stereotaxic coordinates indicated in **Table 2**. Antero-posterior and lateral coordinates were taken relative to bregma. Ventral coordinates were taken relative to the skull at the injection site. The tooth bar was set at -3.3 mm for rats and 0 mm for mice. For rat injections, 4µl of vector diluted in 0.1M PBS with 0.001% pluronic acid was delivered using a microdialysis pump (Stoelting Co., Wood Dale, USA) set at 0.25µl/min. For mice, the volume of injection was set at 2µl and rate of delivery at 0.20µl/min. At the end of injection, the needle was left in place for an additional 5min before removing.

At the end of the surgery procedure, the scalp skin was closed using Michel wound clips. For animals induced with the Ketamine/Domitor mix, anesthesia was then reversed with a subcutaneous injection of Atipamezole (Antisedan, 0,5 mg/kg). All animals were then rehydrated with a subcutaneous injection of warm saline (10ml/kg) and left for 1h in a ventilated heating box (28°C) until they woke up and fully recovered from anesthesia. Post-surgery analgesia was ensured by the administration of Paracetamol (Pracetam 1,6 mg/ml) in drinking water for 48 hours.

Serotype	Transgene	Species	Volume	Dose (per site)	Hemisphere	Hippocampus	Injection coordinates	Experiment	Number of animals
AAV2/8	GFP	Rat (wistar)	4 µl	5.10^{10} Vg	Bilateral	Dorsal/Ventral	**Dorsal** AP: -4,3 L: +/-3 V: -2,8/skull **Ventral** AP: -5,6 L: +/-5 V: -7/skull	Test of injection coordinates	4
AAV2/8	$hTAU^{WT}$ $hTAU^{P301L}$ $hTAU^{ProAggr}$ utGFP PBS	Rat (wistar)	4 µl	$2,5.10^{10}$ Vg	Bilateral	Dorsal/Ventral	**Dorsal** AP: -4,3 L: +/-3 V: -2,8/skull **Ventral** AP: -5,6 L: +/-5 V: -7/skull	Characterization of Tau constructs (histology, biochemistry and RT-qPCR)	14/group
AAV2/8	$hTAU^{WT}$ $hTAU^{ProAggr}$ utGFP PBS	Rat (wistar)	4 µl	$2,5.10^{10}$ Vg	Bilateral	Dorsal/Ventral	**Dorsal** AP: -4,3 L: +/-3 V: -2,8/skull **Ventral** AP: -5,6 L: +/-5 V: -7/skull	Behavioural analysis	14/group
AAV2/8	$hTAU^{P301L}$ $hTAU^{ProAggr}$ utGFP	Rat (wistar)	4 µl	$2,5.10^{10}$ Vg	Bilateral	Dorsal/Ventral	**Dorsal** AP: -4,3 L: +/-3 V: -2,8/skull **Ventral** AP: -5,6 L: +/-5 V: -7/skull	Electron microscopy	2/group
AAV2/9	$hTAU^{P301L}$ $hTAU^{ProAggr}$	Mouse (C57Bl/6J)	2 µl	1.10^{10} Vg	Bilateral	Dorsal	AP: -2,4 L: +/-1,5 V: -1,6/skull	Characterization of glial Tau pathology	6/group
AAV2/9	$hTAU^{P301L}$ $hTAU^{ProAggr}$	Mouse (Aldh1l1-GFP)	2 µl	1.10^{10} Vg	Bilateral	Dorsal	AP: -2,4 L: +/-1,5 V: -1,6/skull	Characterization of glial Tau pathology	5/group

Table 2: Summary table of the different injections performed in this study
Doses of vector are given in number of viral genome (Vg). Coordinates were taken relative to bregma for the antero-posterior (AP) and lateral (L) coordinates. Ventral (V) coordinates were taken relative to the skull at the site of injection.

III – Behavioural analysis

1) Open field

All rats were subjected to a 5 days habituation phase prior to behavioural testing, consisting in 5 min of handling every day. This was followed by an open field test for the assessment of spontaneous locomotion and anxiety behaviour. Briefly, animals were allowed to explore freely a squared open field (Med Associates Inc., St Albans, Vermont, USA) for 10 min. The behaviour of the animal was recorded using Ethovision XT10 software (Noldus Instruments, Wageningen, The Netherlands) and several parameters were computed. Measures of locomotor abilities and exploration included the mean distance travelled (cm), mean velocity (cm/s), frequency of rearing and time spent rearing (s). Measures of anxiety included the frequency of grooming, time spent grooming (s), time spent in centre (s) and the number of entries in centre.

2) Spatial reference memory task in the *Y-Maze*

The test consisted in a 15 min-long training phase during which one arm of the Y-maze (Med Associates Inc., St Albans, Vermont, USA) was blocked and the animals allowed exploring freely the other two arms. After a 3 min inter-trial interval (ITI), animals were re-introduced into the maze for a 5 min-long test period during which they could explore all three arms, including the one that was previously blocked. The behaviour of the animal was recorded using Ethovision XT10 software (Noldus Instruments, Wageningen, The Netherlands) and memory was assessed by computing the percentage of time spent in each arm (time spent in arm * 100 / time spent in all arms).

Introduction of the animal into the maze was always done from the end of the same arm (considered as the “start” arm) and the positions of the blocked (“novel”) and “other” arms were balanced between animals to avoid spatial bias. Given that memory in this test is based on the tendency of animals to explore the environment, animals that presented less than four total arm entries during training were considered as not performing the task and were thus excluded from analysis of the test session.

3) Long-term memory assessment using contextual fear conditioning paradigm

Long term emotional memory was assessed using a standard contextual fear conditioning protocol (Bioseb, Vitrolles, France). During a training phase, animals were introduced in a dark box for a 5 min 30s long-period. After a 3 min habituation to the context, animals received three 0,3 mA electric foot shocks separated by a 1 min interval. After a 24h ITI, animals were re-introduced into the box for an 8 min-long period. Freezing was recorded during the training and test phases using a movement sensor placed at the bottom of the box and considered as a recording bellow a 15% threshold for at least 1s.

IV – Histology

1) Tissue processing

One or three months after injection, rats were anesthetized with 4% isoflurane before receiving a lethal dose (2ml) of sodium pentobarbital (60mg/ml). Animals were then fixed by cardiac perfusion with NaCl 0.9% for 1 min followed by 4% PFA in PBS 0.1M for 9 min at a speed of 30ml/min. The brain was collected and post-fixed overnight in 4% PFA-PBS0.1M. Then, tissue was transferred in a 20% sucrose solution in PBS 0.1M for cryoprotection before sectioning on a freezing microtome (SM2400, Leica, Germany). Fourteen series of 30µm-thick sections were collected, spanning the entire hippocampus and

stored at -20°C in a storage solution containing 30% glycerol, 30% ethylene glycol, 10% 0.1M Phosphate Buffer.

2) Immunohistochemistry and immunofluorescent staining

For free-floating immunohistochemistry, sections were incubated 30 min with 0.3% H_2O_2 in PBS. After rinsing in PBS 0.1M, 0.2% Triton (Sigma X-100), sections were incubated 1h with the blocking buffer containing normal goat serum (NGS) in PBS and transferred into primary antibody solutions diluted in blocking buffer for incubation overnight at 4°C. After rinsing, sections were incubated with the appropriate secondary antibody for 1h at room temperature followed by 30 min incubation in VECTASTAIN ABC Kit (Vector Laboratories, USA) and DAB revelation using DAB Peroxidase Substrate Kit with nickel (Vector Laboratories, USA). Sections were then dehydrated in increasing ethanol concentrations and xylene before mounting using Eukitt (Dutscher, France). For free-floating immunofluorescence staining, sections were incubated directly in blocking solution before transfer into primary antibody solutions diluted in blocking buffer for incubation overnight at 4°C. After rinsing, sections were then transferred into Alexa-coupled secondary antibodies solutions (Thermofisher, USA) for incubation 1h at room temperature. For AT8/Vimentin and AT8/Iba1 colabellings, AT8 immunostaining was amplified using CY3-coupled streptavidin (Sigma-Aldrich, USA). Sections were then mounted directly on slides using fluoromount medium (Sigma-Aldrich, USA). For further description of the antibodies used in this study as well as antibody dilutions, see **Table 3**.

Antibody	Reactivity	Species	Reference	Antibody dilution (blocking)
Immunohistochemistry				
AT8	Human Tau pSer202, pT205	Mouse	Thermofisher	1/400 (PBS + 0,2% Triton)
AT100	Human Tau pS212, pT214	Mouse	Thermofisher	1/4000 (PBS + 0,2% Triton)
GFAP	GFAP	Mouse	Sigma-Aldrich	1/1000 (PBS + 0,2% Triton + 3%NGS)
Anti-mouse (biotinylated)	Mouse Ig	Goat	Vector	1/1000 (PBS + 0,2% Triton)
Immunofluorescence				
HT7	Human total Tau	Mouse	Innogenetics	1/1000 (PBS + 0,2% Triton)
AT8 (biotinylated)	Human Tau pSer202, pT205	Mouse	Thermofisher	1/400 (PBS + 0,2% Triton)
P2A	2A peptide	Rabbit	Millipore	1/1000 (PBS + 0,2% Triton + 3%NGS)
NeuN-A488	NeuN	Mouse	Millipore	1/500 (PBS + 0,2% Triton + 3%NGS)
Vimentin	Vimentin	Mouse	Sigma-Aldrich	1/2000 (PBS + 0,2% Triton + 3%NGS)
Iba1	Iba1	Rabbit	Wako	1/500 (PBS + 0,2% Triton + 3%NGS)
Anti-mouse (Alexa 488/594)	Mouse Ig	Goat	Thermofisher	1/500 (PBS + 0,2% Triton + 3%NGS)
Anti-rabbit (Alexa 488/594)	Rabbit Ig	Goat	Thermofisher	1/500 (PBS + 0,2% Triton + 3%NGS)
Streptavidin-Cy3	Biotin	-	Sigma-Aldrich	1/500 (PBS + 0,2% Triton + 3%NGS)

Table 3: Summary table of antibodies used in this study and the concentrations used for different applications
For each application, primary (top row) and secondary (bottom row) antibody dilutions are given. Ig: Immunoglobulin

3) Gallyas silver impregnation

Sections washed 3 times in sterile 0.1 M PBS, mounted on slides and left for drying overnight prior to Gallyas staining. Sections were then permeabilised by incubation into toluene followed by decreasing ethanol concentrations (100%, 90% and 70%). Slides were then transferred into a 0.25% potassium permanganate for 15 min, incubated 2 min in 2% oxalic acid followed by a 60 min incubation in to a solution containing 0.4g lanthanum nitrate, 2g sodium acetate, and 30% hydrogen peroxide. Slides were then rinsed 3 times in distilled water before incubation for 2 min in a solution containing 0.035% $AgNO_3$, 0.04g/ml of NaOH, 0.1g/ml KI. Reaction was then stopped by rinsing sections in 0.5% acetic acid and development performed by incubation for 20min in a solution containing 2g/L NH_4NO_3, 2g/L $AgNO_3$,

10g/L tungstosilicic acid, 0.28% formaldehyde and 50g/L Na_2CO_3. Sections were then washed again in 0.5% acetic acid, incubated 20 min in 1% gold chloride before rinsing in distilled water. Fixation of the staining was then perfomed by washing sections 3 times in 1% sodium thiosulfate. Sections were then dehydrated in increasing ethanol concentrations and xylene before mounting using Eukitt (Dutscher, France).

4) In situ hybridization

A 200bp sequence of the polyA of beta-globine present in the backbone of our pAAV vectors was cloned in pGEM-T easy vector for in vitro transcription. The DIG-labeled RNA probes (sense and antisense) were synthetized using the Riboprobe SP6/T7 system (Promega, USA) according to manufacturer instructions. Quality of DIG-labeled RNA probes was assessed on microfluidic RNA 6000 Nano chip (Agilent, USA). Sections were first washed 3 times in sterile 0.1 M PBS. Then the sections were mounted on slides and were left for drying overnight. The next day, pre-hybridization was performed by incubating sections for 1h in a solution containing saline-sodium citrate (SSC) 20X and 50% formamide to inhibit non-specific binding. Sections were then hybridized overnight at 72◦C with either the sense or antisense probe diluted to 1/200 in hybridization buffer (50% formamide, 5X denhardts, 1mg/ml yeast tRNA, 500µg/ml salmon sperm DNA). Slides were then washed in SSC 0.2X for 90 min at 72°C and 5 min at room temperature before blocking for 1h in 10% NGS diluted in B1 buffer (Tris-HCl 0.1M pH7.6, NaCl 0.15M, Tween 0.1%). Sections were then transferred in a solution containing anti-DIG-POD Fab fragments (Roche, Switzerland) diluted to 1/5000 in B1 buffer + 1%NGS and left to incubate overnight at room temperature. The final day, sections were rinsed three times in B1 buffer and one time in B3 buffer (Tris-HCl 0.1M pH7.6, NaCl 0.1M, $MgCl_2$ 50mM, Tween 0.1%). DIG revelation was then performed by incubating 24h with colorimetric substrates NBT/BCIP (Roche, Switzerland) according to the manufacturer's instructions. The reaction was then stopped by washing the slides in B1 buffer and sections were incubated with 4% PFA before proceeding to GFAP immunostaining.

5) Image acquisition and quantification

Quantifications were performed on all sections of a series spanning the entire hippocampus in order to be able to perform correlation studies between the different parameters measured.

Counting of AT100-positive neuronal somas and AT100-positive astrocyte-like cells

Following AT100 immunostaining, z-stack images of the entire section were acquired at 20x (10µm, 1µm steps) on an Axioscan (Zeiss, Oberkochen, Germany). Z-project images were then converted into jpeg files and reduced to 70% of full resolution size. Manual counting of AT100-positive somas was then performed using ImageJ software (cell counting plugin) on all sections of a series, spanning the entire hippocampus. Two sub-regions of the hippocampus were defined. The first one, termed Sub-CA1/2, comprised the subiculum as well as the CA1 and CA2 hippocampal subfields. The second one, named CA3/4-DG, was constituted of the CA3 and CA4 hippocampal subfields as well as the dentate gyrus. Total estimate of positive objects in a given sub-region or in total was then calculated by multiplying the obtained number by 14, corresponding to the section sampling.

Cavalieri estimation of hippocampal volume

Estimation of whole hippocampal volume was performed on 5x mosaic images of NeuN staining acquired with a spinning-disk confocal microscope (BX51WI, Olympus Deutschland GmbH, Germany). Manual segmentation of the hippocampus was performed on those images and area of the structure determined

using Stereo Investigator software (MBF Bioscience, USA). Volume of the structure was then estimated using the following formula:

$$V = \sum (A \times n \times T)$$

Where ***V*** is the estimated volume, ***A*** is the hippocampal area segmented on each section, ***n*** corresponds to the section sampling and ***T*** the section thickness.

Image processing of AT8/Iba1 co-staining

AT8/Iba1 immunolabelled sections were scanned at 20x using a Nanozoomer (Hamamatsu, Japan). Manual segmentation of the entire hippocampus was then performed before thresholding of each fluorescent channel (FITC for Iba1 and TRITC for AT8) using Visiopharm Integrator System software (Visiopharm, Denmark). Pre-processing of images was performed prior to thresholding using a series of image transformations implemented into the software. This was done in order to increase the signal to noise ratio, enabling more accurate segmentation of the staining (**Figure 22**). As a result, thresholding on AT8 channel led to the precise segmentation of strong somatic and neuritic staining but left out weakly stained processes. Similar processing was performed on the FITC channel allowing fine identification of individual Iba1-positive microglia.

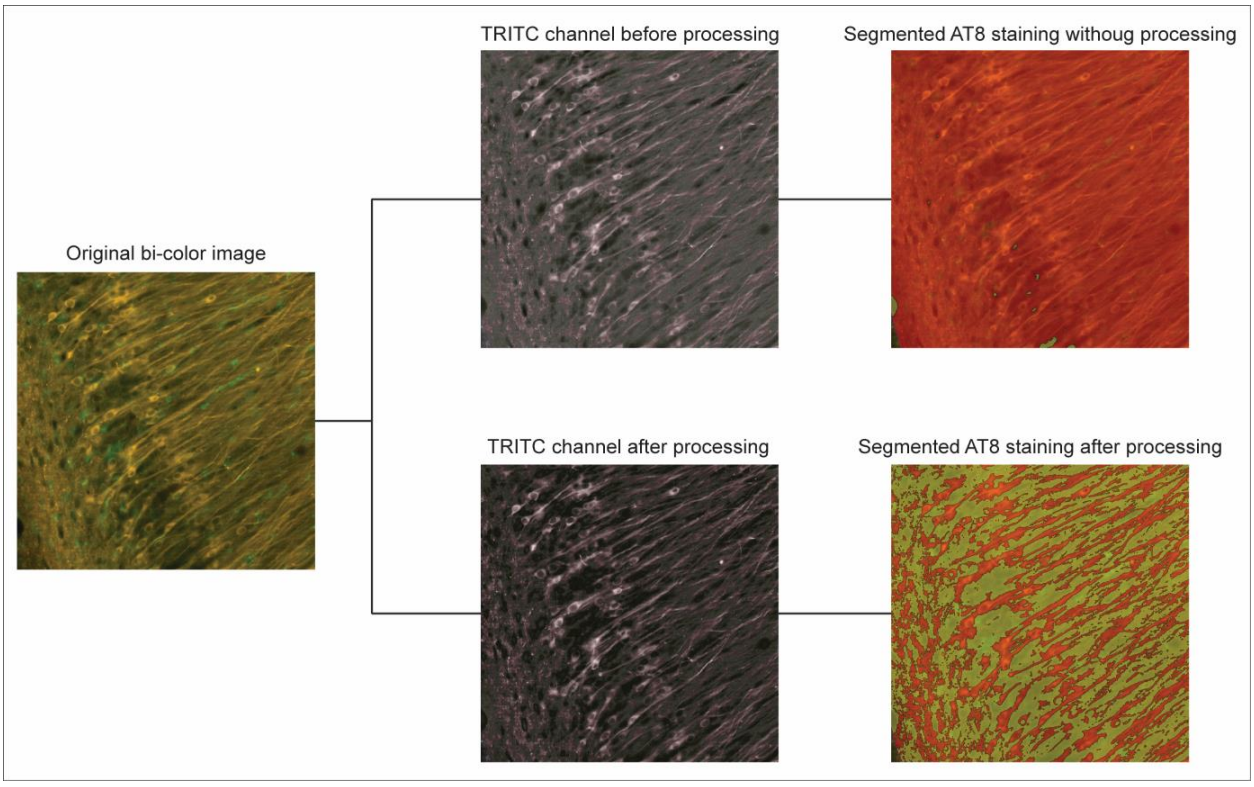

Figure 22: Image pre-processing before thresholding of AT8-positive and Iba1-positive tissue
A series of image transformations is applied on each fluorescence channel of the bi-color image prior to thresholding, allowing to increase the signal to noise ratio. This permitted fine segmentation of each staining, as evidence here by the segmentation of individualised stained neurites on the AT8 channel.

Quantification of AT8 and Iba1 stainings

After pre-processing and thresholding, the mean AT8-positive area and the mean fluorescence intensity (MFI) of this area were computed. Estimation of the percentage of hippocampal volume occupied by AT8 staining was then calculated using the following formula:

$$\%V_{HC} = \frac{A_{AT8}}{A_{ROI}} \times n \times T \times 100$$

Where $\%V_{HC}$ is the proportion of HC volume occupied by AT8 staining, A_{AT8} is the sum of thresholded area of AT8 staining on each section, A_{ROI} the total manually segmented HC area, T the cut section thickness and n the section sampling (i.e. 14).

For Iba1 quantification, two thresholds were applied simultaneously (**Figure 23**). This design allowed the segmentation of whole microglia (Iba1 "low") and specifically of microglial somas (Iba1 "high"). Because microglial activation is associated with strong somatic Iba1 expression, the increase in parameters computed using Iba1 "high" threshold could be considered as an index of microglial activation. Two parameters were thus computed from the Iba1 "high" threshold and compared between groups: the mean area of Iba1 staining and the mean number of Iba1-positive objects. Estimation of Iba1-positive volume was then computed similarly to previously described.

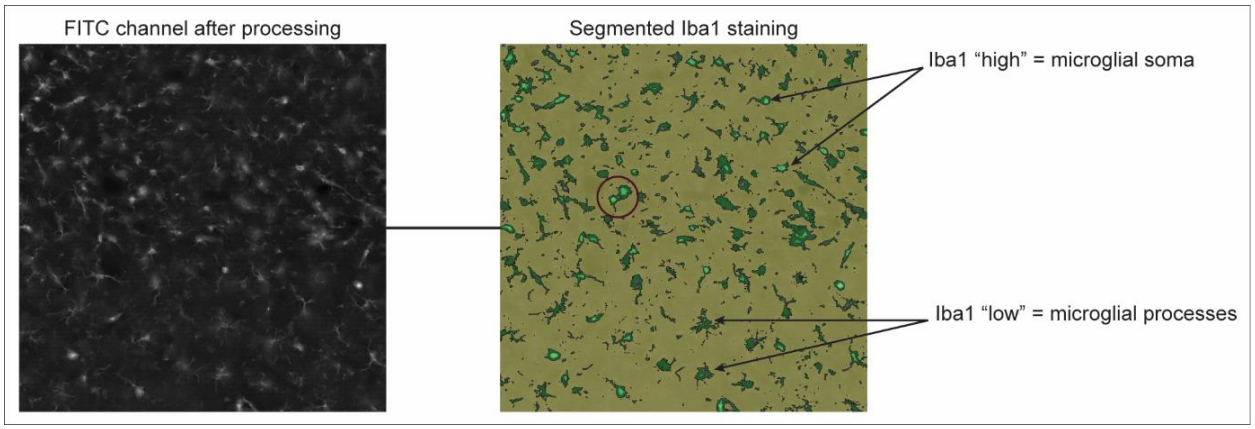

Figure 23: Thresholding of Iba1 staining
Two different thresholds were used, allowing a more precise identification of activation microglias. While Iba1 "low" threshold (dark green) allowed segmentation of the entire staining, Iba1 "high" threshold (light green) lead to the identification of individual microglial somas.

Quantification of Vimentin staining

Vimentin immunolabelled sections were scanned using an Axioscan (Zeiss, Germany). Z-stack images were acquired at 20x (12µm, 2 µm steps). Manual segmentation of the Vimentin-positive region was then performed using Morphostrider software (Exploranova, France) followed by thresholding. The mean Vimentin-positive area was then compared between groups.

Confocal imaging and additional image acquisition

Stacked images (15 steps, z-step: 0.5µm) of AT100 staining on Aldh1l1-GFP transgenic mice were acquired using a confocal microscope (SPM, Leica, Germany) using the 40x objective and a zoom of two. Orthogonal projection was then performed on those images using Leica SPM microscope

associated software in order to investigate colocalization. Images of additional immunostainings were acquired using brightfield or epifluorescence microscopy (DM6000, Leica, Germany).

6) <u>Stereological counting of the number of pyramidal neurons in the CA1/2 hippocampal subfield</u>

Unbiased stereological counting of CA1/2 pyramidal neurons was performed using Stereo Investigator software (MBF Bioscience, Williston, Vermont, USA) on every fourteenth sections (30µm thick sections) spanning the entire hippocampus. 40x z-stack (1µm steps) images of NeuN staining in the CA1/2 region were acquired on a spinning-disk confocal microscope (BX51WI, Olympus Deutschland GmbH, Germany) and analysed with the optical fractionator (**Figure 24**). The tissue thickness was measured at every counting frame location and was found to be of 17.65 µm ± 0.34 (mean ± SD). The height of the counting frame was set to 10 µm with a 2 µm guard zone above and below. The counting frame size was set to 20 x 20 µm with a grid size of 100 x 100 µm. This led to an average counting of 506.20 ± 13.70 cells (mean ± SD). A mean coefficient of error (CE) < 0.1 per group was used as the criterion for assessment of the validity of counting. The average CE for all animals was found to be 0.070 ± 0.002(mean ± SD). Neurons were counted if they came into focus within the height of the counting frame. The centre of the NeuN-stained nucleus was taken as reference points. Neurons were counted when this reference point was found inside the counting frame or hitting the inclusion lines (green). Conversely, neurons were excluded from counting it the reference point lied outside of the counting frame or was hitting the exclusion lines (red).

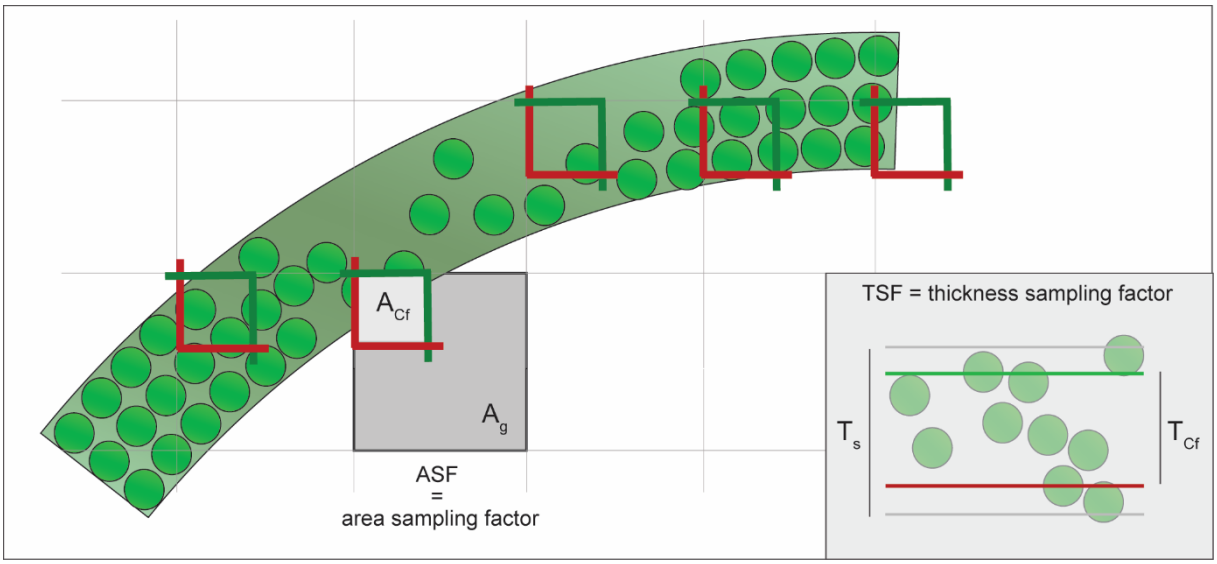

Figure 24: Principle of design-based stereological counting
Counting of neurons is performed in randomly positioned counting frames (of given area A_{Cf}) projected onto the section according to a grid of given area Ag. The area sampling factor ASF used for final calculation of the estimated cell number, corresponding to A_g/A_{Cf}, represents the number of counting frames that could virtually be placed into a given grid. Sampling is also performed within section thickness (TSF) and is defined by the section thickness (T_s) divided by the height of the counting frame (T_{Cf}), this parameter thus corresponding to the number of counting frames that could virtually be placed into section thickness. Definition of those parameters as well as section sampling factor (SSF) allow the estimation of total cell number from the number of counted cells in a given structure.

Estimation of the total number of CA1/2 pyramidal cells per animal was then performed, using the following formula:

$$N = n \times SSF \times ASF \times TSF$$

Where ***N*** is the estimated number of pyramidal neurons, ***n*** is the number of counted cells, ***SSF*** corresponds to the section sampling factor, ***ASF*** to the area sampling factor and ***TSF*** to the thickness sampling factor. And where:

$$\mathrm{SSF} = 14$$

$$ASF = Area\ of\ the\ grid \div area\ of\ the\ counting\ frame$$

$$TSF = Mean\ measured\ section\ thickness \div height\ of\ the\ counting\ frame$$

7) <u>Point-counting/Cavalieri estimation of volume of the pyramidal cell layer</u>

Along with stereological counting of neurons, point-counting/Cavalieri estimation of volume was also performed at each stereological counting site. Briefly, a grid (100µm side) was sur-imposed onto the section and each object hitting an intersection was counted. For more precise estimation of the volume occupied by CA1/2 pyramidal cells, two categories were defined (**Figure 25**): pyramidal cells (PYR^{Cells}) and parenchyma of the pyramidal layer ($PYR^{Parenchyma}$).

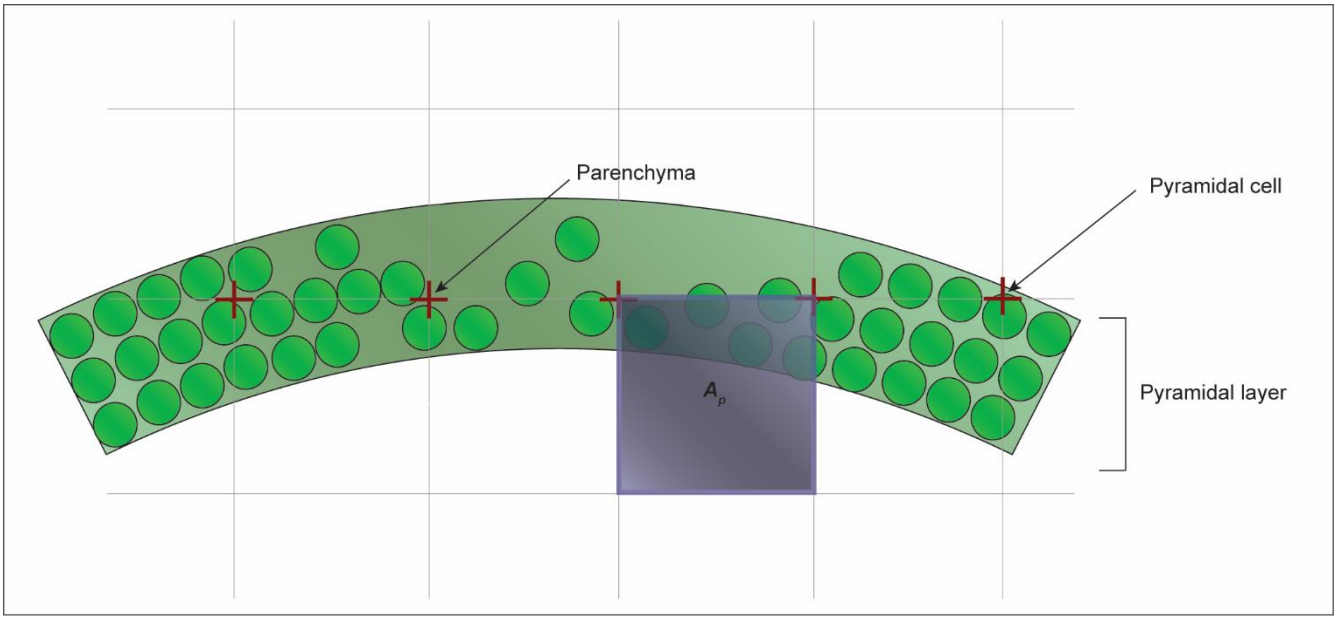

Figure 25: Principle of the point-counting/Cavalieri estimation of volume
A grid is sur-imposed on the section. Each object hitting an intersection of the grid (red cross) is counted. Two categories were used: Pyramidal cells (PYR^{Cells}) and parenchyma of the pyramidal cell layer ($PYR^{Parenchyma}$). A_p represents the area of the grid.See text for the formula used for calculation of the estimated volume.

Then, estimation of volume was performed using the following formula:

$$V_i = A_p \times m \times t \times \sum P_i$$

Where ***i*** represents a given category (PYR^{Cells} or $PYR^{Parenchyma}$), ***V*** is the estimated volume, $\boldsymbol{A_p}$ is the area of the grid, ***m*** the section sampling, ***t*** the measured thickness and ***P*** the points counted on grid.

V – Electron microscopy

Two months after injection, rats were anesthetized with 4% isoflurane before receiving a lethal dose of sodium pentobarbital. Animals were then fixed by cardiac perfusion with NaCl 0.9% for 1 min followed by 2% glutaraldehyde and 2% paraformaldehyde in 0.1M phosphate buffer for 9 min. Whole brains were removed and placed in fresh fixative overnight at 4°C. Transverse slabs of 1 mm thickness across the entire hippocampus from both right and left hemispheres were dissected. The tissue was then post-fixed in 1% osmium tetroxide, 1,5% potassium hexacyanoferrate and 0,1M PHEM buffer pH 7,4 for 1 h, stained in 2% uranyl acetate in water for 1 h and dehydrated through graded series of ethanol and embedding in Epon resin (Epoxy embedding medium kit, Fluka). Blocks were polymerized at 60°C for 48 h. Ultrathin sections of 80nm were cut on an UC7 ultramicrotome (Leica microsystems) with a diamond knife (DiATOME) and mounted on 100 mesh formvar-carbon coated copper grids. Sections were then stained with 2% uranyl acetate and Reynold's lead citrate. For each animal, digital images were acquired from a FEI Tecnai G2 Spirit BioTwin transmission electron microscope operating at 120kV using an Orius SC1000B CCD camera.

VI – Biochemistry

1) Tissue processing

One or three months after injection, rats were anesthetized with 4% isoflurane before receiving a lethal dose of pentobarbital. Brains were then extracted and briefly rinsed in PBS 0.1M before dissection of the hippocampus. The structure was then weighted and 3 volumes of a solution containing Tris 10mM (pH 7.6 – HCl) and sucrose 0.32M were added, before freezing in liquid nitrogen for long-term storage. Samples were then thawed and protease inhibitors (Complete, Roche, Bâle, Switzerland) were added before lysis using Precellys 24 homogenizer (Bertin Technologies, Montigny-le-Bretonneux, France). After BCA dosage (Thermofisher, Carlsbad, California, USA), all samples were aliquoted by 20µl at 1.3µg/µl. For whole homogenate western blots, 20µl of 2x LDS (containing NuPAGE LDS Sample Buffer 4x and NuPAGE Sample Reducing Agent 10x in H_2O, Thermofisher, Carlsbad, California, USA) were added to the samples before heating at 95°C for 5 min.

2) Sarkosyl extraction of insoluble Tau fibrils

For sarkosyl extraction (**Figure 26**), 700µl of Tris 10mM, sucrose 0.32M, Triton 0.23% were added to 100µl of sample (1.3µg/µl). The sample was then sonicated before centrifugation at 5 000 g for 10 min at 4°C. The supernatant was collected for ultracentrifugation at 100 000 g for 1h at 4°C. The second supernatant containing the triton soluble fraction was then collected and diluted in one volume of 2X LDS. The pellet was re-suspended in 800µl of Tris 10mM, sucrose 0.32M, sarkosyl 1%, sonicated and went through a second ultracentrifugation at 100 000 g for 1h at 4°C. The third supernatant containing

the sarkosyl-soluble fraction was diluted in one volume of 2X LDS and the pellet containing the sarkosyl-insoluble fraction re-suspended in 100 µl of 1X LDS.

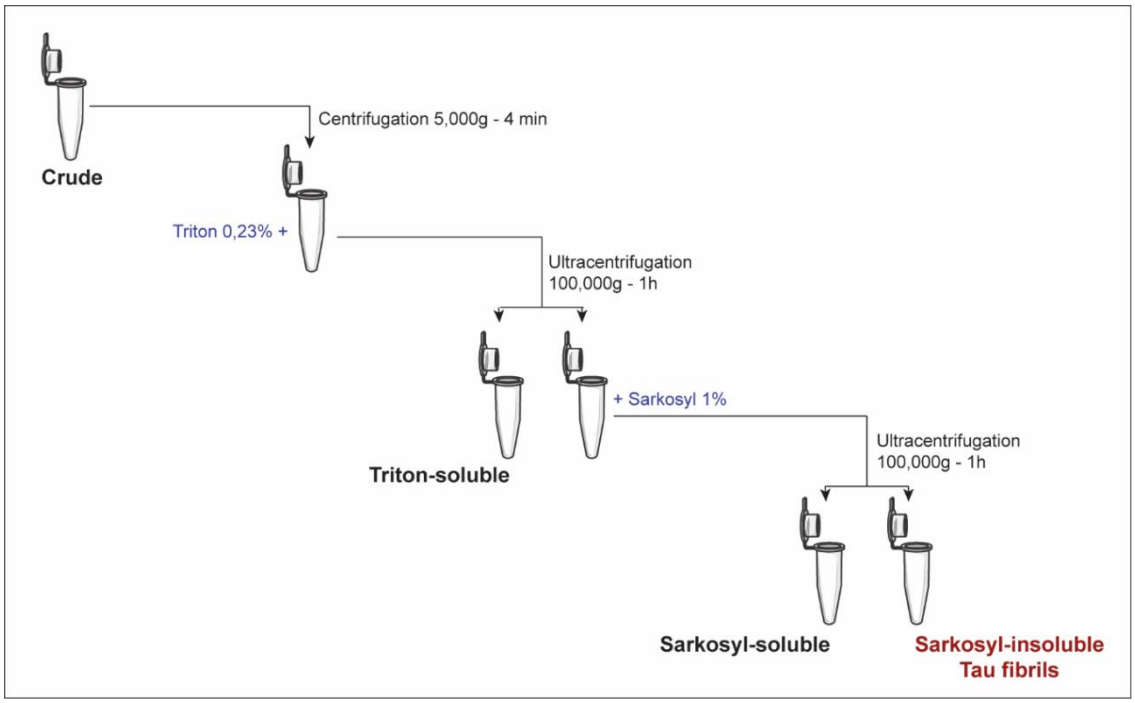

Figure 26: Sarkosyl fractionation protocol used for isolation of Tau fibrils

3) Western blots and dot blots

For western blot analysis, 15µg of samples were loaded onto a 4-12% Bis-Tris NuPAGE Novex gel (Invitrogen, Carlsbad, California, USA). This was followed by transfer onto a 0.2 µm nitrocellulose membrane using iBlot Dry Blotting System (Thermofisher, Carlsbad, California, USA). The membrane was incubated in a blocking solution containing 5% BSA (for AT100 immunoblotting) or 5% milk in TBS, 0.1% Tween for 1h at room temperature. Then, it was transferred in the antibody solution diluted in the blocking solution for incubation overnight at 4°C. The signal was then amplified by incubating the membrane 1h with the appropriate secondary antibody diluted in the blocking solution. The fluorescent signal was then visualized using Odyssey CLx Imager (Li-cor Biosciences, Germany) and analysis performed using Image Studio software (Li-cor Biosciences, Germany). For dot blot analysis, 15µg of non-denatured whole homogenates were deposed onto a 0.2 µm nitrocellulose membrane and allowed to pass through the membrane using a vaccum pump. The membrane was then processed for T22 immunoblotting as previously described (refce). Briefly, the membrane was incubated overnight in a 10% milk blocking solution. After three washes, it was transferred in the primary antibody solution diluted in 5% milk for incubation during 1h. The membrane was then rinsed 3 times and incubated 1h in the secondary antibody solution in 5% milk. Signal was then visualized as described above. For further description of antibodies and antibody dilutions, see **Table 4**.

Antibody	Reactivity	Species	Reference	Antibody dilution (blocking)
Western blot				
P2A	2A peptide	Rabbit	Millipore	1/5000 (5% milk in TBS + 0,1% Tween)
HT7	Human total Tau	Mouse	Innogenetics	1/2000 (5% milk in TBS + 0,1% Tween)
Tau46	Mouse, Rat and Human total Tau	Mouse	Santacruz	1/500 (5% milk in TBS + 0,1% Tween)
AT100	Human Tau pS212, pT214	Mouse	Thermofisher	1/4000 (5% BSA in TBS + 0,1% Tween)
Actin	Actin	Rabbit	Sigma-Aldrich	1/2000 (5% milk in TBS + 0,1% Tween)
Anti-mouse (HRP)	Mouse Ig	Sheep	GE Healthcare	1/5000 (blocking buffer used for primary)
Anti-rabbit (HRP)	Rabbit Ig	Donkey	GE Healthcare	1/5000 (blocking buffer used for primary)
Anti-mouse (800CW)	Mouse Ig	Goat	Licor	1/5000 (blocking buffer used for primary)
Anti-rabbit (680RD)	Rabbit Ig	Goat	Licor	1/5000 (blocking buffer used for primary)
Dot blot				
T22	Tau oligomers	Rabbit	Millipore	1/1000 (5% milk in TBS + 0,1% Tween)
Anti-rabbit (680RD)	Rabbit Ig	Goat	Licor	1/5000 (blocking buffer used for primary)

Table 4: Summary table of antibodies used in this study and the concentrations used for different applications
For each application, primary (top row) and secondary (bottom row) antibody dilutions are given. Ig: Immunoglobulin

4) MSD dosage of CSF total Tau

For MSD dosage, terminal CSF sampling from the cisterna magna was performed. 100-150µl of CSF samples were then vortexed before centrifugation at4 000 g for 10 min at 4°C. Samples were then aliquoted by 30µl and stored at -80°C. For human total Tau dosage (V-plex, MSD, USA), triplicates of each sample diluted to 1/4 in diluent 35 (MSD) were loaded onto plates. Dosage was then performed following manufacturer's instruction. CSF samples that were heavily contaminated with blood during collection were excluded from further analysis.

VII – Real-time quantitative PCR (RT-qPCR)

One or three months after injection, rats were anesthetized with 4% isoflurane before receiving a lethal dose of pentobarbital. Brains were then extracted and briefly rinced in PBS 0.1M before dissection of the hippocampus. The structure was then lysed in 1ml of trizol using Precellys 24 homogenizer (Bertin Technologies, Montigny-le-Bretonneux, France) and total RNA (including miRNAs) isolated using miRNeasy mini kit (Qiagen, Germany), following manufacturer's instructions. RNAs (0.125 µg) were then reverse-transcribed into cDNA using SuperScript VILO cDNA Synthesis Kit (Invitrogen, USA). Cycling parameter were 25°C for 10 min, 42°c for 1h and 85°C for 5 min. RT-qPCR was then performed using iTaq Universal SYBR Green Supermix (Biorad, USA) and primers (Biorad, USA or Eurofin Genomics, Les Ulis, France) specific to different targets on 1ng of cDNA, using 3nM of primers. See **Table 5** for the complete list of the primers used. Reactions were run in triplicates in 384-well PCR plates and the cDNA of four non-injected wistar rats served as an inter-plate reference. PCR cycling parameters were as follows: 95°C for 3 min, 40 cycles at 95°C for 10 s, and 60°C for 30 s. Dissociation temperature mounted 0.5°C/min from 60°c to 95°C. Cycle threshold (Ct) values were generated using Bio-Rad CFX manager software (regression mode). Results for each sample were then expressed using the following formula:

$$\Delta\Delta Ct = \frac{RQ_{G_{interest}}}{\sqrt{RQ_{G_{reference\,1}} \times RQ_{G_{reference\,2}}}}$$

Where:

$$RQ = (2^{E})^{Ct_{min} - Ct_{sample}}$$

And, where ***E*** represents the efficiency of each primer and ***Ct_{min}*** the minimum Ct value of all samples. Peptidylprolyl isomerase A (Ppia) and hypoxanthine phosphoribosyltransferase 1 (Hprt1) were used as the reference genes pair for quantification.

VIII – Statistical analysis

Results are presented as mean ± SEM. Statistical analysis was carried out using Statistica 13 software (Statsoft Inc., Tulsa, Oklahoma, USA). Prior to analysis, the data was assessed for normality and homogeneity of variance. If it fulfilled the criteria for general linear model, it was analysed by one-way ANOVA or factorial ANOVA followed by a Bonferroni's post-hoc test. Otherwise, a non-parametric equivalent was used. When no statistical difference between PBS and utGFP groups could be observed, those were pooled into a single control group for comparison to Tau constructs. For correlation studies, all data passed normality testing, allowing the use of Pearson correlation test. This was performed uniquely on Tau groups with exclusion of control animals. Annotations used throughout the manuscript to indicate level of significance are as follows: *p<0,05; **p<0,01; ***p<0,001.

Biorad PrimePCR primers

Gene symbol	Gene Name	Comment	Amplicon context sequence
Map1lc3a	Microtubule-associated proteins 1A/1B light chain 3A	= LC3-I = Atg8 Involved in autophagy	CATCGCTGACATCTATGAACAGGAGAAGGATGAAGACGGATTCCTCTACATGGTC TATGCCTCCCAAGAAACCTTCGGCTTCTGAGTCAAGAGGAGGGGTGGGGGGTGG CTGGGAGTTCTGGTCAGGTTCTCCCCAGGGAG
Becn1	Beclin-1	Involved in autophagy	CGAGTTTCAATAAATGGCTCCTCTCCTGAGTTAGCCTCTTCCTCCTGGCTCTCTCCT GGTTTCGCCTGGGCTGTGGTAAGTAATGGAGCTGTGAGTTCCTGAATGGTCACTC GGTCCAGGAT
Lamp1	Lysosome-associated membrane glycoprotein 1	Involved in autophagy	ACCACAAGAGCTGCTATTCTTCAGGACTTCTGCAGAGGCTGGCAGGGTCATATTC GAGACCTTAGAAACATGTCCAGCATCATAGGTGGTCAGAAAGGAGGCAGAGAA GCTGGCCATTATACACGCTGTGCCGTTGTTGTCTTTC
Stub1	STIP1 homology and U-Box containing protein 1	= CHIP = E3 ubiquitin-protein ligase Component of the proteasome	AGCTCACTCTCCTGGTGGATGCGCCGTTCCTCGATACTGTTCCAGCGCTTCTTCTT AGCAATGCGAAGGGCACTAGGAATATCATCCCCAAAGTTGAGTCGCTGCTCCTTG GC
Htra1	Serine protease HTRA1		GATCGACAGGCCAAAGGGAAAACTGTCACCAAGAAGAAGTATATTGGGATACGA ATGATGTCGCTTACATCTAGCAAAGCCAAAGAACTGAAGGATCGTCACCGAGACT TCCCG
Casp3	Caspase-3, Caspase-3 subunits p12 and p17	Component of the apoptosis pathway	TTTTGTAACTGCTGTCCAGATATATTCCAGAGTCCATCGACTTGCTTCCATGGATAG TCTTTGTTTCAAAATTATTAATGGATTTTGAATCCACGGAGGTTTCGTTGTTGTCCAT GGTCACTTTTCTTCGCGTTCCAAGCTCCGC
Casp6	Caspase 6	Component of the apoptosis pathway	TGAAGTGAAATGCTTTAACGACCTCCGGGCAGAAGAACTACTGCTCAAGATTCAC GAGGTGTCGACTTCCAGCCACGTAGATGCCGATTGCTTCCTGTGTGTCTTCC
Dlg4	Disks large homolog 4	= PSD95 Component of the post-synaptic density	CAATGCCTACCTGAGTGACAGCTATGCTCCCCCAGACATCACAACCTCGTATTCT CAGCACCTGGACAATGAGATCAGTCATAGCAGCTACTTGGGCACTGACTACCCC ACAGCCATGACCCC
Syp	Synaptophysin	Component of the pre-synaptic vesicles	GGGGCTGCCCAGCCTGTCTCCTTGAACACGAACCATAAGTTGCCAACCCAGAGC ACCAGGTTCAGGAAGCCAAACACCACTGAGGTGTTGAGTCCTGAAGTCACAGGG TCCCTCAGTTCCTTGCATGTGTTCCCTGTCTGGCGG
Aif1	Allograft inflammatory factor 1	= Iba1 Microglial marker	AGGGAGCATTATTTATTTAGTTTGACTCTGGCTCACAACTGCTTCTTCTTTTCCCATG CTGCTGTCATTAGAAGGTCCTCGGTCCCACCGTGTTATATCCACC
Mertk	Tyrosine-protein kinase Mer	Glial phagocytosis receptor	TATCCGGGAATATAGCAGGAAGGTGTGGAGGTCTCCGTATTTCATGAAGGGTAAA ATCACCATGGGCTTCGGGATGCCTTGAGAGCTCAGTTCTATACACACGCCTAGAA GCCGGATGACGTTTGGGTGAT
C1qa	Complement C1q subcomponent subunit A		GCTCTGCAGACATCTTCAGCCACTGTCCATACCAGGGTCACGGCCAGCACACAA GCCACCAGCCATCCCTGAGAGGTCTCCATGATGTTCCTGCCTCCGTGGTCCGC
C3	Complement C3 precursor		GTGAAGGACTCCTGTGTAGGCACGCTGGTGGTGAAAGGTGACCCAAGAGATAAC CGACAGCCCGCGCCTGGGCATCAAACGACACTAAGGATCGAGGGGAACCAGG GGGCCCGAGTGGGGCTAGTGGCTGTGGACAAGGGGGTGT
Clu	Clusterin precursor	Chaperone protein Genetic risk factor for Alzheimer's disease	CCTGGACGGCGTTCTGAATCTCCTTATTAACATACCTACTTCCTTGAGTGGACAGT TCTTGGAGCTCATTGTCAGAGAACTCCTGCTCTCCCAGGACCATGCCATTGTC

Inhouse designed primers

Gene symbol	Gene Name	Comment	Forward sequence	Reverse sequence
Tau46	Human Tau	No cross-reactivity with murine Tau	TGGGGGACAGGAAAGA	CCTCAGATCCGTCCTCAGTG
Grin2a	Glutamate receptor, ionotropic, N-methyl D-aspartate 2A	= NMDA post-synaptic receptor	ACAGGGACCCTAAGTGGCGAC	CCAGCAGCACCGCAATG
Snap25	synaptosome associated protein 25	Pre-synaptic vesicle-associated protein	TCCGCAGGGTAACAAACGATG	TCCGATGATGCCGCTCAC
GFAP	Glial fibrillary acidic protein	Astrocytic marker	AATGACTATCGCCGCCAAC	CTCCTGGTAACTCGCCGACT
Vim	Vimentin	Astrocytic marker	GCAAAGCAGGAGTCAAACGA	AATTCTCTTCCATTTCACGCATCT
TNFα	Tumor necrosis factor alpha	Cytokine	CACCACGCTCTTCTGTCTACTGAAC	TGTGAGGGTCTGGGCCATAG
Hprt1	Hypoxanthine-guanine phosphoribosyltransferase 1	Reference gene	GGACCTCTCGAAGTGTTGGATAC	CCCTGAAGTGCTCATTATAGTCAAG
Ppia	Peptidylprolyl isomerase A	= Cyclophilin Reference gene	ATGGCAAATGCTGGACCAAA	GCCTTCTTTCACCTTCCCAAA

Table 5: List of the different primers used in the RT-qPCR experiment

The sequence amplified during RT-qPCR is given for genes studied using Biorad primers. For in-house designed primer pairs, the sequence of forward and reverse primers is given.

RESULTS

RESULTS

I – Optimization of injection conditions for optimal vector expression

1) *In vitro* and *in vivo* validation of Tau constructs

Before AAV production and injection, the expression of Tau constructs was validated *in vitro*. For this purpose, HEK-293T cells were transfected with Tau plasmids. Western blot analysis was then performed using antibodies detecting either full-length Tau (HT7) or the pro-aggregation peptide (P2A; **Figure 27 – A**). HT7 detected Tau at the correct molecular weight in all constructs, confirming that Tau was correctly expressed in all conditions. In addition, the 2A peptide, which remains attached to the pro-aggregation peptide (TauRD-ΔK280) after cleavage, was detected at the expected molecular weight of TauRD-ΔK280 after transfection of the hTAU^{ProAggr} construct. This suggests that the chimeric protein was indeed cleaved *in vitro*, releasing TauRD-ΔK280 and hTAU^{WT} in similar proportions. Consistent with this result, no HT7 or P2A staining could be observed at 90 kDa, corresponding to the molecular weight of the uncleaved chimeric protein. Cleavage was confirmed *in vivo* by means of HT7 and P2A co-labelling in rats injected with the hTAU^{ProAggr} vector (**Figure 27 – B**). Both epitopes were found in the same cells, but the sub-cellular localization only partially overlapped, suggesting cleavage of the protein *in vivo*.

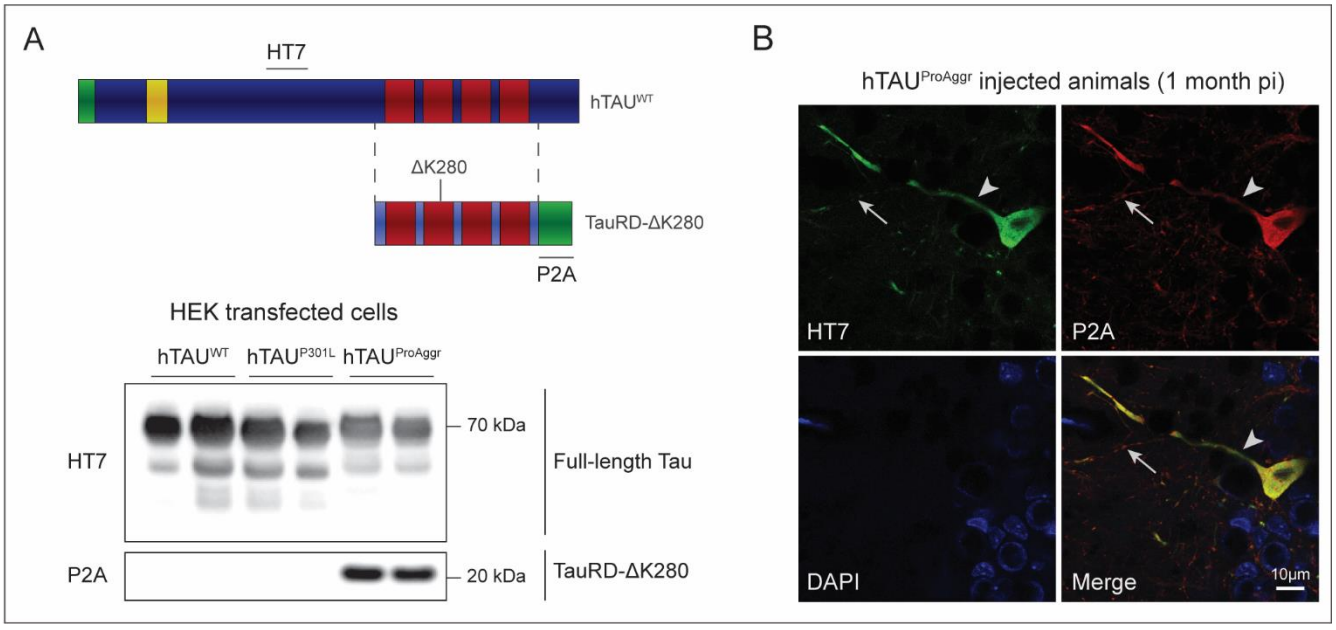

Figure 27: Validation of Tau constructs – Expression and cleavage of the 2A peptide

A) *Western blot analysis on HEK-293T cells transfected with Tau constructs. HT7 antibody detected full-length Tau (but not the pro-aggregation peptide) at the molecular weight of monomeric Tau. The epitope of the anti-P2A antibody remained attached to the pro-aggregation peptide (TauRD-ΔK280), allowing its detection. P2A signal was observed only in the hTAU^{ProAggr} construct, at the expected molecular weight.* ***B)*** *HT7/P2A co-labelling in hTAU^{ProAggr} expressing animals 1 month post-injection. Hippocampal neurons were positive for both HT7 and P2A. Some processes were HT7 positive but only weakly P2A positive (arrowhead) while some neurites were P2A positive but negative for HT7 (arrow).*

2) <u>Validation of injection coordinates for optimal transduction of the entire HC</u>

To determine the optimal injection coordinates, rats were injected with AAV2/8 vectors expressing green fluorescent protein (GFP) under the control of the CBA promoter. Injection coordinates were chosen in order to achieve good transduction of the CA1 hippocampal subfield, a sub-region affected at an early stage in AD and related tauopathies (Braak and Braak, 1991). Two weeks after injection, rats were perfused and direct fluorescence was assessed using epifluorescence microscopy (**Figure 28**). Animals injected in the dorsal and ventral hippocampus at two different antero-posterior levels presented GFP expression in most of the hippocampal subfields, including CA1/2 and CA3/4 sub-regions as well as the dentate gyrus (DG). Hence a good transduction of both dorsal and ventral HC with large diffusion to the entire structure on the antero-posterior axis was achieved, with no diffusion to adjacent regions.

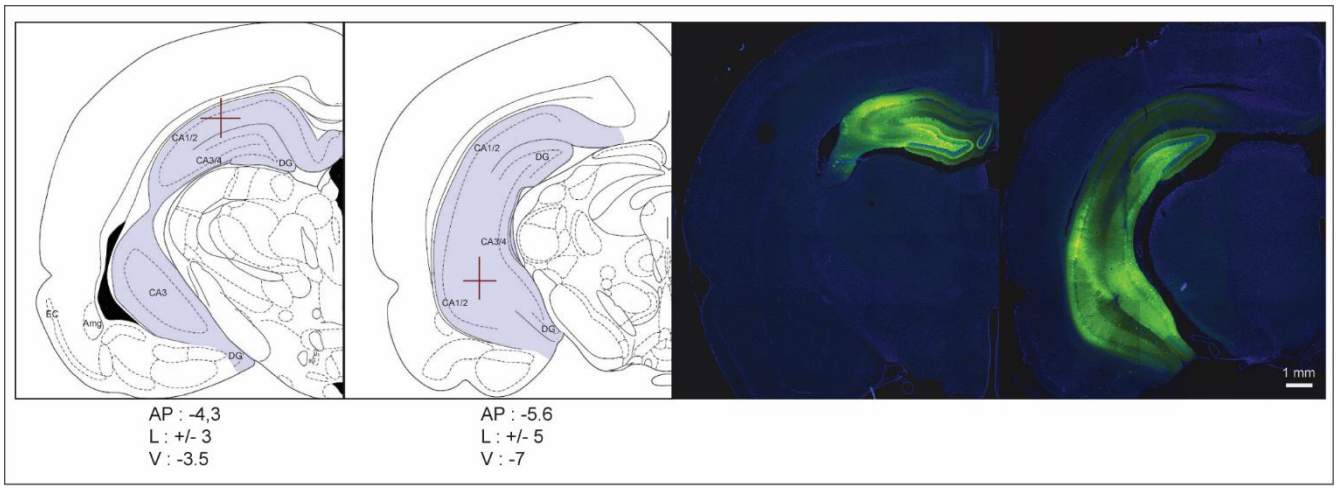

Figure 28: GFP expression analysis for validation of injection coordinates
Rats were injected with AAV2/8-CBA-GFP vector at two distinct sites, one in the anterior dorsal HC (AP: -4,3mm; L: +/- 3mm; V: -3,5mm) and one in the posterior ventral HC (AP: -5,6mm; L: +/-5mm; V: -7mm). Direct fluorescence was observed 2 weeks post-injection, showing large diffusion of the vector on the antero-posterior axis and good transduction of both dorsal and ventral HC with no expression in adjacent regions at this time-point. Abbreviations: Amg, Amygdala; AP, antero-posterior; DG, Dentate gyrus; EC, Entorhinal cortex; L, lateral; V, ventral.

II – Induction of Tau pathology in the HC of adult rats after overexpression of Tau constructs

Once all injection conditions were optimized, rats were injected with each of the 3 Tau constructs (hTAU^{WT}, hTAU^{P301L} and hTAU^{ProAggr}). In addition, animals were injected with AAV vectors encoding an untranslated GFP protein (utGFP) as a control for vector expression. Lastly, rats injected with PBS served as a control for the mechanical lesion induced by the injection. Characterization of those different models was performed at 1 and 3 months post-injection to determine whether the induced Tau pathology was similar in all Tau groups.

1) <u>Expression levels of Tau constructs in vivo</u>

First, we aimed to assess the amount of Tau overexpression induced by the different constructs. To this purpose, rats were injected with AAV2/8 vectors encoding each construct and Tau protein level in the hippocampus was assessed by western blot 1 month post-injection (**Figure 29, A**) using the Tau46 antibody that recognizes both human and murine Tau (**Figure 29, B**). Total Tau expression was found to be 6 to 7-fold the level of endogenous Tau in hTAU^{WT} and hTAU^{P301L} groups (**Figure 29, C**).

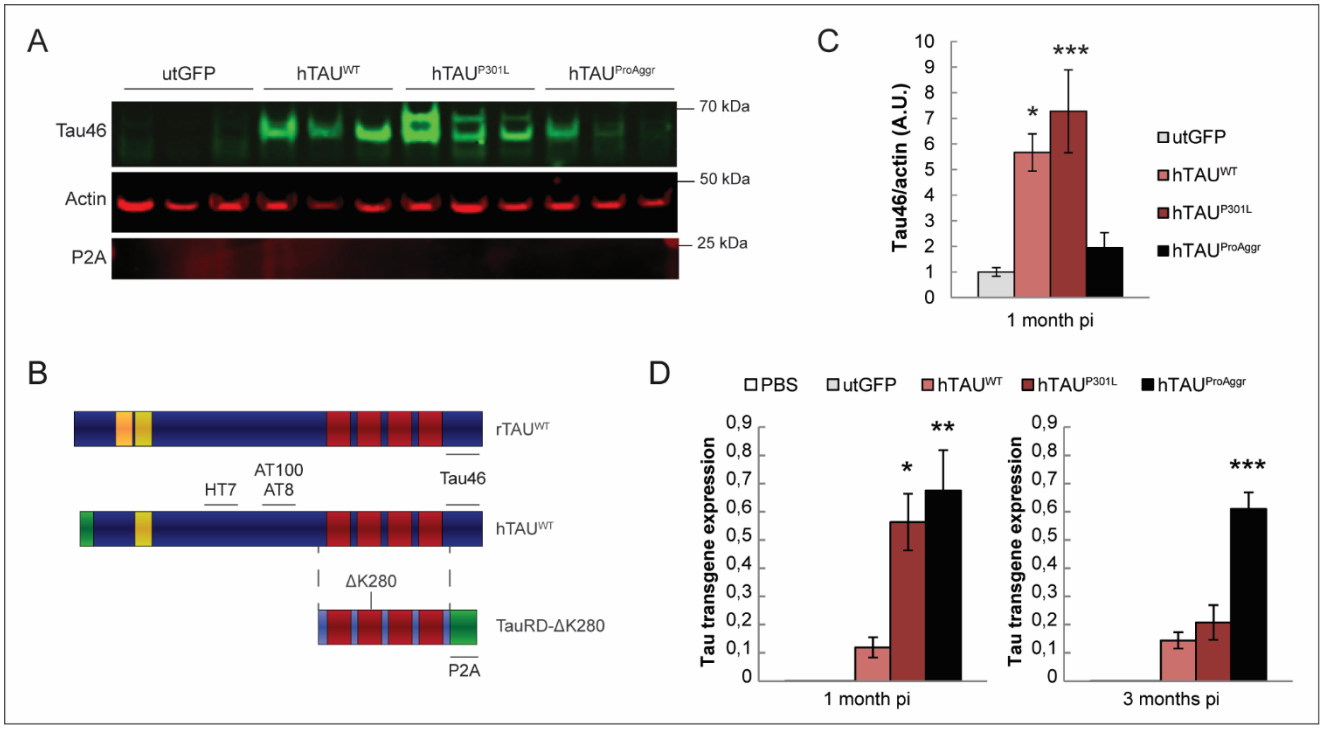

Figure 29: Evaluation of the level of Tau over-expression induced by each construct on crude hippocampal homogenates

A) *Representative blot for total Tau (Tau46) and actin expression at 1 month post-injection.* ***B)*** *Schematic representation of murine and human Tau showing the localisation of antibody epitopes.* ***C)*** *Quantification of Tau expression by western blot in all groups, normalized to actin (n=6/group). A significant increase in Tau expression was observed in both hTAU^{WT} and hTAU^{P301L} but not hTAU^{ProAggr} when compared to utGFP (One-way ANOVA, p<0.001, Bonferroni post-hoc test). Stars represent the result of post-hoc comparisons to utGFP.* ***D)*** *RT-qPCR for the Tau transgene showed a significant increase in both hTAU^{P301L} and hTAU^{ProAggr} groups but not hTAU^{WT} group when compared to controls at 1 month post-injection (Kruskal-Wallis non parametric test, p < 0.001, Dunn's multiple comparison test, n=3-6/group). Conversely, only animals from the hTAU^{ProAggr} group were found to be significantly elevated when compared to controls at 3 months post-injection (Kruskal-Wallis non parametric test, p < 0.001, Dunn's multiple comparison test). Stars represent the result of post-hoc comparisons to PBS group. *p< 0.05, **p<0.01, ***p< 0.001.*

In contrast, Tau expression was found to be only weakly elevated in hTAU^{ProAggr} group when compared to utGFP (representing about 1,5-fold the endogenous level). Surprisingly, no staining for P2A could be detected in any of the animals from the hTAU^{ProAggr} group.

We next aimed to determine whether those differences in human Tau protein levels were resulting from differences in transgene expression. To this purpose, RT-qPCR was performed, using primers targeting an N-terminal sequence present uniquely in human Tau, to assess the level of transgenes mRNAs (**Figure 29, D**). Transgene mRNA was detected specifically in all Tau groups at 1 month post-injection. Differences in expression levels were observed, however, with a significant increase in both hTAU^{P301L} and hTAU^{ProAggr} groups, but not in the hTAU^{WT} group, when compared to controls. In contrast, at 3 months post-injection, only animals from the hTAU^{ProAggr} group showed increased transgene expression when compared to controls. Those differences in expression and the diminution observed in the hTAU^{P301L} group over time may be related to the selective loss of transgene-expressing cells. Indeed, analysis of Tau overexpression was performed at 1 month post-injection because this time-point coincides with the peak of transgene expression with AAV8 vectors (Klein et al., 2008a). However, pathological processes may already be in place at this time. This hypothesis will be addressed in later sections. The finding that hTAU^{ProAggr} animals present the highest level of transgene mRNA suggest that the low level of Tau protein observed by western blot in this group is not related to a reduced transgene expression compared to the other Tau constructs. This will also be discussed in later sections.

2) <u>Hyperphosphorylation of Tau and missorting to the dendrosomatic compartment</u>

We next aimed to study if Tau overexpression was able to recapitulate the main features of tauopathies. To this purpose, immunohistochemistry was performed on all animals using the AT8 antibody (**Figure 30**) that detects a phospho-epitope commonly found in patients with a tauopathy (phospho-Ser202, phospho-Thr205). This antibody is commonly used for Braak staging for the diagnosis of post-mortem samples (Braak and Braak, 1991).

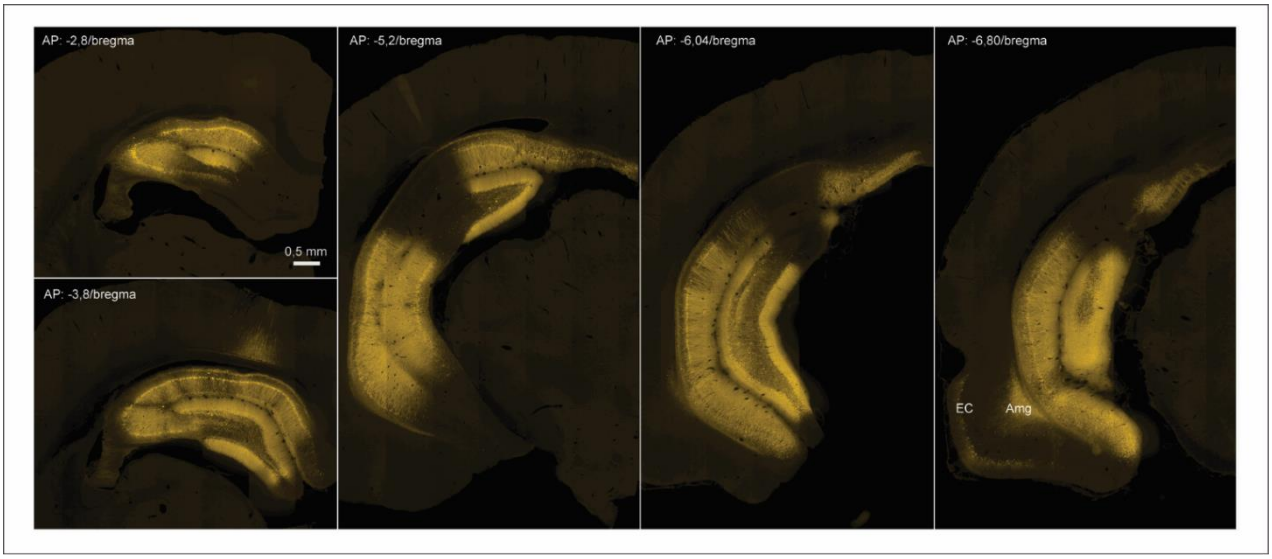

Figure 30: Extent of AT8 Tau pathology on the rostro-caudal axis of the hippocampus
Representative images of the extent of Tau pathology in the HC of one animal of the hTAU^{P301L} group 1 month post-injection. Brain sections were processed for immunohistological analysis using AT8 antibody (yellow). Tau hyperphosphorylation could be detected in the entire hippocampus, both in dentate gyrus and hippocampal subfields. Hyperphosphorylated Tau could sometimes be observed in neighbouring regions such as the amygdala (Amg) and the entorhinal cortex (EC). Similar pattern of Tau pathology could be observed in hTAU^{WT} and hTAU^{ProAggr} groups.

Extensive hyperphosphorylation of Tau was detected in all groups, spanning the entire hippocampus on the antero-posterior axis. In addition, AT8 staining was sometimes observed in neighbouring regions, including entorhinal cortex and amygdala.

This hyperphosphorylation was associated in all Tau groups with missorting of the protein to the somatodendritic compartment, as opposed to its major axonal localisation in physiological conditions (**Figure 31, A, inserts**). Conversely, no AT8 staining could be observed in either utGFP or PBS control group (data not shown). Quantification of AT8 immunofluorescent staining showed differences between groups in the extent of Tau hyperphosphorylation. Hence, mean fluorescence intensity (MFI, **Figure 31, B**) at 1 month post-injection was found to be 30 to 40% higher in the $hTAU^{WT}$ group compared to $hTAU^{P301L}$ and $hTAU^{ProAggr}$ group respectively.

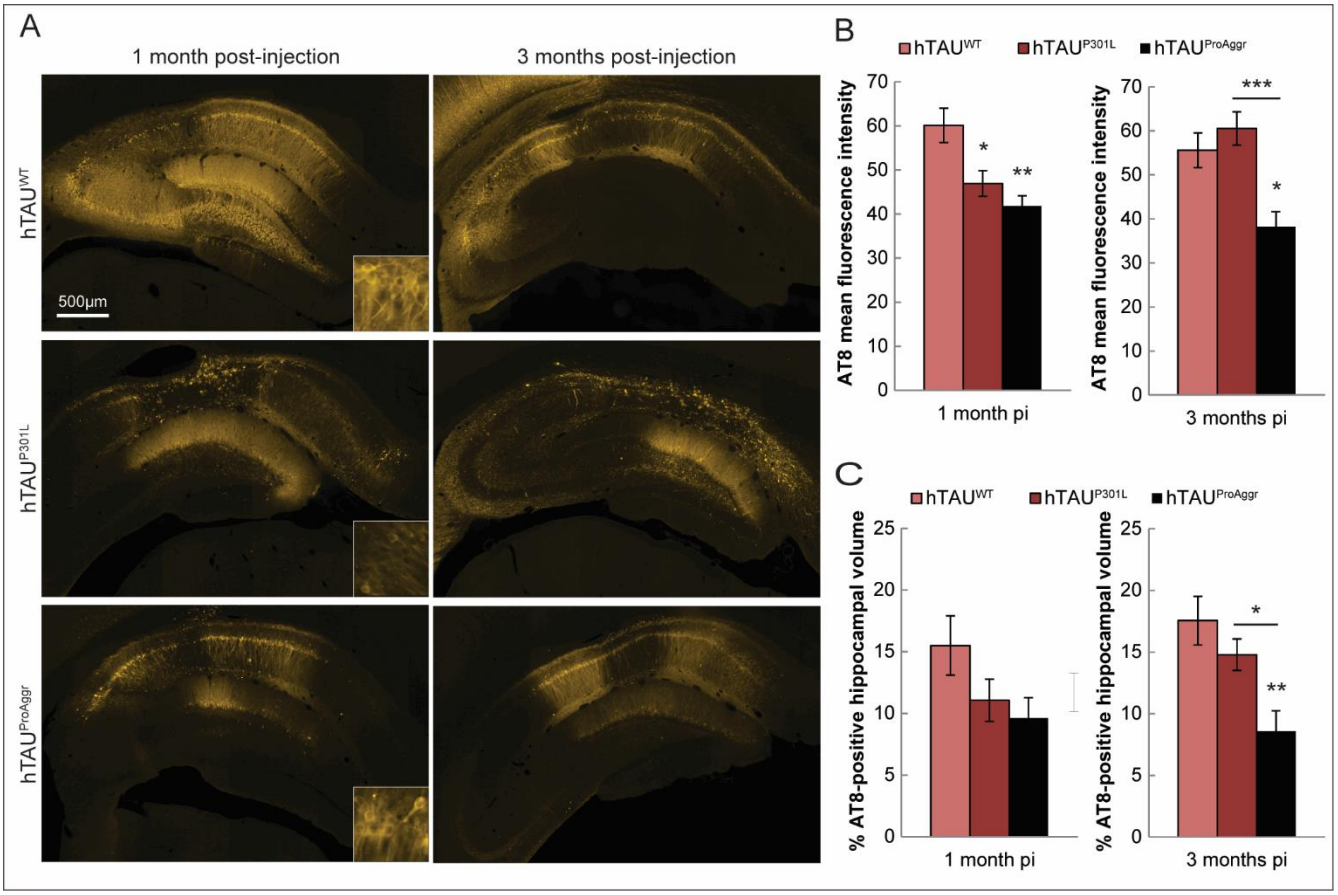

Figure 31: Histological assessment of the extent of Tau hyperphosphorylation induced by different constructs using AT8 antibody

A) *Representative images of AT8 immunofluorescent staining in all groups at 1 and 3 months post-injection. Inserts show missorting of AT8-positive Tau to the somatodendritic compartment.* ***B)*** *Quantification of AT8 mean fluorescence intensity (MFI) showed higher extent of Tau hyperphosphorylation in the $hTAU^{WT}$ group at 1 month post-injection compared to $hTAU^{P301L}$ and $hTAU^{ProAggr}$ groups (One-way ANOVA, p<0.01, Bonferroni post-hoc test). Conversely, both $hTAU^{WT}$ and $hTAU^{P301L}$ showed elevated AT8 MFI compared to $hTAU^{ProAggr}$ group at 3 months post-injection (One-way ANOVA, p<0.001, Bonferroni post-hoc test).* ***C)*** *Quantification of the percentage of AT8-positive hippocampal volume yielded quite similar results. Indeed, while no difference between groups could be observed at 1 month post-injection (One-way ANOVA, p=0.11), both $hTAU^{WT}$ and $hTAU^{P301L}$ groups were found elevated compared to $hTAU^{ProAggr}$ group at 3 months post-injection (One-way ANOVA, p<0.01, Bonferroni post-hoc test). Stars in B) and C) represent results of the post-hoc comparison to $hTAU^{WT}$. Additional group differences are also indicated. *p<0.05, **p<0.01, ***p<0.001.*

Interestingly, while this difference between hTAU^{WT} and hTAU^{ProAggr} groups remained at 3 months post-injection, MFI in the hTAU^{P301L} group increased at this time-point, to a level similar to hTAU^{WT}. Altogether, those results suggest that Tau constructs may differ in the extent and kinetics of Tau hyperphosphorylation. Similar results were obtained when looking at the percentage of hippocampal volume occupied by AT8 staining (**Figure 31, C**), although with less obvious group differences. Indeed, although no significant difference could be observed between groups at 1 month post-injection (10-15% of AT8-positive HC volume), hTAU^{WT} and hTAU^{P301L} groups were found to be significantly increased at 3 months compared to the hTAU^{ProAggr} group. This relatively low percentage of AT8-positive hippocampal volume observed in all groups may be related to the stringent thresholding parameters applied here (see section IV – 5 of the material & methods section).

3) <u>Differential induction of Tau aggregation with Tau constructs</u>

We next aimed to study whether Tau constructs were able to induce Tau aggregation. Immunohistochemistry using AT100 antibody, that recognizes a phospho-epitope (phospho-Thr212, phospho-Ser214) found to be enriched in PHFs in human tauopathies, was performed on all groups at 1 and 3 months post-injection (**Figure 32**).

AT100-positive neurons were observed in all hippocampal subfields in both hTAU^{P301L} and hTAU^{ProAggr} groups as early as 1 month post-injection (**Figure 32, A**). More precisely, AT100 staining was observed filling the somatic compartment. Additional neuritic staining, in the form of “string of beads”, was also observed in both groups, thus mirroring missorting of pathological Tau observed with AT8 antibody. In contrast, the overexpression of hTAU^{WT} construct did not lead to significant Tau aggregation up to 3 months post-injection. Counting of AT100-positive somas indeed showed a large increase in both hTAU^{P301L} and hTAU^{ProAggr} groups when compared to hTAU^{WT}, this difference being more pronounced in the CA3/4-DG region owing to a large number of AT100-positive somas observed in the ventral DG (**Figure 32, B, C and D**). The AT100 epitope is located outside of the repeated regions, which means that only aggregates containing full-length Tau were visualized with this antibody, whereas pure aggregates of TauRD-ΔK280 would not be detected. Thus, the co-expression of TauRD-ΔK280 with hTAU^{WT} in the hTAU^{ProAggr} group strongly promoted the aggregation of the wild-type form of human full-length Tau, which alone was not able to aggregate.

No difference in the number of AT100-positive somas could be observed between hTAU^{P301L} and hTAU^{ProAggr} groups at 1 month post-injection, suggesting that both constructs presented with the same ability to induce aggregation. However, while the number of AT100-positive somas increased in the hTAU^{P301L} group between 1 and 3 months post-injection, aggregation in the hTAU^{ProAggr} group peaked at 1 month and decreased at 3 months post-injection. This suggests that the kinetics of aggregation may be different between those two groups or that they differ in clearance processes.

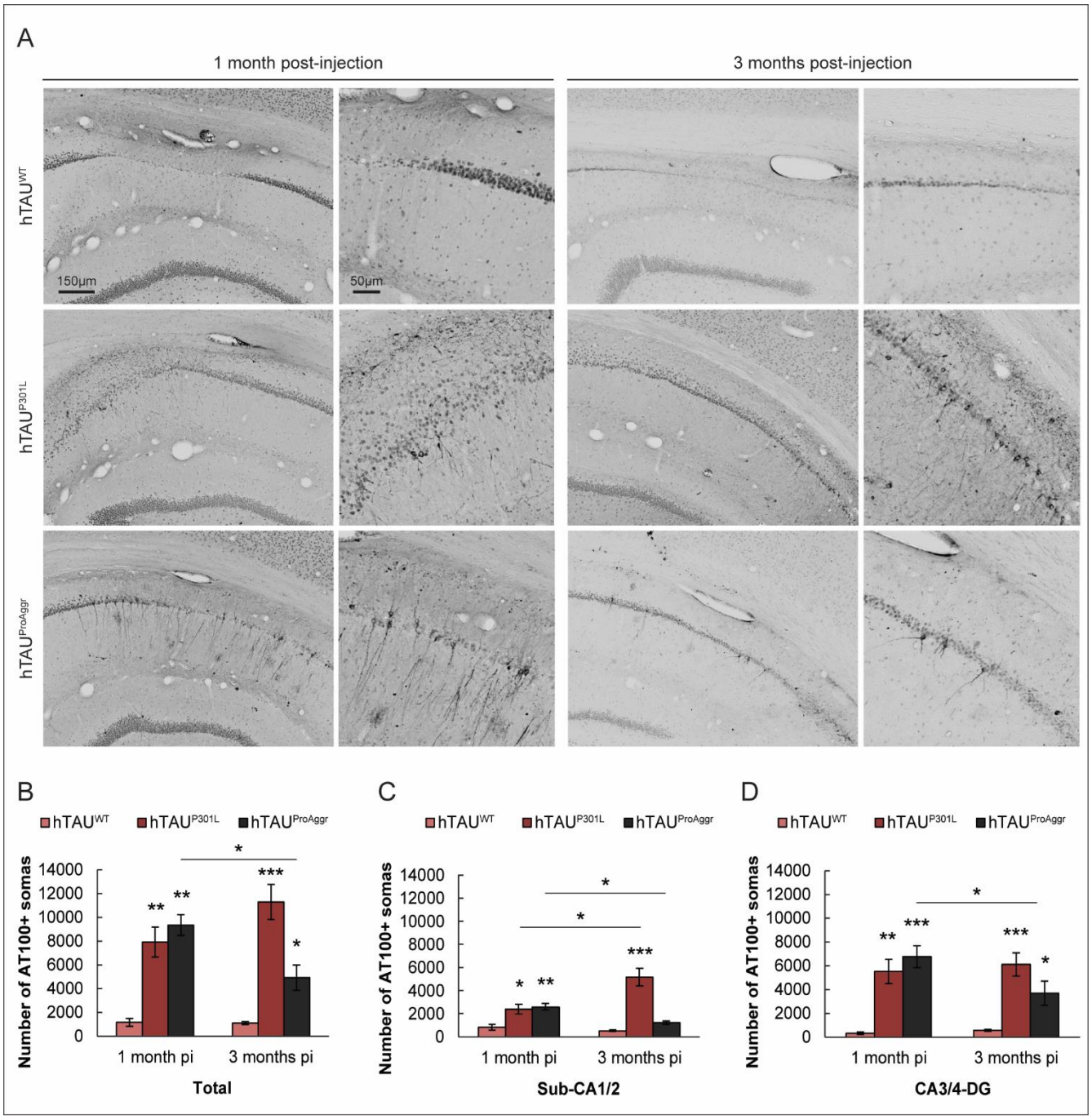

Figure 32: Histological assessment of the level of aggregation induced by Tau constructs

A) *Representative images of AT100 staining in hTAU^{WT}, hTAU^{P301L} and hTAU^{ProAggr} groups.* ***B, C*** *and* ***D)*** *Number of AT100-positive neuronal somas in a given hippocampal subregion: B, Total; C, Sub-CA1/2-; D, CA3/4-DG. A significant increase in the number of AT100-positive somas was observed in both hTAU^{P301L} and hTAU^{ProAggr} groups when compared to hTAU^{WT} at 1 and 3 months post-injection (Kruskal-Wallis non parametric between group comparison at each time-point, p<0.001 (Total and CA3/4-DG), p<0.01 (Sub-CA1/2) at 1 month and p<0.001 (Total, Sub-CA1/2 and CA3/4-DG) at 3 months post-injection. Dunn's multiple comparison test, n=7-8/group). An increase in the number of AT100-positive somas was observed in the hTAU^{P301L} group between 1 and 3 month post-injection while the number of positive somas in the hTAU^{ProAggr} group diminished (Kruskal-Wallis between time-points comparison on each group separately, hTAU^{P301L}, p<0.05 (Sub-CA1/2), hTAU^{ProAggr}, p<0.05 (Total, Sub-CA1/2 and CA3/4-DG). Dunn's multiple comparison test, n=7-8/group). Stars above each bar represent the result of post-hoc comparisons to hTAU^{WT}. Significance between 1 and 3 months post-injection for each group is represented. *p<0.05, **p<0.01, ***p<0.001*

The total quantity of Tau aggregates was further assessed by western blot analysis on whole HC homogenates (**Figure 33, A**). Interestingly, asignificant AT100 signal was observed only in the hTAU^{P301L} group, with a trend towards an increase between 1 and 3 months post-injections (**Figure 33, B**). Conversely, no AT100 signal was observed in both hTAU^{WT} and hTAU^{ProAggr} groups.

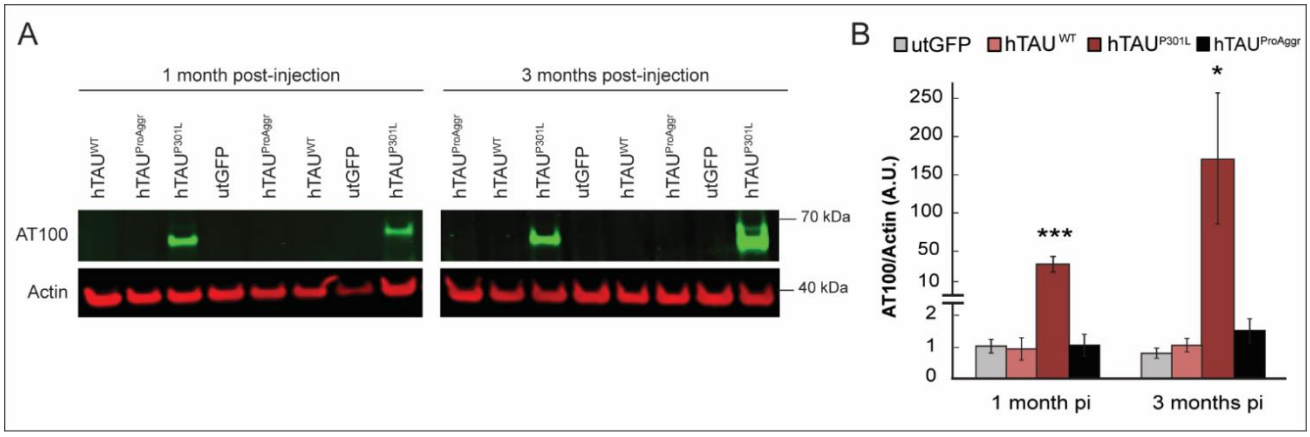

Figure 33: Western blot analysis of the extent of Tau aggregation using AT100 antibody
A) *Representative blots for AT100 signal on whole HC homogenates.* ***B)*** *Quantification of AT100 signal normalized to Actin (Kruskal-Wallis between group comparison at each time-point, p<0.01 at 1 and 3 months post-injection. Dunn's multiple comparison test, n=6/group). Stars represent result of post-hoc comparisons to utGFP. *p< 0.05, ***p< 0.001.*

The discrepancy between histological and biochemical results could be explained by the fact that analysis of Tau aggregation by counting of AT100-positive somas does not take into account the quantity of aggregated Tau in neurites. The total quantity of Tau aggregates in the hTAU^{ProAggr} may thus be reduced compared to hTAU^{P301L} and here failed to reach the detection threshold. Alternatively, it could be that an excessive size of aggregates in the hTAU^{ProAggr} group may preclude them to enter the gel. Ultrastructural studies of aggregates morphology should help resolve this issue.

We next aimed to assess more precisely the nature of Tau aggregates produced by each construct. More specifically, we wanted to determine the stage of aggregation achieved with different Tau constructs. To this purpose, Gallyas silver impregnation was performed (**Figure 34, A**), a staining frequently used to detect mature NFT pathology. Consistent with previous histological results obtained using AT100 antibody, Gallyas-positive neuronal somas and neurites, forming tangle-like lesions, were observed in both hTAU^{P301L} and hTAU^{ProAggr} groups but not in the hTAU^{WT} group as early as 1 month post-injection. The number of Gallyas-positive somas seemed qualitatively higher in the hTAU^{ProAggr} group compared to the hTAU^{P301L} at both time-points. Although this result remains to be confirmed by proper quantification, it suggests that the hTAU^{ProAggr} construct may induce stronger aggregation than the hTAU^{P301L} vector.

To confirm those results, sarkosyl fractionation was performed on hippocampal homogenates from the different groups in order to isolate Tau fibrils. Tau fibrils were detected in both hTAU^{WT} and hTAU^{P301L} groups as early as 1 month post-injection using HT7 antibody (**Figure 34, B**). Surprisingly, only little sarkosyl-insoluble material could be detected in the hTAU^{ProAggr} group. This was consistent with western blot results showing no AT100 staining in this group but showed strong discrepancy with histological results. Interestingly, isolated Tau fibrils in hTAU^{WT} and hTAU^{P301L} groups were only weakly stained with AT100 antibody (**Figure 34, C**) at 1 month post-injection.

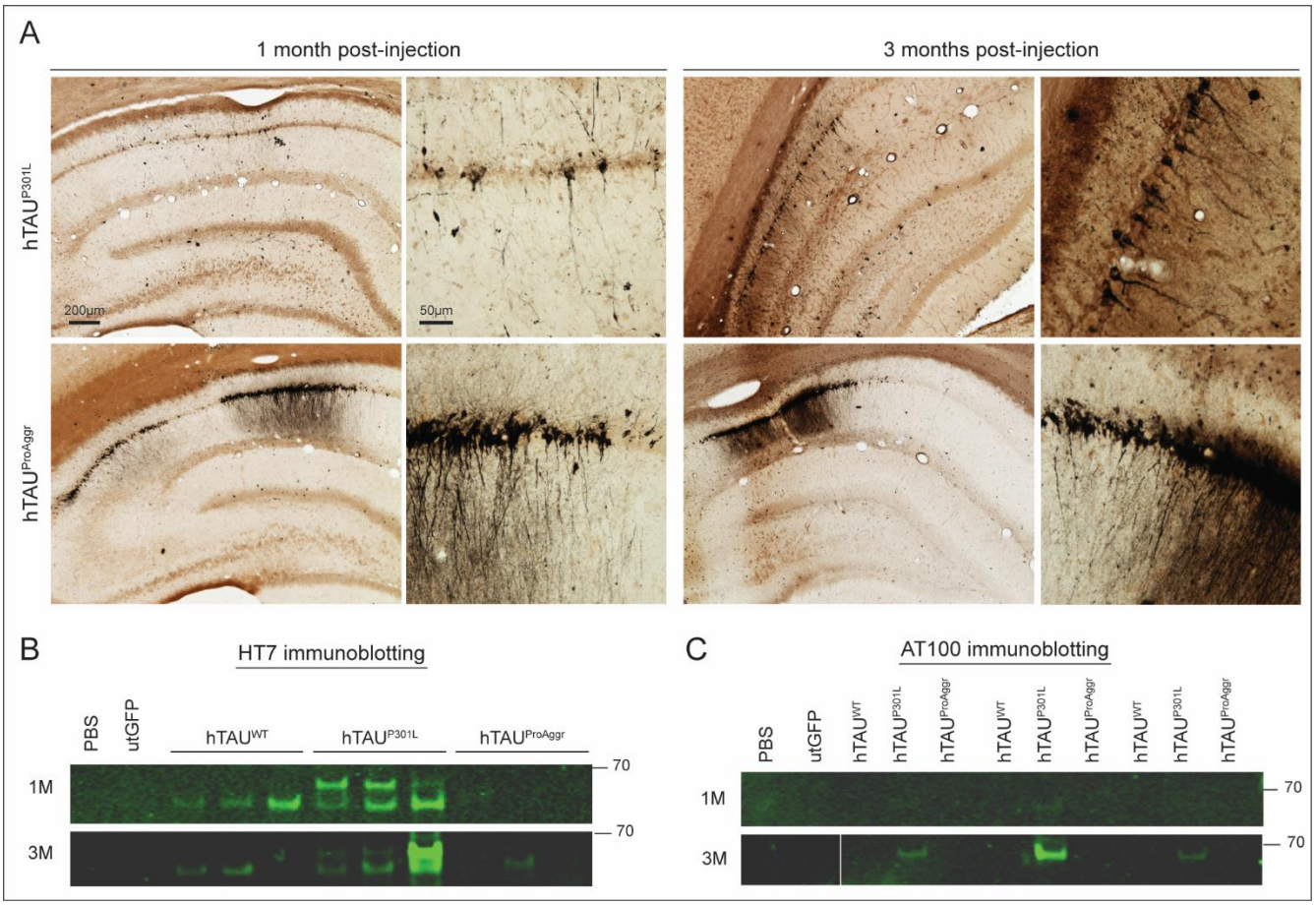

Figure 34: Characterization of the stage of Tau aggregation achieved with different constructs
A) *Representative images of Gallyas silver impregnation (in black) showing the presence of argyrophilic tangle-like lesions in hTAU^{P301L} and hTAU^{ProAggr} animals as early as 1 month post-injection. The number of tangle-like structure seemed qualitatively higher in the hTAU^{ProAggr} group at both time-points.* ***B)*** *Western blot of sarkosyl-insoluble fraction using HT7 antibody at 1 month (1M) and 3 months post-injection (3M) detected fibrillar material in both hTAU^{WT} and hTAU^{P301L} groups as early as 1 month post-injection. Conversely, only weak HT7 signal was detected in the hTAU^{ProAggr} group at 3 months post-injection.* ***C)*** *Western blot of sarkosyl-insoluble fraction using AT100 antibody showed only weak signal in hTAU^{P301L} group at 1 month post-injection (1M). Strong increase in AT100 signal was observed in this group between 1 and 3 months post-injection (3M) while no staining was detected in hTAU^{WT} and hTAU^{ProAggr} groups.*

This is consistent with our previous result of few AT100-stained somas in the hTAU^{WT} group. This also suggests that the majority of AT100-positive material in the hTAU^{P301L} group was non-fibrillar. The observation of HT7-positive and AT100-negative Tau fibrils at this time-point suggests that AT100 epitope may not necessarily be a pre-requisite to fibril formation. The number of AT100-positive fibrils in the hTAU^{P301L} group seemed to increase between 1 month and 3 months post-injection. This followed the progression of AT100-positive somas observed in histological analyses and may suggest conversion of AT100-positive non-fibrillar aggregates into a fibrillary form. Interestingly, two bands were observed in the hTAU^{P301L} group stained with HT7. This is reminiscent of the shift in apparent molecular weight observed in human tauopathies, characterizing Tau hyperphosphorylation. This observation uniquely in the hTAU^{P301L} group, may suggest that this construct induces more post-translational modifications of the protein compared the other groups, in addition to the AT8 epitope that was not significantly increased in this group compared to hTAU^{WT} (see *Figure 31* in section II - 2 of those results).

Following the finding that Tau constructs differed by their ability to induce aggregation as well as in the type of aggregates generated, we next aimed to assess whether those also presented differences in the amount of oligomeric Tau species produced. To this purpose, dot blot analysis using T22 antibody, which was found to selectively bind Tau oligomers *in vitro* and in the brain of AD patients (Lasagna-Reeves et al., 2012a), was performed at 1 month post-injection on whole hippocampal homogenates (**Figure 35, A**). Quantification of T22 staining in all groups (**Figure 35, B**) did not reveal differences between any of the Tau groups and utGFP control animals. Considering the high background signal observed in the utGFP group, however, it may be possible that analysis on whole homogenates may have hindered correct detection of oligomers in Tau-expressing animals. Further analysis should thus be performed to assess the level of Tau oligomers in our models.

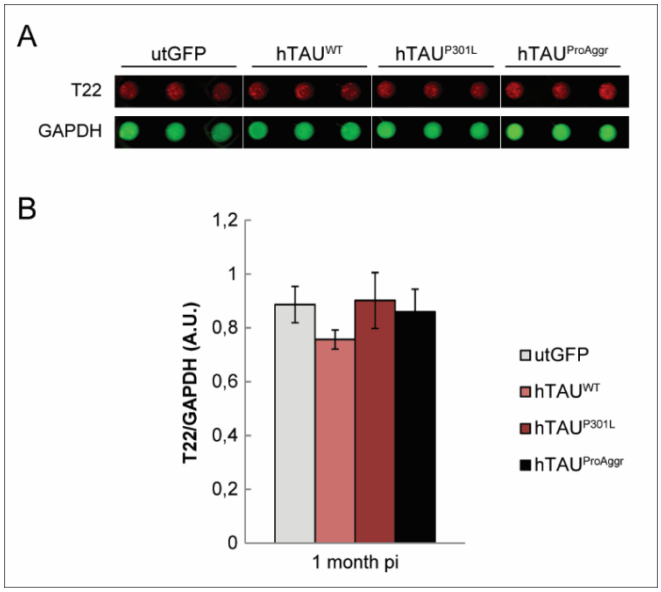

Figure 35: No significant difference in the amount of Tau oligomers detected by T22 antibody
A) *Representative dot blots for Tau oligomers (T22) and Glyceraldehyde-3-phosphate deshydrogenase (GAPDH) at 1 month post-injection.* ***B)*** *Quantification of T22 staining, normalised to GAPDH expression, in all groups failed to reveal differences between Tau constructs and utGFP-injected animals (One-way ANOVA, p=0.233, n=6/group).*

4) Biomarker of Tau pathology in the periphery

We next aimed to determine whether markers of the induced Tau pathology could be detected in peripheral fluids. MSD dosage of total Tau in CSF was thus performed in all animals (**Figure 36**). A dramatic and significant increase in CSF total Tau was observed in all Tau groups compared to controls as early as 1 month post-injection. This increase was highest in the hTAU^{P301L} group, that showed a significant difference when compared to the hTAU^{ProAggr} group. Elevation of CSF total Tau in the hTAU^{WT} group was also higher than in hTAU^{ProAggr} animals, although this failed to reach significance. Interestingly, a strong reduction in CSF Tau level was observed in all groups at 3 months post-injection although Tau level remained significantly higher in hTAU^{WT} and hTAU^{P301L} groups when compared to controls.

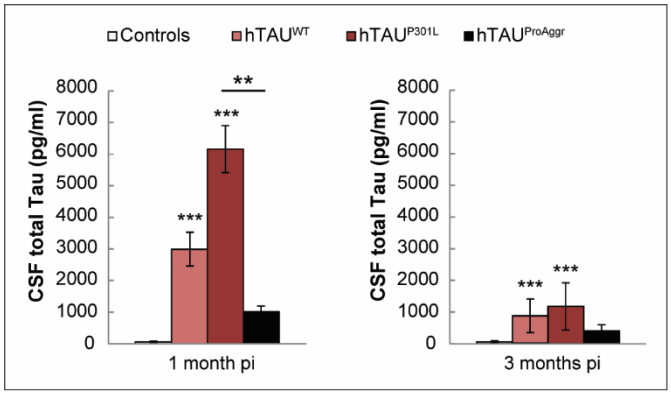

Figure 36: Elevated total Tau levels in CSF observed for all Tau groups
*Increase in CSF total Tau was observed in all Tau groups compared to controls at 1 month post-injection (Kruskall-Wallis non parametric test, p< 0,001, Dunn's multiple comparison test, n=5-13/group). CSF Tau levels was reduced in all Tau groups at 3 months post-injection but were still higher than controls (Kruskall-Wallis non parametric test, p<0,001, Dunn's multiple comparison test, n=4-9/group). Stars represent post-hoc comparisons to controls. Significant difference between Tau groups is also indicated. **p<0.01, ***p< 0.001.*

To conclude, the characterization of the pathology induced by Tau constructs showed that those differ in the extent of Tau aggregation. While AT8-positive hyperphosphorylated Tau is was observed in all groups as early as 1 month post-injection, only hTAU^{P301L} and hTAU^{ProAggr} constructs were able to induce aggregation, in the form of AT100-positive somas. In addition, Gallyas silver impregnation allowed us to identify differences between those two groups in the stage of Tau aggregation. Indeed, hTAU^{ProAggr} animals seemed to exhibit more end-stage tangle-like lesions suggesting that this construct led to stronger aggregation.

Surprisingly, biochemical analysis failed to reproduce histological results. Indeed, no Tau aggregate could be detected in the hTAU^{ProAggr} independently of the biochemical technique used. Interestingly, this was associated with a reduction in detected Tau protein level compared to the other two groups which could not be explained by differences in transgene expression. One possible explanation for this discrepancy may thus be related to the structural nature of Tau aggregated in the hTAU^{ProAggr} group. Indeed, here all biochemical analysis were performed using final SDS denaturation in order to dissolve Tau aggregates. However, it was recently demonstrated that some sort of large Tau aggregates may be highly SDS-resistant which may hinder their detection using standard western blot protocols (Cowan and Mudher, 2013).

Altogether, this first characterization allowed us to demonstrate that co-expression of wild-type human Tau with the pro-aggregation peptide TauRD-ΔK280 strongly promoted its aggregation, while hTAU^{WT} construct on its own was unable to aggregate in the rat brain. The hTAU^{P301L} construct seemed to produce an intermediate phenotype with aggregation detected as early as 1 month post-injection, mostly in the form of soluble non-fibrillar aggregates.

III – The toxicity of Tau constructs is inversely correlated to their ability to aggregate

1) Differences in the level of neurodegeneration induced by Tau constructs

We next wanted to assess whether these differences observed in the extent of Tau pathology were associated with differences in the ability of Tau constructs to induce neurodegeneration. To this purpose, NeuN staining was performed on all groups at 1 and 3 months post-injection (**Figure 37, A**).

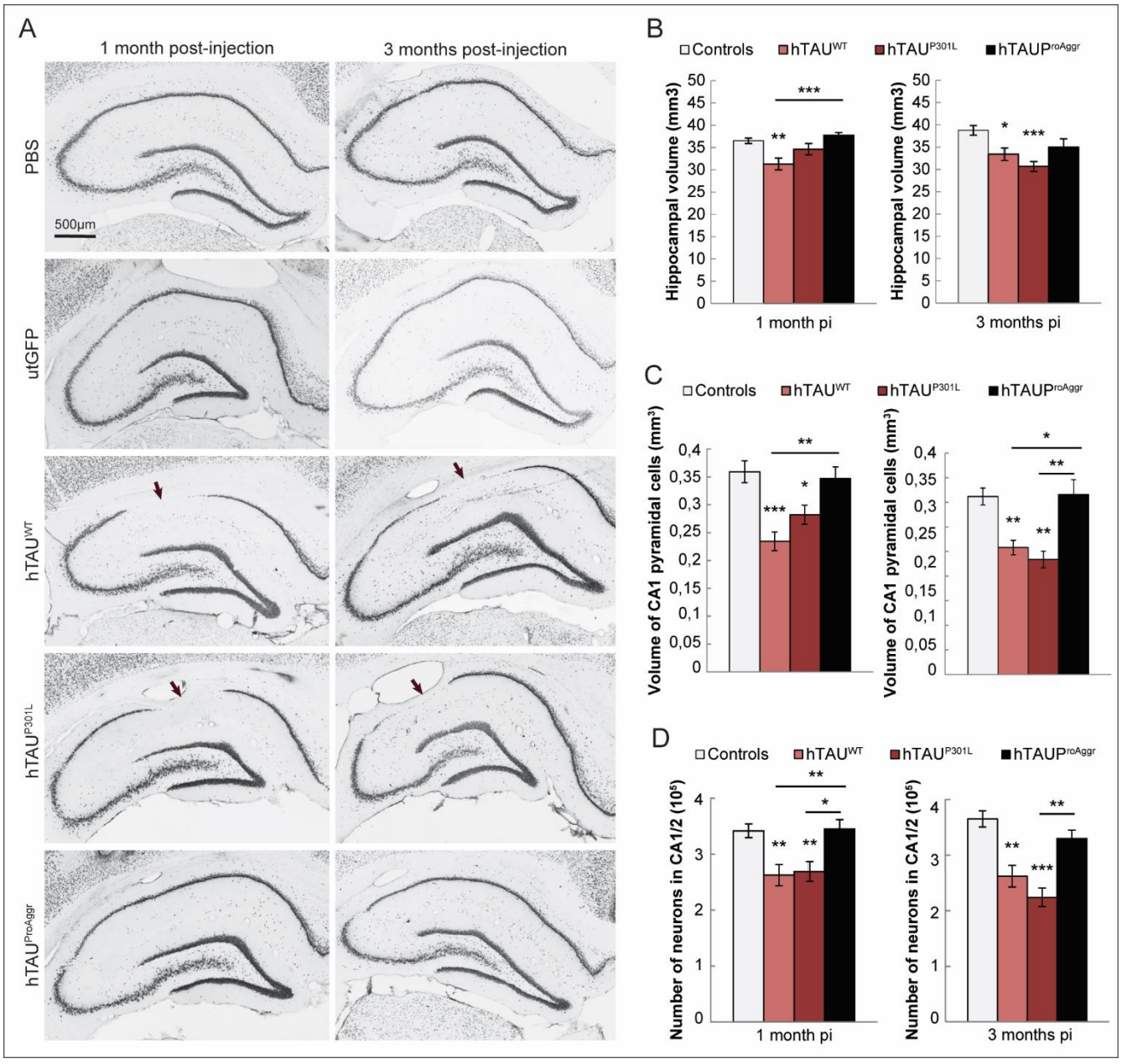

Figure 37: Differences in levels of neurodegeneration associated with the expression of Tau constructs
A) *Representative images of NeuN staining in all groups showing significant loss (arrow) of CA1 pyramidal neurons in hTAU^{WT} and hTAU^{P301L} groups at 1 month post-injection.* ***B)*** *Measure of hippocampal volume shows a significant reduction in hTAU^{WT} group at 1 month post-injection (left) and in both hTAU^{WT} and hTAU^{P301L} (right) at 3 months post-injection, when compared to controls (One-way ANOVA for each time-point, followed by Bonferroni post-hoc test, 1 month post-injection p<0.001, n=7-13/group, months post-injection, p<0.001, n=8-16/group). No difference could be observed between control and hTAU^{ProAggr} animals.* ***C)*** *Cavalieri estimation of the volume of CA1/2 pyramidal neurons shows a significant reduction in hTAU^{WT} and hTAU^{P301L} groups but not hTAU^{ProAggr} group at both 1 and 3 months post-injection when compared to controls*

(One-way ANOVA done separately for each time-point followed by Bonferroni post-hoc comparison, p<0.001 for each time-point, n=5-12/group). ***D)*** *Stereological counting showing significant reduction in the number of CA1 pyramidal neurons in both hTAU^{WT} and hTAU^{P301L} groups at 1 and 3 months post-injection when compared to controls and hTAU^{ProAggr} (One-way ANOVA done separately for each time-point, Bonferroni post-hoc test, p<0.001 for each time-point, n=5-12/group). In contrast, no difference could be observed at any of the time-points between control and hTAU^{ProAggr} animals. Stars above each bar represent the result of post-hoc comparisons to controls. Additional significance between groups is represented. *p<0.05, **p<0.01, ***p<0.001*

Estimation of the whole hippocampal volume was then performed on the same animals (**Figure 37, B**). Expression of hTAU^{WT} construct led to a small reduction in hippocampal volume as early as 1 month post-injection, this atrophy being fairly stable over time (-14.3% at 1 month and -13.9% at 3 months post-injection). Conversely, the atrophy induced by hTAU^{P301L} overexpression was only visible at 3 months post-injection (-20.9%), suggesting that this construct presented with a less acute toxicity than hTAU^{WT}. In contrast, no obvious hippocampal atrophy could be observed with the hTAU^{ProAggr} construct at any of the time-points. Similar results were observed using Cavalieri estimation of the volume occupied by CA1/2 pyramidal cells (**Figure 37, C**). Indeed, hTAU^{WT} and hTAU^{P301L} expressing animals showed a reduction in the volume of pyramidal cells at 1 month post-injection, when compared to controls (-28.8% and -21.4% respectively). Conversely, no significant atrophy of the pyramidal cell layer could be observed at this time-point in the hTAU^{ProAggr} group. Consistent with previous results, the volume occupied by pyramidal cells was relatively stable over time in the hTAU^{WT} group while animals expressing hTAU^{P301L} construct exhibited increased atrophy at 3 months post-injection (-28.6% and -35.4% respectively).

This difference in the toxicity of Tau constructs was further confirmed by the stereological counting of CA1/2 pyramidal neurons (**Figure 37, D**). Indeed, a significant reduction in neuron number could be observed in hTAU^{WT} and hTAU^{P301L} groups when compared to controls as well as to hTAU^{ProAggr} construct as early as 1 month post-injection (-23,2% for hTAU^{WT} and -21,3% for hTAU^{P301L} when compared to controls). No significant difference in the number of CA1 pyramidal neurons could be observed between hTAU^{ProAggr} and control animals, further confirming the absence of toxicity of this Tau construct at this time-point. Again, the extent of neuronal loss seemed fairly stable over time in the hTAU^{WT} group (-28.2% at 3 month post-injection). Conversely, neurodegeneration progressed in the hTAU^{P301L} group, leading to a near 40% loss of CA1/2 pyramidal neurons at 3 months post-injection. Interestingly, expression of the hTAU^{ProAggr} was still neuroprotective at this time-point, as no difference in neurons number could be observed between this group and control animals. A few patches of neuronal loss were observed in one animal from this group, evidenced by a loss in NeuN staining, but it was occasional and never reached the level of neurodegeneration observed in the other two groups. This suggests that long-term expression of this construct may still have small detrimental effects. This should be assessed by characterizing our model at a later time-point. Altogether, those results however suggest that the co-expression of human wild-type Tau with TauRD-ΔK280, which strongly promotes its aggregation, protects neurons from strong acute toxicity exerted by hTAU^{WT} alone.

2) Neurodegeneration induced by Tau constructs correlates with Tau hyperphosphorylation

Based on the observation that hTAU^{ProAggr} construct produced the strongest aggregation in absence of any obvious toxicity, we next aimed to assess whether the extent of neuronal loss could be correlated to the degree of Tau pathology (**Figure 38**)..

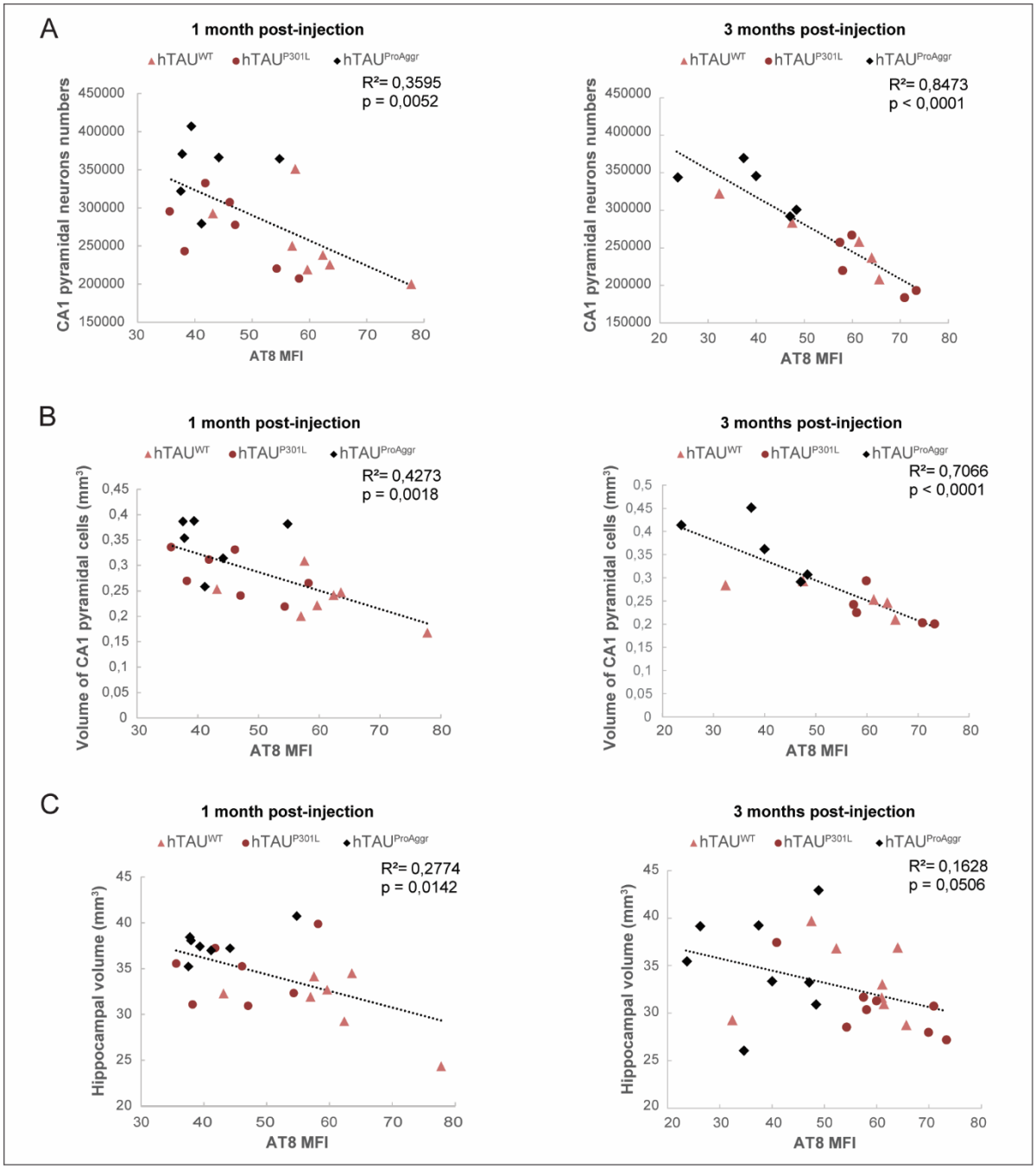

Figure 38: Negative correlation observed between hyperphosphorylation of Tau and neuronal integrity
A) *A negative correlation was observed at 1 and 3 months post-injection between AT8 mean fluorescence intensity (MFI) and number of CA1/2 pyramidal neurons (Pearson correlation test done separately for each time-point, p=0.0052, 95% confidence interval [-0.8236;-0.2137], n=20 at 1 month, p<0.0001, 95% confidence interval [-0.9737;-0.7724], n=15 at 3 months).* ***B)*** *MFI of the AT8 staining was also negatively correlated at both time-points to the volume occupied by CA1 pyramidal cells (p=0.0018, 95% confidence interval [-0.8504;-0.2975], n=20 at 1 month, p<0.0001, 95% confidence interval [-0.9457;-0.5765], n=15 at 3 months).* ***C)*** *Negative correlation was also observed with whole hippocampal volume at both 1 month (p=0.0142, 95% confidence interval [-0.7809;-0.1229], n=21) and 3 months post-injection (p=0.0052, 95% confidence interval [-0.6940;0], n=24), although it failed to reach significance at the latest time-point.*

Significant negative correlations were observed between the mean fluorescence intensity of AT8 staining and all parameters used to assess the extent of neurodegeneration at 1 and 3 months post-injection, including stereological counting of CA1/2 pyramidal neurons (**Figure 38, A**), Cavalieri estimation of the volume of CA1 pyramidal cells layer (**Figure 38, B**) and whole hippocampal volume (**Figure 38, C**). Thus, increased hyperphosphorylation of Tau in our models correlated with an increase in the extent of neuronal loss, confirming an association between this feature of Tau pathology and neurodegeneration. Interestingly, no correlation could be observed between markers of neuronal loss and the number of AT100-positive somas (data not shown). Considering that AT100-positive objects may represent either non-fibrillar aggregates such as observed in the $hTAU^{P301L}$ group, or highly aggregated argyrophilic lesions such as in the $hTAU^{ProAggr}$ group, this absence of correlation may be associated with the inhomogeneity of AT100-positive aggregates. Further correlation analyses between markers of neurodegeneration and numbers of argyrophilic lesions or oligomeric species should help us resolve the nature of the toxic Tau species.

3) <u>Morphological neuronal and synaptic alterations associated with Tau pathology</u>

To confirm that $hTAU^{ProAggr}$ expression did not induce significant neuronal damage, electron microscopy was performed on hippocampal tissue from injected animals at 2 months post-injection. Animals from utGFP and $hTAU^{P301L}$ groups were used as negative and positive controls, respectively. As expected, no obvious neuronal abnormality could be observed in the utGFP group (**Figure 39, A**). In contrast, $hTAU^{P301L}$ animals presented with several signs of neuronal damage (**Figure 39, B**), notably including signs of axonal and dendritic degeneration. Surprisingly, similar abnormalities could be observed in the $hTAU^{ProAggr}$ group as well (**Figure 39, C**) along with a few degenerating cells. Those results may suggest that $hTAU^{ProAggr}$ expression may be associated with some synaptic and neuronal defects, although its toxic effect may not be strong enough to induce significant neurodegeneration. To note, no typical Tau fibril usually observed in the brain of patients suffering from tauopathies could be observed in any of the Tau groups.

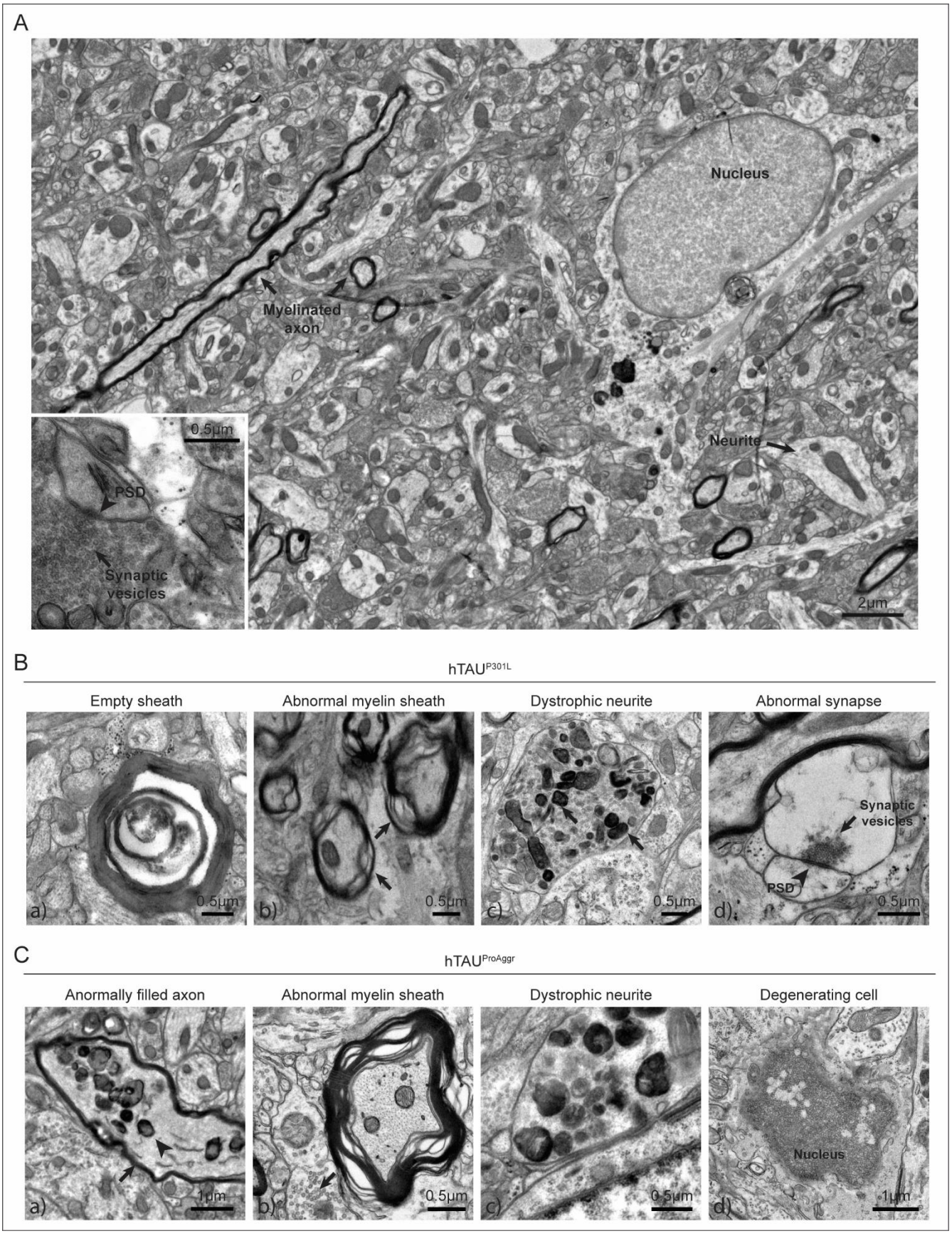

Figure 39: Electron microscopy reveals neuronal abnormalities in both hTAU^{P301L} and hTAU^{ProAggr} groups
A) *Low magnification image of hippocampal tissue in utGFP group shows no obvious morphological abnormality at 2 months post-injection. Key elements of tissue structure are highlighted. Insert: High magnification image of a synapse.* ***B)*** *Several abnormalities can be observed in the hTAU^{P301L} group at 2 months post-injection. Those include: Empty sheaths of myelin (a) surrounding degenerating axons, loose sheaths (b) characterized by splitting of the myelin lamellas (arrows),*

dystrophic neurites (c) presenting a dark cytoplasm filled with autophagic vacuoles (arrows) and synaptic abnormalities (d) with swollen presynaptic terminal and heterogeneous synaptic vesicles distribution. ***C)*** *Similar signs of neuronal distress could be observed in hTAU^{ProAggr} group, including degenerating axons (a, characterized by the myelin shreath, arrow) filled with autophagic vacuoles (arrowhead), loose sheaths of myelin (b) associated with abnormal synapses (arrow), dystrophic neurites (c) and degenerating cells (d) characterized by a dark cell body and a nucleus presenting abnormal chromatin organization as well as signs of degradation.*

4) No significant functional consequence of Tau overexpression revealed by RT-qPCR

Following the finding that both hTAU^{WT} and hTAU^{P301L} constructs induced strong neurodegeneration and that hTAU^{ProAggr} overexpression was associated with neuronal and synaptic morphological abnormalities, we aimed to further assess the effect of these constructs on neuronal integrity. To this purpose, RT-qPCR was performed on whole HC homogenates using target genes involved in the apoptosis pathway (**Figure 40, A and B**). No difference was observed between any of the Tau groups and controls in the expression of caspases 3 and 6, suggesting that neuronal loss in hTAU^{WT} and hTAU^{P301L} groups was not associated with apoptotic pathways.

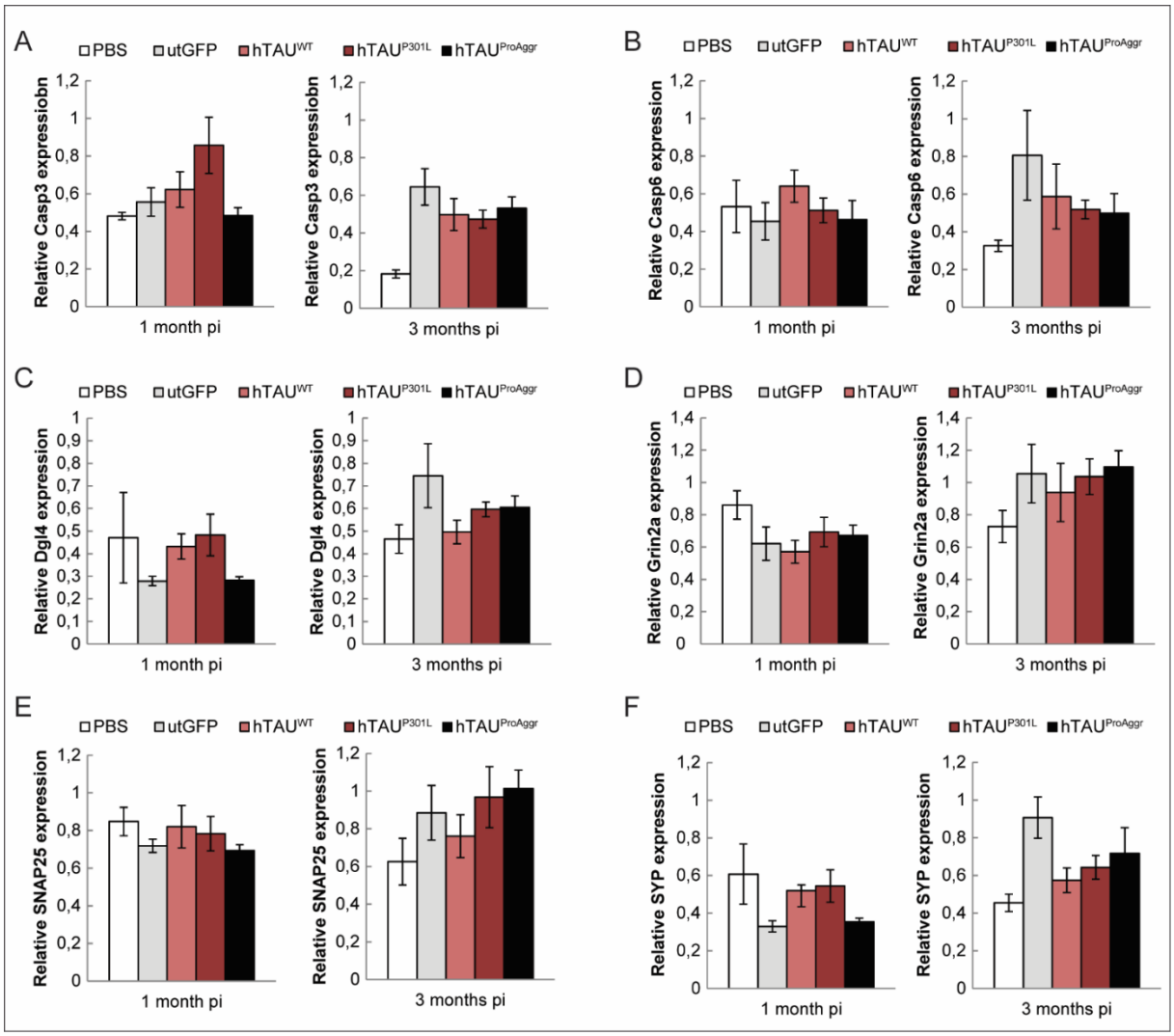

Figure 40: RT-qPCR assay for apoptosis and synaptic markers did not reveal gross abnormalities in Tau groups
No gross modification of caspases 3 ***(A)*** *and 6* ***(B)*** *expression levels were observed in Tau groups compared to controls, suggesting that there was no specific activation of the apoptotic pathways. No difference between groups could be observed in expression of post-synaptic (PSD95, Dgl4,* ***(C)****; NMDA receptor, Grin2a* ***(D)****) or presynaptic markers (Snap25* ***(E)****, Synaptophysin, SYP,* ***(F)****). Kruskall-Wallis non parametric test for each time-point (n=2/6/group).*

Alternatively, caspase activation being a rapid and transient mechanism, it is possible that this would have occurred prior to 1 month post-injection, as strong neuronal loss was already evident at this time-point. In addition, qPCR for post-synaptic markers PSD95 and NMDA receptor (**Figure 40, C and D**) as well as pre-synaptic proteins SNAP25 and synaptophysin (**Figure 40, E and F**) did not reveal significant difference between groups.

We next aimed to assess whether differences in the toxicity of Tau constructs was associated with altered expression of genes involved in protein degradation pathways. To this purpose, RT-qPCR was performed for markers of proteolysis (**Figure 41, A**), the ubiquitin-proteasome system (UPS; **Figure 41, B**) or autophagy-lysosome system (ALS, **Figure 41, C-E**).

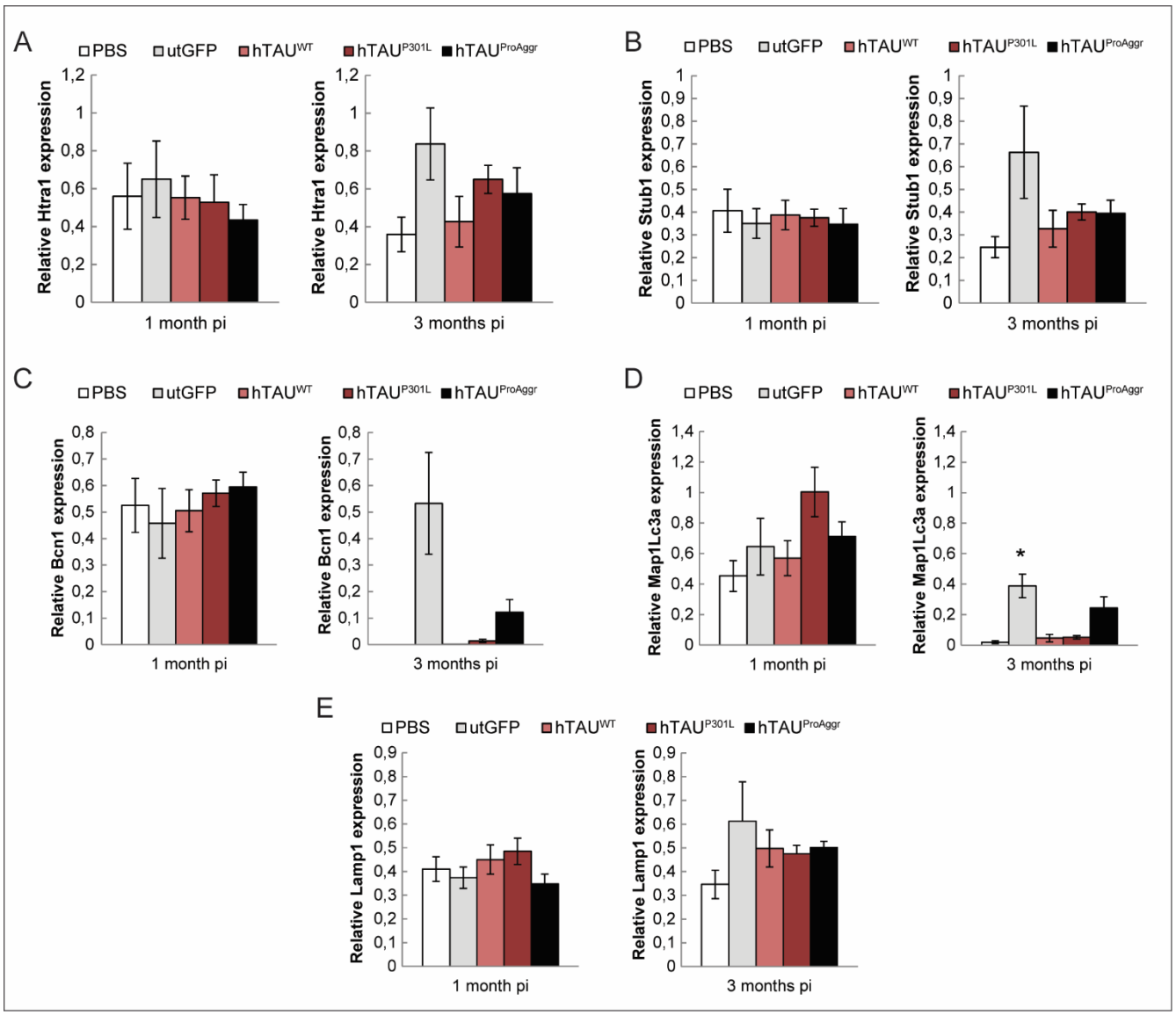

Figure 41: RT-qPCR assay for markers of degradation pathways did not reveal abnormalities in Tau groups
*No gross modification in the expression level of HTRA1 **(A)**, a protease involved in Tau degradation**,** was observed in Tau groups compared to controls, suggesting that Tau degradation was not affected by its overexpression. There was also no difference between groups in expression of CHIP ubiquitin-ligase (Stub1, **(B)**), a marker of the ubiquitin-proteasome system (UPS), or for markers of autophagy (Beclin 1, Bcn1, **(C)**; LC3, Map1Lc3a **(D)**; LAMP1, **(E)**). Kruskall-Wallis non parametric test at each time-point (n=2-6/group). *p<0.05*

No difference between Tau-expressing and control animals could be observed in any of the target genes investigated, although a tendency towards an increase was observed in hTAUproAggr animals at 3 months post-injection when compared to the other Tau groups. This suggests that Tau overexpression did not significantly affect those pathways. Conversely, those results suggest that Tau aggregation in $hTAU^{P301L}$ and $hTAU^{ProAggr}$ groups may not be related to defects in Tau clearance. Considering that neuronal loss in our models, although consequent, was spatially localised, it may also be possible that effects of Tau expression on gene expression may have been diluted when taking whole HC for analysis. Similar analysis on cells sorted using antibodies directed against pathological Tau epitopes such as AT100 may allow to evidence small differences that would have not been detected here.

5) <u>Absence of functional consequences on behaviour at 1,5 months pi</u>

To assess whether the tauopathy induced by Tau constructs led to cognitive impairment, new cohorts of rats were injected with either PBS, utGFP, $hTAU^{WT}$ or $hTAUPro^{Aggr}$ and subjected to behavioural testing 1,5 months after injection. This time-point was chosen because of the relatively rapid time-course of pathology in our different models. This allowed the study of behavioural impairment at a time where neuronal loss was still quite limited and where synaptic deficits may occur. Indeed, the strong reduction observed over time in transgene mRNA suggests selective loss of transgene-expressing neurons. Behavioural deficits and synaptic impairment may be either associated with neuronal death or more likely to impairment of neuronal and synaptic function by pathological Tau species, which may be rescued when transgene-expressing neurons are lost. Testing at an early stage thus allowed studying the specific effect of Tau pathology on cognition.

Animals were first tested in an open field for assessment of locomotor activity and spontaneous exploratory behaviour (**Table 6**). There was no difference between groups in any of the parameters computed, either in measures of locomotor abilities (e.g. mean velocity), spontaneous exploration (e.g. distance travelled, frequency of rearing) or anxiety (e.g. time spent in centre). This suggests that Tau overexpression did not induce gross alteration of locomotion or anxiety level, allowing us to proceed with the assessment of short-term memory.

		PBS (n=14)	utGFP (n=14)	$hTAU^{WT}$ (n=13)	$hTAU^{ProAggr}$ (n=14)
Locomotor abilities & exploratory behaviour					
	Distance travelled (cm)	4495,64 ± 257,18	4558,52 ± 264,55	3621,90 ± 410,02	4410,84 ± 232,53
	Mean velocity (cm/s)	12,44 ± 0,48	12,57 ± 0,41	10,94 ± 0,46	12,36 ± 0,41
	Time spent rearing (s)	107,05 ± 5,96	106,77 ± 5,96	103,14 ± 11,52	121,29 ± 7,58
	Frequency of rearing	61,86 ± 3,88	61,29 ± 4,17	54,77 ± 5,54	69,71 ± 4,57
Measures of anxiety					
	Time spent grooming (s)	11,94 ± 1,61	9,93 ± 3,68	8,67 ± 2,02	8,13 ± 1,40
	Frequency of grooming	2,79 ± 0,41	1,71 ± 0,49	2,00 ± 0,44	1,86 ± 0,29
	Time spent in centre (s)	23,15 ± 3,26	24,64 ± 2,95	23,02 ± 4,82	30,65 ± 5,00
	Number of entries in centre	6,64 ± 1,18	7,93 ± 1,36	5,54 ± 1,35	8,57 ± 1,49

Table 6: No gross alteration of behaviour in Tau-injected animals
Summary table of the parameters measured during the Open-field spontaneous exploration test. No significant difference was observed between groups in any of the parameters computed. Data given as mean ± SEM. One-way ANOVA or Kruskall-Wallis non-parametric test when necessary.

We next wanted to assess whether the neurodegeneration observed after hTAU^{WT} overexpression was associated with memory deficits and if those could be rescued in the hTAU^{ProAggr} group. To this purpose, rats were injected then tested for a working memory task in the Y-maze at 1.5 months post-injection (**Figure 42, A**). All control animals made significantly more entries in the novel arm compared to the other two arms, confirming that those were able to remember the familiar arm in the training phase (**Figure 42, B**). However, this was also the case for both hTAU^{WT} and hTAU^{ProAggr} groups, suggesting that Tau overexpression did not lead to significant impairment in working memory. Similar results were obtained when looking at the time spent in arm (**Figure 42, C**).

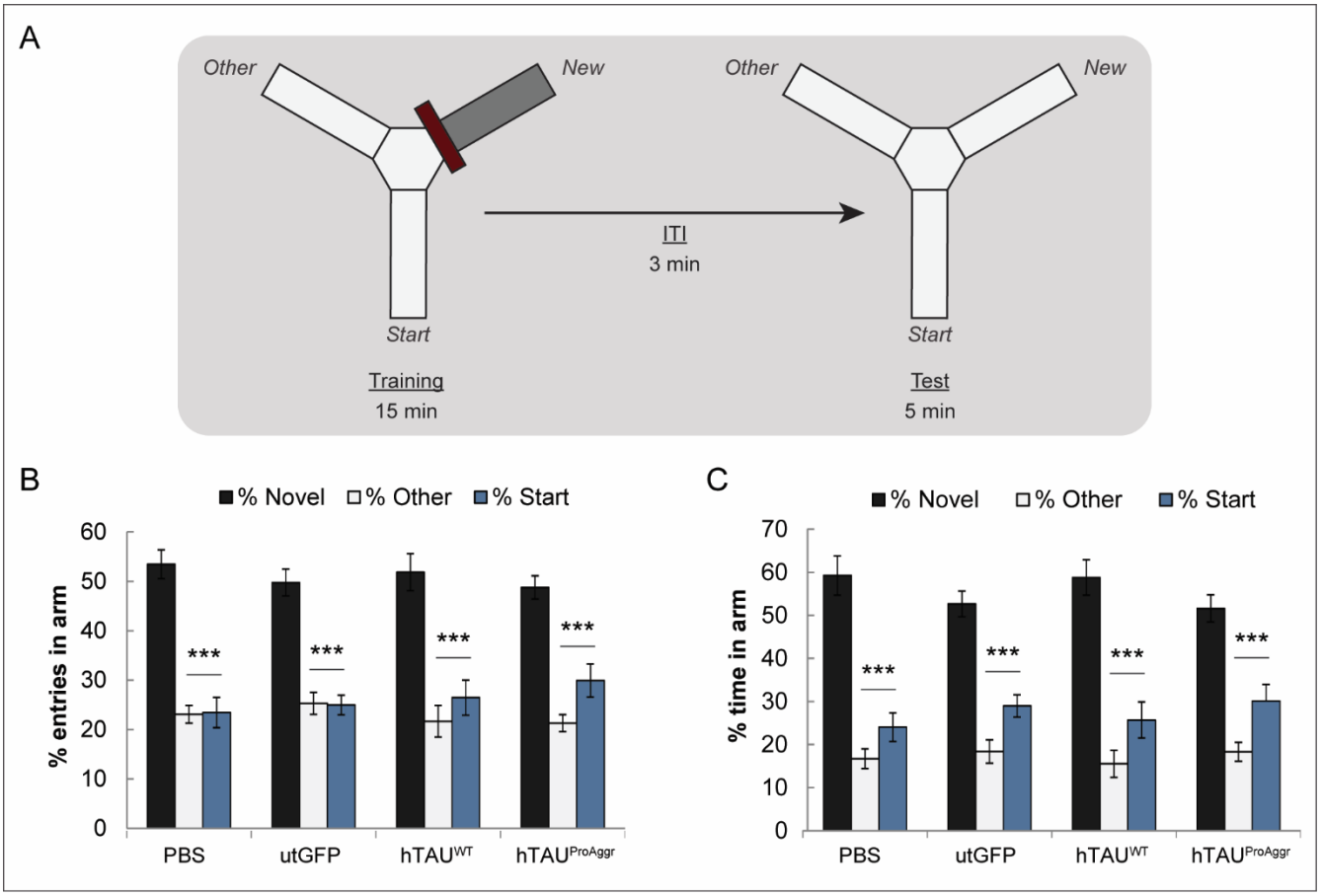

Figure 42: Tau overexpression did not lead to any defect in spatial working memory

A) *Principle of the spatial working memory task in the Y-maze. During a training phase, the animal is allowed to explore 2 arms of the Y-maze for 15 min while the third arm is blocked. After an inter-trial interval (ITI) of 3 min, the animal is reintroduced into the maze for a test trial where all arms are accessible for exploration. If the animal remembers the training phase, it will spend significantly more time in the novel arm (previously blocked) compared to the other two.* ***B)*** *Percentage of entries done in an arm over the total entries in arms. All groups enter more in the Novel arm compared to Other and Start arms (two-way ANOVA, Arm factor, p<0,001, Bonferroni post-hoc test).* ***C)*** *Percentage of time spent in an arm over the total time spent in arms. All groups spend more time in the Novel arm compared to Other and Start arms (two-way ANOVA, Arm factor, p<0,001, Bonferroni post-hoc test, n=13-14/group). ***p<0,001*

Assessment of long-term emotional memory was then performed using a contextual fear conditioning paradigm (**Figure 43**). Percentage of freezing, an index of emotional memory, was measured during the training phase before and after shocks as well as in a test phase performed after a 24h retention interval. As expected, PBS and utGFP-injected showed increased freezing after shock compared to before shock during the training phase (**Figure 43, A**). Increased freezing was also observed but to a lesser extent in both hTAU^{WT} and hTAU^{ProAggr} groups, with significant reduction in freezing after the second shock in hTAU^{ProAggr} compared to controls. This may be related to altered stress-related behaviour in those animals. Percentage of freezing during test, however, did not differ between Tau-expressing animals and controls (**Figure 43, B**) suggesting that behavioural alterations evidenced during the training phase did not lead to significant deficit in long-term emotional memory.

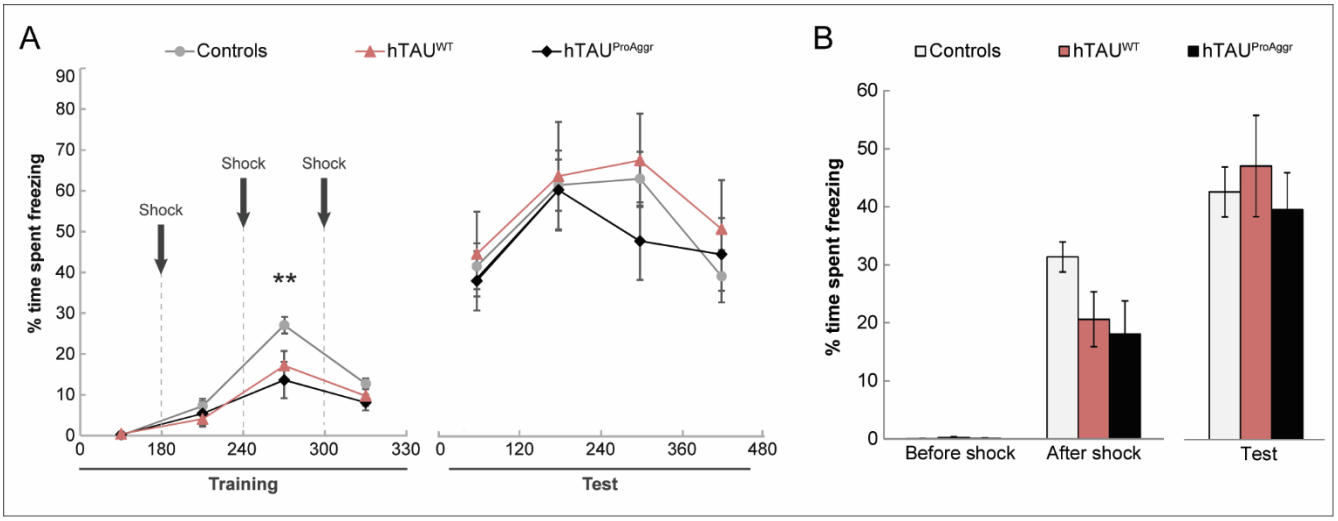

Figure 43: No long-term memory deficit observed in contextual fear conditioning test

A) *Kinetics of the percentage of time spent freezing during the training phase and test trial. Increase freezing was observed after each foot shock in control groups, suggesting associative learning. Increase in freezing over time was also observed in Tau-expressing animals with, however, a small reduction (star) compared to controls after the second shock (Repeated-measure ANOVA, significant group x time effect, p<0.01, Bonferroni post-hoc test, p<0.001 for utGFP-hTAU^{ProAggr} comparison on the 240-300s interval, n=11-13/group). No difference could be observed between groups during the test trial (Repeated-measure ANOVA, no group x time effect, p=0.50, n=11-13/group). **p<0.01.* ***B)*** *Total results obtained for the training phase (before and after shock) showed similar results, with an increase over time in the percentage of freezing. Again, a slight difference was observed between utGFP and hTAU^{ProAggr} animals in the percentage of freezing after shock (one-way ANOVA, p<0.05, Bonferroni post-hoc test, p=0.054 for utGFP-hTAU^{ProAggr} comparison, n=11-13/group). No difference between groups could be observed during test, suggesting no impairment of long-term memory following overexpression of human Tau in our models (One-way ANOVA, p=0.745, n=11-13/group).*

Analysis of the neurodegeneration associated with Tau overexpression allowed us to unravel differences in the toxicity of Tau constructs. Indeed, while significant neuronal loss was observed in both $hTAU^{WT}$ and $hTAU^{P301L}$ groups as early as 1 month post-injection, overexpression of the $hTAU^{ProAggr}$ construct was associated with only limited neurotoxicity. Those results suggest that potentiating the aggregation of wild-type human Tau may be associated with neuroprotection against the toxicity associated with soluble Tau species.

Slight signs of neuronal and synaptic distress, such as morphological abnormalities, where observed at later time-points in the $hTAU^{ProAggr}$ group, suggesting that on a longer term maintenance of Tau aggregates may be detrimental. No significant difference, however, was observed between Tau-expressing animals and controls in the expression of synaptic markers or pathways involved in neurodegeneration. However, it is worth noting that neuronal loss in both $hTAU^{WT}$ and $hTAU^{P301L}$ groups was dramatic but spatially restricted. The use of whole HC homogenates in the RT-qPCR analysis may have thus been associated with diluted effects of Tau constructs, precluding their detection.

Lastly, no significant memory deficit could be observed in any of Tau-expressing models at 1,5 months post-injection. Again, the relatively spatially restricted neuronal loss may not be sufficient to induce significant functional impairment. Alternatively, other types of memory may be affected in our model. Further behavioural analysis should allow better characterization of the functional consequences of Tau overexpression in our models.

IV – Toxicity is associated in Tau groups with distinct phenotypes of inflammation

1) Tau constructs present differences in the extent and kinetics of microglial activation

Neuronal loss is commonly associated with neuroinflammation in several neurodegenerative diseases, including tauopathies (Ishizawa and Dickson, 2001; Sheng et al., 1997). To determine whether this was the case in our models, we studied markers of astrocytic and microglial activation. First, Iba1 immunofluorescent staining was performed to assess the extent microgliosis in the whole HC (**Figure 44, A**). Microglial activation was observed in all Tau groups at 1 month post-injection and, to a lesser extent, in utGFP animals, suggesting that microgliosis may be partly induced by vector expression.

Microglia in $hTAU^{WT}$ and $hTAU^{P301L}$ were found to populate strongly around the injection site, suggesting that they were participating in the formation of the glial scar associated with neuronal loss. Consistent with this idea, morphological changes were observed in those groups with somatic thickening and, in some cases, polarisation of the processes perpendicular to the lesion site suggesting migration of activated microglia to the lesion (**Figure 44, A, inserts**). Quantification of Iba1 staining confirmed microglial activation. Indeed, increase in Iba1-positive volume (**Figure 44, B**) as well as in the number of Iba1 cells (**Figure 44, C**) was observed in all Tau groups at 1 month post-injection. A small increase in both parameters was also observed in utGFP, although it failed to reach significance.

Interestingly, the kinetics of microglial activation strongly differed between groups at 3 months post-injection. Indeed, while microgliosis almost completely resolved in $hTAU^{WT}$ and $hTAU^{ProAggr}$ groups, animals overexpressing the $hTAU^{P301L}$ construct showed maintenance of strong microglial activation at this stage. This suggests that pathological processes induced by Tau constructs may differ and that maintained microgliosis may be associated with the toxicity of $hTAU^{P301L}$ construct. Interestingly, RT-qPCR for Iba1 showed similar results at 1 month post-injection, with strong increase in all Tau groups (**Figure 44, D**). Strongest expression at this time-point was observed in the $hTAU^{P301L}$ group. However, Iba1 mRNA levels dropped drastically at 3 months post-injection, including in the $hTAU^{P301L}$ group, in contrast with histological data. Lastly, RT-qPCR for the pro-inflammatory cytokine tumor necrosis factor α (TNFα) did not yield any significant group difference (**Figure 44, E**).

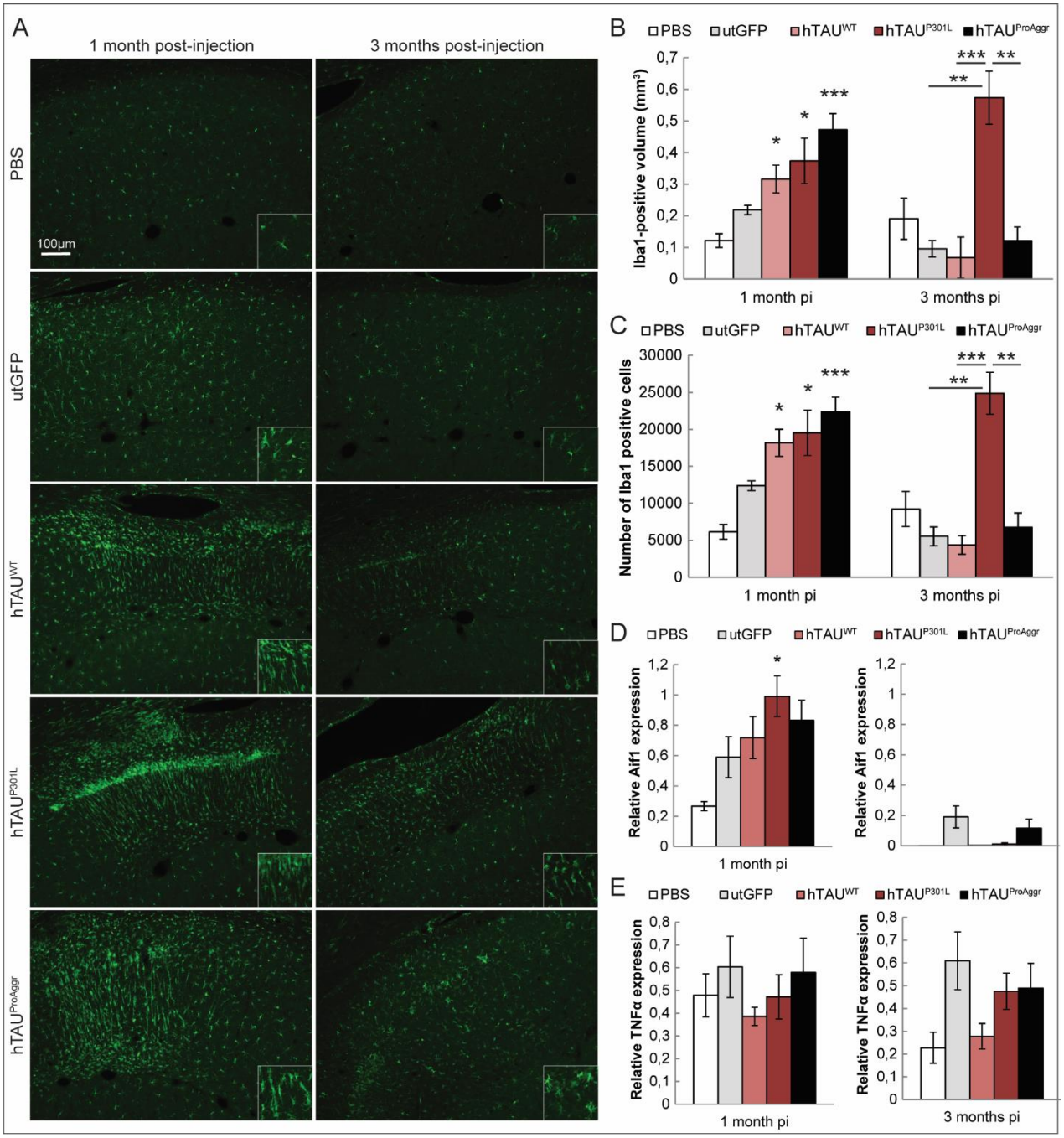

Figure 44: Microgliosis is observed following AAV injection and persists in hTAU^{P301L} group

A) *Representative images of Iba1 staining showing microglial activation at 1 month post-injection following Tau overexpression in all groups and, to a lesser, in utGFP animals. Morphological changes were also observed with thickening of microglial soma and, in some cases, polarisation of the processes perpendicular to the lesion site suggesting migration of activated microglia to the lesion site (e.g. insert in hTAU^{WT} and hTAU^{P301L} groups).* ***B)*** *Quantification of the Iba1-positive volume revealed an increase in microglial activation in all Tau groups compared to PBS-injected animals at 1 month post-injection (Kruskal-Wallis non parametric test, p<0.001, Dunn's multiple comparison test). Microglial activation was also observed in the utGFP group, although this failed to reach significance. Microgliosis resolved at 3 months post-injection in all groups except hTAU^{P301L} (Kruskal-Wallis non parametric test, p<0.001, Dunn's multiple comparison test, n=5/8/group).* ***C)*** *Quantification of the number of activated microglia yielded similar results with an increase in all Tau groups at 1 month that persisted to 3 months post-injection in hTAU^{P301L} (Kruskal-Wallis between group comparison for each time-point, p<0.01 at 1 and 3 months post-injection, Dunn's multiple comparison test, n=5/8/group).* ***D)*** *Iba1 mRNA increase was also found in all groups at 1 month post-injection before returning to basal at 3 months post-injection (Kruskal-Wallis between group comparison for each time-point, p<0.05 at 1 and 3 months post-injection, Dunn's multiple comparison test, n=5/8/group). Highest Iba1 expression was found in hTAU^{P301L} at 1 month post-injection, thus preceding increase observed at the protein level.* ***E)*** *RT-qPCR for the pro-inflammatory cytokine tumor necrosis factor α (TNFα) did not show a significant change.*

2) Different extents of astrogliosis observed in all Tau groups

We next aimed to study the extent of astrogliosis induced by Tau constructs. AT8/Vimentin co-immunofluorescent staining was thus performed to measure astrocytic reactivity in the whole HC (**Figure 45, A**).

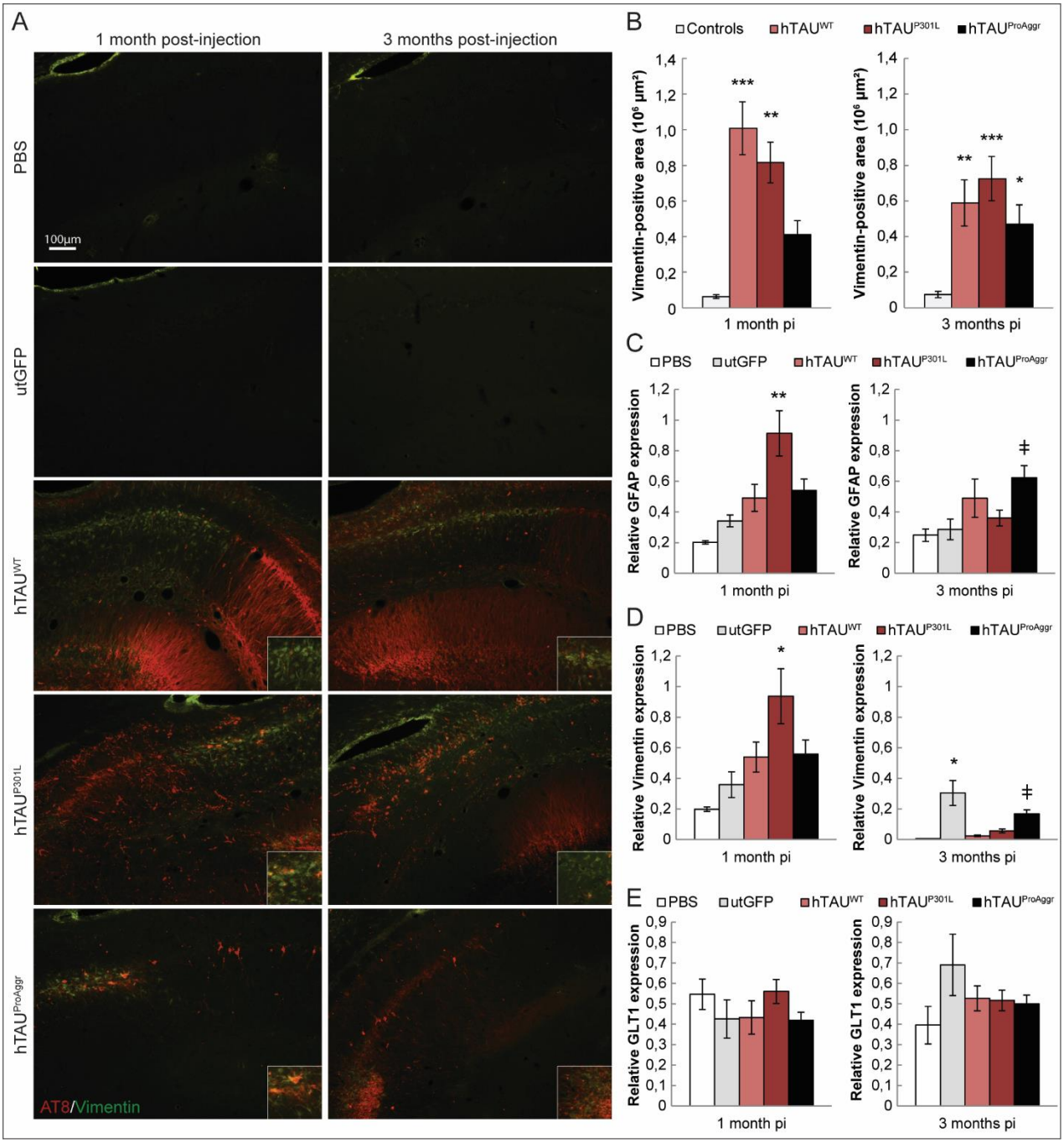

Figure 45: Astrogliosis is induced following overexpression of all Tau constructs

A) *Representative images of AT8/Vimentin colabelling showing strong astrocytic reactivity in all Tau groups at 1 and 3 months post-injection. Interestingly, the localisation of Vimentin reactivity differed between constructs. While Vimentin-positive astrocytes were localised in the vicinity of AT8-positives neurons in the hTAU^{ProAggr} group, there was a clear spatial segregation in both hTAU^{WT} and hTAU^{P301L} groups. Reactive astrocytes in these groups were localised in regions negative for AT8 staining, forming a glial scar at the site where neurons had died.* ***B)*** *Quantification of the Vimentin-positive area showed strong astrogliosis in all Tau groups at 1 month post-injection, this being the highest for hTAU^{WT} and hTAU^{P301L} groups (Kruskall-Wallis non parametric test, p<0.001, Dunn's multiple comparison test, n=6-10/group). Astrogliosis then partially resolved in those groups at 3 months post-injection, falling at the level of hTAU^{ProAggr} (Kruskall-Wallis non parametric test, p<0.001, Dunn's multiple comparison test, n=5-10/group). RT-qPCR for GFAP* ***(C)*** *and Vimentin genes* ***(D)***

showed an increase in expression at 1 month post-injection, found to be the highest in the hTAU^{P301L} group, that resolved at 3 month post-injection (Kruskall-Wallis non parametric test at each time-point, p<0,01 for both genes at 1 month, p<0.05 and p<0.001 for GFAP and Vimentin respectively at 3months, Dunn's multiple comparison test, n=4-9/group). Expression of the astrocytic glutamate transporter GLT1 ***(E)*** *was not affected in any of the Tau groups, suggesting that there was no impairment of astrocytic function of glutamate recapture (Kruskall-Wallis non parametric test at each time-point, Dunn's multiple comparison test, n=2-6/group).*

Vimentin-positive astrocytes were observed in all Tau groups as early as 1 month post-injection. In contrast, no Vimentin reactivity could be observed in control animals at any of the time-points observed, suggesting that the strong astrocytic reactivity observed in the other groups was selectively induced by Tau pathology. Interestingly, the localisation of reactive astrocytes differed between groups. Those were found in the hTAU^{ProAggr} group in the close vicinity of AT8-positive neurons. In contrast, Vimentin-positive astrocytes in the hTAU^{WT} and hTAU^{P301L} group populated places devoid of AT8 reactivity and characterized by shrinkage of the cellular layer, suggesting that they were involved in the formation of the glial scar following neurodegeneration. Differences in the topography of astrogliosis observed between Tau groups may suggest that reactive astrocytes may play distinct functions in those models.

Quantification of Vimentin-positive area also revealed group differences in the extent of astrogliosis (**Figure 45, B**). Indeed, although all Tau groups presented with an increase in Vimentin-positive area, this astroglial activation was the highest in hTAU^{WT} and hTAU^{P301L} groups at 1 month post-injection. Interestingly, astrogliosis in those groups seemed to partially resolve at 3 months post-injection, as the area of vimentin reactivity was found to drop to the level of the hTAU^{ProAggr} group at this time.

Slightly different results were obtained when looking at the expression of the markers of astrocytic activation GFAP (**Figure 45, C**) and Vimentin (**Figure 45, D**) by RT-qPCR. Indeed, increase in both markers was observed at 1 month post-injection, with this increase being the highest in the hTAU^{P301L} group, before dropping down again at 3 months post-injection. Lastly, RT-qPCR for the astrocytic glutamate transporter GLT1 (**Figure 45, E**) did not reveal any difference between groups, which may suggest that Tau pathology did not induce impairment of this astrocytic function. Alternatively, much alike what we previously observed, it may be possible that a dilution effect due to analysis on the whole HC may have prevented us from observing effects of Tau expression on gene expression. RT-qPCR on sorted astrocytes may allow to evidence modifications of astrocytic activity and reactivity.

3) <u>Astroglial Tau pathology occurs concurrently to Tau aggregation in our models</u>

Interestingly, glial Tau pathology reminiscent of that observed in several human tauopathies (**Figure 46, A**) was observed in both hTAU^{P301L} and hTAU^{ProAggr} groups (**Figure 46, B**) but not in hTAU^{WT} group using AT100 staining. Different morphological subtypes could be observed, including inclusions resembling astrocytic plaques, thorn-shaped and tufted astrocytes. Similar glial Tau pathology could occasionally be observed with AT8 antibody and Gallyas silver impregnation.

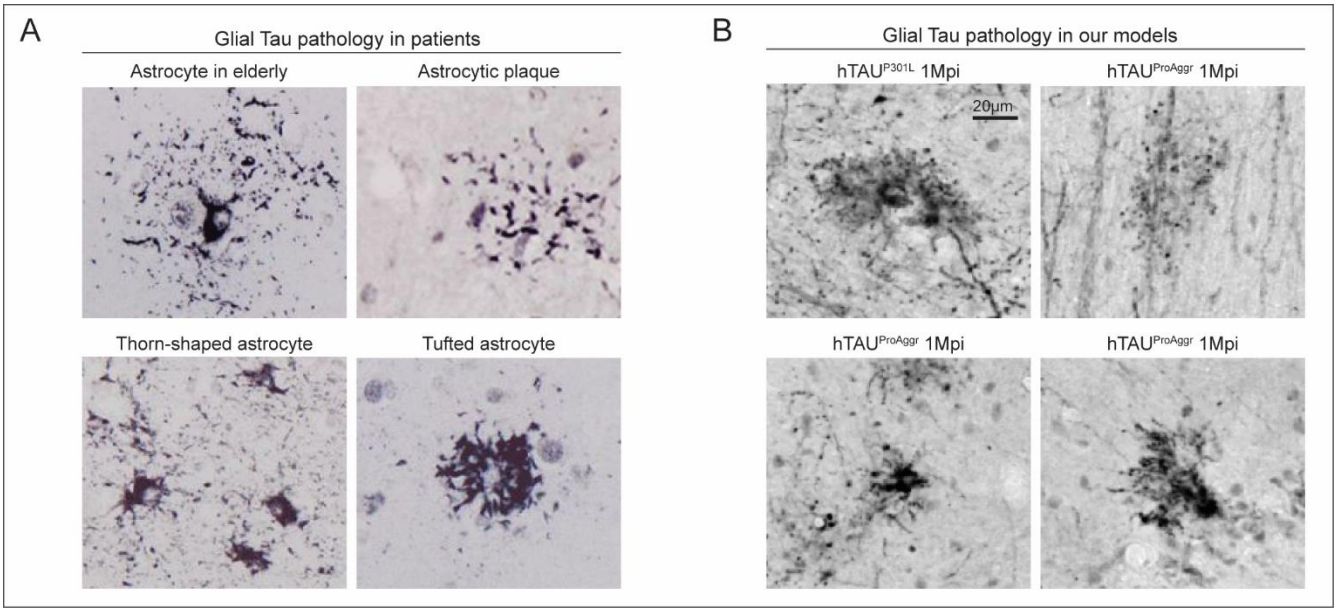

Figure 46: Amount of glial pathology induced by different Tau constructs
A) *Different morphological subtypes of astroglial Tau inclusions observed in human tauopathies (AT8 antibody). Adapted from Ferrer et al, 2014, Journal of Neuropathology & Experimental Neurology.* ***B)*** *Representative images of AT100 staining showing astrocyte-like Tau inclusions of different morphologies in hTAU^{P301L} and hTAU^{ProAggr} groups.*

To assess the extent of glial Tau pathology in those groups, counting of hippocampal astrocytic-like inclusions was performed at 1 and 3 months post-injection on AT100 staining (**Figure 47, A**), with no attempt to differentiate the various types of inclusions. Both groups displayed AT100-positive glial inclusions as early as 1 month post-injection, those being more numerous in the hTAU^{P301L} group when compared to the hTAU^{ProAggr} group, especially in the Sub-CA1/2 sub-region (**Figure 47, B, C and D**). This could be associated with the fact that neuronal loss is observed at this point only in the hTAU^{P301L} group. Interestingly, the amount of glial Tau pathology increased in the hTAU^{ProAggr} between 1 and 3 months post-injection while it remained stable in the hTAU^{P301L} group. This increase may be consecutive to the apparition of neuronal defects in the hTAU^{ProAggr} group, as evidenced by electron microscopy at 2 months post-injection (see *Figure 39* in section III - 4 of the results). Together, those results suggest that glial Tau accumulation may be secondary to the degenerating process in neurons.

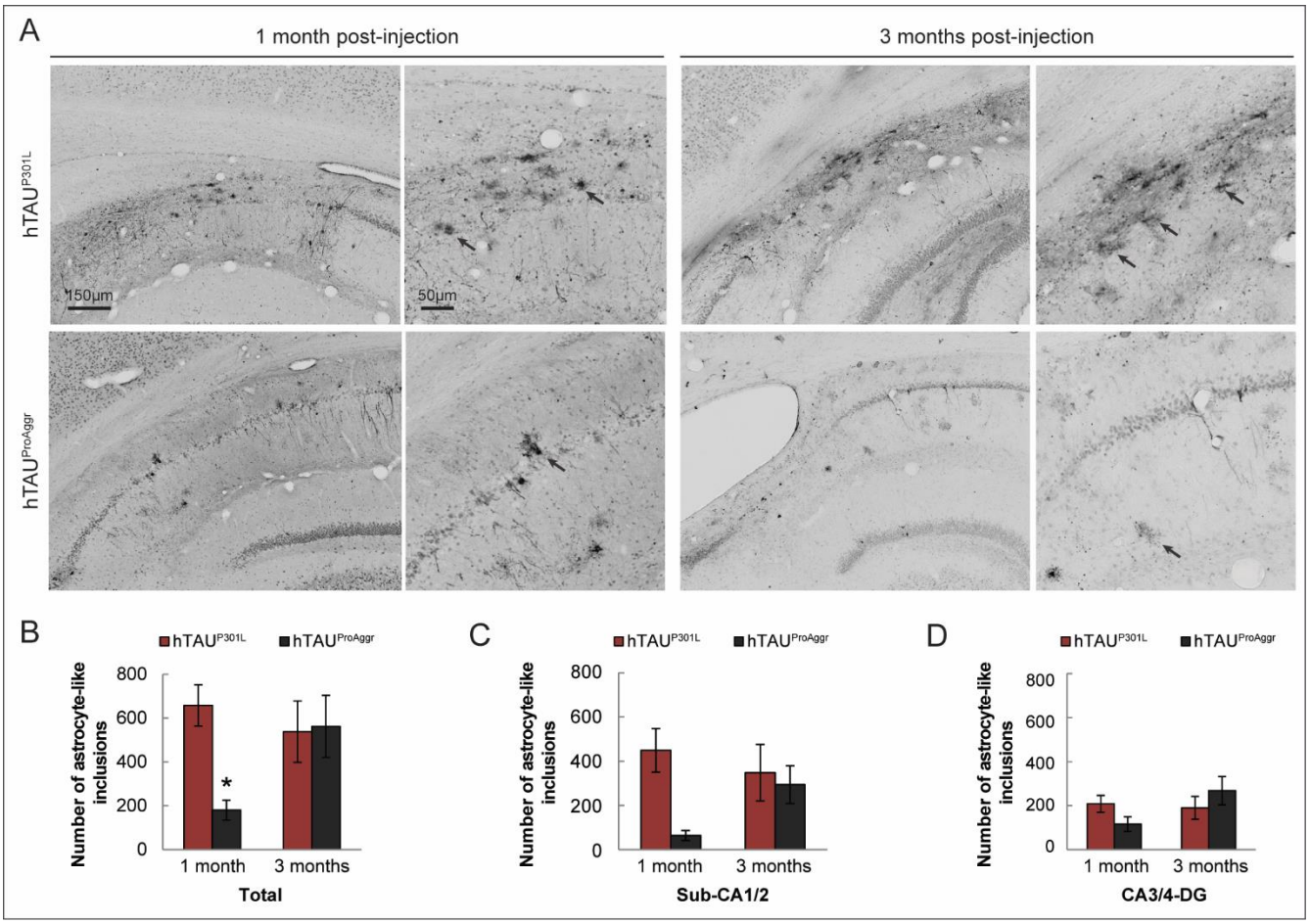

Figure 47: Amount of glial pathology induced by different Tau constructs

A) *Representative images of AT100 staining in both groups at 1 and 3 months post-injection. Arrows indicate astrocyte-like inclusions.* ***B)****,* ***C)*** *and* ***D)*** *Quantification of AT100-positive astrocyte-like inclusions in the entire hippocampus (B), in the Subiculum-CA1/2 subfield (C) and in the CA3-4/Dentate Gyrus sub-field (D). Two-way ANOVA with time and group factors, significant group x time effect for Total (B, p<0.05), near significant effect for Sub-CA1/2 (C, p=.077) and CA3/4-DG (D, p=0.069), Bonferroni post-hoc test, n=7-8/group. Stars represent the result of the post-hoc comparison to hTAU^{P301L}. *p<0,05*

To further characterize those glial lesions, wild-type mice were injected with hTAU^{P301L} and hTAU^{ProAggr} vectors. Similarly to rats, glial Tau lesions appeared in mice at 1 month post-injection, as visualized using AT100 antibody (**Figure 48, A**). In situ hybridization was also performed on those animals to detect the transgene, using a probe against the polyA tail of the β-globin (bGHpA) that is present in all AAV backbones, associated with GFAP immunostaining (**Figure 48, B**). This was done in order to determine whether these Tau-positive astrocyte-like lesions arose from transgene expression in those cells. The transgene mRNA was observed mainly in the pyramidal layer of the hippocampus, confirming that our AAV vectors target mainly neuronal cells. A few cells were marked in the molecular layer but no obvious colocalization was observed with GFAP, suggesting that those may not be astrocytes. Altogether, these results suggest that AT100-positive astrocyte-like inclusions may arise from a secondary process, maybe from phagocytosis of neuronal debris or extracellular Tau by the astrocytes. AT100 immunofluorescent staining, performed on transgenic mice expressing GFP under the promoter of aldehyde dehydrogenase 1 family, member L1 (Aldh1l1), an astrocytic enzyme (Cahoy et al., 2008), injected with either hTAU^{P301L} or hTAU^{ProAggr} construct further supports this hypothesis (**Figure 48, C**). AT100 staining in these glial profiles did colocalize with GFP, confirming that these were indeed astrocytes. In addition, some polynuclear Tau-positive astrocytes were observed, suggesting that those may have phagocytosed cell corpses.

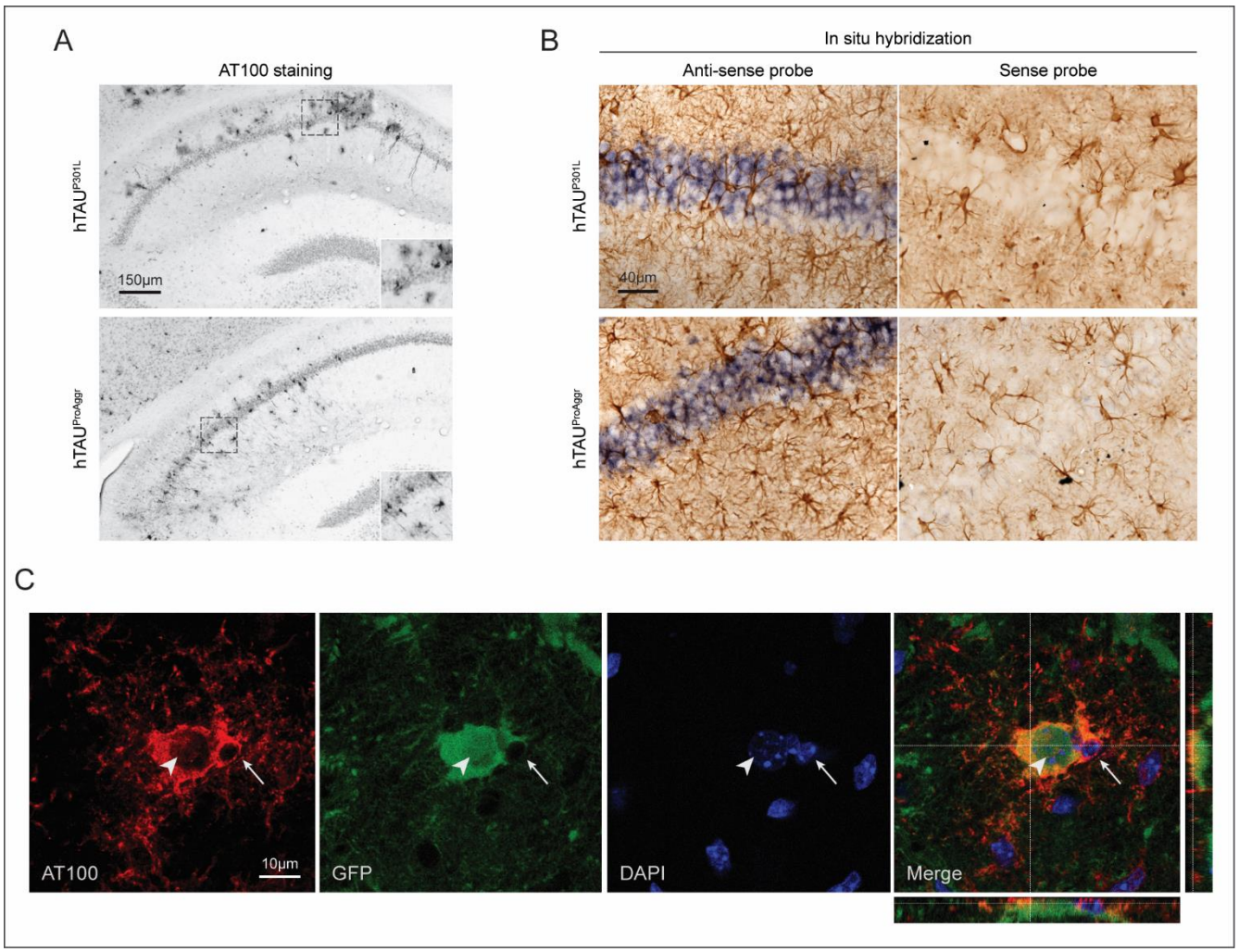

Figure 48: Astrocytic Tau inclusions are not the consequence of transgene expression in those cells
A) *AT100 immunohistological staining on mice injected with hTAU^{P301L} and hTAU^{ProAggr} constructs showed the presence of astrocytic-like Tau lesions in this model (insert) at 1 month post-injectino.* ***B)*** *In situ hybridization using bGHpA-directed probe (blue) shows localization of the transgene mainly in the pyramidal layer. No obvious colocalization can be observed with GFAP (brown). Hybridization with the sense probe was used as negative control.* ***C)*** *AT100 immunofluorescent staining in Aldh1l1-GFP transgenic mice injected with hTAU^{P301L} construct shows that those glial inclusions are indeed astrocytes. In addition to the GFP-positive astrocyte nucleus (arrowhead) a small DAPI-stained nucleus (arrow) is observed in the cytoplasm, suggesting that the astrocyte may have phagocytosed a cell corpse.*

This increase in phagocytic activity of glial cells was confirmed by RT-qPCR analysis for Multiple EGF-like-domains 10 (MEGF10; **Figure 49, A**) and Myeloid-epithelial-reproductive Tyrosine Kinase (MERTK; **Figure 49, B**) genes coding for glial phagocytic receptors known to be involved in synaptic pruning during development and at adult age (Chung et al., 2013). The expression of components of the complement cascade was assessed as well (**Figure 49, C, D and E**). High expression levels of those different markers were observed in all groups at 1 month post-injection, including in utGFP and PBS-injected animals. This result mirrored the increased Iba1 reactivity observed also in utGFP at 1 month post-injection and suggests that increased glial phagocytic activity at this time-point may be, at least in part, related to clearance of cellular debris consecutive to the mechanical lesion induced by injection. However, differences in the expression level of those markers was observed between groups, with the highest upregulation observed in the hTAU^{P301L} group, which reached significance compared to PBS animals in the case of clusterin (CLU, **Figure 49, E**). Interestingly, while expression then reduced in most groups at 3 months post-injection, maintained upregulation was observed in the hTAU^{ProAgg}r group,

notably in complement proteins C1q (**Figure 49, C**) and C3 (**Figure 49, D**). To note, the kinetics of expression of genes involved in phagocytosis mirrored the kinetics of glial Tau aggregation in hTAU^{P301L} and hTAU^{ProAggr} groups. Although those results, obtained on whole HC homogenates, could not allow us to make any inference on the relative contribution of microglia and astrocytes, similar analysis on sorted glial cells may allow us to confirm this association between activation of phagocytic pathways and astroglial Tau aggregation. Lastly, RT-qPCR for Psmb9 (**Figure 49, F**), coding for the inducible β1i subunit of the proteasome, was performed to study protein degradation pathways specifically in glia. Increased expression was observed in all Tau-expressing animal at 1 month post-injection, especially in the hTAU^{ProAggr} group, thus suggesting that activated glial cells may indeed be in a process of cleansing of the injection site.

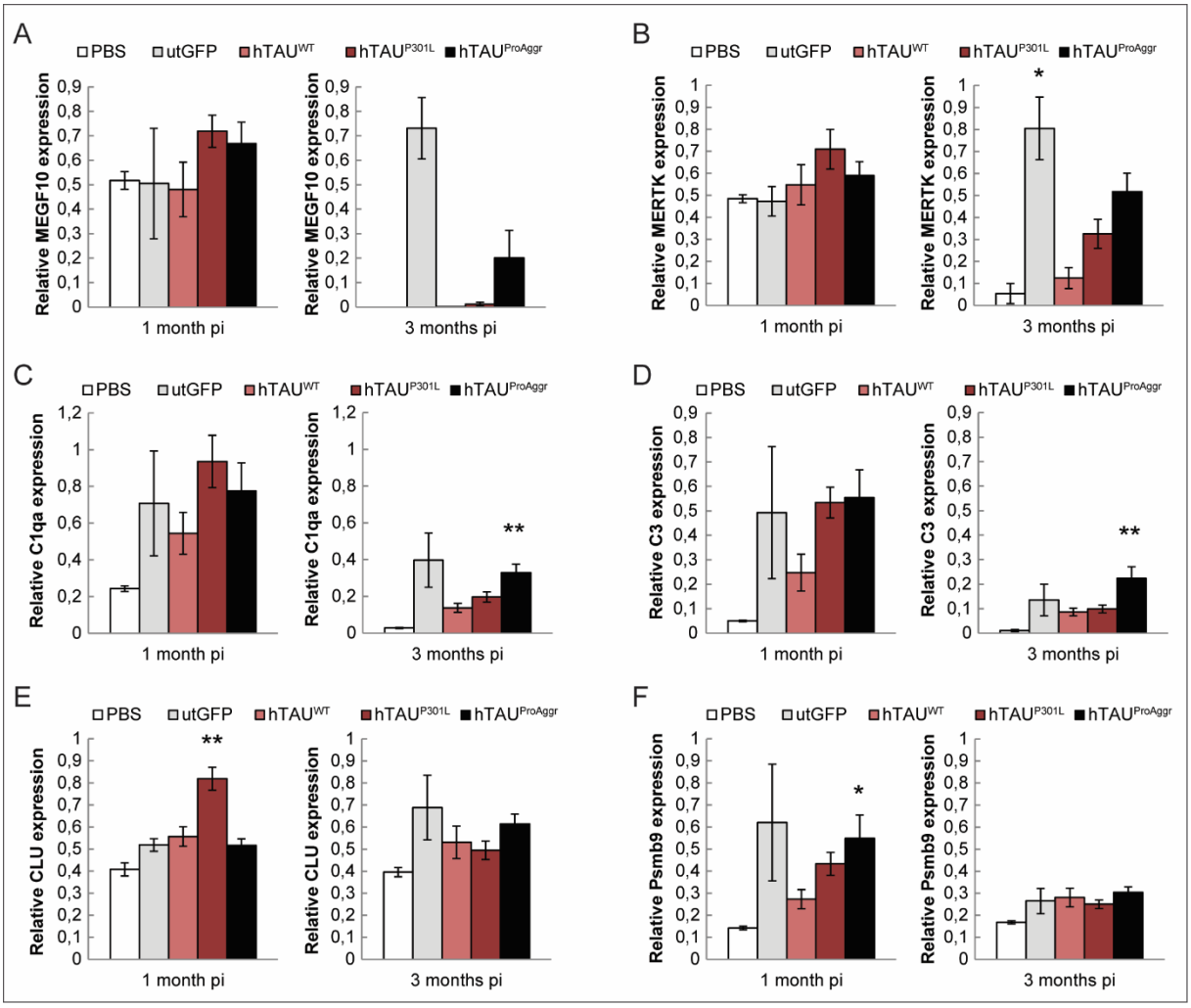

Figure 49: RT-qPCR assay showed an increase in markers of phagocytotic and degradation pathways concomitant to the apparition of glial Tau lesions

*Markers of glial phagocytic pathways MEGF10 (**A**) and MERTK (**B**) as well as components of the complement cascade (**C**, **D** and **E**) were found to be elevated in all groups at 1 month post-injection, suggesting that those may be involved in clearance of cellular debris consecutive to the mechanical lesion induced by the injection of AAV vectors and PBS. Interestingly, among Tau groups, highest mRNA levels were observed in both Tau groups showing glial inclusions, hTAU^{P301L} and hTAU^{ProAggr}, although this failed to reach significance in most cases. Significant difference was however observed between PBS and hTAU^{P301L} groups in CLU levels (**E**, Kruskal-Wallis non parametric test, p<0.01, Dunn's multiple comparison test, n=2-6/group). While reduction in the expression level of those different markers was observed at 3 months post-injection in most groups, maintained elevated levels were observed in the hTAUProAggr group and, to a lesser extent, in animals expressing hTAUP301L construct. Indeed, hTAUProAggr animals exhibited increased C1qa (**C**, Kruskal-Wallis non parametric test, p<0.01, Dunn's multiple comparison test, n=2-6/group) and C3 (**D**, p<0.05) levels at this time-point,*

suggesting maintained activation of the complement cascade. ***F)*** *Elevated expression of Psmb9 gene, coding for the β1i subunit of the immunoproteasome, a component of protein degradation observed selectively in glial cells, was found to be elevated at 1 month post-injection in hTAU^{ProAggr} group (Kruskal-Wallis non parametric test, p<0.05, Dunn's multiple comparison test, n=3-6/group), and to a lesser extent in hTAU^{P301L} animals, suggesting that glial cells associated with the tauopathy had active processes of degradation. Stars represent results of the post-hoc comparison to PBS control group. *p<0.05, **p<0.01*

Reminiscent of what observed in human neurodegenerative diseases, including tauopathies, microglial and astroglial activation was observed following overexpression of different Tau constructs. Microgliosis was observed in all Tau groups at 1 month post-injection as well as, to a lesser extent, in utGFP animals suggesting that initial microglial activation may be related to inflammatory processes following AAV injection. Consistent with this finding, initial elevation of phagocytic markers was observed in all groups including PBS-injected animals suggesting that glial cells may be recruited to eliminate cellular debris at the site of injection. Interestingly, while initial microgliosis resolved at 3 months post-injection in most groups, hTAUP301L animals exhibited maintenance in microglial activation at this stage. This may suggest that Tau pathology induced by different constructs is associated with the differential recruitment of inflammatory cells, which may in turn underlie functional differences.

Astrogliosis, on the other hand, was found to be induced specifically by Tau pathology as increased astrocytic reactivity was observed only in animals expressing Tau constructs. Interestingly, no significant difference in the extent of astrogliosis could be observed between 1 and 3 months post-injection, which may be related to the relative stability of Tau pathology (i.e. Tau hyperphosphorylation and aggregation). Surprisingly, however, astrocytic activation in hTAU^{P301L} and hTAU^{ProAggr} groups was associated with the formation of astrocytic Tau lesions. Preliminary studies done in mice allowed to confirm that Tau accumulation was not consecutive to transgene expression in those cells. In addition, the finding that the kinetics of expression of phagocytic markers in the hTAU^{ProAggr} mirrored that of glial Tau accumulation suggest that those lesions may be related to Tau uptake by astrocytes secondary to neuronal degeneration.

DISCUSSION

DISCUSSION

I – Generation of gene-transfer based rat models of human tauopathies

The main objective of this project was the development of several models of pure tauopathy in rodents. To this purpose, we chose to use AAV-mediated gene transfer of human Tau to induce a tauopathy in the HC of adult rats, a species that is more practical for brain imaging and fluid analysis of biomarkers than mice. Expression of human Tau led to the rapid development of a tauopathy starting at 1 month post-injection, each construct recapitulating specific features of Tau pathology, associated with different involvement of neuroinflammation. Indeed, overexpression of human wild-type Tau led to its hyperphosphorylation associated with neurodegeneration but no aggregation. In contrast, its co-expression with the pro-aggregation peptide TauRD-ΔK280 strongly promoted its aggregation, which was associated with strong neuroprotective effects.

We will describe here how the phenotypes observed following injection of our different constructs relate to what was described in other models of tauopathy. We will then discuss the possible applications of our different models as well as the implications of our results for the comprehension of Tau-induced neurodegeneration.

1) <u>Characterization of the pathology induced by wild-type human Tau</u>

Gene-transfer of the human wild-type Tau protein led to the induction of an early stage tauopathy, reminiscent of what is observed in transgenic models. Indeed, overexpression of wild-type human Tau in the hTAU^{WT} group led to the strong hyperphosphorylation of the protein (*Figure 31 in the results section*) but with only limited aggregation (*Figures 32 and 33*). This is consistent with what was observed in most transgenic models where overexpression of wild-type Tau led to early Tau pathology with hyperphosphorylation of Tau but only little tangle formation (Andorfer et al., 2003; Probst et al., 2000; Spittaels et al., 1999). Tau pathology in those models, however, was associated with very limited neurodegeneration which is in strong contrast with our finding of drastic neuronal loss following hTAU^{WT} expression (*Figure 37*).

Several reasons could explain the discrepancy between our results and those in transgenic models. One would be the setting of compensatory mechanisms in transgenic animals due to long-term transgene expression. Differences in expression levels may also be involved, as vector-based approaches may allow stronger transgene expression in transduced cells than what could be achieved in transgenic animals. A relationship between Tau expression levels and the extent of pathology was indeed observed in animal models (Jaworski et al., 2009; Klein et al., 2005) and the modulation of Tau expression in humans was found to be associated with the development of several tauopathies (Hooli et al., 2014; Myers et al., 2007; Rovelet-Lecrux et al., 2010). Increased expression of pathological Tau species in our model may thus be associated with strong acceleration of the pathological process. The finding that AAV-mediated gene transfer of human wild-type Tau in mice leads to neurodegeneration starting at 3 weeks post-injection also supports this hypothesis (Jaworski et al., 2009).

Lastly, this discrepancy between our results and those obtained in transgenic mice may be related to species differences between rats and mice. Indeed, the contribution of endogenous murine Tau to the pathological processes induced by the human protein is still unclear and contradictory results have been

obtained in other labs. The fact that hTAU mice, expressing all 6 isoforms of human Tau on a Tau KO background, exhibit stronger phenotype than their parent line may suggest that the endogenous protein may counteract pathology (Andorfer et al., 2003). In contrast, recruitment of the endogenous protein to aggregates was found in a model expressing human ΔK280 mutant Tau (Sydow et al., 2011b) and knock-out of murine Tau was found to reduce the toxicity induced by the overexpression of human mutant P301L Tau (Wegmann et al., 2015). The strong neurotoxicity of $hTAU^{WT}$ observed in our study in absence of significant aggregation may thus be related to its inhibitory effect on the function of the endogenous protein. Indeed, in vitro studies have demonstrated that soluble hyperphosphorylated Tau is able to inhibit MT assembly by sequestering the normal protein and that this inhibitory effect is lost upon polymerization (Alonso et al., 2006). In addition, species differences can be observed in the expression ratio of different Tau isoforms. While human adult brain shows similar expression of 3R and 4R isoforms, mice present with a strong enrichment of 4R isoforms (Takuma et al., 2003). This imbalance is also observed in rats but to a much lesser extent (Hanes et al., 2009). The much closer to human cellular environment in this species may thus be associated with increased susceptibility to Tau pathology by overexpression of the human protein. It remains that the link between 3R/4R ratio and toxicity is still not well established.

Surprisingly, despite the strong toxicity exerted by $hTAU^{WT}$, no significant cognitive impairment could be observed in those animals (*Figures 42 and 43*). This is again in strong contrast with what observed in transgenic animals where even light Tau pathology could induce significant cognitive (Andorfer et al., 2003) or locomotor (Probst et al., 2000; Spittaels et al., 1999) defects, those occurring before or in absence of neurodegeneration. Several reasons could explain those differences. First, it may be that mice present stronger vulnerability than rats to neuronal injury, thus developing larger functional impairment associated with mild Tau pathology. The finding that induction of Tau pathology by AAV-mediated gene-transfer in the HC of rats did not lead to any cognitive defect may be in support of this hypothesis (Dayton et al., 2012) and is in agreement with our own data. Alternatively, this may be related to the spatial restriction of Tau pathology in vector-based models. Although both hypotheses may explain our results, the fact that Tau pathology induced by AAV-mediated gene transfer in the subtantia nigra is associated with motor deficits (Klein et al., 2005) suggest that this approach can lead to functional impacts.

Lastly, the absence of cognitive deficits in our model could be associated with the selective loss of transgene-expressing neurons. Indeed, RT-qPCR for the transgene mRNA showed a strong reduction in this group compared to the other two constructs (*Figure 29*) prior to behavioural testing. It is generally believed that behavioural deficits are either associated with neurodegeneration or impairment of neuronal/synaptic function by pathological Tau species. This last hypothesis if supported by data obtained in the rTg4510 transgenic model, where transgene suppression was associated with rescue of cognitive deficits, even at stages where strong neuronal loss had already occurred (SantaCruz et al., 2005). This suggests that impairment of cognitive function may be more associated with the expression of pathogenic proteins than with neurodegeneration per se. Thus, the absence of cognitive deficits in our model may be related to the fact that neurons expressing pathological Tau had disappeared, the remaining healthy neurons being able to compensate for this loss. Lastly, the absence of memory deficits in our models may be associated to the type of test used. Indeed, a short 3 min interval was used in the Y-maze paradigm that may not have been sufficiently stringent to detect subtle memory impairments.

2) <u>Characterization of the pathology induced by mutant Tau constructs</u>

In contrast to the limited Tau pathology observed in the hTAU^{WT} group, co-expression of human wild-type Tau with the pro-aggregation peptide TauRD-ΔK280 in the hTAU^{ProAggr} group strongly potentiated its aggregation (*Figures 32 and 34*). This is consistent with the known strong pro-aggregation properties of the ΔK280 mutation (Barghorn et al., 2000; Von Bergen et al., 2001). This may also be related to the increased amyloidogenic properties of truncated forms of Tau (Barghorn et al., 2000; Gamblin et al., 2003) that may occur through the removal of inhibitory activity from the C-terminal and N-terminal regions on Tau aggregation. This also reminiscent of what was observed in transgenic models expressing this TauRD-ΔK280 construct, where strong aggregation was observed in the form of Gallyas-positive NFT-like lesions starting at 3 months of age (Mocanu et al., 2008). Interestingly, another model expressing full-length Tau bearing the same ΔK280 mutation did not induce as much aggregation (Eckermann et al., 2007), confirming the potentiating effect of truncation on the pro-aggregation properties of the ΔK280 mutation.

Intriguingly, stronger aggregation in ΔK280 transgenic models was associated with worsening of functional impairment. Indeed, while synaptic defects and cognitive impairment were observed in both transgenic models (Decker et al., 2015; Sydow et al., 2011a; Van der Jeugd et al., 2012), significant neuronal loss was observed only in the model expressing TauRD-ΔK280 peptide. This is in strong contrast with our results showing that stronger aggregation in the hTAU^{ProAggr} was associated with neuroprotective effects (*Figure 37*).

Several reasons could explain the discrepancy of our results compared to transgenic models. First, one key feature of transgenic mice was the finding that human Tau constructs recruited the endogenous murine protein into aggregates. Neurodegeneration in mice may have thus occurred through a toxic loss of function of the endogenous protein that, when aggregated, would not be able to promote MT stabilization (Fischer et al., 2009; Tepper et al., 2014). The effect of hTAU^{ProAggr} construct on the endogenous murine Tau was not assessed during our study. However, one possible explanation for the robust neuroprotective effect of hTAU^{ProAggr} may be that strong seeding of TauRD-ΔK280 peptide is exerted on human wild-type Tau instead of on murine protein. Promoted aggregation of wild-type human Tau would protect from its toxicity. In the same time, TauRD-ΔK280 peptide being trapped into aggregates, it would not be able to exert its inhibitory function on endogenous Tau. In other words while both hTAU^{WT} and TauRD- ΔK280 are toxic individually, they counteract each other when present in the same cell. Further studies should be performed to study this hypothesis, notably by evaluating the effect of TauRD-ΔK280 overexpression alone in rats on the endogenous protein. Differences between hTAU^{ProAggr} expression level and that observed in transgenic mice may also underlie those differences of phenotype. Indeed, in both transgenic models, transgene was found to be only weakly expressed, representing 1 to 3-fold the endogenous protein (Eckermann et al., 2007; Mocanu et al., 2008). Stronger overexpression was observed in our model (*Figure 29*) that may be associated with higher local concentration of the protein, which could in turn lead to stronger aggregation when proteins are missorted to the somatodendritic compartment (*Figure 31*).

The pathology developed in the hTAU^{P301L} group seemed to represent an intermediate phenotype between hTAU^{WT} and hTAU^{ProAggr}. Indeed, consistent with its amyloidogenic properties (Hong et al., 1998), P301L mutation was associated with stronger aggregation than in the hTAU^{WT} group. However, aggregates in the hTAU^{P301L} group seemed less mature than with the hTAU^{ProAggr} construct. Indeed, while a similar number of AT100-positive somas was observed in both groups (*Figure 32*), less Gallyas-positive NFT-like lesions could be observed in the hTAU^{P301L} group (*Figure 34*). This suggests that most

of those aggregates were in a soluble non-fibrillar form. Tau pathology in this group was associated with neurodegeneration, although to a lesser extent than in hTAU^{WT} animals (*Figure 37*). This is consistent with what observed in transgenic animals expressing different Tau mutants, where cognitive deficits and neuronal and synaptic impairment usually occur before the apparition of argyrophylic tangle-like structures (Maurin et al., 2014; Oddo et al., 2003; Ramsden et al., 2005; Schindowski et al., 2006; Terwel et al., 2005). The implications of those results and those obtained using the other two constructs for the study of Tau-induced neurodegeneration will be described in more details in the second part of this discussion.

3) Advantages & drawbacks of our models for different applications

Advantages of vector-based transgene expression for the development of disease-models in rodents

During this project, we were able to develop three fast-developing models of pure tauopathy, each recapitulating key features of Tau pathology. Viral-based tools were chosen for the development of those models because they present several advantages compared to other approaches. First, injection of viral vectors can be performed in adult animals, thus avoiding adverse effects of transgene expression during development. Alternatively, transgene expression from early developmental stages, where brain structure is highly flexible, can in turn lead to compensatory mechanisms that could slow down pathology in adult animals (as seen in transgenic animals). This may be the reason for the very late development of Tau pathology in most transgenic animals and would be avoided using vector-based approaches. Expression of pathogenic proteins at adult age also proves relevant for the study of tauopathies, such as AD, that usually develop with aging (Blennow et al., 2006). Dementia in tauopathies, however, seems to arise from a very long process starting at early age, as suggested by the finding of pretangle pathology in the locus coeruleus of young adult subjects (Braak and Del Tredici, 2011). However, as soon as cognitive deficits appear, the rate of progression of the pathology can be strikingly rapid. This suggests that once pathological Tau species have started to accumulate, the process may accelerate in a snow-ball effect. The use of gene-transfer to induce overexpression of pathological Tau species in animals may allow bypassing the slow process leading to the triggering of the pathology. This would not allow the study of the mechanisms inducing Tau aggregation but may prove useful for the study of the pathways involved in its toxicity.

The second advantage of vector-based models is the possibility to target transgene expression not only to a specific cell-type but also to a spatially restricted brain region. Indeed, the main issue with most transgenic models of tauopathy is the high transgene expression often observed in brainstem and spinal cord, in addition to cortical and limbic structures (Allen et al., 2002; Lewis et al., 2000; Terwel et al., 2005; Yoshiyama et al., 2007; Hrnkova et al., 2007). This led in most cases to the apparition of strong locomotor impairment which interfered with cognitive testing, thus limiting the interest of those models for translational research. Transgene expression in vector based models is mostly restricted to the injection site, allowing to control the structure and associated functions to be targeted. On a longer term, propagation of the pathology is sometimes observed to downstream connected regions (Dujardin et al., 2014b; Peeraer et al., 2015), but this can be controlled by considering the anatomical connectivity of the targeted structure. In addition, because connectivity is often associated with function of the structure, it can even allow increased specificity of the affected cognitive function (Stancu et al., 2015). Lastly, many tauopathies such as AD are associated with the sequential involvement of anatomically connected regions (Braak and Braak, 1991). Progression of the pathology in vector-based models may thus be more relevant to what observed in human.

Lastly, another advantage of gene-transfer for the development of disease models is its versatility, allowing the modulation and direct comparison of several parameters in a given study. This approach can be used for example to study the impact of Tau pathology on young or aging animals (Klein et al., 2010). The use of similar vector tools can also allow the direct comparison of the pathology induced by wild-type or mutant Tau (Caillierez et al., 2013). Lastly, injection of Tau vectors in transgenic mice expressing mutant amyloid precursor protein (APP), allowing the study of the interaction between amyloid and Tau pathologies (Osinde et al., 2008). Such questions could not be easily addressed in transgenic animals because of the difficulty to directly compare several models. Indeed, phenotypic variability can sometimes be observed between models expressing the same pathological form of Tau, which may be related to the location of transgene insertion (Schindowski et al., 2006). The use of non-integrative viral vectors, such as adeno-associated viruses (AAV) could prevent such issues to arise and allow direct comparison of different experimental conditions.

Potential applications of our different models

The models that we developed may be used for several applications. For example, the availability of models showing strong aggregation in a such short time-course (1 month post-injection in the case of $hTAU^{P301L}$ and $hTAU^{ProAggr}$ constructs) may be of great use for screening of drugs targeting aggregation processes. Direct comparison of those two models may, in addition, allow studying the beneficial and adverse effects of targeting different stages of aggregation on neuronal integrity. Indeed, while $hTAU^{P301L}$ group was associated with mostly non-fibrillar aggregates, overexpression of $hTAU^{ProAggr}$ construct led to the formation of large argyrophilic lesions. $hTAU^{WT}$ construct, on the other hand, may be used to study the efficiency of compounds potentiating fibrillation to inhibit Tau toxicity or to trap soluble toxic forms.

This rapidity in the development of pathology in our models may, however, be a drawback for the study of disease progression. Phenotypes developed by each of the constructs seem relatively stable over the time of our study, suggesting that they may represent end-stage pathologies. Testing the efficiency of treatment strategies would thus need to rely on the study of how those affect the apparition of given parameters, such as neuronal loss or behavioural deficits. However, no behavioural deficit could be detected in our models. In the case of the $hTAU^{ProAggr}$ construct this may be related to its relatively neuroprotective effect. Testing at later time-points may still allow to evidence significant cognitive impairment. In the case of the $hTAU^{WT}$ group, we suggest that this lack of impairment may be related to the rapid and specific loss of transgene-expressing neurons, that may be compensated for by remaining neurons. Because pathology may, at least in part, be related to levels in transgene expression (Klein et al., 2008a), lowering the viral titers used offers the possibility to slow down the process.

In addition, further studies should assess in more details the effect of Tau overexpression on neuronal function. No significant difference could be observed between our models in the expression of synaptic markers. However, this may be due to the technique used here to assess synaptic defects on the whole of the HC. More precise characterization of the synaptic effect of Tau constructs should be performed, for example by means of electrophysiological studies within the transduced region. This could allow identifying biomarkers of the neurotoxicity associated with Tau pathology. Those would then be used as outcome measures for the evaluation of treatment strategies.

Lastly, the development of those models in rats may also allow the study of biomarkers that are not readily accessible in mice, such as dosage of Tau in CSF and *in vivo* imaging. Multimodal study of our different models may allow identifying which biomarkers represent the best correlate of underlying pathology and how those respond to treatment. This approach has already been used in a transgenic rat

model of tauopathy in which worsening of cognitive deficits was found to be associated with an increase in CSF p-Tau181 (Zilka et al., 2010).

In our study, increase in CSF total Tau was observed in all Tau-expressing animals (*Figure 36*) suggesting that it may be a correlate of Tau pathology. This increase could be due to the release of Tau from degenerating neurons. Indeed, increased levels were observed in $hTAU^{WT}$ and $hTAU^{P301L}$ animals compared to $hTAU^{ProAggr}$ group at 1 month post-injection, a time-point where both constructs exhibited neuronal loss. Interestingly, the highest level was found in the $hTAU^{P301L}$ group that also exhibited continuous neurodegeneration processes from 1 to 3 months post-injection, while neuronal loss peaked in the $hTAU^{WT}$ group at 1 month post-injection. Alternatively, release of Tau in CSF may reflect an attempt of clearance of the aggregates from degenerating neurons and may not solely rely on passive release from already dead neurons.

A strong decrease in CSF Tau levels was observed in all groups at 3 months post-injection. Interestingly, it occurred in the $hTAU^{P301L}$ along with a concomitant increase in the number of AT100-positive somas (*Figure 32*) as well as conversion of non-fibrillar aggregates into fibrils (*Figure 34*). This decrease in CSF Tau may thus be a consequence of Tau aggregation into large fibrillar aggregates that could not be released into the extracellular space, as was suggested for Aβ peptide which parenchymal aggregation is associated with decreased CSF levels (Blennow et al., 2010). This is consistent with the low CSF Tau level observed at all time-points in the $hTAU^{ProAggr}$ groups that presents strong NFT-like pathology. This is also consistent with data from the literature that showed reduced 4R isoforms in CSF of PSP patients, a tauopathy associated with selective aggregation of 4R Tau (Barthélemy et al., 2016). In addition, this is reminiscent of what was found in AD patients where initial elevated CSF Tau levels were found to drop down after onset of symptoms (Fagan et al., 2014). The variability observed between Tau constructs in CSF Tau levels also closely resembles what is observed in human tauopathies. Indeed, while elevated CSF Tau is observed in AD and CBD, no such increase can be found in PSP (Urakami et al., 2001; Wagshal et al., 2015). Studying how CSF Tau levels relate to the pathology in our models could thus allow a better understanding of the mechanisms underlying those differences between tauopathies, thus permitting to determine its clinical significance.

Another advantage of our rat models is the possibility of imaging those animals in vivo using positon emission tomography (PET). Indeed, current research for the identification of biomarkers focuses on the development of Tau-directed PET tracers (Shah and Catafau, 2014). Most of those tracers are chemical derivatives of amyloid dyes, i.e. composites able to bind aggregates enriched in β-pleated sheets such as Tau and amyloid β (Aβ) proteins. Because of those origins, one of the main challenges in the field is to develop compounds that specifically bind to Tau aggregates compared other amyloids. Several of currently developed compounds were described as selectively binding to Tau lesions in AD brain (Fodero-Tavoletti et al., 2014). However, the co-occurrence of several types of amyloid lesions in the brain of patients may hinder definite conclusions on the specificity of those tracers. PET imaging of our models, which develop tauopathy in the absence of any other proteinopathy may permit to conclude on this matter. The other main issue for the development of Tau-binding PET tracers is the question of selectivity for different types of aggregates. While some compounds may bind uniquely to aggregates found in AD, others have been found to recognize Tau in several tauopathies (Maruyama et al., 2013). The study of those tracers in our models, that exhibit different stages of aggregation, could permit to determine whether those differences in binding may rely on selectivity for different types of aggregates. Further characterizing the target of those tracers seems necessary before PET imaging can be used as a biomarker in patients.

II – Relationship between Tau aggregation and its toxicity

1) Aggregation of Tau into tangle-like lesions in the hTAU^{ProAggr} is associated with neuroprotection

One striking result of our study is the negative relationship observed between the degree of Tau aggregation and its toxicity (**Table 7**). Indeed, while expression of human wild-type Tau in the hTAU^{WT} group led to a strong hyperphosphorylation but no significant aggregation, its co-expression with the pro-aggregation peptide TauRD-ΔK280 in hTAU^{ProAggr} animals strongly potentiated its aggregation, with the formation of numerous argyrophilic NFT-like lesions as early as 1 month post-injection (*Figure 34 in the results section*). This was associated with neuroprotection against the strong toxicity exerted by hTAU^{WT} alone (*Figure 37*). This is in accordance with several studies that identified NFTs as either relatively inoffensive or even protective. Indeed, spatial dissociation between NFT formation and neurodegeneration was observed in the brain of AD patients and transgenic mouse models (Spires et al., 2006; Vogt et al., 1998), suggesting that those may not represent the primary cause of Tau-induced neurodegeneration.

		hTAU^{WT}		hTAU^{P301L}		hTAU^{ProAggr}	
		1M	3M	1M	3M	1M	3M
Tau pathology	Hyperphosphorylation	+++	+++	++	+++	++	++
	Aggregation	+	+	+++	+++	+++	++
	NFT-like lesions	-	-	++	++	+++	+++
Toxicity	Neuronal loss	+++	+++	++	+++	-	+
	Morphological defects			++		++	
	Behavioural impairment	-				-	
Inflammation	Microgliosis	++	-	++	+++	++	-
	Astrogliosis	+++	++	+++	++	++	++
	Glial Tau pathology	-	-	++	++	+	++

Table 7: Recapitulative table of the main results obtained in this study
Intensity of a given effect is indicated for each group at 1 month (1M) and 3 months (3M) post-injection, classified by type of effect (Tau pathology, toxicity and neuroinflammation). A negative relation could be observed between the extent of argyrophilic NFT-like lesions and neurotoxicity (red contour).

On the contrary, NFTs may instead allow delaying Tau toxicity. Indeed, not only Tau accumulation can be found in morphologically normal neurons (Andorfer et al., 2005; van de Nes et al., 2008; Rocher et al., 2010), but those tangle-bearing neurons can live for decades after somatic Tau aggregation started (Morsch et al., 1999). Those can be fully integrated into neural networks and be even more functional than cells containing only soluble Tau (Fox et al., 2011; Kuchibhotla et al., 2014; Rudinskiy et al., 2014). Our finding of strong Gallyas reactivity in hTAU^{ProAggr} animals suggests that tangle formation may represent a protective mechanism allowing neurons to escape acute neurodegeneration (de Calignon et al., 2010; Spires-Jones et al., 2008).

Surprisingly, strong discrepancy was observed in our study between histological and biochemical results, with no visible sarkosyl-insoluble material (*Figure 34*) detected by western-blot. Interestingly, this was associated with a reduction in the level of human Tau protein compared to the other two Tau constructs

that could not be explained by differences in transgene expression since it was found to be the highest in the hTAU^{ProAggr} group (*Figure 29*). Altogether, those observations led us to hypothesize that the size and structural nature of Tau aggregates in the hTAU^{ProAggr} group may have hindered their detection in standard SDS-PAGE denaturing conditions, thus explaining differences between histological and biochemical results. Interestingly, another class of Tau aggregates was recently identified, termed granular Tau oligomers (GTOs), which exhibit very similar biochemical properties. These large amorphous aggregates, composed of approximately 40 Tau proteins, are indeed highly insoluble but do not sediment in standard fractionation protocols (Maeda et al., 2007). In addition, it was noted that their high resistance to reduction prevents them from entering standard gels and be detected (Cowan and Mudher, 2013), which may explain our finding of little sarkosyl-insoluble material in hTAU^{ProAggr} animals. This is consistent with the strong amyloidogenic properties of the ΔK280 mutation that was found to exceed that of many other mutations (Barghorn et al., 2000).

Interestingly, the accumulation of such GTOs, thought to be an intermediary state of aggregation before tangle formation (Maeda et al., 2006), was found to be associated with neuroprotection in *Drosophila* models. In one study, chaperones-induced aggregation of Tau into large aggregates reminiscent of human GTOs was associated with improvement of cognition and halted neurodegeneration (Ali et al., 2012). Similarly, in another study, the rescue of motor deficits and disrupted axonal transport observed following treatment with GSK3-β inhibitors was associated with the formation of GTO-like structures (Cowan et al., 2015). This may suggest that the neuroprotective effect observed in our hTAU^{ProAggr} model may be associated with the formation of such GTO-like aggregates. Ultrastructural studies of the morphology of Tau aggregates induced by the hTAU^{ProAggr} construct may allow us to confirm this hypothesis by identifying which type is present in this model.

Scarce morphological abnormalities were however observed in the hTAU^{ProAggr} by means of electron microscopy at 2 months post-injection (*Figure 39*), which suggests that accumulation of large insoluble aggregates may not be entirely benign. This is consistent with current hypothesis posing that initially neuroprotective NFT formation may, in the longer term, induce slow neuronal death. Indeed, the observation of “ghost-tangles” in the brain of patients (Bancher et al., 1989) suggests that somatic aggregation of Tau in the form of PHFs may lead to the loss of neuronal integrity. It may also be possible that accumulation of large fibrillary aggregates into neurons would affect normal neuronal function. Indeed, several studies have found strong decrease in several pre- and post-synaptic markers in NFT-bearing neurons when compared to neighbouring neurons, implying that synaptic transmission may be impaired due to tangle formation (Callahan et al., 1999; Ginsberg et al., 2000), probably by the sequestering of essential cellular components into Tau aggregates (Wang and Mandelkow, 2016). In addition, a recent *in vitro* study demonstrated that Tau inclusions are dynamic structures, constantly undergoing fission and fusion events (Guo et al., 2016). Thus, long-term toxicity of the seemingly inert NFTs could also be associated with the continuous release of soluble aggregates.

Interestingly, although no significant neuronal loss observed in the hTAU^{ProAggr} group even at 3 months post-injection (*Figure 37*), a reduction in the number of neurons presenting somatic Tau aggregation was observed at this time-point (*Figure 32*). This reduction could be associated with clearance processes that may occur specifically with this construct. Indeed, it was demonstrated in several models that large Tau aggregates can be cleared following transgene suppression, notably via the autophagy-lysosome pathway (Guo et al., 2016; Hochgräfe et al., 2013; Polydoro et al., 2013). Although no significant changes in the expression of genes involved in degradation processes could be observed between groups, a tendency towards an increase was observed in the hTAU^{ProAggr} group (*Figure 41*), suggesting that there may be an active clearance of aggregates in this model. To note, this absence of statistically

significant increase may be related to a surprisingly elevated expression of those genes in the utGFP group that, on the other hand, often presented aberrant mRNA expression. This suggests that despite the fact that no neuronal loss was detected in this group, overexpression of the GFP mRNA without protein translation may have noticeable impact on some cellular functions, which questions the validity of this construct as a control.

Lastly, no modification in the expression of synaptic proteins (*Figure 40*) could be observed in the hTAU^{ProAggr} group, despite some indications of synaptic defects after longer hTAU^{ProAggr} expression. It may be possible that those defects were too sparse, such that RT-qPCR analysis on whole HC homogenates would have failed to detect them. It is also possible that upregulation of synaptic proteins in neighbouring neurons may have occurred to compensate for deficits observed in cells expressing pathological Tau. Further analysis on isolated synaptosome preparations as well as electrophysiological studies could allow us to assess more precisely the effect of long-term hTAU^{ProAggr} expression on synaptic function. Characterizing the progression of the pathology on a longer term should allow us to determine if increased toxicity can be observed past 3 months post-injection, and whether this can lead to functional consequences. Indeed, no behavioural impairment could be observed in our model at 1,5 months post-injection (*Figures 42 and 43*), confirming that the pathology at this time-point was still at an early stage. But this does not preclude the possibility that functional deficits could occur at a later stage.

2) Identification of the toxic species in hTAU^{WT} and hTAU^{P301L} groups

Strong neurotoxicity was observed in two of the Tau constructs, hTAU^{WT} and hTAU^{P301L}, as early as 1 month post-injection (*Figure 37*). Those, however, exhibited very different pattern of Tau pathology suggesting that they may differ in the type of toxic Tau species.

Indeed, while both presented strong Tau hyperphosphorylation (*Figure 31*), significant aggregation was observed only in the hTAU^{P301L} group using AT100 antibody (*Figures 32 and 33*). AT100-positive aggregates in this group, however, were found to be largely in a non-fibrillar state (*Figure 34*), thus pointing towards toxicity of soluble oligomeric species. This is in accordance with a growing body of evidence suggesting that Tau oligomers may represent the major contributor of Tau-induced neurodegeneration. Injection of both recombinant and brain-derived Tau oligomers in wild-type mice was indeed found to induce a large variety of cellular defects, including reduction of synaptic and mitochondrial markers, caspase activation and neuronal loss, leading to cognitive deficits (Lasagna-Reeves et al., 2011, 2012b). Those effects appeared prior to tangle formation (Fá et al., 2016), thus suggesting that oligomers exert direct toxicity irrespective of the presence of NFTs. The amount of oligomeric forms in rTg4510 mice, expressing mutant P301L human Tau protein, was found to tightly correlate with cognitive performance in those animals (Berger et al., 2007). Interestingly, Tau oligomers in this model were observed even before the apparition of cognitive deficits, suggesting that it had to accumulate before affecting neuronal function. Tau oligomers were also observed in the brain of AD patients, being an important component of neurons bearing pre-tangles and intracellular NFTs, but mostly absent from ghost tangles (Lasagna-Reeves et al., 2012a). This further supports the hypothesis that toxicity exerted by oligomeric Tau occurs prior to NFT formation. To investigate the possibility that overexpression of hTAU^{P301L} generates toxic oligomeric species, dot blot analysis was performed using T22 antibodies which has been described to bind specifically to Tau oligomers *in vitro* and in the brain of AD patients (Lasagna-Reeves et al., 2012a). No significant between groups difference could be observed (*Figure 35*). However, the strong background staining observed even in control animals suggest that analysis performed on whole homogenates may have hindered the detection of oligomers. Similar analysis on different fractions obtained during sarkosyl extraction may allow a better detection of

those soluble species. Alternatively, more precise measures, e.g. by means of mass spectrometry, could allow us to better quantify the amount of oligomers in our different models and to confirm that the toxicity of hTAU^{P301L} construct is associated with their accumulation.

Such may be the case in the hTAU^{WT} group. Indeed, one surprising result of our study is the finding that wild-type human Tau overexpression led to strong neurotoxicity (*Figure 37*) in absence of any noticeable aggregation detected with AT100 antibody (*Figure 32*) or Gallyas silver impregnation (*Figure 34*). This may be interpreted as evidence for the fact that the toxicity of soluble hyperphosphorylated human Tau may occur without the need for it to aggregate. Others have also demonstrated toxicity of human Tau overexpression in absence of any aggregation in a model of pure tauopathy using AAV-mediated gene transfer of wild-type Tau in the hippocampus of WT mice (Jaworski et al., 2009). One hypothesis for this adverse effect of monomeric human Tau would be through inhibiting the function of the endogenous protein. Indeed, it was shown in vitro that only soluble hyperphosphorylated Tau, but not PHF-Tau, is able to sequester the normal protein, leading to an inhibition of MT assembly (Alonso et al., 2006). Given the strong homology in human and rodent Tau sequence (Kosik et al., 1989a; Lee et al., 1988), an interaction between those may be highly plausible. The phenotypic variability observed between hTAU^{WT} and hTAU^{P301L} may thus be related to distinct pathological processes, those acting respectively through a toxic loss or toxic gain of function. Further studies should be performed to unravel the effect of human Tau overexpression on the expression and function of the endogenous protein, which could allow us to identify which pathways are implicated in Tau-induced toxicity in those different models. However, the absence of AT100 positivity does not necessarily mean that hTAU^{WT} was entirely unable to aggregate. Indeed, some sarkosyl-insoluble material was observed in this group (*Figure 34*), this being largely AT100-negative but HT7-positive. This suggests that wild-type human Tau was indeed capable of aggregation, consistent with previous findings in transgenic and vector-based animal (Andorfer et al., 2005; Caillierez et al., 2013). The AT100 epitope has been found to stain primarily mature NFT pathology in the brain of patients (Augustinack et al., 2002) which led to the suggestion that this pathological phosphorylation may be a marker of fibrillation. Our results however suggest that aggregation of Tau into fibrils can occur independently of the formation of this epitope and that AT100 epitope can also be observed in non-fibrillar aggregates such as what was observed in the hTAU^{P301L} group. It may thus be possible that some kind of aggregates was present in our hTAU^{WT} model, which did not exhibit the AT100 epitope. An alternate hypothesis for the toxicity of hTAU^{WT} construct may thus implicate soluble oligomers that, however, presented distinct biochemical properties and pathological epitopes compared to hTAU^{P301L} animals.

The classical view for the sequence of Tau aggregation starts with hyperphosphorylation at a number of pathological epitopes inducing Tau aggregation. However, growing evidence suggest that the relationship between hyperphosphorylation and aggregation may not be that straightforward. Indeed, while some phosphorylation sites, known to induce detachment of Tau from the MT, have been found to inhibit aggregation (Schneider et al., 1999). Conversely, aggregation into oligomers can occur before phosphorylation at some pathological sites, including AT8 epitope (Lasagna-Reeves et al., 2012a). It is thus possible that toxicity of hTAU^{WT} was due to the accumulation of soluble oligomeric species that formed prior to phosphorylation at AT8 sites and that did not exhibit AT100 reactivity. Interestingly, hTAU^{WT} animals presented the highest degree of phosphorylation of the AT8 epitope at 1 month post-injection (*Figure 31*). This was associated with a stronger toxicity compared to hTAU^{P301L} construct, inducing significant atrophy of the HC region (*Figure 37*). In addition, AT8 reactivity was reduced in the hTAU^{ProAggr} group, which presented the highest amount of argyrophilic lesions. It is thus possible that aggregation of Tau into large insoluble aggregates was associated in this model with the loss of AT8

reactivity. The AT8 epitope could then be considered, in our models, as a marker of soluble Tau aggregates. The negative correlation observed between phosphorylation of AT8 reactivity and all markers of neuronal integrity (*Figure 37*) may then reflect the effect of toxic soluble species.

Differences between constructs in the extent of Tau pathology and associated neurotoxicity may thus be explained by differences in the balance between soluble and insoluble Tau aggregates (**Figure 50**). Indeed, Tau aggregation is thought to follow a stereotyped progression from soluble monomers to fibrils through dimers and oligomeric species (Patterson et al., 2011; Sahara et al., 2007). But this process may not be irreversible and there may be a constant exchange between those different species (Guo et al., 2016; Hochgräfe et al., 2013). Phenotypic variability observed in our models may thus be determined by an imbalance towards one of those species. Hence, hTAU^{WT} construct would produce predominantly soluble and small oligomeric species that would act either through a toxic loss or toxic gain of function. The P301L mutation would instead push a bit more towards aggregation, which is consistent with its described properties (Hong et al., 1998). This will lead to the production of oligomeric species, that may be different in nature from those observed in hTAU^{WT} animals and being able to fibrilize, thus delaying slightly toxicity. Overexpression of the hTAU^{ProAggr}, on the other hand, would strongly shift the balance towards production of highly insoluble aggregates (either GTOs or NFTs) leading to initial strong neuroprotection. Those large aggregates may then eventually affect neuronal function.

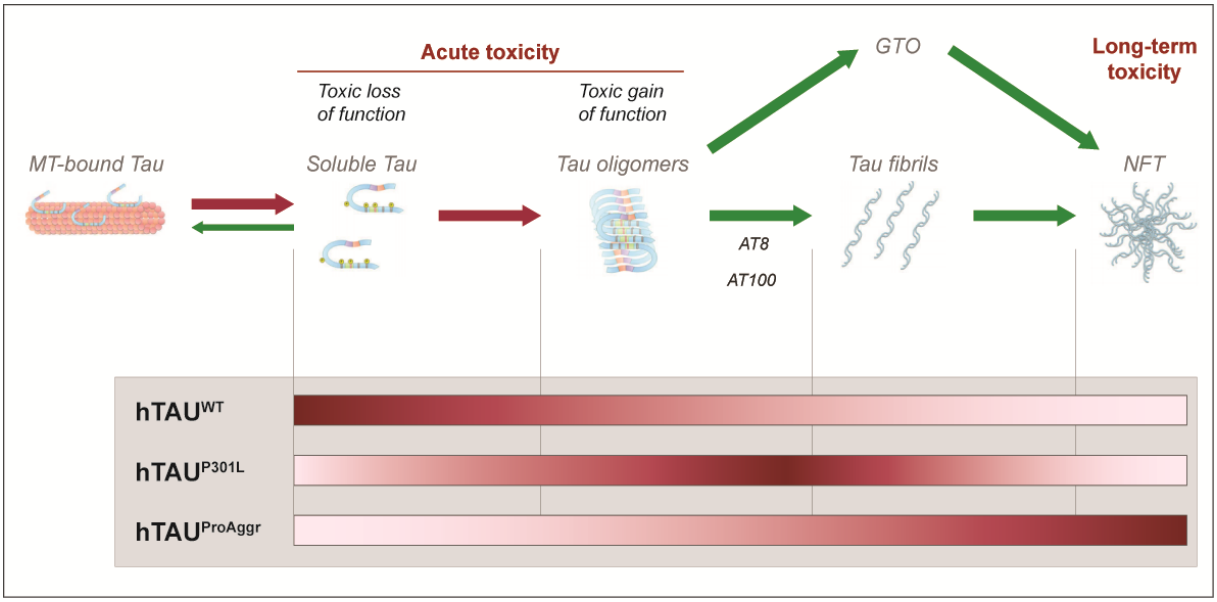

Figure 50: Schematic representation of the hypothesized reason for phenotypic variability of Tau constructs
Differential toxicity observed with Tau constructs may be related to differences in the nature of aggregates, hTAU^{WT} construct inducing an imbalance towards soluble toxic species while hTAU^{ProAggr} expression leading to a strong shift towards the production of large insoluble aggregates. Bars for each group represent the hypothesized relative amount of different Tau species from the highest concentration (dark red) to almost none (light pink). Schematic representation of the sequence of Tau aggregation is represented above. Green and red arrows represent respectively a supposed positive or negative effect of conversion from one type of aggregate to the next on neuronal integrity. Adapted from (Martin et al., 2011).

3) <u>Contribution of neuroinflammation to the pathological processes associated with Tau aggregation</u>

Tau pathology is commonly associated with neuroinflammation in AD and other tauopathies (Ishizawa and Dickson, 2001; Sheng et al., 1997). In addition, correlation is often observed between the extent of Tau pathology and glial reactivity, suggesting that it may play a role in the process of degeneration. Whether it has a positive or deleterious effect, however, is still a matter of debate. Both microgliosis and astrogliosis were associated with Tau pathology in our models, although they seemed to be involved in different processes. Indeed, strong microgliosis was observed following injection of all Tau constructs as well as utGFP control vector (*Figure 44*), suggesting that at least part of the initial microglial activation was induced by AVV vectors expression. Interestingly, while this microglial activation later resolved for most groups, maintained microgliosis was observed in hTAU^{P301L} at 3 months post-injection, a time-point where worsening of neurodegeneration could be observed in this group (*Figure 37*). This suggests that sustained microglial activation was contributing to Tau-induced neuronal loss or, alternatively, that it was associated with the maintained necessity for debris clearance.

Localisation of reactive microglia in our models may be in support for this later idea. Indeed, while general activation could be observed in utGFP animals, strong microgliosis in hTAU^{WT} and hTAU^{P301L} animals was spatially associated with neurodegeneration. Morphological changes were also observed in those groups with, in some cases, polarisation of the processes perpendicular to the pyramidal layer suggesting migration of activated microglia to the lesion (*Figure 44*). Microglia, as brain's professional phagocytes, would probably be recruited in those groups to phagocyte cellular debris. Reduction of microglial activation in hTAU^{WT} group at 3 months post-injection may then be associated with the fact that neuronal loss does not seem to progress over time in this group (*Figure 37*). Similarly, stable microgliosis in the hTAU^{P301L} group may be associated with the maintained necessity for debris clearance as neuronal loss kept progressing in this group. Alternatively, the maintenance of microglial activation be associated with processes of degradation of Tau aggregates, as toxicity in the hTAU^{P301L} group was associated with continuous Tau aggregation. This would be reminiscent of what is observed in humans where both astrocytes (Probst et al., 1982)and microglia (Cras et al., 1991) were found to infiltrate extracellular "ghost" tangles suggesting that they may be involved in the degradation of Tau aggregates. It remains that sustained microglial activation may in turn have adverse effects. Indeed, strong microglial activation could be observed to precede tangle formation in the brain of transgenic mice (Yoshiyama et al., 2007) occurring concurrently to synaptic loss. Interestingly, inhibition of neuro-inflammation in those mice ameliorated phenotype, suggesting that neuro-inflammation triggered by Tau pathology itself may act as a driver or potentiator of Tau-associated neurodegeneration (Zilka et al., 2012). Further studies are needed to determine the specific contribution of microglial activation to the pathological processes in our different models.

Astrogliosis was also evaluated in our different models, using staining for the intermediate filament Vimentin that is upregulated during initial astroglial activation (Pekny and Nilsson, 2005). Reactive astrocytes were observed as early as 1 month post-injection, specifically in Tau-expressing animals (*Figure 45*). Conversely, no sign of astrocytic reactivity could be observed in either PBS or utGFP control groups, suggesting that astrogliosis was specific to Tau pathology. Group differences were however observed between constructs in the extent and topography of astroglial reactivity. Indeed, stronger activation was observed in hTAU^{WT} and hTAU^{P301L} groups, that also exhibited strong neurodegeneration, suggesting that astrocytic activation occurred in those models partly in response to neuronal death. In addition, reactive astrocytes were observed in those groups mainly in regions presenting strong neuronal loss, consistent with their known implication in the formation of the glial scar (Pekny and Nilsson, 2005).

4) Origin and implications of glial Tau pathology in hTAU^{P301L} and hTAU^{ProAggr} groups

The most surprising result regarding neuroinflammation was the finding of glial Tau aggregation in hTAU^{P301L} and hTAU^{ProAggr} groups. Different morphological subtypes could be identified (*Figure 46*), bearing strong similarities to what is observed in several human tauopathies (Berry et al., 2001; Yoshida, 2006). Interestingly, in patients, the morphology of astrocytic Tau lesion is usually highly specific for a given tauopathy, although it is not clear what would be the reason for this disease-specific phenotype. Primary sequence of Tau protein may be involved, as different mutations in Tau gene have been associated with specific morphological subtypes (Ferrer et al., 2014). Differential post-translational modification of Tau (e.g. truncation or phosphorylation) may also be involved in the generation of those distinct phenotypes. Lastly, given the large diversity of astrocytic subtypes, it may be possible that those Tau lesions may be associated with aggregation in different sub-population.

In our model, however, several of those morphological subtypes could be observed within a single animal, suggesting that those may arise from similar pathological processes. It is not clear what would be reason for this discrepancy between our results and human data. However, quantification of the relative proportion of those different subtypes may allow us to determine if some were specifically associated with a given Tau construct. Better characterizing the composition of glial Tau aggregates could also allow us to determine if this morphological diversity is associated with differences in the nature of Tau aggregates (e.g. differences in isoforms composition or post-translational modifications).

Although glial Tau pathology has been extensively described on an anatomo-pathological level, not much has been discovered on the processes underlying the apparition of Tau inclusions in those cells. The occurrence of glial Tau inclusions was described in mice following injection of brain homogenates originating from patients with different tauopathies such as PSP or CBD (Boluda et al., 2015; Clavaguera et al., 2013). Interestingly, the morphological specificity of each tauopathy was transmitted as well. Glial Tau pathology was also described in several transgenic mouse models next to neuronal Tau aggregation (Lin et al., 2003; Murakami et al., 2006). Tau aggregates in those mice bore strong resemblance in composition with that present in neurons, i.e. similar Gallyas reactivity. Given the strong enrichment of Tau in neurons compared to other neuronal cell types (Binder et al., 1985), it is possible that glial Tau aggregation may in some cases be related to neurodegeneration.

Data from our study support this second hypothesis. Indeed, our preliminary data in mice showed that astroglial Tau inclusions were not associated with transgene expression in those cells (*Figure 48*), suggesting that they appeared through a secondary process. In addition, quantification of AT100-positive glial inclusions in hTAU^{P301L} and hTAU^{ProAggr} groups of injected rats revealed group differences in the kinetics of glial Tau aggregation (*Figure 47*). Indeed, while strong Tau accumulation in astrocytes was already observed in the hTAU^{P301L} group at 1 month post-injection, glial Tau pathology increased over time in hTAU^{ProAggr} animals. Interestingly, the kinetics of glial Tau aggregation mirrored that of neuronal defects as the increase in glial Tau pathology occurred in the hTAU^{ProAggr} along with the apparition of mild neuronal defects (*Figure 39*). Those results thus confirm that glial Tau pathology in our models was associated with neurodegenerative processes.

One likely way Tau pathology arose in astrocytes may be through phagocytosis of cell debris or even whole degenerating neurons. Indeed, astrocytes were recently found to mediate synapse and neurons elimination during development through the activation of different phagocytic pathways, including those mediated by MEGF10 and MERTK receptors (Chung et al., 2013). Maintained activation of those pathways was also observed into adult age suggesting that astrocytes may be able to engulf

degenerating neurons or synapses in pathological conditions. In addition, phagocytosis of organelles of neuronal origin, such as mitochondria, was also observed in astrocytes (Davis et al., 2014). Interestingly, RT-qPCR analysis in our different models showed a trend for increased expression of different phagocytic markers (*Figure 49*), including MEGF10 and MERTK. Although analysis on whole HC homogenates could not allow inference on the glial cell type involved, the observation that the kinetics of expression of those genes mirrored that of glial Tau aggregation in hTAU^{P301L} and hTAU^{ProAggr} groups suggest that those pathways may be, at least in part, activated in astrocytes. Activation of those phagocytic pathways also occurred along with neurodegeneration in hTAU^{P301L} model, suggesting that it may be triggered by signals sent by degenerating cells. This process of degradation of cell debris may have beneficial effects. Indeed, the phagocytic activity of astrocytes was recently found to be useful in the context of neuronal injury where phagocytosis of degenerating neurons prevented bystander cell death of neighbouring neurons (Lööv et al., 2012).

What remains to be determined, however, is the impact of Tau aggregation on astrocytes function and viability in our models. Indeed, studies on transgenic mouse models of glial Tau pathology showed that Tau aggregation in astrocytes was associated with impairment of their functions, including redistribution of the intermediate filament GFAP, mild disruption of the blood brain barrier (Forman et al., 2005), and impaired glutamate transport (Dabir et al., 2006). RT-qPCR analysis in our models did not evidence significant differences in expression levels of the glutamate transporter GLT1 (*Figure 49*). However, accumulation of Tau aggregates in astrocytes may already be a sign of astrocytic defects. Increased expression of Psmb9 gene, coding for the inducible β1i subunit of the proteasome specifically expressed in activated glial cells (Orre et al., 2013), was observed in the hTAU^{ProAggr} group at 1 month post-injection, suggesting that activated glial cells were indeed attempting to degrade Tau aggregates. This accumulation of Tau in astrocytes may, in turn, have adverse effects on neurons. Indeed, glial Tau aggregation was found in different models to be associated not only with astrocytic death but also with neurodegeneration (Colodner and Feany, 2010; Forman et al., 2005). Further studies should be performed in our models to determine the long-term effect of glial Tau accumulation.

5) <u>Conclusion and perspectives</u>

The characterization and comparison of our different models allowed us to better understand the relationship between Tau aggregation and its toxicity, confirming the current hypothesis that posits soluble aggregates, supposedly oligomers, as the toxic players in Tau-induced neurodegeneration. Tau pathology in our models was associated with differential involvement of neuro-inflammation, further suggesting its implication in tauopathies. Lastly, Tau aggregation in glial cells could be observed in some models, accompanying neurodegeneration and probably arising from phagocytic activity of those cells. Expression of those different Tau constructs in similar proportions thus led to strong phenotypic variability, reminiscent of the disparities observed in human tauopathies.

One following axis of study could thus be focussed on the reasons and mechanisms involved in the induction of those distinct phenotypes. It was recently suggested that different Tau prion-like strains may underlie the distinct phenotypes observed in human tauopathies. Such strains where identified in the brain of patients (Sanders et al., 2014), that produced Tau aggregates with different morphologies, biochemical properties and associated degrees of toxicity when transfected into cellular models. One may hypothesize that the production of several such prion-like strains may underlie phenotypic variability produced by our different Tau constructs. Further ultrastructural and biochemical characterization of Tau species in our different models would be necessary to determine if this is the case. Notably, it would be interesting to determine how biochemical properties of Tau can govern the balance between small

soluble and large highly insoluble aggregates and how this relates to toxicity. This would have potential implications for the development of therapies, by allowing better design of drugs targeting Tau aggregation.

The direct comparison of our different models could also prove useful for the study of the mechanisms involved in Tau-induced neurodegeneration. More precisely, it would be interesting to study whether similar pathways are involved in the acute toxicity exerted by $hTAU^{WT}$ and $hTAU^{P301L}$ constructs, in order to determine if similar therapeutic strategies could be applied in the context of sporadic and genetic tauopathies. Similarly, direct comparison of $hTAU^{WT}$ and $hTAU^{ProAggr}$ constructs should allow us to compare pathways involved in acute toxicity triggered by oligomeric species to those activated following tangle formation. Because diagnosis of tauopathies still occurs at a late stage due to the lack of early biomarkers, this would could prove useful by allowing to adapt therapeutic strategies to patients at different stages.

III – Conclusion

The aim of this project was the development of rat models of sporadic and genetic tauopathies using AAV-mediated gene transfer of human Tau protein. Characterization and comparison of those different models showed strong phenotypic variability, reminiscent of that observed in human tauopathies. Indeed, while $hTAU^{WT}$ expression led to hyperphosphorylation of Tau and strong neurodegeneration in absence of significant aggregation, $hTAU^{ProAggr}$ construct strongly promoted aggregation into NFTs, with neuroprotective effect. The $hTAU^{P301L}$ group represented an intermediate phenotype with the formation of toxic soluble aggregates and fully mature tangles. Our different models thus bear close resemblance with human tauopathies where Tau aggregation is associated with neurodegeneration as well as induction inflammatory processes. The results obtained in this study also come in further support for the current hypothesis identifying soluble Tau oligomers as the toxic players in Tau-induced neurodegeneration. What remains to be determined, however, is the cause of the phenotypic variability observed between our different models. Further characterization of our models should allow us to address this question.

First dosage of oligomeric species would be necessary to confirm that those indeed represent the toxic species involved in Tau-induced neurodegeneration in our study. Morphological and biochemical characterization of the different types of aggregates should also be done, in order to determine if differences in the biochemical properties of Tau may underlie the differential toxicity exerted by Tau constructs. Further characterization of the potential synaptic defects triggered by Tau vectors, by means of biochemical or electrophysiological analysis, should also be done to identify pathways of Tau-induced neurodegeneration. This could also permit to determine the long term effect of the accumulation of large insoluble aggregates. Indeed, it would also be interesting to study the progression of the pathology past 3 months post-injection, the latest time-point investigated here.

Our results further identify Tau aggregation as a relevant target for disease-modifying therapies. Several approaches have been suggested, from inhibiting the induction of aggregation (e.g. through inhibitors of Tau phosphorylation) to dissolution of long formed aggregates with the use of passive or active immunotherapy (Pedersen and Sigurdsson, 2015). Our results, along with a growing body of evidence from the literature, point towards the inhibition of oligomers formation as a valid therapeutic strategy. But this will necessitate first to determine why and how those appear. Alternatively, promoting fibrils formation to trap pre-existing oligomers may also be a valid approach, although more needs to be done before to assess the long term effect of those aggregates. Our fast-developing models, that each exhibit different stages of Tau aggregation may be of great use to study these different questions.

These different therapeutic approaches may not be mutually exclusive and efficiency may depend on the stage of Tau pathology. To this respect, success of Tau-directed therapies would gain from the visualisation of disease staging that, in turn, necessitates development of biomarkers allowing the follow up of the progression of the pathology. Among those, much effort has been done recently for the development of Tau-directed PET tracers (Shah and Catafau, 2014). The specificity of those compounds for Tau remains to be clearly established and imaging of our models where Tau aggregates in absence of any proteinopathy should help resolve this question. Our data also suggest that, instead of the large fibrillar aggregates that are the target of current tracers, imaging Tau oligomers may represent a better correlate of the pathology. Indeed, imaging early stages of Tau aggregation, which in addition may represent the toxic species in tauopathies, could allow diagnosis before extensive degeneration. This should also prove useful to follow the effect of disease-modifying therapies on the progression of the pathology. Screening of PET-tracers with differential selectivity for specific stages of Tau aggregation could be performed in our models.

REFERENCES

Ahmed, T., Van der Jeugd, A., Blum, D., Galas, M.-C., D'Hooge, R., Buee, L., and Balschun, D. (2014). Cognition and hippocampal synaptic plasticity in mice with a homozygous tau deletion. Neurobiol. Aging *35*, 2474–2478.

Ali, Y.O., Ruan, K., and Zhai, R.G. (2012). NMNAT suppresses Tau-induced neurodegeneration by promoting clearance of hyperphosphorylated Tau oligomers in a Drosophila model of tauopathy. Hum. Mol. Genet. *21*, 237–250.

Allen, B., Ingram, E., Takao, M., Smith, M.J., Jakes, R., Virdee, K., Yoshida, H., Holzer, M., Craxton, M., Emson, P.C., et al. (2002). Abundant Tau Filaments and Nonapoptotic Neurodegeneration in Transgenic Mice Expressing Human P301S Tau Protein. J. Neurosci. *22*, 9340–9351.

Alonso, A. del C., Li, B., Grundke-Iqbal, I., and Iqbal, K. (2006). Polymerization of hyperphosphorylated tau into filaments eliminates its inhibitory activity. Proc. Natl. Acad. Sci. *103*, 8864–8869.

Andorfer, C., Kress, Y., Espinoza, M., De Silva, R., Tucker, K.L., Barde, Y.-A., Duff, K., and Davies, P. (2003). Hyperphosphorylation and aggregation of tau in mice expressing normal human tau isoforms. J. Neurochem. *86*, 582–590.

Andorfer, C., Acker, C.M., Kress, Y., Hof, P.R., Duff, K., and Davies, P. (2005). Cell-Cycle Reentry and Cell Death in Transgenic Mice Expressing Nonmutant Human Tau Isoforms. J. Neurosci. *25*, 5446–5454.

Arai, T., Ikeda, K., Akiyama, H., Nonaka, T., Hasegawa, M., Ishiguro, K., Iritani, S., Tsuchiya, K., Iseki, E., Yagishita, S., et al. (2004). Identification of amino-terminally cleaved tau fragments that distinguish progressive supranuclear palsy from corticobasal degeneration. Ann. Neurol. *55*, 72–79.

Aronov, S., Aranda, G., Behar, L., and Ginzburg, I. (2001). Axonal Tau mRNA Localization Coincides with Tau Protein in Living Neuronal Cells and Depends on Axonal Targeting Signal. J. Neurosci. *21*, 6577–6587.

Aschauer, D.F., Kreuz, S., and Rumpel, S. (2013). Analysis of Transduction Efficiency, Tropism and Axonal Transport of AAV Serotypes 1, 2, 5, 6, 8 and 9 in the Mouse Brain. PLOS ONE *8*, e76310.

Augustinack, J.C., Schneider, A., Mandelkow, E.-M., and Hyman, B.T. (2002). Specific tau phosphorylation sites correlate with severity of neuronal cytopathology in Alzheimer's disease. Acta Neuropathol. (Berl.) *103*, 26–35.

Aurnhammer, C., Haase, M., Muether, N., Hausl, M., Rauschhuber, C., Huber, I., Nitschko, H., Busch, U., Sing, A., Ehrhardt, A., et al. (2012). Universal real-time PCR for the detection and quantification of adeno-associated virus serotype 2-derived inverted terminal repeat sequences. Hum. Gene Ther. Methods *23*, 18–28.

de Backer, M.W., Fitzsimons, C.P., Brans, M.A., Luijendijk, M.C., Garner, K.M., Vreugdenhil, E., and Adan, R.A. (2010). An adeno-associated viral vector transduces the rat hypothalamus and amygdala more efficient than a lentiviral vector. BMC Neurosci. *11*, 81.

Ballatore, C., Lee, V.M.-Y., and Trojanowski, J.Q. (2007). Tau-mediated neurodegeneration in Alzheimer's disease and related disorders. Nat. Rev. Neurosci. *8*, 663–672.

Bancher, C., Brunner, C., Lassmann, H., Budka, H., Jellinger, K., Wiche, G., Seitelberger, F., Grundke-Iqbal, I., Iqbal, K., and Wisniewski, H.M. (1989). Accumulation of abnormally phosphorylated τ precedes the formation of neurofibrillary tangles in Alzheimer's disease. Brain Res. *477*, 90–99.

Barghorn, S., Zheng-Fischhöfer, Q., Ackmann, M., Biernat, J., von Bergen, M., Mandelkow, E.-M., and Mandelkow, E. (2000). Structure, Microtubule Interactions, and Paired Helical Filament Aggregation by Tau Mutants of Frontotemporal Dementias. Biochemistry (Mosc.) *39*, 11714–11721.

Barrachina, M., and Ferrer, I. (2009). DNA methylation of Alzheimer disease and tauopathy-related genes in postmortem brain. J. Neuropathol. Exp. Neurol. *68*, 880–891.

Barthélemy, N.R., Gabelle, A., Hirtz, C., Fenaille, F., Sergeant, N., Schraen-Maschke, S., Vialaret, J., Buée, L., Junot, C., Becher, F., et al. (2016). Differential Mass Spectrometry Profiles of Tau Protein in the Cerebrospinal Fluid of Patients with Alzheimer's Disease, Progressive Supranuclear Palsy, and Dementia with Lewy Bodies. J. Alzheimers Dis. JAD *51*, 1033–1043.

Bergen, M. von, Friedhoff, P., Biernat, J., Heberle, J., Mandelkow, E.-M., and Mandelkow, E. (2000). Assembly of τ protein into Alzheimer paired helical filaments depends on a local sequence motif (306VQIVYK311) forming β structure. Proc. Natl. Acad. Sci. *97*, 5129–5134.

von Bergen, M., Barghorn, S., Li, L., Marx, A., Biernat, J., Mandelkow, E.M., and Mandelkow, E. (2001). Mutations of tau protein in frontotemporal dementia promote aggregation of paired helical filaments by enhancing local beta-structure. J. Biol. Chem. *276*, 48165–48174.

Berger, A., Lorain, S., Joséphine, C., Desrosiers, M., Peccate, C., Voit, T., Garcia, L., Sahel, J.-A., and Bemelmans, A.-P. (2015). Repair of rhodopsin mRNA by spliceosome-mediated RNA trans-splicing: a new approach for autosomal dominant retinitis pigmentosa. Mol. Ther. J. Am. Soc. Gene Ther. *23*, 918–930.

Berger, Z., Roder, H., Hanna, A., Carlson, A., Rangachari, V., Yue, M., Wszolek, Z., Ashe, K., Knight, J., Dickson, D., et al. (2007). Accumulation of pathological tau species and memory loss in a conditional model of tauopathy. J. Neurosci. Off. J. Soc. Neurosci. *27*, 3650–3662.

Berriman, J., Serpell, L.C., Oberg, K.A., Fink, A.L., Goedert, M., and Crowther, R.A. (2003). Tau filaments from human brain and from in vitro assembly of recombinant protein show cross-β structure. Proc. Natl. Acad. Sci. *100*, 9034–9038.

Berry, R.W., Quinn, B., Johnson, N., Cochran, E.J., Ghoshal, N., and Binder, L.I. (2001). Pathological glial tau accumulations in neurodegenerative disease: review and case report. Neurochem. Int. *39*, 469–479.

Binder, L.I., Frankfurter, A., and Rebhun, L.I. (1985). The distribution of tau in the mammalian central nervous system. J. Cell Biol. *101*, 1371–1378.

Black, M.M., Slaughter, T., Moshiach, S., Obrocka, M., and Fischer, I. (1996). Tau Is Enriched on Dynamic Microtubules in the Distal Region of Growing Axons. J. Neurosci. *16*, 3601–3619.

Blennow, K., de Leon, M.J., and Zetterberg, H. (2006). Alzheimer's disease. The Lancet *368*, 387–403.

Blennow, K., Hampel, H., Weiner, M., and Zetterberg, H. (2010). Cerebrospinal fluid and plasma biomarkers in Alzheimer disease. Nat. Rev. Neurol. *6*, 131–144.

Blom, E.S., Giedraitis, V., Zetterberg, H., Fukumoto, H., Blennow, K., Hyman, B.T., Irizarry, M.C., Wahlund, L.-O., Lannfelt, L., and Ingelsson, M. (2009). Rapid progression from mild cognitive impairment to Alzheimer's disease in subjects with elevated levels of tau in cerebrospinal fluid and the APOE epsilon4/epsilon4 genotype. Dement. Geriatr. Cogn. Disord. *27*, 458–464.

Blum, D., Herrera, F., Francelle, L., Mendes, T., Basquin, M., Obriot, H., Demeyer, D., Sergeant, N., Gerhardt, E., Brouillet, E., et al. (2015). Mutant huntingtin alters Tau phosphorylation and subcellular distribution. Hum. Mol. Genet. *24*, 76–85.

Boluda, S., Iba, M., Zhang, B., Raible, K.M., Lee, V.M.-Y., and Trojanowski, J.Q. (2015). Differential induction and spread of tau pathology in young PS19 tau transgenic mice following intracerebral injections of pathological tau from Alzheimer's disease or corticobasal degeneration brains. Acta Neuropathol. (Berl.) *129*, 221–237.

Braak, H., and Braak, E. (1991). Neuropathological stageing of Alzheimer-related changes. Acta Neuropathol. (Berl.) *82*, 239–259.

Braak, H., and Del Tredici, K. (2011). The pathological process underlying Alzheimer's disease in individuals under thirty. Acta Neuropathol. (Berl.) *121*, 171–181.

Braak, H., and Tredici, K.D. (2011). Alzheimer's pathogenesis: is there neuron-to-neuron propagation? Acta Neuropathol. (Berl.) *121*, 589–595.

Braak, H., and Tredici, K.D. (2015). The preclinical phase of the pathological process underlying sporadic Alzheimer's disease. Brain *138*, 2814–2833.

Braak, E., Braak, H., and Mandelkow, E.M. (1994). A sequence of cytoskeleton changes related to the formation of neurofibrillary tangles and neuropil threads. Acta Neuropathol. (Berl.) *87*, 554–567.

Braak, H., Thal, D.R., Ghebremedhin, E., and Del Tredici, K. (2011). Stages of the Pathologic Process in Alzheimer Disease. J. Neuropathol. Exp. Neurol. *70*, 960–969.

Brandt, R., Léger, J., and Lee, G. (1995). Interaction of tau with the neural plasma membrane mediated by tau's amino-terminal projection domain. J. Cell Biol. *131*, 1327–1340.

Buée, L., Bussière, T., Buée-Scherrer, V., Delacourte, A., and Hof, P.R. (2000). Tau protein isoforms, phosphorylation and role in neurodegenerative disorders11These authors contributed equally to this work. Brain Res. Rev. *33*, 95–130.

Bugiani, O., Murrell, J.R., Giaccone, G., Hasegawa, M., Ghigo, G., Tabaton, M., Morbin, M., Primavera, A., Carella, F., Solaro, C., et al. (1999). Frontotemporal dementia and corticobasal degeneration in a family with a P301S mutation in tau. J. Neuropathol. Exp. Neurol. *58*, 667–677.

Caceres, A., and Kosik, K.S. (1990). Inhibition of neurite polarity by tau antisense oligonucleotides in primary cerebellar neurons. Nature *343*, 461–463.

Cahoy, J.D., Emery, B., Kaushal, A., Foo, L.C., Zamanian, J.L., Christopherson, K.S., Xing, Y., Lubischer, J.L., Krieg, P.A., Krupenko, S.A., et al. (2008). A transcriptome database for astrocytes, neurons, and oligodendrocytes: a new resource for understanding brain development and function. J. Neurosci. Off. J. Soc. Neurosci. *28*, 264–278.

Caillet-Boudin, M.-L., Buée, L., Sergeant, N., and Lefebvre, B. (2015). Regulation of human MAPT gene expression. Mol. Neurodegener. *10*, 28.

Caillierez, R., Bégard, S., Lécolle, K., Deramecourt, V., Zommer, N., Dujardin, S., Loyens, A., Dufour, N., Aurégan, G., Winderickx, J., et al. (2013). Lentiviral Delivery of the Human Wild-type Tau Protein Mediates a Slow and Progressive Neurodegenerative Tau Pathology in the Rat Brain. Mol. Ther.

Calafate, S., Buist, A., Miskiewicz, K., Vijayan, V., Daneels, G., de Strooper, B., de Wit, J., Verstreken, P., and Moechars, D. (2015). Synaptic Contacts Enhance Cell-to-Cell Tau Pathology Propagation. Cell Rep. *11*, 1176–1183.

de Calignon, A., Fox, L.M., Pitstick, R., Carlson, G.A., Bacskai, B.J., Spires-Jones, T.L., and Hyman, B.T. (2010). Caspase activation precedes and leads to tangles. Nature *464*, 1201–1204.

Callahan, L.M., Vaules, W.A., and Coleman, P.D. (1999). Quantitative Decrease in Synaptophysin Message Expression and Increase in Cathepsin D Message Expression in Alzheimer Disease Neurons Containing Neurofibrillary Tangles. J. Neuropathol. Exp. Neurol. *58*, 275–287.

Chesser, A.S., Pritchard, S.M., and Johnson, G.V.W. (2013). Tau clearance mechanisms and their possible role in the pathogenesis of Alzheimer disease. Front. Neurol. *4*, 122.

Cho, J.-H., and Johnson, G.V.W. (2003). Glycogen Synthase Kinase 3β Phosphorylates Tau at Both Primed and Unprimed Sites DIFFERENTIAL IMPACT ON MICROTUBULE BINDING. J. Biol. Chem. *278*, 187–193.

Cho, J.-H., and Johnson, G.V.W. (2004). Primed phosphorylation of tau at Thr231 by glycogen synthase kinase 3β (GSK3β) plays a critical role in regulating tau's ability to bind and stabilize microtubules. J. Neurochem. *88*, 349–358.

Chung, W.-S., Clarke, L.E., Wang, G.X., Stafford, B.K., Sher, A., Chakraborty, C., Joung, J., Foo, L.C., Thompson, A., Chen, C., et al. (2013). Astrocytes mediate synapse elimination through MEGF10 and MERTK pathways. Nature *504*, 394–400.

Chung, W.-S., Welsh, C.A., Barres, B.A., and Stevens, B. (2015). Do glia drive synaptic and cognitive impairment in disease? Nat. Neurosci. *18*, 1539–1545.

Clavaguera, F., Bolmont, T., Crowther, R.A., Abramowski, D., Frank, S., Probst, A., Fraser, G., Stalder, A.K., Beibel, M., Staufenbiel, M., et al. (2009). Transmission and spreading of tauopathy in transgenic mouse brain. Nat. Cell Biol. *11*, 909–913.

Clavaguera, F., Akatsu, H., Fraser, G., Crowther, R.A., Frank, S., Hench, J., Probst, A., Winkler, D.T., Reichwald, J., Staufenbiel, M., et al. (2013). Brain homogenates from human tauopathies induce tau inclusions in mouse brain. Proc. Natl. Acad. Sci. U. S. A. *110*, 9535–9540.

Cleveland, D.W., Hwo, S.-Y., and Kirschner, M.W. (1977a). Purification of tau, a microtubule-associated protein that induces assembly of microtubules from purified tubulin. J. Mol. Biol. *116*, 207–225.

Cleveland, D.W., Hwo, S.-Y., and Kirschner, M.W. (1977b). Physical and chemical properties of purified tau factor and the role of tau in microtubule assembly. J. Mol. Biol. *116*, 227–247.

Cohen, R.M., Rezai-Zadeh, K., Weitz, T.M., Rentsendorj, A., Gate, D., Spivak, I., Bholat, Y., Vasilevko, V., Glabe, C.G., Breunig, J.J., et al. (2013). A transgenic Alzheimer rat with plaques, tau pathology, behavioral impairment, oligomeric aβ, and frank neuronal loss. J. Neurosci. Off. J. Soc. Neurosci. *33*, 6245–6256.

Cohen, T.J., Guo, J.L., Hurtado, D.E., Kwong, L.K., Mills, I.P., Trojanowski, J.Q., and Lee, V.M.Y. (2011). The acetylation of tau inhibits its function and promotes pathological tau aggregation. Nat. Commun. *2*, 252.

Colodner, K.J., and Feany, M.B. (2010). Glial Fibrillary Tangles and JAK/STAT-Mediated Glial and Neuronal Cell Death in a Drosophila Model of Glial Tauopathy. J. Neurosci. *30*, 16102–16113.

Colom-Cadena, M., Gelpi, E., Martí, M.J., Charif, S., Dols-Icardo, O., Blesa, R., Clarimón, J., and Lleó, A. (2013). MAPT H1 haplotype is associated with enhanced α-synuclein deposition in dementia with Lewy bodies. Neurobiol. Aging *34*, 936–942.

Cook, C., Carlomagno, Y., Gendron, T.F., Dunmore, J., Scheffel, K., Stetler, C., Davis, M., Dickson, D., Jarpe, M., DeTure, M., et al. (2014). Acetylation of the KXGS motifs in tau is a critical determinant in modulation of tau aggregation and clearance. Hum. Mol. Genet. *23*, 104–116.

Cook, C., Kang, S.S., Carlomagno, Y., Lin, W.-L., Yue, M., Kurti, A., Shinohara, M., Jansen-West, K., Perkerson, E., Castanedes-Casey, M., et al. (2015). Tau deposition drives neuropathological, inflammatory and behavioral abnormalities independently of neuronal loss in a novel mouse model. Hum. Mol. Genet. *24*, 6198–6212.

Coppola, G., Chinnathambi, S., Lee, J.J., Dombroski, B.A., Baker, M.C., Soto-Ortolaza, A.I., Lee, S.E., Klein, E., Huang, A.Y., Sears, R., et al. (2012). Evidence for a role of the rare p.A152T variant in MAPT in increasing the risk for FTD-spectrum and Alzheimer's diseases. Hum. Mol. Genet. *21*, 3500–3512.

Cowan, C.M., and Mudher, A. (2013). Are tau aggregates toxic or protective in tauopathies? Front. Neurol. *4*, 114.

Cowan, C.M., Quraishe, S., Hands, S., Sealey, M., Mahajan, S., Allan, D.W., and Mudher, A. (2015). Rescue from tau-induced neuronal dysfunction produces insoluble tau oligomers. Sci. Rep. *5*, 17191.

Crary, J.F., Trojanowski, J.Q., Schneider, J.A., Abisambra, J.F., Abner, E.L., Alafuzoff, I., Arnold, S.E., Attems, J., Beach, T.G., Bigio, E.H., et al. (2014). Primary age-related tauopathy (PART): a common pathology associated with human aging. Acta Neuropathol. (Berl.) *128*, 755–766.

Cras, P., Kawai, M., Siedlak, S., and Perry, G. (1991). Microglia are associated with the extracellular neurofibrillary tangles of alzheimer disease. Brain Res. *558*, 312–314.

Crowther, R.A., and Goedert, M. (2000). Abnormal Tau-Containing Filaments in Neurodegenerative Diseases. J. Struct. Biol. *130*, 271–279.

Crowther, R.A., and Wischik, C.M. (1985). Image reconstruction of the Alzheimer paired helical filament. EMBO J. *4*, 3661–3665.

Cruchaga, C., Vidal-Taboada, J.M., Ezquerra, M., Lorenzo, E., Martinez-Lage, P., Blazquez, M., Tolosa, E., Iberian Atypical Parkinsonism Study Group Researchers, and Pastor, P. (2009). 5'-Upstream variants of CRHR1 and MAPT genes associated with age at onset in progressive supranuclear palsy and cortical basal degeneration. Neurobiol. Dis. *33*, 164–170.

Dabir, D.V., Robinson, M.B., Swanson, E., Zhang, B., Trojanowski, J.Q., Lee, V.M.-Y., and Forman, M.S. (2006). Impaired Glutamate Transport in a Mouse Model of Tau Pathology in Astrocytes. J. Neurosci. *26*, 644–654.

Dassie, E., Andrews, M.R., Bensadoun, J.-C., Cacquevel, M., Schneider, B.L., Aebischer, P., Wouters, F.S., Richardson, J.C., Hussain, I., Howlett, D.R., et al. (2013). Focal expression of adeno-associated viral-mutant tau induces widespread impairment in an APP mouse model. Neurobiol. Aging *34*, 1355–1368.

Davis, C.O., Kim, K.-Y., Bushong, E.A., Mills, E.A., Boassa, D., Shih, T., Kinebuchi, M., Phan, S., Zhou, Y., Bihlmeyer, N.A., et al. (2014). Transcellular degradation of axonal mitochondria. Proc. Natl. Acad. Sci. *111*, 9633–9638.

Dawson, H.N., Ferreira, A., Eyster, M.V., Ghoshal, N., Binder, L.I., and Vitek, M.P. (2001). Inhibition of neuronal maturation in primary hippocampal neurons from tau deficient mice. J. Cell Sci. *114*, 1179–1187.

Dayton, R.D., Wang, D.B., Cain, C.D., Schrott, L.M., Ramirez, J.J., King, M.A., and Klein, R.L. (2012). Frontotemporal lobar degeneration-related proteins induce only subtle memory-related deficits when bilaterally overexpressed in the dorsal hippocampus. Exp. Neurol. *233*, 807–814.

de Calignon, A., Polydoro, M., Suárez-Calvet, M., William, C., Adamowicz, D.H., Kopeikina, K.J., Pitstick, R., Sahara, N., Ashe, K.H., Carlson, G.A., et al. (2012). Propagation of Tau Pathology in a Model of Early Alzheimer's Disease. Neuron *73*, 685–697.

Decker, J.M., Krüger, L., Sydow, A., Zhao, S., Frotscher, M., Mandelkow, E., and Mandelkow, E.-M. (2015). Pro-aggregant Tau impairs mossy fiber plasticity due to structural changes and Ca++ dysregulation. Acta Neuropathol. Commun. *3*, 23.

Delacourte, A., David, J.P., Sergeant, N., Buée, L., Wattez, A., Vermersch, P., Ghozali, F., Fallet-Bianco, C., Pasquier, F., Lebert, F., et al. (1999). The biochemical pathway of neurofibrillary degeneration in aging and Alzheimer's disease. Neurology *52*, 1158–1158.

Dickson, D.W., Crystal, H.A., Bevona, C., Honer, W., Vincent, I., and Davies, P. (1995). Correlations of synaptic and pathological markers with cognition of the elderly. Neurobiol. Aging *16*, 285–298.

Dickson, D.W., Kouri, N., Murray, M.E., and Josephs, K.A. (2011). Neuropathology of frontotemporal lobar degeneration-tau (FTLD-tau). J. Mol. Neurosci. MN *45*, 384–389.

Dixit, R., Ross, J.L., Goldman, Y.E., and Holzbaur, E.L.F. (2008). Differential Regulation of Dynein and Kinesin Motor Proteins by Tau. Science *319*, 1086–1089.

Do Carmo, S., and Cuello, A.C. (2013). Modeling Alzheimer's disease in transgenic rats. Mol. Neurodegener. *8*, 37.

Dotti, C.G., Banker, G.A., and Binder, L.I. (1987). The expression and distribution of the microtubule-associated proteins tau and microtubule-associated protein 2 in hippocampal neurons in the rat in situ and in cell culture. Neuroscience *23*, 121–130.

Drubin, D.G., Caput, D., and Kirschner, M.W. (1984). Studies on the expression of the microtubule-associated protein, tau, during mouse brain development, with newly isolated complementary DNA probes. J. Cell Biol. *98*, 1090–1097.

Duff, K., Knight, H., Refolo, L.M., Sanders, S., Yu, X., Picciano, M., Malester, B., Hutton, M., Adamson, J., Goedert, M., et al. (2000). Characterization of Pathology in Transgenic Mice Over-Expressing Human Genomic and cDNA Tau Transgenes. Neurobiol. Dis. *7*, 87–98.

Dujardin, S., Bégard, S., Caillierez, R., Lachaud, C., Delattre, L., Carrier, S., Loyens, A., Galas, M.-C., Bousset, L., Melki, R., et al. (2014a). Ectosomes: A New Mechanism for Non-Exosomal Secretion of Tau Protein. PLoS ONE *9*, e100760.

Dujardin, S., Lecolle, K., Caillierez, R., Begard, S., Zommer, N., Lachaud, C., Carrier, S., Dufour, N., Auregan, G., Winderickx, J., et al. (2014b). Neuron-to-neuron wild-type Tau protein transfer through a trans-synaptic mechanism: relevance to sporadic tauopathies. Acta Neuropathol. Commun. *2*, 14.

Duyckaerts, C., Braak, H., Brion, J.-P., Buée, L., Del Tredici, K., Goedert, M., Halliday, G., Neumann, M., Spillantini, M.G., Tolnay, M., et al. (2015). PART is part of Alzheimer disease. Acta Neuropathol. (Berl.) *129*, 749–756.

Eckermann, K., Mocanu, M.-M., Khlistunova, I., Biernat, J., Nissen, A., Hofmann, A., Schönig, K., Bujard, H., Haemisch, A., Mandelkow, E., et al. (2007). The β-Propensity of Tau Determines Aggregation and Synaptic Loss in Inducible Mouse Models of Tauopathy. J. Biol. Chem. *282*, 31755–31765.

Ezquerra, M., Pastor, P., Gaig, C., Vidal-Taboada, J.M., Cruchaga, C., Muñoz, E., Martí, M.-J., Valldeoriola, F., Aguilar, M., Calopa, M., et al. (2011). Different MAPT haplotypes are associated with Parkinson's disease and progressive supranuclear palsy. Neurobiol. Aging *32*, 547.e11-16.

Fá, M., Puzzo, D., Piacentini, R., Staniszewski, A., Zhang, H., Baltrons, M.A., Li Puma, D.D., Chatterjee, I., Li, J., Saeed, F., et al. (2016). Extracellular Tau Oligomers Produce An Immediate Impairment of LTP and Memory. Sci. Rep. *6*, 19393.

Fagan, A.M., Xiong, C., Jasielec, M.S., Bateman, R.J., Goate, A.M., Benzinger, T.L.S., Ghetti, B., Martins, R.N., Masters, C.L., Mayeux, R., et al. (2014). Longitudinal change in CSF biomarkers in autosomal-dominant Alzheimer's disease. Sci. Transl. Med. *6*, 226ra30.

Falcon, B., Cavallini, A., Angers, R., Glover, S., Murray, T.K., Barnham, L., Jackson, S., O'Neill, M.J., Isaacs, A.M., Hutton, M.L., et al. (2015). Conformation Determines the Seeding Potencies of Native and Recombinant Tau Aggregates. J. Biol. Chem. *290*, 1049–1065.

Farah, C.A., Perreault, S., Liazoghli, D., Desjardins, M., Anton, A., Lauzon, M., Paiement, J., and Leclerc, N. (2006). Tau interacts with Golgi membranes and mediates their association with microtubules. Cell Motil. Cytoskeleton *63*, 710–724.

Feinstein, S.C., and Wilson, L. (2005). Inability of tau to properly regulate neuronal microtubule dynamics: a loss-of-function mechanism by which tau might mediate neuronal cell death. Biochim. Biophys. Acta BBA - Mol. Basis Dis. *1739*, 268–279.

Fernández-Nogales, M., Cabrera, J.R., Santos-Galindo, M., Hoozemans, J.J.M., Ferrer, I., Rozemuller, A.J.M., Hernández, F., Avila, J., and Lucas, J.J. (2014). Huntington's disease is a four-repeat tauopathy with tau nuclear rods. Nat. Med. *20*, 881–885.

Ferrer, I., López-González, I., Carmona, M., Arregui, L., Dalfó, E., Torrejón-Escribano, B., Diehl, R., and Kovacs, G.G. (2014). Glial and neuronal tau pathology in tauopathies: characterization of disease-specific phenotypes and tau pathology progression. J. Neuropathol. Exp. Neurol. *73*, 81–97.

Filipcik, P., Zilka, N., Bugos, O., Kucerak, J., Koson, P., Novak, P., and Novak, M. (2012). First transgenic rat model developing progressive cortical neurofibrillary tangles. Neurobiol. Aging *33*, 1448–1456.

Fischer, D., Mukrasch, M.D., Biernat, J., Bibow, S., Blackledge, M., Griesinger, C., Mandelkow, E., and Zweckstetter, M. (2009). Conformational Changes Specific for Pseudophosphorylation at Serine 262 Selectively Impair Binding of Tau to Microtubules. Biochemistry (Mosc.) *48*, 10047–10055.

Flach, K., Hilbrich, I., Schiffmann, A., Gärtner, U., Krüger, M., Leonhardt, M., Waschipky, H., Wick, L., Arendt, T., and Holzer, M. (2012). Tau oligomers impair artificial membrane integrity and cellular viability. J. Biol. Chem. *287*, 43223–43233.

Fodero-Tavoletti, M.T., Furumoto, S., Taylor, L., McLean, C.A., Mulligan, R.S., Birchall, I., Harada, R., Masters, C.L., Yanai, K., Kudo, Y., et al. (2014). Assessing THK523 selectivity for tau deposits in Alzheimer's disease and non–Alzheimer's disease tauopathies. Alzheimers Res Ther *6*, 11.

Forman, M.S., Lal, D., Zhang, B., Dabir, D.V., Swanson, E., Lee, V.M.-Y., and Trojanowski, J.Q. (2005). Transgenic Mouse Model of Tau Pathology in Astrocytes Leading to Nervous System Degeneration. J. Neurosci. *25*, 3539–3550.

Fox, L.M., William, C.M., Adamowicz, D.H., Pitstick, R., Carlson, G.A., Spires-Jones, T.L., and Hyman, B.T. (2011). Soluble tau Species, Not Neurofibrillary Aggregates, Disrupt Neural System Integration in a tau Transgenic Model. J. Neuropathol. Exp. Neurol. *70*, 588–595.

Frost, B., Jacks, R.L., and Diamond, M.I. (2009). Propagation of Tau Misfolding from the Outside to the Inside of a Cell. J. Biol. Chem. *284*, 12845–12852.

Furler, S., Paterna, J.C., Weibel, M., and Büeler, H. (2001). Recombinant AAV vectors containing the foot and mouth disease virus 2A sequence confer efficient bicistronic gene expression in cultured cells and rat substantia nigra neurons. Gene Ther. *8*, 864–873.

Galván, M., David, J.P., Delacourte, A., Luna, J., and Mena, R. (2001). Sequence of neurofibrillary changes in aging and Alzheimer's disease: A confocal study with phospho-tau antibody, AD2. J. Alzheimers Dis. *3*, 417–425.

Gamblin, T.C., Chen, F., Zambrano, A., Abraha, A., Lagalwar, S., Guillozet, A.L., Lu, M., Fu, Y., Garcia-Sierra, F., LaPointe, N., et al. (2003). Caspase cleavage of tau: Linking amyloid and neurofibrillary tangles in Alzheimer's disease. Proc. Natl. Acad. Sci. *100*, 10032–10037.

Giannakopoulos, P., Herrmann, F.R., Bussière, T., Bouras, C., Kövari, E., Perl, D.P., Morrison, J.H., Gold, G., and Hof, P.R. (2003). Tangle and neuron numbers, but not amyloid load, predict cognitive status in Alzheimer's disease. Neurology *60*, 1495–1500.

Giasson, B.I., Forman, M.S., Higuchi, M., Golbe, L.I., Graves, C.L., Kotzbauer, P.T., Trojanowski, J.Q., and Lee, V.M.-Y. (2003). Initiation and synergistic fibrillization of tau and alpha-synuclein. Science *300*, 636–640.

Gilley, J., Ando, K., Seereeram, A., Rodríguez-Martín, T., Pooler, A.M., Sturdee, L., Anderton, B.H., Brion, J.-P., Hanger, D.P., and Coleman, M.P. (2016). Mislocalization of neuronal tau in the absence of tangle pathology in phosphomutant tau knockin mice. Neurobiol. Aging *39*, 1–18.

Ginsberg, S.D., Hemby, S.E., Lee, V.M., Eberwine, J.H., and Trojanowski, J.Q. (2000). Expression profile of transcripts in Alzheimer's disease tangle-bearing CA1 neurons. Ann. Neurol. *48*, 77–87.

Goedert, M., and Jakes, R. (1990). Expression of separate isoforms of human tau protein: correlation with the tau pattern in brain and effects on tubulin polymerization. EMBO J. *9*, 4225–4230.

Goedert, M., Wischik, C.M., Crowther, R.A., Walker, J.E., and Klug, A. (1988). Cloning and sequencing of the cDNA encoding a core protein of the paired helical filament of Alzheimer disease: identification as the microtubule-associated protein tau. Proc. Natl. Acad. Sci. U. S. A. *85*, 4051–4055.

Goedert, M., Spillantini, M.G., Jakes, R., Rutherford, D., and Crowther, R.A. (1989a). Multiple isoforms of human microtubule-associated protein tau: sequences and localization in neurofibrillary tangles of Alzheimer's disease. Neuron *3*, 519–526.

Goedert, M., Spillantini, M.G., Potier, M.C., Ulrich, J., and Crowther, R.A. (1989b). Cloning and sequencing of the cDNA encoding an isoform of microtubule-associated protein tau containing four tandem repeats: differential expression of tau protein mRNAs in human brain. EMBO J. *8*, 393–399.

Gómez-Isla, T., Hollister, R., West, H., Mui, S., Growdon, J.H., Petersen, R.C., Parisi, J.E., and Hyman, B.T. (1997). Neuronal loss correlates with but exceeds neurofibrillary tangles in Alzheimer's disease. Ann. Neurol. *41*, 17–24.

Gómez-Ramos, A., Díaz-Hernández, M., Rubio, A., Miras-Portugal, M.T., and Avila, J. (2008). Extracellular tau promotes intracellular calcium increase through M1 and M3 muscarinic receptors in neuronal cells. Mol. Cell. Neurosci. *37*, 673–681.

Gratuze, M., Cisbani, G., Cicchetti, F., and Planel, E. (2016). Is Huntington's disease a tauopathy? Brain *139*, 1014–1025.

Grundke-Iqbal, I., Iqbal, K., Tung, Y.C., Quinlan, M., Wisniewski, H.M., and Binder, L.I. (1986). Abnormal phosphorylation of the microtubule-associated protein tau (tau) in Alzheimer cytoskeletal pathology. Proc. Natl. Acad. Sci. *83*, 4913–4917.

Guerreiro, R., Bilgic, B., Guven, G., Brás, J., Rohrer, J., Lohmann, E., Hanagasi, H., Gurvit, H., and Emre, M. (2013). A novel compound heterozygous mutation in TREM2 found in a Turkish frontotemporal dementia-like family. Neurobiol. Aging *34*, 2890.e1-2890.e5.

Guillozet-Bongaarts, A.L., Garcia-Sierra, F., Reynolds, M.R., Horowitz, P.M., Fu, Y., Wang, T., Cahill, M.E., Bigio, E.H., Berry, R.W., and Binder, L.I. (2005). Tau truncation during neurofibrillary tangle evolution in Alzheimer's disease. Neurobiol. Aging *26*, 1015–1022.

Guillozet-Bongaarts, A.L., Cahill, M.E., Cryns, V.L., Reynolds, M.R., Berry, R.W., and Binder, L.I. (2006). Pseudophosphorylation of tau at serine 422 inhibits caspase cleavage: in vitro evidence and implications for tangle formation in vivo. J. Neurochem. *97*, 1005–1014.

Guo, H., Albrecht, S., Bourdeau, M., Petzke, T., Bergeron, C., and LeBlanc, A.C. (2004). Active Caspase-6 and Caspase-6-Cleaved Tau in Neuropil Threads, Neuritic Plaques, and Neurofibrillary Tangles of Alzheimer's Disease. Am. J. Pathol. *165*, 523–531.

Guo, J.L., Buist, A., Soares, A., Callaerts, K., Calafate, S., Stevenaert, F., Daniels, J.P., Zoll, B.E., Crowe, A., Brunden, K.R., et al. (2016). The Dynamics and Turnover of Tau Aggregates in Cultured Cells INSIGHTS INTO THERAPIES FOR TAUOPATHIES. J. Biol. Chem. *291*, 13175–13193.

Hanes, J., Zilka, N., Bartkova, M., Caletkova, M., Dobrota, D., and Novak, M. (2009). Rat tau proteome consists of six tau isoforms: implication for animal models of human tauopathies. J. Neurochem. *108*, 1167–1176.

Harada, A., Oguchi, K., Okabe, S., Kuno, J., Terada, S., Ohshima, T., Sato-Yoshitake, R., Takei, Y., Noda, T., and Hirokawa, N. (1994). Altered microtubule organization in small-calibre axons of mice lacking tau protein. Nature *369*, 488–491.

Hardy, J.A., and Higgins, G.A. (1992). Alzheimer's disease: the amyloid cascade hypothesis. Science *256*, 184–185.

Himmelstein, D.S., Ward, S.M., Lancia, J.K., Patterson, K.R., and Binder, L.I. (2012). Tau as a therapeutic target in neurodegenerative disease. Pharmacol. Ther. *136*, 8–22.

Himmler, A. (1989). Structure of the bovine tau gene: alternatively spliced transcripts generate a protein family. Mol. Cell. Biol. *9*, 1389–1396.

Himmler, A., Drechsel, D., Kirschner, M.W., and Martin, D.W. (1989). Tau consists of a set of proteins with repeated C-terminal microtubule-binding domains and variable N-terminal domains. Mol. Cell. Biol. *9*, 1381–1388.

Hirokawa, N., Shiomura, Y., and Okabe, S. (1988). Tau proteins: the molecular structure and mode of binding on microtubules. J. Cell Biol. *107*, 1449–1459.

Hochgräfe, K., Sydow, A., and Mandelkow, E.-M. (2013). Regulatable transgenic mouse models of Alzheimer disease: onset, reversibility and spreading of Tau pathology. FEBS J. n/a–n/a.

Hochgräfe, K., Sydow, A., Matenia, D., Cadinu, D., Könen, S., Petrova, O., Pickhardt, M., Goll, P., Morellini, F., Mandelkow, E., et al. (2015). Preventive methylene blue treatment preserves cognition in mice expressing full-length pro-aggregant human Tau. Acta Neuropathol. Commun. *3*, 25.

Holmes, B.B., DeVos, S.L., Kfoury, N., Li, M., Jacks, R., Yanamandra, K., Ouidja, M.O., Brodsky, F.M., Marasa, J., Bagchi, D.P., et al. (2013). Heparan sulfate proteoglycans mediate internalization and propagation of specific proteopathic seeds. Proc. Natl. Acad. Sci. U. S. A. *110*, E3138-3147.

Holtzman, D.M., Carrillo, M.C., Hendrix, J.A., Bain, L.J., Catafau, A.M., Gault, L.M., Goedert, M., Mandelkow, E., Mandelkow, E.-M., Miller, D.S., et al. (2016). Tau: From research to clinical development. Alzheimers Dement. J. Alzheimers Assoc. *0*.

Hong, M., Zhukareva, V., Vogelsberg-Ragaglia, V., Wszolek, Z., Reed, L., Miller, B.I., Geschwind, D.H., Bird, T.D., McKeel, D., Goate, A., et al. (1998). Mutation-Specific Functional Impairments in Distinct Tau Isoforms of Hereditary FTDP-17. Science *282*, 1914–1917.

Hooli, B.V., Kovacs-Vajna, Z.M., Mullin, K., Blumenthal, M.A., Mattheisen, M., Zhang, C., Lange, C., Mohapatra, G., Bertram, L., and Tanzi, R.E. (2014). Rare autosomal copy number variations in early-onset familial Alzheimer's disease. Mol. Psychiatry *19*, 676–681.

Hoover, B.R., Reed, M.N., Su, J., Penrod, R.D., Kotilinek, L.A., Grant, M.K., Pitstick, R., Carlson, G.A., Lanier, L.M., Yuan, L.-L., et al. (2010). Tau Mislocalization to Dendritic Spines Mediates Synaptic Dysfunction Independently of Neurodegeneration. Neuron *68*, 1067–1081.

Hrnkova, M., Zilka, N., Minichova, Z., Koson, P., and Novak, M. (2007). Neurodegeneration caused by expression of human truncated tau leads to progressive neurobehavioural impairment in transgenic rats. Brain Res. *1130*, 206–213.

Hutton, M., Lendon, C.L., Rizzu, P., Baker, M., Froelich, S., Houlden, H., Pickering-Brown, S., Chakraverty, S., Isaacs, A., Grover, A., et al. (1998). Association of missense and 5′-splice-site mutations in tau with the inherited dementia FTDP-17. Nature *393*, 702–705.

Hyman, B.T., Hoesen, G.V., Damasio, A.R., and Barnes, C.L. (1984). Alzheimer's disease: cell-specific pathology isolates the hippocampal formation. Science *225*, 1168–1170.

Ikeda, C., Yokota, O., Nagao, S., Ishizu, H., Oshima, E., Hasegawa, M., Okahisa, Y., Terada, S., and Yamada, N. (2015). The Relationship Between Development of Neuronal and Astrocytic Tau Pathologies in Subcortical Nuclei and Progression of Argyrophilic Grain Disease. Brain Pathol. n/a-n/a.

Ikeda, K., Akiyama, H., Arai, T., Oda, T., Kato, M., Iseki, E., Kosaka, K., Wakabayashi, K., and Takahashi, H. (1999). Clinical aspects of "senile dementia of the tangle type"-- a subset of dementia in the senium separable from late-onset Alzheimer's disease. Dement. Geriatr. Cogn. Disord. *10*, 6–11.

Ikegami, S., Harada, A., and Hirokawa, N. (2000). Muscle weakness, hyperactivity, and impairment in fear conditioning in tau-deficient mice. Neurosci. Lett. *279*, 129–132.

Iqbal, K., Liu, F., and Gong, C.-X. (2016). Tau and neurodegenerative disease: the story so far. Nat. Rev. Neurol. *12*, 15–27.

Ishizawa, K., and Dickson, D.W. (2001). Microglial activation parallels system degeneration in progressive supranuclear palsy and corticobasal degeneration. J. Neuropathol. Exp. Neurol. *60*, 647–657.

Ittner, L.M., Ke, Y.D., Delerue, F., Bi, M., Gladbach, A., van Eersel, J., Wölfing, H., Chieng, B.C., Christie, M.J., Napier, I.A., et al. (2010). Dendritic Function of Tau Mediates Amyloid-β Toxicity in Alzheimer's Disease Mouse Models. Cell *142*, 387–397.

Iwata, A., Nagata, K., Hatsuta, H., Takuma, H., Bundo, M., Iwamoto, K., Tamaoka, A., Murayama, S., Saido, T., and Tsuji, S. (2014). Altered CpG methylation in sporadic Alzheimer's disease is associated with APP and MAPT dysregulation. Hum. Mol. Genet. *23*, 648–656.

Jaworski, T., Dewachter, I., Lechat, B., Croes, S., Termont, A., Demedts, D., Borghgraef, P., Devijver, H., Filipkowski, R.K., Kaczmarek, L., et al. (2009). AAV-Tau Mediates Pyramidal Neurodegeneration by Cell-Cycle Re-Entry without Neurofibrillary Tangle Formation in Wild-Type Mice. PLoS ONE *4*, e7280.

Jaworski, T., Lechat, B., Demedts, D., Gielis, L., Devijver, H., Borghgraef, P., Duimel, H., Verheyen, F., Kügler, S., and Van Leuven, F. (2011). Dendritic Degeneration, Neurovascular Defects, and Inflammation Precede Neuronal Loss in a Mouse Model for Tau-Mediated Neurodegeneration. Am. J. Pathol. *179*, 2001–2015.

Jeganathan, S., von Bergen, M., Brutlach, H., Steinhoff, H.-J., and Mandelkow, E. (2006). Global Hairpin Folding of Tau in Solution†. Biochemistry (Mosc.) *45*, 2283–2293.

Jeganathan, S., Hascher, A., Chinnathambi, S., Biernat, J., Mandelkow, E.-M., and Mandelkow, E. (2008). Proline-directed Pseudo-phosphorylation at AT8 and PHF1 Epitopes Induces a Compaction of the Paperclip Folding of Tau and Generates a Pathological (MC-1) Conformation. J. Biol. Chem. *283*, 32066–32076.

Jellinger, K.A., Alafuzoff, I., Attems, J., Beach, T.G., Cairns, N.J., Crary, J.F., Dickson, D.W., Hof, P.R., Hyman, B.T., Jr, C.R.J., et al. (2015). PART, a distinct tauopathy, different from classical sporadic Alzheimer disease. Acta Neuropathol. (Berl.) *129*, 757–762.

Kadavath, H., Jaremko, M., Jaremko, Ł., Biernat, J., Mandelkow, E., and Zweckstetter, M. (2015a). Folding of the Tau Protein on Microtubules. Angew. Chem. Int. Ed. *54*, 10347–10351.

Kadavath, H., Hofele, R.V., Biernat, J., Kumar, S., Tepper, K., Urlaub, H., Mandelkow, E., and Zweckstetter, M. (2015b). Tau stabilizes microtubules by binding at the interface between tubulin heterodimers. Proc. Natl. Acad. Sci. *112*, 7501–7506.

Kanaan, N.M., Morfini, G.A., LaPointe, N.E., Pigino, G.F., Patterson, K.R., Song, Y., Andreadis, A., Fu, Y., Brady, S.T., and Binder, L.I. (2011). Pathogenic Forms of Tau Inhibit Kinesin-Dependent Axonal Transport through a Mechanism Involving Activation of Axonal Phosphotransferases. J. Neurosci. *31*, 9858–9868.

Kanemaru, K., Takio, K., Miura, R., Titani, K., and Ihara, Y. (1992). Fetal-Type Phosphorylation of the τ in Paired Helical Filaments. J. Neurochem. *58*, 1667–1675.

Kempf, M., Clement, A., Faissner, A., Lee, G., and Brandt, R. (1996). Tau Binds to the Distal Axon Early in Development of Polarity in a Microtubule- and Microfilament-Dependent Manner. J. Neurosci. *16*, 5583–5592.

Khlistunova, I., Biernat, J., Wang, Y., Pickhardt, M., Bergen, M. von, Gazova, Z., Mandelkow, E., and Mandelkow, E.-M. (2006). Inducible Expression of Tau Repeat Domain in Cell Models of Tauopathy AGGREGATION IS TOXIC TO CELLS BUT CAN BE REVERSED BY INHIBITOR DRUGS. J. Biol. Chem. *281*, 1205–1214.

Kimura, T., Whitcomb, D.J., Jo, J., Regan, P., Piers, T., Heo, S., Brown, C., Hashikawa, T., Murayama, M., Seok, H., et al. (2014). Microtubule-associated protein tau is essential for long-term depression in the hippocampus. Phil Trans R Soc B *369*, 20130144.

Klein, R.L., Hamby, M.E., Gong, Y., Hirko, A.C., Wang, S., Hughes, J.A., King, M.A., and Meyer, E.M. (2002). Dose and Promoter Effects of Adeno-Associated Viral Vector for Green Fluorescent Protein Expression in the Rat Brain. Exp. Neurol. *176*, 66–74.

Klein, R.L., Lin, W.-L., Dickson, D.W., Lewis, J., Hutton, M., Duff, K., Meyer, E.M., and King, M.A. (2004). Rapid Neurofibrillary Tangle Formation after Localized Gene Transfer of Mutated Tau. Am. J. Pathol. *164*, 347–353.

Klein, R.L., Dayton, R.D., Lin, W.-L., and Dickson, D.W. (2005). Tau gene transfer, but not alpha-synuclein, induces both progressive dopamine neuron degeneration and rotational behavior in the rat. Neurobiol. Dis. *20*, 64–73.

Klein, R.L., Dayton, R.D., Leidenheimer, N.J., Jansen, K., Golde, T.E., and Zweig, R.M. (2006). Efficient Neuronal Gene Transfer with AAV8 Leads to Neurotoxic Levels of Tau or Green Fluorescent Proteins. Mol. Ther. *13*, 517–527.

Klein, R.L., Dayton, R.D., Tatom, J.B., Diaczynsky, C.G., and Salvatore, M.F. (2008a). Tau expression levels from various adeno-associated virus vector serotypes produce graded neurodegenerative disease states. Eur. J. Neurosci. *27*, 1615–1625.

Klein, R.L., Dayton, R.D., Tatom, J.B., Henderson, K.M., and Henning, P.P. (2008b). AAV8, 9, Rh10, Rh43 vector gene transfer in the rat brain: effects of serotype, promoter and purification method. Mol. Ther. J. Am. Soc. Gene Ther. *16*, 89–96.

Klein, R.L., Dayton, R.D., Diaczynsky, C.G., and Wang, D.B. (2010). Pronounced microgliosis and neurodegeneration in aged rats after tau gene transfer. Neurobiol. Aging *31*, 2091–2102.

Korenova, M., Zilka, N., Stozicka, Z., Bugos, O., Vanicky, I., and Novak, M. (2009). NeuroScale, the battery of behavioral tests with novel scoring system for phenotyping of transgenic rat model of tauopathy. J. Neurosci. Methods *177*, 108–114.

Korhonen, P., van Groen, T., Thornell, A., Kyrylenko, S., Soininen, M.-L., Ojala, J., Peltomaa, E., Tanila, H., Salminen, A., Mandelkow, E.M., et al. (2011). Characterization of a novel transgenic rat carrying human tau with mutation P301L. Neurobiol. Aging *32*, 2314–2315.

Kosik, K.S., Orecchio, L.D., Bakalis, S., and Neve, R.L. (1989a). Developmentally regulated expression of specific tau sequences. Neuron *2*, 1389–1397.

Kosik, K.S., Crandall, J.E., Mufson, E.J., and Neve, R.L. (1989b). Tau in situ hybridization in normal and alzheimer brain: Localization in the somatodendritic compartment. Ann. Neurol. *26*, 352–361.

Koson, P., Zilka, N., Kovac, A., Kovacech, B., Korenova, M., Filipcik, P., and Novak, M. (2008). Truncated tau expression levels determine life span of a rat model of tauopathy without causing neuronal loss or correlating with terminal neurofibrillary tangle load. Eur. J. Neurosci. *28*, 239–246.

Krylova, S.M., Musheev, M., Nutiu, R., Li, Y., Lee, G., and Krylov, S.N. (2005). Tau protein binds single-stranded DNA sequence specifically--the proof obtained in vitro with non-equilibrium capillary electrophoresis of equilibrium mixtures. FEBS Lett. *579*, 1371–1375.

Ksiezak-Reding, H., Morgan, K., Mattiace, L.A., Davies, P., Liu, W.K., Yen, S.H., Weidenheim, K., and Dickson, D.W. (1994). Ultrastructure and biochemical composition of paired helical filaments in corticobasal degeneration. Am. J. Pathol. *145*, 1496–1508.

Kuchibhotla, K.V., Wegmann, S., Kopeikina, K.J., Hawkes, J., Rudinskiy, N., Andermann, M.L., Spires-Jones, T.L., Bacskai, B.J., and Hyman, B.T. (2014). Neurofibrillary tangle-bearing neurons are functionally integrated in cortical circuits in vivo. Proc. Natl. Acad. Sci. U. S. A. *111*, 510–514.

Lace, G., Savva, G.M., Forster, G., de Silva, R., Brayne, C., Matthews, F.E., Barclay, J.J., Dakin, L., Ince, P.G., Wharton, S.B., et al. (2009). Hippocampal tau pathology is related to neuroanatomical connections: an ageing population-based study. Brain J. Neurol. *132*, 1324–1334.

Lasagna-Reeves, C.A., Castillo-Carranza, D.L., Sengupta, U., Clos, A.L., Jackson, G.R., and Kayed, R. (2011). Tau oligomers impair memory and induce synaptic and mitochondrial dysfunction in wild-type mice. Mol. Neurodegener. *6*, 39.

Lasagna-Reeves, C.A., Castillo-Carranza, D.L., Sengupta, U., Sarmiento, J., Troncoso, J., Jackson, G.R., and Kayed, R. (2012a). Identification of oligomers at early stages of tau aggregation in Alzheimer's disease. FASEB J. *26*, 1946–1959.

Lasagna-Reeves, C.A., Castillo-Carranza, D.L., Sengupta, U., Guerrero-Munoz, M.J., Kiritoshi, T., Neugebauer, V., Jackson, G.R., and Kayed, R. (2012b). Alzheimer brain-derived tau oligomers propagate pathology from endogenous tau. Sci. Rep. *2*.

Lee, G., Cowan, N., and Kirschner, M. (1988). The primary structure and heterogeneity of tau protein from mouse brain. Science *239*, 285–288.

Lee, G., Neve, R.L., and Kosik, K.S. (1989). The microtubule binding domain of tau protein. Neuron *2*, 1615–1624.

Lee, G., Newman, S.T., Gard, D.L., Band, H., and Panchamoorthy, G. (1998). Tau interacts with src-family non-receptor tyrosine kinases. J. Cell Sci. *111 (Pt 21)*, 3167–3177.

Leroy, K., Bretteville, A., Schindowski, K., Gilissen, E., Authelet, M., De Decker, R., Yilmaz, Z., Buee, L., and Brion, J.-P. (2007). Early Axonopathy Preceding Neurofibrillary Tangles in Mutant Tau Transgenic Mice. Am. J. Pathol. *171*, 976–992.

Lewis, J., McGowan, E., Rockwood, J., Melrose, H., Nacharaju, P., Slegtenhorst, M.V., Gwinn-Hardy, K., Murphy, M.P., Baker, M., Yu, X., et al. (2000). Neurofibrillary tangles, amyotrophy and progressive motor disturbance in mice expressing mutant (P301L) tau protein. Nat. Genet. *25*, 402–405.

Li, X., Kumar, Y., Zempel, H., Mandelkow, E.-M., Biernat, J., and Mandelkow, E. (2011). Novel diffusion barrier for axonal retention of Tau in neurons and its failure in neurodegeneration. EMBO J. *30*, 4825–4837.

Li, X.-C., Hu, Y., Wang, Z., Luo, Y., Zhang, Y., Liu, X.-P., Feng, Q., Wang, Q., Ye, K., Liu, G.-P., et al. (2016). Human wild-type full-length tau accumulation disrupts mitochondrial dynamics and the functions via increasing mitofusins. Sci. Rep. *6*, 24756.

Lin, W.-L., Lewis, J., Yen, S.-H., Hutton, M., and Dickson, D.W. (2003). Filamentous Tau in Oligodendrocytes and Astrocytes of Transgenic Mice Expressing the Human Tau Isoform with the P301L Mutation. Am. J. Pathol. *162*, 213–218.

Litman, P., Barg, J., Rindzoonski, L., and Ginzburg, I. (1993). Subcellular localization of tau mRNA in differentiating neuronal cell culture: Implications for neuronal polarity. Neuron *10*, 627–638.

Liu, C., and Götz, J. (2013). Profiling Murine Tau with 0N, 1N and 2N Isoform-Specific Antibodies in Brain and Peripheral Organs Reveals Distinct Subcellular Localization, with the 1N Isoform Being Enriched in the Nucleus. PLOS ONE *8*, e84849.

Liu, F., Iqbal, K., Grundke-Iqbal, I., Hart, G.W., and Gong, C.-X. (2004). O-GlcNAcylation regulates phosphorylation of tau: A mechanism involved in Alzheimer's disease. Proc. Natl. Acad. Sci. U. S. A. *101*, 10804–10809.

Liu, F., Li, B., Tung, E.-J., Grundke-Iqbal, I., Iqbal, K., and Gong, C.-X. (2007). Site-specific effects of tau phosphorylation on its microtubule assembly activity and self-aggregation. Eur. J. Neurosci. *26*, 3429–3436.

Liu, F., Shi, J., Tanimukai, H., Gu, J., Gu, J., Grundke-Iqbal, I., Iqbal, K., and Gong, C.-X. (2009). Reduced O-GlcNAcylation links lower brain glucose metabolism and tau pathology in Alzheimer's disease. Brain *132*, 1820–1832.

Loeb, J.E., Cordier, W.S., Harris, M.E., Weitzman, M.D., and Hope, T.J. (1999). Enhanced Expression of Transgenes from Adeno-Associated Virus Vectors with the Woodchuck Hepatitis Virus Posttranscriptional Regulatory Element: Implications for Gene Therapy. Hum. Gene Ther. *10*, 2295–2305.

Lööv, C., Hillered, L., Ebendal, T., and Erlandsson, A. (2012). Engulfing Astrocytes Protect Neurons from Contact-Induced Apoptosis following Injury. PLoS ONE *7*, e33090.

LoPresti, P., Szuchet, S., Papasozomenos, S.C., Zinkowski, R.P., and Binder, L.I. (1995). Functional implications for the microtubule-associated protein tau: localization in oligodendrocytes. Proc. Natl. Acad. Sci. U. S. A. *92*, 10369–10373.

Ma, Q.-L., Zuo, X., Yang, F., Ubeda, O.J., Gant, D.J., Alaverdyan, M., Teng, E., Hu, S., Chen, P.-P., Maiti, P., et al. (2013). Curcumin suppresses soluble tau dimers and corrects molecular chaperone, synaptic, and behavioral deficits in aged human tau transgenic mice. J. Biol. Chem. *288*, 4056–4065.

Maeda, S., Sahara, N., Saito, Y., Murayama, S., Ikai, A., and Takashima, A. (2006). Increased levels of granular tau oligomers: an early sign of brain aging and Alzheimer's disease. Neurosci. Res. *54*, 197–201.

Maeda, S., Sahara, N., Saito, Y., Murayama, M., Yoshiike, Y., Kim, H., Miyasaka, T., Murayama, S., Ikai, A., and Takashima, A. (2007). Granular Tau Oligomers as Intermediates of Tau Filaments. Biochemistry (Mosc.) *46*, 3856–3861.

Magnani, E., Fan, J., Gasparini, L., Golding, M., Williams, M., Schiavo, G., Goedert, M., Amos, L.A., and Spillantini, M.G. (2007). Interaction of tau protein with the dynactin complex. EMBO J. *26*, 4546–4554.

Mailliot, C., Sergeant, N., Bussière, T., Caillet-Boudin, M.-L., Delacourte, A., and Buée, L. (1998). Phosphorylation of specific sets of tau isoforms reflects different neurofibrillary degeneration processes. FEBS Lett. *433*, 201–204.

Mairet-Coello, G., Courchet, J., Pieraut, S., Courchet, V., Maximov, A., and Polleux, F. (2013). The CAMKK2-AMPK kinase pathway mediates the synaptotoxic effects of Aβ oligomers through Tau phosphorylation. Neuron *78*, 94–108.

Mandelkow, E.-M., and Mandelkow, E. (2012). Biochemistry and Cell Biology of Tau Protein in Neurofibrillary Degeneration. Cold Spring Harb. Perspect. Med. *2*, a006247.

Mandelkow, E., Von Bergen, M., Biernat, J., and Mandelkow, E.-M. (2007). Structural Principles of Tau and the Paired Helical Filaments of Alzheimer's Disease. Brain Pathol. *17*, 83–90.

Maphis, N., Xu, G., Kokiko-Cochran, O.N., Jiang, S., Cardona, A., Ransohoff, R.M., Lamb, B.T., and Bhaskar, K. (2015). Reactive microglia drive tau pathology and contribute to the spreading of pathological tau in the brain. Brain J. Neurol. *138*, 1738–1755.

Martin, L., Latypova, X., and Terro, F. (2011). Post-translational modifications of tau protein: Implications for Alzheimer's disease. Neurochem. Int. *58*, 458–471.

Maruyama, M., Shimada, H., Suhara, T., Shinotoh, H., Ji, B., Maeda, J., Zhang, M.-R., Trojanowski, J.Q., Lee, V.M.-Y., Ono, M., et al. (2013). Imaging of Tau Pathology in a Tauopathy Mouse Model and in Alzheimer Patients Compared to Normal Controls. Neuron *79*, 1094–1108.

Maurin, H., Chong, S.-A., Kraev, I., Davies, H., Kremer, A., Seymour, C.M., Lechat, B., Jaworski, T., Borghgraef, P., Devijver, H., et al. (2014). Early structural and functional defects in synapses and myelinated axons in stratum lacunosum moleculare in two preclinical models for tauopathy. PloS One *9*, e87605.

McKhann, G.M., Knopman, D.S., Chertkow, H., Hyman, B.T., Jack Jr., C.R., Kawas, C.H., Klunk, W.E., Koroshetz, W.J., Manly, J.J., Mayeux, R., et al. (2011). The diagnosis of dementia due to Alzheimer's disease: Recommendations from the National Institute on Aging-Alzheimer's Association workgroups on diagnostic guidelines for Alzheimer's disease. Alzheimers Dement. *7*, 263–269.

Michel, C.H., Kumar, S., Pinotsi, D., Tunnacliffe, A., George-Hyslop, P.S., Mandelkow, E., Mandelkow, E.-M., Kaminski, C.F., and Schierle, G.S.K. (2013). Extracellular Monomeric Tau is Sufficient to Initiate the Spread of Tau Pathology. J. Biol. Chem. jbc.M113.515445.

Min, S.-W., Cho, S.-H., Zhou, Y., Schroeder, S., Haroutunian, V., Seeley, W.W., Huang, E.J., Shen, Y., Masliah, E., Mukherjee, C., et al. (2010). Acetylation of Tau Inhibits Its Degradation and Contributes to Tauopathy. Neuron *67*, 953–966.

Min, S.-W., Chen, X., Tracy, T.E., Li, Y., Zhou, Y., Wang, C., Shirakawa, K., Minami, S.S., Defensor, E., Mok, S.A., et al. (2015). Critical role of acetylation in tau-mediated neurodegeneration and cognitive deficits. Nat. Med. *21*, 1154–1162.

Mirbaha, H., Holmes, B.B., Sanders, D.W., Bieschke, J., and Diamond, M.I. (2015). Tau Trimers Are the Minimal Propagation Unit Spontaneously Internalized to Seed Intracellular Aggregation. J. Biol. Chem. *290*, 14893–14903.

Mitani, K., Furiya, Y., Uchihara, T., Ishii, K., Yamanouchi, H., Mizusawa, H., and Mori, H. (1998). Increased CSF tau protein in corticobasal degeneration. J. Neurol. *245*, 44–46.

Mocanu, M.-M., Nissen, A., Eckermann, K., Khlistunova, I., Biernat, J., Drexler, D., Petrova, O., Schönig, K., Bujard, H., Mandelkow, E., et al. (2008). The Potential for β-Structure in the Repeat Domain of Tau Protein Determines Aggregation, Synaptic Decay, Neuronal Loss, and Coassembly with Endogenous Tau in Inducible Mouse Models of Tauopathy. J. Neurosci. *28*, 737–748.

Mondragón-Rodríguez, S., Basurto-Islas, G., Santa-Maria, I., Mena, R., Binder, L.I., Avila, J., Smith, M.A., Perry, G., and García-Sierra, F. (2008). Cleavage and conformational changes of tau protein follow phosphorylation during Alzheimer's disease. Int. J. Exp. Pathol. *89*, 81–90.

Morris, M., Hamto, P., Adame, A., Devidze, N., Masliah, E., and Mucke, L. (2013). Age-appropriate cognition and subtle dopamine-independent motor deficits in aged tau knockout mice. Neurobiol. Aging *34*, 1523–1529.

Morsch, R., Simon, W., and Coleman, P.D. (1999). Neurons May Live for Decades with Neurofibrillary Tangles. J. Neuropathol. Exp. Neurol. *58*, 188–197.

Mukrasch, M.D., Bibow, S., Korukottu, J., Jeganathan, S., Biernat, J., Griesinger, C., Mandelkow, E., and Zweckstetter, M. (2009). Structural Polymorphism of 441-Residue Tau at Single Residue Resolution. PLOS Biol *7*, e1000034.

Murakami, T., Paitel, E., Kawarabayashi, T., Ikeda, M., Chishti, M.A., Janus, C., Matsubara, E., Sasaki, A., Kawarai, T., Phinney, A.L., et al. (2006). Cortical Neuronal and Glial Pathology in TgTauP301L Transgenic Mice. Am. J. Pathol. *169*, 1365–1375.

Mustroph, M.L., King, M.A., Klein, R.L., and Ramirez, J.J. (2012). Adult-onset focal expression of mutated human tau in the hippocampus impairs spatial working memory of rats. Behav. Brain Res. *233*, 141–148.

Myeku, N., Clelland, C.L., Emrani, S., Kukushkin, N.V., Yu, W.H., Goldberg, A.L., and Duff, K.E. (2016). Tau-driven 26S proteasome impairment and cognitive dysfunction can be prevented early in disease by activating cAMP-PKA signaling. Nat. Med. *22*, 46–53.

Myers, A.J., Kaleem, M., Marlowe, L., Pittman, A.M., Lees, A.J., Fung, H.C., Duckworth, J., Leung, D., Gibson, A., Morris, C.M., et al. (2005). The H1c haplotype at the MAPT locus is associated with Alzheimer's disease. Hum. Mol. Genet. *14*, 2399–2404.

Myers, A.J., Pittman, A.M., Zhao, A.S., Rohrer, K., Kaleem, M., Marlowe, L., Lees, A., Leung, D., McKeith, I.G., Perry, R.H., et al. (2007). The MAPT H1c risk haplotype is associated with increased expression of tau and especially of 4 repeat containing transcripts. Neurobiol. Dis. *25*, 561–570.

van de Nes, J.A.P., Nafe, R., and Schlote, W. (2008). Non-tau based neuronal degeneration in Alzheimer's disease — an immunocytochemical and quantitative study in the supragranular layers of the middle temporal neocortex. Brain Res. *1213*, 152–165.

Neve, R.L., Harris, P., Kosik, K.S., Kurnit, D.M., and Donlon, T.A. (1986). Identification of cDNA clones for the human microtubule-associated protein tau and chromosomal localization of the genes for tau and microtubule-associated protein 2. Mol. Brain Res. *1*, 271–280.

Noble, W., Planel, E., Zehr, C., Olm, V., Meyerson, J., Suleman, F., Gaynor, K., Wang, L., LaFrancois, J., Feinstein, B., et al. (2005). Inhibition of glycogen synthase kinase-3 by lithium correlates with reduced tauopathy and degeneration in vivo. Proc. Natl. Acad. Sci. U. S. A. *102*, 6990–6995.

Noble, W., Hanger, D.P., and Lovestone, S. (2013). The importance of tau phosphorylation for neurodegenerative diseases. Front. Neurodegener. *4*, 83.

Novak, M., Kabat, J., and Wischik, C.M. (1993). Molecular characterization of the minimal protease resistant tau unit of the Alzheimer's disease paired helical filament. EMBO J. *12*, 365–370.

Oddo, S., Caccamo, A., Shepherd, J.D., Murphy, M.P., Golde, T.E., Kayed, R., Metherate, R., Mattson, M.P., Akbari, Y., and LaFerla, F.M. (2003). Triple-transgenic model of Alzheimer's disease with plaques and tangles: intracellular Abeta and synaptic dysfunction. Neuron *39*, 409–421.

Orre, M., Kamphuis, W., Dooves, S., Kooijman, L., Chan, E.T., Kirk, C.J., Smith, V.D., Koot, S., Mamber, C., Jansen, A.H., et al. (2013). Reactive glia show increased immunoproteasome activity in Alzheimer's disease. Brain *136*, 1415–1431.

Osinde, M., Clavaguera, F., May-Nass, R., Tolnay, M., and Dev, K.K. (2008). Lentivirus Tau (P301S) expression in adult amyloid precursor protein (APP)-transgenic mice leads to tangle formation. Neuropathol. Appl. Neurobiol. *34*, 523–531.

Pallas-Bazarra, N., Jurado-Arjona, J., Navarrete, M., Esteban, J.A., Hernández, F., Ávila, J., and Llorens-Martín, M. (2016). Novel function of Tau in regulating the effects of external stimuli on adult hippocampal neurogenesis. EMBO J. *35*, 1417–1436.

Panda, D., Samuel, J.C., Massie, M., Feinstein, S.C., and Wilson, L. (2003). Differential regulation of microtubule dynamics by three- and four-repeat tau: Implications for the onset of neurodegenerative disease. Proc. Natl. Acad. Sci. *100*, 9548–9553.

Patterson, K.R., Remmers, C., Fu, Y., Brooker, S., Kanaan, N.M., Vana, L., Ward, S., Reyes, J.F., Philibert, K., Glucksman, M.J., et al. (2011). Characterization of Prefibrillar Tau Oligomers in Vitro and in Alzheimer Disease. J. Biol. Chem. *286*, 23063–23076.

Pedersen, J.T., and Sigurdsson, E.M. (2015). Tau immunotherapy for Alzheimer's disease. Trends Mol. Med. *21*, 394–402.

Peeraer, E., Bottelbergs, A., Van Kolen, K., Stancu, I.-C., Vasconcelos, B., Mahieu, M., Duytschaever, H., Ver Donck, L., Torremans, A., Sluydts, E., et al. (2015). Intracerebral injection of preformed synthetic tau fibrils initiates widespread tauopathy and neuronal loss in the brains of tau transgenic mice. Neurobiol. Dis. *73*, 83–95.

Pekny, M., and Nilsson, M. (2005). Astrocyte activation and reactive gliosis. Glia *50*, 427–434.

Perry, G., Friedman, R., Shaw, G., and Chau, V. (1987). Ubiquitin is detected in neurofibrillary tangles and senile plaque neurites of Alzheimer disease brains. Proc. Natl. Acad. Sci. U. S. A. *84*, 3033–3036.

Piras, A., Collin, L., Grüninger, F., Graff, C., and Rönnbäck, A. (2016). Autophagic and lysosomal defects in human tauopathies: analysis of post-mortem brain from patients with familial Alzheimer disease, corticobasal degeneration and progressive supranuclear palsy. Acta Neuropathol. Commun. *4*, 22.

Polanco, J.C., Scicluna, B.J., Hill, A.F., and Götz, J. (2016). Extracellular Vesicles Isolated from the Brains of rTg4510 Mice Seed Tau Protein Aggregation in a Threshold-dependent Manner. J. Biol. Chem. *291*, 12445–12466.

Polydoro, M., Acker, C.M., Duff, K., Castillo, P.E., and Davies, P. (2009). Age-dependent impairment of cognitive and synaptic function in the htau mouse model of tau pathology. J. Neurosci. Off. J. Soc. Neurosci. *29*, 10741–10749.

Polydoro, M., Calignon, A. de, Suárez-Calvet, M., Sanchez, L., Kay, K.R., Nicholls, S.B., Roe, A.D., Pitstick, R., Carlson, G.A., Gómez-Isla, T., et al. (2013). Reversal of Neurofibrillary Tangles and Tau-Associated Phenotype in the rTgTauEC Model of Early Alzheimer's Disease. J. Neurosci. *33*, 13300–13311.

Pooler, A.M., Phillips, E.C., Lau, D.H.W., Noble, W., and Hanger, D.P. (2013). Physiological release of endogenous tau is stimulated by neuronal activity. EMBO Rep. *14*, 389–394.

Pooler, A.M., Noble, W., and Hanger, D.P. (2014). A role for tau at the synapse in Alzheimer's disease pathogenesis. Neuropharmacology *76*, *Part A*, 1–8.

Probst, A., Ulrich, J., and Heitz, P.U. (1982). Senile dementia of Alzheimer type: astroglial reaction to extracellular neurofibrillary tangles in the hippocampus. An immunocytochemical and electron-microscopic study. Acta Neuropathol. (Berl.) *57*, 75–79.

Probst, A., Götz, J., Wiederhold, K.H., Tolnay, M., Mistl, C., Jaton, A.L., Hong, M., Ishihara, T., Lee, V.M.-Y., Trojanowski, J.Q., et al. (2000). Axonopathy and amyotrophy in mice transgenic for human four-repeat tau protein. Acta Neuropathol. (Berl.) *99*, 469–481.

Ramirez, J.J., Poulton, W.E., Knelson, E., Barton, C., King, M.A., and Klein, R.L. (2011). Focal expression of mutated tau in entorhinal cortex neurons of rats impairs spatial working memory. Behav. Brain Res. *216*, 332–340.

Ramsden, M., Kotilinek, L., Forster, C., Paulson, J., McGowan, E., SantaCruz, K., Guimaraes, A., Yue, M., Lewis, J., Carlson, G., et al. (2005). Age-Dependent Neurofibrillary Tangle Formation, Neuron Loss, and Memory Impairment in a Mouse Model of Human Tauopathy (P301L). J. Neurosci. *25*, 10637–10647.

Rankin, C.A., Sun, Q., and Gamblin, T.C. (2008). Pre-assembled tau filaments phosphorylated by GSK-3b form large tangle-like structures. Neurobiol. Dis. *31*, 368–377.

Reddy, P.H. (2011). Abnormal tau, mitochondrial dysfunction, impaired axonal transport of mitochondria, and synaptic deprivation in Alzheimer's disease. Brain Res. *1415*, 136–148.

Rewcastle, N.B., and Ball, M.J. (1968). Electron microscopic structure of the "inclusion bodies" in Pick's disease. Neurology *18*, 1205–1213.

Rizzu, P., Van Swieten, J.C., Joosse, M., Hasegawa, M., Stevens, M., Tibben, A., Niermeijer, M.F., Hillebrand, M., Ravid, R., Oostra, B.A., et al. (1999). High Prevalence of Mutations in the Microtubule-Associated Protein Tau in a Population Study of Frontotemporal Dementia in the Netherlands. Am. J. Hum. Genet. *64*, 414–421.

Roberson, E.D., Scearce-Levie, K., Palop, J.J., Yan, F., Cheng, I.H., Wu, T., Gerstein, H., Yu, G.-Q., and Mucke, L. (2007). Reducing Endogenous Tau Ameliorates Amyloid ß-Induced Deficits in an Alzheimer's Disease Mouse Model. Science *316*, 750–754.

Rocher, A.B., Crimins, J.L., Amatrudo, J.M., Kinson, M.S., Todd-Brown, M.A., Lewis, J., and Luebke, J.I. (2010). Structural and functional changes in tau mutant mice neurons are not linked to the presence of NFTs. Exp. Neurol. *223*, 385–393.

Rossi, G., and Tagliavini, F. (2015). Frontotemporal lobar degeneration: old knowledge and new insight into the pathogenetic mechanisms of tau mutations. Front. Aging Neurosci. *7*, 192.

Rovelet-Lecrux, A., Hannequin, D., Guillin, O., Legallic, S., Jurici, S., Wallon, D., Frebourg, T., and Campion, D. (2010). Frontotemporal dementia phenotype associated with MAPT gene duplication. J. Alzheimers Dis. JAD *21*, 897–902.

Rudinskiy, N., Hawkes, J.M., Wegmann, S., Kuchibhotla, K.V., Muzikansky, A., Betensky, R.A., Spires-Jones, T.L., and Hyman, B.T. (2014). Tau pathology does not affect experience-driven single-neuron and network-wide Arc/Arg3.1 responses. Acta Neuropathol. Commun. *2*, 63.

Ryan, M.D., King, A.M., and Thomas, G.P. (1991). Cleavage of foot-and-mouth disease virus polyprotein is mediated by residues located within a 19 amino acid sequence. J. Gen. Virol. *72 (Pt 11)*, 2727–2732.

Sahara, N., Maeda, S., Murayama, M., Suzuki, T., Dohmae, N., Yen, S.-H., and Takashima, A. (2007). Assembly of two distinct dimers and higher-order oligomers from full-length tau. Eur. J. Neurosci. *25*, 3020–3029.

Sämgård, K., Zetterberg, H., Blennow, K., Hansson, O., Minthon, L., and Londos, E. (2010). Cerebrospinal fluid total tau as a marker of Alzheimer's disease intensity. Int. J. Geriatr. Psychiatry *25*, 403–410.

Sanders, D.W., Kaufman, S.K., DeVos, S.L., Sharma, A.M., Mirbaha, H., Li, A., Barker, S.J., Foley, A.C., Thorpe, J.R., Serpell, L.C., et al. (2014). Distinct Tau Prion Strains Propagate in Cells and Mice and Define Different Tauopathies. Neuron *82*, 1271–1288.

SantaCruz, K., Lewis, J., Spires, T., Paulson, J., Kotilinek, L., Ingelsson, M., Guimaraes, A., DeTure, M., Ramsden, M., McGowan, E., et al. (2005). Tau Suppression in a Neurodegenerative Mouse Model Improves Memory Function. Science *309*, 476–481.

Santa-Maria, I., Haggiagi, A., Liu, X., Wasserscheid, J., Nelson, P.T., Dewar, K., Clark, L.N., and Crary, J.F. (2012). The MAPT H1 haplotype is associated with tangle-predominant dementia. Acta Neuropathol. (Berl.) *124*, 693–704.

Schindowski, K., Bretteville, A., Leroy, K., Begard, S., Brion, J.-P., Hamdane, M., and Buee, L. (2006). Alzheimer's Disease-Like Tau Neuropathology Leads to Memory Deficits and Loss of Functional Synapses in a Novel Mutated Tau Transgenic Mouse without Any Motor Deficits. Am. J. Pathol. *169*, 599–616.

Schneider, A., Biernat, J., von Bergen, M., Mandelkow, E., and Mandelkow, E.M. (1999). Phosphorylation that detaches tau protein from microtubules (Ser262, Ser214) also protects it against aggregation into Alzheimer paired helical filaments. Biochemistry (Mosc.) *38*, 3549–3558.

Schönheit, B., Zarski, R., and Ohm, T.G. (2004). Spatial and temporal relationships between plaques and tangles in Alzheimer-pathology. Neurobiol. Aging *25*, 697–711.

Schulz, K.L., Eckert, A., Rhein, V., Mai, S., Haase, W., Reichert, A.S., Jendrach, M., Müller, W.E., and Leuner, K. (2012). A new link to mitochondrial impairment in tauopathies. Mol. Neurobiol. *46*, 205–216.

Sergeant, N., Delacourte, A., and Buée, L. (2005). Tau protein as a differential biomarker of tauopathies. Biochim. Biophys. Acta BBA - Mol. Basis Dis. *1739*, 179–197.

Sergeant, N., Bretteville, A., Hamdane, M., Caillet-Boudin, M.-L., Grognet, P., Bombois, S., Blum, D., Delacourte, A., Pasquier, F., Vanmechelen, E., et al. (2008). Biochemistry of Tau in Alzheimer's disease and related neurological disorders. Expert Rev. Proteomics *5*, 207–224.

Shah, M., and Catafau, A.M. (2014). Molecular Imaging Insights into Neurodegeneration: Focus on Tau PET Radiotracers. J. Nucl. Med. *55*, 871–874.

Shammas, S.L., Garcia, G.A., Kumar, S., Kjaergaard, M., Horrocks, M.H., Shivji, N., Mandelkow, E., Knowles, T.P.J., Mandelkow, E., and Klenerman, D. (2015). A mechanistic model of tau amyloid aggregation based on direct observation of oligomers. Nat. Commun. *6*, 7025.

Shen, Y., Lue, L., Yang, L., Roher, A., Kuo, Y., Strohmeyer, R., Goux, W.J., Lee, V., Johnson, G.V., Webster, S.D., et al. (2001). Complement activation by neurofibrillary tangles in Alzheimer's disease. Neurosci. Lett. *305*, 165–168.

Sheng, J.G., Mrak, R.E., and Griffin, W.S.T. (1997). Glial-Neuronal Interactions in Alzheimer Disease: Progressive Association of IL-1α+ Microglia and S100β+ Astrocytes with Neurofibrillary Tangle Stages. J. Neuropathol. Exp. Neurol. *56*, 285–290.

Siman, R., Lin, Y.-G., Malthankar-Phatak, G., and Dong, Y. (2013). A rapid gene delivery-based mouse model for early-stage Alzheimer disease-type tauopathy. J. Neuropathol. Exp. Neurol. *72*, 1062–1071.

Spires, T.L., Orne, J.D., SantaCruz, K., Pitstick, R., Carlson, G.A., Ashe, K.H., and Hyman, B.T. (2006). Region-specific dissociation of neuronal loss and neurofibrillary pathology in a mouse model of tauopathy. Am. J. Pathol. *168*, 1598–1607.

Spires-Jones, T.L., de Calignon, A., Matsui, T., Zehr, C., Pitstick, R., Wu, H.-Y., Osetek, J.D., Jones, P.B., Bacskai, B.J., Feany, M.B., et al. (2008). In vivo imaging reveals dissociation between caspase activation and acute neuronal death in tangle-bearing neurons. J. Neurosci. Off. J. Soc. Neurosci. *28*, 862–867.

Spires-Jones, T.L., Kopeikina, K.J., Koffie, R.M., Calignon, A. de, and Hyman, B.T. (2011). Are Tangles as Toxic as They Look? J. Mol. Neurosci. *45*, 438–444.

Spittaels, K., Van den Haute, C., Van Dorpe, J., Bruynseels, K., Vandezande, K., Laenen, I., Geerts, H., Mercken, M., Sciot, R., Van Lommel, A., et al. (1999). Prominent Axonopathy in the Brain and Spinal

Cord of Transgenic Mice Overexpressing Four-Repeat Human tau Protein. Am. J. Pathol. *155*, 2153–2165.

Stamer, K., Vogel, R., Thies, E., Mandelkow, E., and Mandelkow, E.-M. (2002). Tau blocks traffic of organelles, neurofilaments, and APP vesicles in neurons and enhances oxidative stress. J. Cell Biol. *156*, 1051–1063.

Stancu, I.-C., Vasconcelos, B., Ris, L., Wang, P., Villers, A., Peeraer, E., Buist, A., Terwel, D., Baatsen, P., Oyelami, T., et al. (2015). Templated misfolding of Tau by prion-like seeding along neuronal connections impairs neuronal network function and associated behavioral outcomes in Tau transgenic mice. Acta Neuropathol. (Berl.) *129*, 875–894.

Sultan, A., Nesslany, F., Violet, M., Bégard, S., Loyens, A., Talahari, S., Mansuroglu, Z., Marzin, D., Sergeant, N., Humez, S., et al. (2011). Nuclear Tau, a Key Player in Neuronal DNA Protection. J. Biol. Chem. *286*, 4566–4575.

Swieten, J.C. van, Bronner, I.F., Azmani, A., Severijnen, L.-A., Kamphorst, W., Ravid, R., Rizzu, P., Willemsen, R., and Heutink, P. (2007). The ΔK280 Mutation in MAP tau Favors Exon 10 Skipping In Vivo. J. Neuropathol. Exp. Neurol. *66*, 17–25.

Sydow, A., Jeugd, A.V. der, Zheng, F., Ahmed, T., Balschun, D., Petrova, O., Drexler, D., Zhou, L., Rune, G., Mandelkow, E., et al. (2011a). Tau-Induced Defects in Synaptic Plasticity, Learning, and Memory Are Reversible in Transgenic Mice after Switching Off the Toxic Tau Mutant. J. Neurosci. *31*, 2511–2525.

Sydow, A., Jeugd, A.V. der, Zheng, F., Ahmed, T., Balschun, D., Petrova, O., Drexler, D., Zhou, L., Rune, G., Mandelkow, E., et al. (2011b). Reversibility of Tau-Related Cognitive Defects in a Regulatable FTD Mouse Model. J. Mol. Neurosci. *45*, 432.

Tai, H.-C., Serrano-Pozo, A., Hashimoto, T., Frosch, M.P., Spires-Jones, T.L., and Hyman, B.T. (2012). The Synaptic Accumulation of Hyperphosphorylated Tau Oligomers in Alzheimer Disease Is Associated With Dysfunction of the Ubiquitin-Proteasome System. Am. J. Pathol. *181*, 1426–1435.

Tai, H.-C., Wang, B.Y., Serrano¿Pozo, A., Frosch, M.P., Spires-Jones, T.L., and Hyman, B.T. (2014). Frequent and symmetric deposition of misfolded tau oligomers within presynaptic and postsynaptic terminals in Alzheimer's disease. Acta Neuropathol. Commun. *2*, 146.

Takuma, H., Arawaka, S., and Mori, H. (2003). Isoforms changes of tau protein during development in various species. Dev. Brain Res. *142*, 121–127.

Tatebayashi, Y., Miyasaka, T., Chui, D.-H., Akagi, T., Mishima, K., Iwasaki, K., Fujiwara, M., Tanemura, K., Murayama, M., Ishiguro, K., et al. (2002). Tau filament formation and associative memory deficit in aged mice expressing mutant (R406W) human tau. Proc. Natl. Acad. Sci. *99*, 13896–13901.

Taymans, J.-M., Vandenberghe, L.H., Haute, C.V.D., Thiry, I., Deroose, C.M., Mortelmans, L., Wilson, J.M., Debyser, Z., and Baekelandt, V. (2007). Comparative Analysis of Adeno-Associated Viral Vector Serotypes 1, 2, 5, 7, And 8 in Mouse Brain. Hum. Gene Ther. *18*, 195–206.

Tepper, K., Biernat, J., Kumar, S., Wegmann, S., Timm, T., Hübschmann, S., Redecke, L., Mandelkow, E.-M., Müller, D.J., and Mandelkow, E. (2014). Oligomer Formation of Tau Protein Hyperphosphorylated in Cells. J. Biol. Chem. *289*, 34389–34407.

Terwel, D., Lasrado, R., Snauwaert, J., Vandeweert, E., Van Haesendonck, C., Borghgraef, P., and Van Leuven, F. (2005). Changed conformation of mutant Tau-P301L underlies the moribund tauopathy, absent in progressive, nonlethal axonopathy of Tau-4R/2N transgenic mice. J. Biol. Chem. *280*, 3963–3973.

Thies, E., and Mandelkow, E.-M. (2007). Missorting of Tau in Neurons Causes Degeneration of Synapses That Can Be Rescued by the Kinase MARK2/Par-1. J. Neurosci. *27*, 2896–2907.

Tian, H., Davidowitz, E., Lopez, P., Emadi, S., Moe, J., and Sierks, M. (2013). Trimeric tau is toxic to human neuronal cells at low nanomolar concentrations. Int. J. Cell Biol. *2013*, 260787.

Togo, T., Sahara, N., Yen, S.-H., Cookson, N., Ishizawa, T., Hutton, M., de Silva, R., Lees, A., and Dickson, D.W. (2002). Argyrophilic grain disease is a sporadic 4-repeat tauopathy. J. Neuropathol. Exp. Neurol. *61*, 547–556.

Tomonaga, M. (1977). Ultrastructure of neurofibrillary tangles in progressive supranuclear palsy. Acta Neuropathol. (Berl.) *37*, 177–181.

Tucker, K.L., Meyer, M., and Barde, Y.-A. (2001). Neurotrophins are required for nerve growth during development. Nat. Neurosci. *4*, 29–37.

Ubhi, K., Rockenstein, E., Doppler, E., Mante, M., Adame, A., Patrick, C., Trejo, M., Crews, L., Paulino, A., Moessler, H., et al. (2009). Neurofibrillary and neurodegenerative pathology in APP-transgenic mice injected with AAV2-mutant TAU: neuroprotective effects of Cerebrolysin. Acta Neuropathol. (Berl.) *117*, 699–712.

Urakami, K., Wada, K., Arai, H., Sasaki, H., Kanai, M., Shoji, M., Ishizu, H., Kashihara, K., Yamamoto, M., Tsuchiya-Ikemoto, K., et al. (2001). Diagnostic significance of tau protein in cerebrospinal fluid from patients with corticobasal degeneration or progressive supranuclear palsy. J. Neurol. Sci. *183*, 95–98.

Van der Jeugd, A., Hochgräfe, K., Ahmed, T., Decker, J.M., Sydow, A., Hofmann, A., Wu, D., Messing, L., Balschun, D., D'Hooge, R., et al. (2012). Cognitive defects are reversible in inducible mice expressing pro-aggregant full-length human Tau. Acta Neuropathol. (Berl.) *123*, 787–805.

Violet, M., Chauderlier, A., Delattre, L., Tardivel, M., Chouala, M.S., Sultan, A., Marciniak, E., Humez, S., Binder, L., Kayed, R., et al. (2015). Prefibrillar Tau oligomers alter the nucleic acid protective function of Tau in hippocampal neurons in vivo. Neurobiol. Dis. *82*, 540–551.

Vogt, B.A., Vogt, L.J., Vrana, K.E., Gioia, L., Meadows, R.S., Challa, V.R., Hof, P.R., and Van Hoesen, G.W. (1998). Multivariate Analysis of Laminar Patterns of Neurodegeneration in Posterior Cingulate Cortex in Alzheimer's Disease. Exp. Neurol. *153*, 8–22.

Vuono, R., Winder-Rhodes, S., de Silva, R., Cisbani, G., Drouin-Ouellet, J., REGISTRY Investigators of the European Huntington's Disease Network, Spillantini, M.G., Cicchetti, F., and Barker, R.A. (2015). The role of tau in the pathological process and clinical expression of Huntington's disease. Brain J. Neurol. *138*, 1907–1918.

Wagshal, D., Sankaranarayanan, S., Guss, V., Hall, T., Berisha, F., Lobach, I., Karydas, A., Voltarelli, L., Scherling, C., Heuer, H., et al. (2015). Divergent CSF τ alterations in two common tauopathies: Alzheimer's disease and progressive supranuclear palsy. J. Neurol. Neurosurg. Psychiatry *86*, 244–250.

Wang, Y., and Mandelkow, E. (2016). Tau in physiology and pathology. Nat. Rev. Neurosci. *17*, 22–35.

Wang, Y., Martinez-Vicente, M., Krüger, U., Kaushik, S., Wong, E., Mandelkow, E.-M., Cuervo, A.M., and Mandelkow, E. (2009). Tau fragmentation, aggregation and clearance: the dual role of lysosomal processing. Hum. Mol. Genet. *18*, 4153–4170.

Wang, Y.P., Biernat, J., Pickhardt, M., Mandelkow, E., and Mandelkow, E.-M. (2007). Stepwise proteolysis liberates tau fragments that nucleate the Alzheimer-like aggregation of full-length tau in a neuronal cell model. Proc. Natl. Acad. Sci. *104*, 10252–10257.

Wegmann, S., Maury, E.A., Kirk, M.J., Saqran, L., Roe, A., DeVos, S.L., Nicholls, S., Fan, Z., Takeda, S., Cagsal-Getkin, O., et al. (2015). Removing endogenous tau does not prevent tau propagation yet reduces its neurotoxicity. EMBO J.

Weingarten, M.D., Lockwood, A.H., Hwo, S.Y., and Kirschner, M.W. (1975). A protein factor essential for microtubule assembly. Proc. Natl. Acad. Sci. *72*, 1858–1862.

Weller, R.O. (2008). Greenfield's Neuropathology (8th Edition). Neuropathol. Appl. Neurobiol. *34*, 573–574.

Wischik, C.M., Novak, M., Thøgersen, H.C., Edwards, P.C., Runswick, M.J., Jakes, R., Walker, J.E., Milstein, C., Roth, M., and Klug, A. (1988). Isolation of a fragment of tau derived from the core of the paired helical filament of Alzheimer disease. Proc. Natl. Acad. Sci. U. S. A. *85*, 4506–4510.

Yamada, K., Cirrito, J.R., Stewart, F.R., Jiang, H., Finn, M.B., Holmes, B.B., Binder, L.I., Mandelkow, E.-M., Diamond, M.I., Lee, V.M.-Y., et al. (2011). In Vivo Microdialysis Reveals Age-Dependent Decrease of Brain Interstitial Fluid Tau Levels in P301S Human Tau Transgenic Mice. J. Neurosci. *31*, 13110–13117.

Yamada, K., Patel, T.K., Hochgräfe, K., Mahan, T.E., Jiang, H., Stewart, F.R., Mandelkow, E.-M., and Holtzman, D.M. (2015). Analysis of in vivo turnover of tau in a mouse model of tauopathy. Mol. Neurodegener. *10*, 55.

Yoshida, M. (2006). Cellular tau pathology and immunohistochemical study of tau isoforms in sporadic tauopathies. Neuropathology *26*, 457–470.

Yoshiyama, Y., Higuchi, M., Zhang, B., Huang, S.-M., Iwata, N., Saido, T.C., Maeda, J., Suhara, T., Trojanowski, J.Q., and Lee, V.M.-Y. (2007). Synapse Loss and Microglial Activation Precede Tangles in a P301S Tauopathy Mouse Model. Neuron *53*, 337–351.

Zempel, H., Thies, E., Mandelkow, E., and Mandelkow, E.-M. (2010). Aβ Oligomers Cause Localized Ca2+ Elevation, Missorting of Endogenous Tau into Dendrites, Tau Phosphorylation, and Destruction of Microtubules and Spines. J. Neurosci. *30*, 11938–11950.

Zhang, Z., Song, M., Liu, X., Kang, S.S., Kwon, I.-S., Duong, D.M., Seyfried, N.T., Hu, W.T., Liu, Z., Wang, J.-Z., et al. (2014). Cleavage of tau by asparagine endopeptidase mediates the neurofibrillary pathology in Alzheimer's disease. Nat. Med. *20*, 1254–1262.

Zilka, N., Filipcik, P., Koson, P., Fialova, L., Skrabana, R., Zilkova, M., Rolkova, G., Kontsekova, E., and Novak, M. (2006). Truncated tau from sporadic Alzheimer's disease suffices to drive neurofibrillary degeneration in vivo. FEBS Lett. *580*, 3582–3588.

Zilka, N., Korenova, M., Kovacech, B., Iqbal, K., and Novak, M. (2010). CSF phospho-tau correlates with behavioural decline and brain insoluble phospho-tau levels in a rat model of tauopathy. Acta Neuropathol. (Berl.) *119*, 679–687.

Zilka, N., Kazmerova, Z., Jadhav, S., Neradil, P., Madari, A., Obetkova, D., Bugos, O., and Novak, M. (2012). Who fans the flames of Alzheimer's disease brains? Misfolded tau on the crossroad of neurodegenerative and inflammatory pathways. J. Neuroinflammation *9*, 47.

RESUME SUBSTANTIEL EN FRANCAIS

Introduction

Tau est une protéine associée aux microtubules (MT) qui exerce de nombreuses fonctions au sein du neurone, ces différentes fonctions faisant de la protéine Tau un facteur important pour la survie neuronale. Celles-ci sont finement régulées par différents facteurs tels que l'épissage alternatif de Tau (et l'expression de différents isoformes ; Kosik et al., 1989a), sa localisation subcellulaire (Binder et al., 1985), ainsi que de nombreuses modifications post-traductionnelles, à commencer par la phosphorylation (Kanemaru et al., 1992). Ceci revêt une importance cruciale durant le développement post-natal, une période où Tau joue un rôle majeur dans la formation de la polarité axonale (Caceres and Kosik, 1990), mais aussi à l'âge adulte via son impact sur la morphologie cellulaire et le transport axonal (Dixit et al., 2008). Des dérégulations de la phosphorylation de Tau (Grundke-Iqbal et al., 1986) ou dans le rapport d'expression des isoformes (Hutton et al., 1998) peuvent donc avoir un impact significatif sur la survie neuronale. C'est le cas dans une grande famille de maladies, appelées tauopathies, où des dysfonctionnements de Tau sont associés à une neurodégénérescence.

Les tauopathies sont caractérisées par l'agrégation pathologique de la protéine Tau dans le soma des cellules neuronales et gliales, associée à une neurodégénérescence et menant à des déficiences cognitives. Cette classe de pathologies, bien que présentant de nombreuses similitudes, est phénotypiquement très hétérogène. Il est donc difficile de déterminer quels mécanismes peuvent être responsables de la neurodégénérescence associée à Tau. En effet, alors que la pathologie Tau semble n'être qu'un effecteur en aval de la pathologie Aβ dans la maladie d'Alzheimer (MA ; Hardy et Higgins, 1992), le fait que les cas familiaux de démence frontotemporale avec parkinsonisme liée au chromosome 17 (FTDP-17) soient associés à des mutations dans le gène codant pour Tau (MAPT ; Hong et al., 1998, Swieten et al., 2007), suggère que Tau joue lui-même un rôle actif dans la dégénérescence. Le large spectre de présentation clinique observé dans les tauopathies pose la question de savoir quel mécanisme sous-tend l'implication de régions cérébrales et de populations de cellules spécifiques dans différentes tauopathies. De plus, bien que l'agrégation d'isoformes spécifiques puisse conduire à des phénotypes remarquablement différents (c'est-à-dire tauopathies 3R opposées aux tauopathies 4R), une forte hétérogénéité peut également être trouvée dans le même trouble (FTDP-17 qui peut être associée à l'agrégation d'isoformes 3R, 4R ou de tous les isoformes de Tau, Sergeant et al., 2005). Enfin, bien qu'une seule mutation puisse conduire à plusieurs troubles (Bugiani et al., 1999), les cas sporadiques et familiaux sont souvent indiscernables cliniquement au sein d'une seule tauopathie. En d'autres termes, bien que la séquence d'agrégation de Tau depuis le dimère jusqu'à l'accumulation de fibrilles (PHFs) constitutives des dégénérescences neurofibrillaires (DNFs), en passant par des espèces oligomériques solubles, est maintenant bien caractérisée, peu de choses sont connues à ce jour sur le lien entre l'agrégation de Tau et sa toxicité.

Depuis la découverte que la progression spatiale de la pathologie de Tau est associée à une aggravation des symptômes dans la MA (Braak et Braak, 1991), il a été suggéré que la formation des DNFs joue un rôle actif dans la neurodégénérescence. En effet, plusieurs études ont trouvé une forte corrélation entre le nombre de DNFs et la perte neuronale ainsi que le score clinique, ce qui suggère que la neurodégénérescence liée aux DNFs joue un rôle important dans le déclin cognitif chez les patients (Dickson et al., 1995; Giannakopoulos et al. ., 2003). Les neurones porteurs de DNF présentent

également une forte diminution de plusieurs marqueurs pré- et post-synaptiques par rapport aux neurones voisins, ce qui implique que la transmission synaptique est altérée (Callahan et al., 1999).

Cette vue classique des DNFs comme étant la principale espèce toxique de Tau est cependant fortement remise en question. En effet, une dissociation spatiale a été observée entre la formation de DNFs et la neurodégénérescence dans le cerveau des patients atteints de la MA (Vogt et al., 1998) ainsi que dans des modèles de souris transgéniques (Spiers et al., 2006). De plus, bien que le nombre de DNFs soit corrélé à la neurodégénérescence, il a été démontré que la quantité de perte neuronale dépasse fortement le nombre de neurones présentant des DNFs (Gómez-Isla et al., 1997, Vogt et al., 1998) suggérant que les neurones meurent via un autre mécanisme. Ainsi, la formation de DNFs ne semble pas nécessaire ni suffisante pour que la perte neuronale se produise. Au contraire, les neurones semblent pouvoir vivre pendant des décennies après que Tau ait commencé à s'accumuler dans le soma (Morsch et al., 1999), être complètement intégrés dans les réseaux neuronaux, et sembleraient même plus fonctionnels que ceux contenant uniquement de la protéine Tau soluble (Fox et al., 2011).

Il a ensuite été suggéré que les espèces solubles de Tau pourraient être responsables de la toxicité. En effet, seule la protéine Tau hyperphosphorylée soluble, mais pas celle agrégée en PHFs, est capable de séquestrer la protéine normale, conduisant à une inhibition de l'assemblage des MT (Alonso et al., 2006). Dans un modèle utilisant le transfert de gène de la protéine Tau mutée, médié par des virus adéno-associés (AAV), une forte perte neuronale est observée dans l'hippocampe en l'absence de gros agrégats de Tau (Jaworski et al., 2009). D'autres preuves de l'implication d'espèces toxiques solubles de Tau proviennent de l'étude de modèles de souris inductibles. En effet, dans le modèle rTg4510, la suppression du transgène Tau est capable d'arrêter la neurodégénérescence, de restaurer la plasticité synaptique (Fox et al., 2011) et de conduire à la récupération comportementale alors que les DNFs continuent de se former (SantaCruz et al., 2005). De façon intéressante, la suppression prolongée du transgène entraîne une augmentation de la formation de DNFs, ce qui suggère que ceux-ci peuvent représenter une forme stable moins nocive, utilisée par la cellule pour piéger des espèces solubles toxiques. Le travail d'une équipe différente, utilisant des souris exprimant conditionnellement des formes mutantes de Tau aux propriétés pro-agrégeantes, a donné des résultats similaires. Dans ces modèles, les performances cognitives et les marqueurs synaptiques sont restaurés après la suppression du transgène, tandis que les gros agrégats positifs pour la coloration Gallyas sont toujours observés jusqu'à 4 mois après le traitement par la doxycycline (Sydow et al., 2011a). Il est intéressant de noter cependant que la composition de ces agrégats semble très dynamique, car contenant uniquement la Tau murine après suppression du transgène (Sydow et al., 2011b). Cela pourrait servir de preuve que les DNFs servent effectivement de piège pour des espèces solubles toxiques.

La première preuve de la toxicité des oligomères de Tau provient d'études anatomo-pathologiques dans lesquelles des oligomères de Tau, composés de Tau phosphorylé, ont été observés dans le cerveau de patients atteints de MA (Lasagna-Reeves et al., 2012a, Patterson et al., 2011). Ces oligomères peuvent être observés dans le cortex frontal des patients atteints de la MA, même à des stades où les DNFs ne sont pas encore présents dans cette région (Maeda et al., 2006). Ceci suggère que la formation des oligomères de Tau précède l'apparition des DNFs, les impliquant en amont dans la cascade pathologique. Ceci est cohérent avec la découverte récente selon laquelle une mutation non causative du gène MAPT, qui augmente la formation d'oligomères, est associée à un risque accru de développer une MA (Coppola et al., 2012). Après injection dans des souris sauvage, les oligomères de Tau sont les seules espèces capables d'induire une grande variété de défauts cellulaires, incluant la réduction des marqueurs synaptiques et mitochondriaux, l'activation des caspases et la perte neuronale, conduisant à des déficits cognitifs (Lasagna -Reeves et al., 2011, 2012b), ces effets pouvant être observés dans une

autre étude avant l'apparition des DNFs (Fá et al., 2016). Ceci confirme que les oligomères exercent une toxicité directe indépendamment de la présence des DNFs.

Bien qu'un grand nombre de preuves pointent vers les formes oligomèriques solubles comme principaux contributeurs de la toxicité induite par Tau, il reste que la formation de DNFs peut ne pas être totalement bénigne. L'observation de «DNFs fantômes », caractérisés par une rupture de la membrane cellulaire, dans le cerveau des patients (Bancher et al., 1989) suggère que l'agrégation somatique de Tau sous la forme de PHF peut tout de même avoir des effets indésirables. Les neurones contenant des DNFs présentent bien souvent des anomalies structurelles (Andorfer et al., 2005). Cela suggère un nouveau modèle dans lequel les espèces solubles seraient responsables de la toxicité aiguë. La formation de DNFs représenterait dans ce cas un mécanisme de défense mis en place par la cellule pour piéger des espèces solubles toxiques. L'accumulation de matériel fibrillaire aurait à son tour des effets indésirables, conduisant à une mort neuronale lente. De plus, des données récentes suggèrent que les DNFs ne sont pas totalement inertes mais subissent plutôt des événements de fusion et de fission et sont en échange constant avec des agrégats solubles (Guo et al., 2016). La toxicité à long terme de ces grandes espèces pourrait ainsi être liée à la production continue de formes solubles toxiques.

La notion de souches de type prion a été développée récemment afin d'expliquer la diversité phénotypique observée dans les tauopathies. Cette théorie suggère que les différences dans la conformation des agrégats de Tau peuvent sous-tendre des différences dans la capacité à déclencher des mécanismes toxiques responsables des phénotypes spécifiques observés dans les tauopathies, notamment le type cellulaire affecté (Clavaguera et al., 2013; Sanders et al., 2014). Il reste à déterminer si ces différences peuvent être dues à des morphologies différentes des agrégats de Tau ou si elles sont la conséquence d'une production différentielle d'espèces solubles par rapport aux espèces insolubles. L'utilisation d'outils polyvalents permettant le développement de modèles récapitulant des caractéristiques spécifiques de la pathologie Tau devrait nous aider à résoudre la question des points communs dans les processus pathologiques sous-jacents aux tauopathies, mais aussi nous permettre de déterminer ce qui les distingue.

À ce jour, un large choix de modèles de tauopathies chez le rongeur est disponible, ce qui a déjà permis une meilleure compréhension des mécanismes pathologiques associés à la neurodégénérescence induite par Tau. Chacun d'entre eux présente cependant ses avantages et inconvénients spécifiques et l'utilisation d'un modèle en particulier doit donc être guidée par le type de question à laquelle répondre. Par conséquent, bien que les modèles transgéniques constitutifs "classiques" puissent être d'une grande utilité pour l'étude des processus à long terme sous-jacents à la pathologie de Tau, le développement plus récent de modèles inductibles a permis une meilleure compréhension du lien entre Tau soluble, toxicité et agrégation (Hochgräfe et Al., 2013; SantaCruz et al., 2005). Cependant, la comparaison directe de plusieurs modèles transgéniques peut être entravée par la variabilité phénotypique induite par l'emplacement de l'insertion du transgène (Schindowski et al., 2006).

Des approches alternatives ont donc été développées au cours des années afin d'étudier les points communs et les différences entre les tauopathies. Par exemple, l'injection d'agrégats Tau dérivés de cerveau de patients a été utilisée pour déterminer si ceux-ci reproduisaient la variabilité phénotypique observée chez les patients atteints de tauopathie (Clavaguera et al., 2013). De même, l'injection d'agrégats de Tau de différents ordres a confirmé le rôle pathogène des oligomères solubles par rapport aux espèces fibrillaires (Lasagna-Reeves et al., 2011). Plus récemment, le développement de modèles de tauopathie à l'aide de vecteurs viraux a également permis d'étudier des questions qui auraient été difficiles à aborder avec d'autres approches. Ainsi, l'injection de vecteurs lentiviraux codant pour la

protéine Tau sauvage ou portant la mutation P301L a permis une comparaison directe de la pathologie dans des modèles de pathologie Tau sporadique et génétique (Caillierez et al., 2013).

Objectifs de la thèse

Le terme tauopathie désigne une grande famille de maladies neurodégénératives caractérisées par l'agrégation de la protéine Tau à l'intérieur du cerveau. Malgré cette caractéristique commune, les tauopathies présentent une grande diversité, que ce soit par le type cellulaire affecté ou les régions du cerveau impliquées, conduisant à des déficits cognitifs spécifiques. Plusieurs mécanismes de toxicité de Tau ont été proposés qui peuvent être liés à la grande contribution de Tau à différentes fonctions neuronales. L'identification de ces différents effets toxiques de Tau a toutefois été principalement effectuée chez des animaux transgéniques exprimant la protéine mutante. Il reste à établir si des mécanismes similaires se produisent également dans les tauopathies sporadiques. Compte tenu de ces questions, le développement de thérapies gagnerait à l'étude des tauopathies dans leur ensemble et à l'identification des points communs et des différences dans les mécanismes qui sous-tendent la neurodégénérescence associée au Tau. Plus précisément, une question qui reste à aborder est de savoir si les mécanismes qui lient l'agrégation de Tau à sa toxicité sont différents dans les tauopathies génétiques et sporadiques. À cet égard, le développement de modèles animaux permettant la comparaison directe des déficits associés à Tau sous-tendant diverses tauopathies serait d'une grande utilité. Par conséquent, le premier objectif de ce projet était de développer des modèles rongeurs de tauopathies sporadiques et génétiques par transfert de gène de la protéine Tau humaine à l'aide de vecteurs AAV. L'utilisation de vecteurs viraux, par sa polyvalence, permet la comparaison directe de différents modèles. Le développement de ces modèles chez les rats a également permis une approche multimodale avec l'étude de biomarqueurs périphériques qui ne sont pas facilement accessibles chez la souris, tels que les niveaux de Tau dans le LCR.

Nous avons également cherché à étudier le lien entre l'agrégation de Tau et sa toxicité et la façon dont celles-ci peuvent se rapporter aux déficiences cognitives. Nous avons donc choisi d'injecter ces différents vecteurs dans une structure cérébrale commune (l'hippocampe) afin de déterminer comment différents types de pathologie Tau peuvent être associés à la détérioration d'une fonction donnée. A cet égard, nos modèles n'ont donc pas été développés pour tenter de récapituler le spectre complet d'une tauopathie donnée, mais afin de servir d'outils pour l'étude différentielle des effets pathogènes de l'agrégation de Tau dans les tauopathies sporadiques et génétiques en général. L'utilisation de différents vecteurs pour sur-exprimer la protéine Tau sauvage ($hTAU^{WT}$), mutante ($hTAU^{P301L}$) ou pro-agrégeante ($hTAU^{ProAggr}$) dans nos modèles nous a permis d'aborder ces différentes questions.

Résultats & Discussion

L'objectif principal de ce projet était donc de développer plusieurs modèles de tauopathie pure chez le rongeur. Dans ce but, nous avons choisi d'utiliser le transfert de gènes de la protéine Tau humaine médié par des vecteurs AAV pour induire une tauopathie chez le rat adulte, une espèce plus pratique pour l'imagerie cérébrale et l'analyse des biomarqueurs que les souris. L'expression de la protéine Tau humaine conduit au développement rapide d'une tauopathie à partir d'un mois après l'injection, chaque construction récapitulant des caractéristiques spécifiques de la pathologie Tau, associée à une implication différente de la neuroinflammation.

Caractérisation de la pathologie induite par la protéine Tau sauvage

Le transfert de gène de la protéine Tau sauvage ($hTAU^{WT}$) conduit à l'induction d'une tauopathie au stade précoce, rappelant ce qui est observé dans les modèles transgéniques. En effet, la surexpression dans le groupe $hTAU^{WT}$ a conduit à une hyperphosphorylation forte de la protéine (visualisée avec l'anticorps AT8) mais avec une agrégation très limitée (marqueurs AT100 et Gallyas). Ceci est cohérent avec ce qui a été observé dans la plupart des modèles transgéniques où la surexpression de Tau sauvage conduit à une pathologie Tau précoce avec une hyperphosphorylation de Tau mais seulement une faible formation de DNFs (Andorfer et al., 2003 ; Spittaels et al., 1999). Cependant, la pathologie Tau dans ces modèles était associée à une neurodégénérescence très limitée, ce qui contraste fortement avec notre découverte d'une perte neuronale drastique après l'expression de $hTAU^{WT}$. En effet, une perte de 25% des neurones du CA1 est observée dans ce modèle dès 1 mois post-injection, mesurée par comptage stéréologique sur le marquage NeuN. La forte neurotoxicité de $hTAU^{WT}$ observée dans notre étude en l'absence d'agrégation significative pourrait être liée à son effet inhibiteur sur la fonction de la protéine endogène. En effet, des études in vitro ont démontré que la protéine Tau hyperphosphorylé soluble est capable d'inhiber l'assemblage MT par séquestration de la protéine normale et que cet effet inhibiteur est perdu lors de la polymérisation (Alonso et al., 2006).

De façon surprenante, malgré la forte toxicité exercée par $hTAU^{WT,}$ aucune altération cognitive significative n'a pu être observée chez ces animaux. Ceci est à nouveau fortement en contraste avec ce qui a été observé chez les animaux transgéniques où même une faible pathologie Tau pouvait induire des déficiences cognitives (Andorfer et al., 2003) ou locomotrices (Probst et al., 2000, Spittaels et al., 1999) importantes, avant ou en l'absence de neurodégénérescence. Plusieurs raisons peuvent expliquer ces différences. Tout d'abord, cela peut être lié à la restriction spatiale de la pathologie Tau dans les modèles basés sur l'injection de vecteurs viraux. Bien que cette hypothèse puisse expliquer nos résultats, le fait qu'une pathologie Tau induite par transfert de gêne dans la substance noire soit associée à des déficits moteurs (Klein et al., 2005) suggère que cette approche peut conduire à des impacts fonctionnels. L'absence de déficits cognitifs dans notre modèle pourrait être associée à la perte sélective des neurones exprimant le transgène. En effet, la quantification de l'ARNm du transgène par RT-qPCR montre une forte réduction dans ce groupe par rapport aux deux autres constructions. Les déficits comportementaux peuvent être associés soit à une neurodégénération soit à une altération de la fonction neuronale/synaptique par des espèces Tau pathologiques. Cette dernière hypothèse est étayée par des données obtenues dans le modèle transgénique rTg4510, où la suppression du transgène est associée à la restauration des fonctions cognitifs, même aux stades où une forte perte neuronale a déjà eu lieu (SantaCruz et al., 2005). Cela suggère que l'altération de la fonction cognitive pourrait être associée plus à l'expression de protéines pathogènes qu'à la neurodégénérescence en soi. Ainsi, l'absence de déficits cognitifs dans notre modèle peut être liée au fait que les neurones exprimant le Tau pathologique ont disparu, les autres neurones pouvant compenser cette perte.

Caractérisation de la pathologie induite par des formes mutées de la protéine

Contrairement à la pathologie Tau limitée observée dans le groupe hTAU^{WT}, la co-expression de Tau sauvage avec le peptide pro-agrégeant TauRD-ΔK280 dans le groupe hTAU^{ProAggr} potentialise fortement son agrégation. Ceci est cohérent avec les fortes propriétés pro-agrégation de la mutation ΔK280 (Barghorn et al., 2000, Von Bergen et al., 2001). Cela peut également être lié aux propriétés amyloïdogéniques accrues des formes tronquées de Tau (Barghorn et al., 2000, Gamblin et al., 2003) dues à l'élimination de l'activité inhibitrice des régions C-terminale et N-terminale de Tau. Cela rappelle également ce qui est observé dans les modèles transgéniques exprimant cette construction TauRD-ΔK280, où une forte agrégation est observée sous la forme de lésions de type DNF positives pour la coloration Gallyas à partir de l'âge de 3 mois (Mocanu et al., 2008). De façon intéressante, une agrégation plus forte dans les modèles transgéniques ΔK280 est associée à l'aggravation de l'atteinte fonctionnelle (Decker et al., 2015, Sydow et al., 2011a, Van der Jeugd et al., 2012). Ceci est fortement en contraste avec nos résultats montrant qu'une agrégation plus forte dans le hTAU^{ProAggr} est associée à des effets neuroprotecteurs.

Plusieurs raisons pourraient expliquer l'écart de nos résultats par rapport aux modèles transgéniques. Premièrement, une caractéristique clé des souris transgéniques est le recrutement de la protéine murine endogène dans les agrégats. La neurodégénérescence chez la souris peut donc se produire par une perte de fonction toxique de la protéine endogène qui, une fois agrégée, ne pourrait plus favoriser la stabilisation des MT (Fischer et al., 2009; Tepper et al., 2014). L'effet de la construction hTAU^{ProAggr} sur la protéine Tau endogène n'a pas été évalué au cours de notre étude. Cependant, une explication possible de l'effet neuroprotecteur robuste de hTAU^{ProAggr} peut être que le peptide TauRD-ΔK280 potentialise fortement l'agrégation de la Tau humaine sauvage au lieu de la protéine murine. L'agrégation promue de hTAU^{WT} protégerait de sa toxicité. Dans le même temps, le peptide TauRD-ΔK280 étant piégé dans des agrégats, il ne pourrait pas exercer sa fonction inhibitrice sur la protéine endogène. En d'autres termes, alors que hTAU^{WT} et TauRD-ΔK280 sont toxiques individuellement, ils se neutralisent mutuellement lorsqu'ils sont présents dans la même cellule. D'autres études devraient être réalisées pour étudier cette hypothèse, notamment en évaluant l'effet de la surexpression du peptide TauRD-ΔK280 seul chez le rat sur la protéine endogène.

La pathologie développée dans le groupe hTAU^{P301L} semble représenter un phénotype intermédiaire entre hTAU^{WT} et hTAU^{ProAggr}. En effet, conformément à ses propriétés amyloïdogènes (Hong et al., 1998), la mutation P301L est associée à une agrégation plus forte que dans le groupe hTAU^{WT}. Cependant, les agrégats dans le groupe hTAU^{P301L} semblent moins matures qu'avec la construction hTAU^{ProAggr}. En effet, alors qu'un nombre similaire de somas AT100-positif est observé dans les deux groupes, moins de lésions de type DNF (positifs pour la coloration Gallyas) sont observées dans le groupe hTAU^{P301L} Cela suggère que la plupart des agrégats dans ce groupe sont sous une forme non fibrillaire soluble. La pathologie Tau dans ce groupe est associée à une neurodégénérescence qui progresse dans le temps jusqu'à atteindre une perte de 40% des neurones du CA1. Ceci est cohérent avec ce qui est observé chez les animaux transgéniques exprimant différents mutants de Tau, où les déficits cognitifs et les altérations neuronales et synaptiques se produisent habituellement avant l'apparition de structures argyrophiles de type DNF (Maurin et al., 2014, Odda et al. 2005, Schindowski et al., 2006, Terwel et al., 2005).

Caractérisation de la relation entre l'agrégation de Tau et sa toxicité

Un résultat frappant de notre étude est la relation négative observée entre le degré d'agrégation de Tau et sa toxicité. En effet, bien que l'expression de Tau sauvage dans le groupe hTAU^{WT} conduit à une hyperphosphorylation forte mais sans agrégation significative, sa co-expression avec le peptide pro-agrégation TauRD-ΔK280 chez les animaux hTAU^{ProAggr} potentialise fortement son agrégation, avec la formation de nombreux DNFs dès 1 mois après l'injection. Ceci est associé à une neuroprotection contre la forte toxicité exercée par hTAU^{WT} seul. Ceci est en accord avec plusieurs études qui ont identifié les DNFs comme relativement inoffensifs ou même protecteurs. En effet, non seulement l'accumulation de Tau peut être trouvée dans les neurones morphologiquement normaux (Andorfer et al., 2005, van de Nes et al., 2008; Rocher et al., 2010), mais ces neurones peuvent vivre pendant des décennies après que l'agrégation somatique de Tau ai commencé (Morsch et al., 1999). Ceux-ci peuvent être totalement intégrés dans les réseaux neuronaux et être encore plus fonctionnels que les cellules contenant uniquement des agrégats solubles de Tau (Fox et al., 2011; Kuchibhotla et al., 2014, Rudinskiy et al., 2014). Notre observation d'une forte réactivité au Gallyas dans les animaux hTAU^{ProAggr} suggère que la formation de DNFs peut représenter un mécanisme protecteur permettant aux neurones d'échapper à la neurodégénérescence aiguë (de Calignon et al., 2010; Spires-Jones et al., 2008).

Étonnamment, une forte divergence est observée dans notre étude entre les résultats histologiques et biochimiques, aucune fibrille sarkosyl-insoluble ne pouvant être détectée par western-blot. Ceci est associé à une réduction du niveau de protéine Tau humaine par rapport aux deux autres constructions qui ne peut être expliquées par des différences dans l'expression du transgène. Ces observations nous ont amené à faire l'hypothèse que la taille et la nature structurelle des agrégats de Tau dans le groupe hTAU^{ProAggr} peuvent avoir empêché leur détection dans des conditions de dénaturation classiques, expliquant ainsi les différences entre les résultats histologiques et biochimiques. Il est intéressant de noter qu'une autre classe d'agrégats de Tau a récemment été identifiée, appelés oligomères granulaires de Tau (GTO), qui présentent des propriétés biochimiques très similaires (Maeda et al., 2007 ; Cowan et Mudher, 2013). L'accumulation de ces GTO est associée à une neuroprotection chez la Drosophile. Dans une étude, l'agrégation induite de Tau en grands agrégats rappelant les GTO est associée à une amélioration de la cognition et à une neurodégénérescence stoppée (Ali et al., 2012). De même, dans une autre étude, la restauration des fonctions locomotrices et du transport axonal observé après traitement par des inhibiteurs de GSK3-β est associé à la formation de structures de type GTO (Cowan et al., 2015). Ceci peut suggérer que l'effet neuroprotecteur observé dans notre modèle hTAU^{ProAggr} peut être associé à la formation de tels agrégats de type GTO. Des études ultra-structurales de la morphologie des agrégats de Tau induites par la construction de hTAU^{ProAggr} devraient nous permettre de confirmer cette hypothèse en identifiant quel type d'agrégat.

Des anomalies morphologiques rares ont toutefois été observées dans le groupe hTAU^{ProAggr} par microscopie électronique à 2 mois post-injection, ce qui suggère que l'accumulation de gros agrégats insolubles peut ne pas être entièrement bénigne. Ceci est cohérent avec l'hypothèse actuelle selon laquelle la formation initialement neuroprotectrice de DNFs peut, à plus long terme, induire une mort neuronale lente. En effet, plusieurs études ont révélé une forte diminution de plusieurs marqueurs pré- et post-synaptiques dans les neurones porteurs de DNF par rapport aux neurones voisins, ce qui implique que la transmission synaptique peut être altérée (Callahan et al., 1999; ., 2000), probablement par le séquestration de composants cellulaires essentiels dans des agrégats de Tau (Wang et Mandelkow, 2016). De plus, une récente étude in vitro a démontré que les inclusions de Tau sont des structures dynamiques, subissant constamment des événements de fission et de fusion (Guo et al., 2016). Ainsi, la toxicité à long terme des NFT apparemment inertes pourrait également être associée à la libération

continue d'agrégats solubles. Caractériser l'évolution de la pathologie à plus long terme devrait nous permettre de déterminer si une toxicité accrue peut être observée au bout de 3 mois après l'injection et si cela peut entraîner des conséquences fonctionnelles. En effet, aucune dégradation comportementale n'a pu être observée dans notre modèle à 1,5 mois après l'injection, ce qui confirme que la pathologie à ce moment-là était encore à un stade précoce. Mais cela n'empêche pas la possibilité que des déficits fonctionnels se produisent à un stade ultérieur.

Identification de l'espèce toxique dans les groupes hTAU^{WT} et hTAU^{P301L}

Une forte neurotoxicité est observée après la surexpression de hTAU^{WT} et hTAU^{P301L}, dès 1 mois après l'injection. Ceux-ci, cependant, présentent de fortes différences dans la pathologie Tau associée, suggérant qu'ils peuvent différer par le type d'espèce toxique de Tau. En effet, bien que tous deux présentent une forte hyperphosphorylation de Tau, une agrégation significative n'est observée que dans le groupe hTAU^{P301L} principalement sous la forme d'agrégats non fibrillaires. Ceci est en accord avec un nombre croissant d'études suggérant que les oligomères de Tau représenteraient le principal contributeur de la neurodégénérescence induite par Tau. L'injection d'oligomères de Tau dans des souris sauvages induit une grande variété de défauts cellulaires, incluant une diminution des marqueurs synaptiques et mitochondriaux, l'activation des caspases et la perte neuronale et conduisant à des déficits cognitifs (Lasagna-Reeves et al. Al., 2011, 2012b). Ces effets apparaissent avant la formation de DNFs (Fá et al., 2016), ce qui suggère que les oligomères exercent une toxicité directe indépendamment de la présence de DNF. La quantité de formes oligomères dans les souris rTg4510, est étroitement corrélée avec les performances cognitives chez ces animaux (Berger et al., 2007).

Pour étudier la possibilité que la surexpression de hTAU^{P301L} génère des espèces oligomèriques toxiques, une analyse par dot blot a été réalisée en utilisant l'anticorps T22, décrit comme se liant spécifiquement aux oligomères de Tau in vitro et dans le cerveau de patients atteints de la MA (Lasagna-Reeves et al., 2012a). Aucune différence significative entre les groupes n'a pu être observée dans notre étude. Cependant, le fort marquage de fond observé même chez les animaux témoins suggère que l'analyse effectuée sur des homogénats complets peut avoir empêché la détection d'oligomères. Une analyse similaire sur les différentes fractions obtenues lors de l'extraction au sarkosyl devrait permettre une meilleure détection des espèces solubles. Des mesures plus précises, par exemple par spectrométrie de masse, pourrait aussi nous permettre de mieux quantifier la quantité d'oligomères dans nos différents modèles mais aussi de déterminer si différents degrés d'oligomérisation pourrait être associés à la toxicité de hTAU^{WT} et hTAU^{P301L}.

En effet, un résultat surprenant de notre étude est la découverte que la surexpression de Tau sauvage conduit à une neurotoxicité forte en l'absence d'agrégation notable. Ceci peut être interprété comme une preuve du fait que la toxicité du Tau humain hyperphosphorylé soluble peut se produire sans qu'il soit nécessaire de l'agréger. D'autres ont également démontré une toxicité de la surexpression de Tau humaine en l'absence d'agrégation dans un modèle de tauopathie pure en utilisant un transfert de gêne médié par AAV de Tau sauvage dans l'hippocampe de souris (Jaworski et al., 2009). Cependant, l'absence de positivité AT100 ne signifie pas nécessairement que hTAU^{WT} était totalement incapable d'agréger. En effet, une faible quantité de fibrilles sarkosyl-insolubles a été observé dans ce groupe suggérant que Tau sauvage est effectivement capable d'agrégation, conformément aux résultats antérieurs dans différents modèles (Andorfer et al., 2005; Caillierez et al., 2013). La vue classique de la séquence d'agrégation de Tau commence par l'hyperphosphorylation à un certain nombre d'épitopes pathologiques, induisant ensuite l'agrégation. Cependant, un certain nombre de données suggère que la relation entre l'hyperphosphorylation et l'agrégation peut ne pas être aussi simple. En effet, certains sites de phosphorylation, connus pour induire un détachement de Tau du MT, s'avèrent inhiber l'agrégation

(Schneider et al., 1999). Inversement, l'agrégation en oligomères peut se produire avant la phosphorylation à certains sites pathologiques, y compris l'épitope AT8 (Lasagna-Reeves et al., 2012a). Il est donc possible que la toxicité de hTAU^{WT} soit due à l'accumulation d'espèces oligomèriques qui se sont formées avant la phosphorylation aux sites AT8 et qui ne présentent pas de réactivité AT100.

Les différences entre les constructions dans l'étendue de la pathologie Tau et la neurotoxicité associée peuvent donc être expliquées par des différences dans l'équilibre entre les agrégats solubles et insolubles de Tau. En effet, l'agrégation de Tau suit une progression stéréotypée à partir de monomères solubles en fibrilles via des dimères et des espèces oligomériques (Patterson et al., 2011; Sahara et al., 2007). Mais ce processus peut ne pas être irréversible et il peut y avoir un échange constant entre ces différentes espèces (Guo et al., 2016; Hochgräfe et al., 2013). La variabilité phénotypique observée dans nos modèles pourrait donc être expliquée par un déséquilibre vis-à-vis de l'une de ces espèces. Par conséquent, la construction hTAU^{WT} produirait principalement des petits oligomères solubles qui agiraient soit par une perte de fonction, soit par un gain de fonction toxique. La mutation P301L pousserait un peu plus vers l'agrégation, ce qui est cohérent avec ses propriétés décrites (Hong et al., 1998). Ceci conduirait à la production d'espèces oligomèriques, qui peuvent être de nature différente de celles observées chez les animaux de hTAU^{WT} et capables de s'agréger en fibrilles, retardant ainsi sa toxicité. La surexpression de hTAU^{ProAggr}, d'autre part, déplacerait fortement l'équilibre vers la production d'agrégats fortement insolubles (GTO ou DNF) menant à une forte neuroprotection, ces gros agrégats pouvant à terme affecter la fonction neuronale.

Implication de la neuro-inflammation dans la tauopathie

La pathologie Tau est couramment associée à une neuroinflammation dans la MA et d'autres tauopathies (Ishizawa et Dickson, 2001; Sheng et al., 1997). En outre, une corrélation est souvent observée entre l'étendue de la pathologie Tau et la réactivité gliale, ce qui suggère qu'elle peut jouer un rôle dans le processus de dégénérescence. Une microgliose ainsi qu'une astrogliose sont observées dans nos modèles, associées à la pathologie Tau, bien que les deux semblent être impliqués dans des processus différents. En effet, une forte microgliose est observée après l'injection de toutes les constructions Tau ainsi que du vecteur contrôle, suggérant qu'au moins une partie de l'activation microgliale initiale est induite par l'expression des vecteurs AVV. Bien que cette activation microgliale soit plus tard résolue pour la plupart des groupes, celle-ci se maintient dans le groupe hTAU^{P301L} 3 mois après l'injection, un temps où une aggravation de la neurodégénérescence est observée dans ce groupe. L'activation microgliale pourrait donc contribuer à la perte neuronale induite par Tau ou, alternativement, être associée à la nécessité maintenue pour la clairance des débris cellulaires.

L'astrogliose a également été évaluée dans nos différents modèles. Des astrocytes réactifs sont observés dès 1 mois après l'injection, en particulier chez les animaux exprimant Tau. Inversement, aucun signe de réactivité astrocytaire n'a pu être observé dans les groupes contrôles, ce qui suggère que l'astrogliose est spécifique de la pathologie Tau. Des différences sont toutefois observées entre les constructions dans l'étendue et la topographie de la réactivité astrogliale. En effet, une activation plus forte est observée dans les groupes hTAU^{WT} et hTAU^{P301L}, qui présentent également une forte neurodégénérescence, ce qui suggère que l'activation astrocytaire s'est produite dans ces modèles en partie en réponse à la mort neuronale. De plus, des astrocytes réactifs sont observés dans ces groupes principalement dans des régions présentant une forte perte neuronale, ce qui est compatible avec leur implication connue dans la formation de la cicatrice gliale (Pekny et Nilsson, 2005).

Enfin, une agrégation de Tau dans les cellules gliales est observée dans les groupes hTAU^{P301L} et hTAU^{ProAggr}, différents sous-types morphologiques pouvant être identifiés, présentant de fortes

similitudes avec ce qui est observé dans plusieurs tauopathies humaines (Berry et al., 2001; Yoshida, 2006). Bien que la pathologie Tau gliale ait été largement décrite à un niveau anatomo-pathologique, peu est connu sur les processus entrainant son apparition. Des inclusions de Tau dans les cellules gliales ont été décrite chez des souris suite à l'injection d'homogénats cérébraux provenant de patients souffrant de différentes tauopathies (Clavaguera et al., 2013), la spécificité morphologique de chaque tauopathie ayant également été transmise. L'agrégation de Tau dans la glie a également été décrite dans plusieurs modèles de souris transgéniques (Lin et al., 2003; Murakami et al., 2006). Les agrégats de Tau chez ces souris présentaient une forte ressemblance de composition avec celle présente dans les neurones. Compte tenu du fort enrichissement de Tau dans les neurones (Binder et al., 1985), il est possible que l'agrégation gliale de Tau soit dans certains cas liée à la neurodégénérescence.

Les données de notre étude appuient cette deuxième hypothèse. En effet, nos données préliminaires chez la souris ont montré que les inclusions de Tau dans les astrocytes n'étaient pas associées à l'expression du transgène dans ces cellules, suggérant qu'elles apparaissent par un processus secondaire. De plus, la quantification des inclusions gliales positives à AT100 dans les groupes $hTAU^{P301L}$ et $hTAU^{ProAggr}$ chez le rat révèle des différences dans la cinétique d'agrégation. En effet, alors qu'une forte accumulation de Tau dans les astrocytes soit déjà observée dans le groupe $hTAU^{P301L}$ à 1 mois post-injection, la pathologie gliale augmente au cours du temps dans les animaux $hTAU^{ProAggr}$. De manière intéressante, la cinétique d'agrégation dans les astrocytes reflète celle des défauts neuronaux. Ces résultats confirment ainsi que la pathologie gliale dans nos modèles serait associée à des processus neurodégénératifs.

Une des causes probables de cette pathologie Tau dans les astrocytes pourrait être par la phagocytose de débris cellulaires ou même de neurones entiers en dégénérescence. En effet, il a été récemment découvert que les astrocytes étaient impliqués dans l'élimination de synapses et de neurones au cours du développement par l'activation de différentes voies phagocytaires, notamment celles médiées par les récepteurs MEGF10 et MERTK (Chung et al., 2013). L'activation maintenue de ces voies a également été observée dans l'âge adulte suggérant que les astrocytes pourraient être capables de phagocyter des neurones ou des synapses en dégénérescence dans des conditions pathologiques. De plus, la phagocytose des organelles d'origine neuronale, comme les mitochondries, a également été observée dans les astrocytes (Davis et al., 2014). Il est intéressant de noter que l'analyse par RT-qPCR dans nos différents modèles a montré une tendance à l'expression accrue de différents marqueurs phagocytaires, y compris MEGF10 et MERTK. Bien que l'analyse sur des homogénats complets de HC ne puisse pas permettre d'inférence sur le type de cellule gliale impliquée, l'observation que la cinétique d'expression de ces gènes reflétait celle de l'agrégation astrocytaire de Tau dans les groupes $hTAU^{P301L}$ et $hTAU^{ProAggr}$ suggère que ces voies pourraient être, activées dans les astrocytes.

Ce processus de dégradation des débris cellulaires peut avoir des effets bénéfiques. En effet, l'activité phagocytaire des astrocytes s'est révélée récemment utile dans le contexte d'une lésion neuronale où la phagocytose de neurones en dégénérescence empêcherait la mort cellulaire des neurones voisins (Lööv et al., 2012). Cependant, il reste à déterminer l'impact de l'agrégation de Tau sur la fonction et la viabilité des astrocytes dans nos modèles. En effet, des études portant sur des modèles de souris transgéniques montrent que l'agrégation de Tau dans les astrocytes est associée à une altération de leurs fonctions, y compris la redistribution du filament intermédiaire GFAP et une perturbation légère de la barrière hémato-encéphalique (Forman et al., 2005 ; Dabir et al., 2006). D'autres études devraient être effectuées dans nos modèles pour déterminer l'effet à long terme de l'accumulation de Tau dans les astrocytes sur la fonctions astrocytaire mais aussi sur la survie neuronale.

Conclusions

Le but de ce projet était le développement de modèles de rat de tauopathies sporadiques et génétiques en utilisant le transfert de gène de la protéine Tau humaine médié par des vecteurs AAV. La caractérisation et la comparaison de ces différents modèles ont montré une forte variabilité phénotypique, rappelant celle observée chez les tauopathies humaines. En effet, alors que l'expression de $hTAU^{WT}$ conduit à une hyperphosphorylation de Tau et à une forte neurodégénérescence en l'absence d'agrégation significative, la construction de $hTAU^{ProAggr}$ favorise fortement l'agrégation en DNF, avec un effet neuroprotecteur. Le groupe $hTAU^{P301L}$ représente un phénotype intermédiaire avec la formation d'agrégats solubles toxiques et de DNFs totalement matures. Nos différents modèles ont donc une grande ressemblance avec les tauopathies humaines où l'agrégation Tau est associée à la neurodégénérescence ainsi que des processus inflammatoires. Les résultats obtenus dans cette étude viennent également en appui à l'hypothèse actuelle identifiant les oligomères solubles de Tau comme les acteurs principaux de la neurodégénérescence induite par Tau. Ce qui reste à déterminer, cependant, est la cause de la variabilité phénotypique observée entre nos différents modèles. Une caractérisation plus poussée de nos modèles devrait nous permettre de répondre à cette question.

Tout d'abord, le dosage des oligomères serait nécessaire pour confirmer que celles-ci représentent effectivement les espèces toxiques impliquées dans la neurodégénérescence induite par Tau dans notre étude. La caractérisation morphologique et biochimique des différents types d'agrégats doit également être effectuée afin de déterminer si des différences dans les propriétés biochimiques de Tau peuvent sous-tendre la toxicité différentielle exercée par nos différents vecteurs. Une caractérisation supplémentaire des défauts synaptiques potentiels déclenchés par nos vecteurs, au moyen d'une analyse biochimique ou électrophysiologique, doit également être effectuée pour identifier les voies impliquées dans neurodégénérescence induite par Tau. Enfin, il serait également intéressant d'étudier la progression de la pathologie passé 3 mois après l'injection.

Nos résultats permettent d'identifier l'agrégation de Tau comme une cible thérapeutiques pertinente. Plusieurs approches ont été suggérées, depuis l'inhibition de l'induction de l'agrégation (par exemple par des inhibiteurs de la phosphorylation de Tau) jusqu'à la dissolution d'agrégats grâce à l'immunothérapie passive ou active (Pedersen et Sigurdsson, 2015). Nos résultats, ainsi qu'un nombre croissant d'études, pointent vers l'inhibition de la formation d'oligomères comme une stratégie thérapeutique valide. Mais il faudrait d'abord déterminer pourquoi et comment ceux-ci apparaissent. D'autre part, la promotion de la formation de fibrilles pour piéger des oligomères préexistants pourrait également constituer une approche valide, bien qu'il faille d'abord mieux caractériser l'effet à long terme de ces agrégats. Nos modèles à développement rapide, qui présentent chacun des stades différents de l'agrégation de Tau peuvent être d'une grande utilité pour étudier ces différentes questions.

Ces différentes approches thérapeutiques peuvent ne pas s'exclure mutuellement et l'efficacité dépendre du stade de la pathologie Tau. À cet égard, le succès des thérapies dirigées contre Tau profiterait du développement de biomarqueurs permettant le suivi de la progression de la pathologie. Parmi ceux-ci, beaucoup d'efforts ont été faits récemment pour le développement de traceurs d'imagerie dirigés contre Tau (Shah et Catafau, 2014). La spécificité de ces composés pour Tau reste à être clairement établie et l'imagerie de nos modèles où Tau agrège en absence de toute autree protéinopathie devrait aider à résoudre cette question. Nos données suggèrent également que, au lieu des grands agrégats fibrillaires qui sont la cible des traceurs actuels, images les oligomères de Tau pourrait représenter un meilleur corrélat de la pathologie. Le criblage de traceurs avec une sélectivité

PUBLICATION AND COMMUNICATIONS

Publications

Potentiating tangles formation prevents from acute toxicity exerted by soluble Tau species in a novel rat model of tauopathy. **d'Orange M, Aurégan G, Cheramy D, Gaudin- Guérif M, Guillermier M, Stimmer L, Joséphine C, Gaillard MC, Petit F, Diguet E, Kiessling M, Aschauer B, Schmitz C, Colin M, Buée L, Brouillet E, Hantraye P, Bemelmans AP, Cambon K**

In preparation

Oral presentation

Functional and biochemical characterization of the link between the aggregation of Tau and its toxicity in a novel gene transfer-based rat model of tauopathy **d'Orange M, Bemelmans AP, Auregan G, Joséphine C, Guillermier M, Dufour N, Gaillard MC, Guerif M, Cheramy D, Diguet E, Colin M, Buée L, Brouillet M, Hantraye P, Cambon K**

Society for Neuroscience (SfN) annual meeting, Chicago, Illinois, USA October 2015

Poster presentations

Progressive tauopathy induced in the rat brain by AAV-mediated gene transfer of wild type or mutant forms of Tau **d'Orange M, Bemelmans AP, Auregan G, Joséphine C, Guillermier M, Dufour N, Gaillard MC, Colin M, Buée L, Brouillet E, Hantraye P, Cambon K**

12th International Conference on Alzheimer's and Parkinson's Diseases and Related Neurological Disorders – AD/PD, Nice, France Mars 2015

Progressive tauopathy induced in the rat brain by AAV-mediated gene transfer of wild type or mutant forms of Tau **d'Orange M, Cambon K, Bemelmans AP, Van Camp N, Bramoullé Y, Auregan G, Joséphine C, Guillermier M, Dufour N, Gaillard MC, Colin M, Buée L, Brouillet E, Hantraye P**

13th International Springfield Symposium on Advances in Alzheimer Therapy, Geneva, Switzerland Mars 2014

Titre : Utilisation de nouveaux modèles rongeurs de tauopathie pure, obtenus par transfert de gène, pour caractériser le lien entre l'agrégation de Tau et sa toxicité

Mots clés : Modèle rongeur, virus adéno-associés, agrégation et tauopathies

Résumé : Les tauopathies sont des maladies neurodégénératives caractérisées par l'agrégation de protéine Tau. Mis à part ce marqueur pathologique commun, les tauopathies présentent une grande diversité, tant sur le plan clinique qu'anatomo-pathologique, qui pourrait résulter de mécanismes pathologiques différents. Un mécanisme commun pourrait impliquer de petits agrégats de type oligomériques comme étant l'espèce toxique dans les tauopathies.

L'objectif de ce projet est de développer plusieurs modèles de tauopathies, génétiques ou sporadiques, par transfer de gène de la protéine Tau humaine à l'aide de vecteurs adéno-associés. Trois vecteurs sont utilisés, chacun induisant un phénotype spécifique. Tout d'abord, la surexpression de $hTAU^{WT}$ induit une hyperphosphorylation de la protéine associée à une forte mort neuronale, mais en absence d'agrégation. Sa co-expression avec le peptide pro-agrégant TauRD-ΔK280 dans le groupe $hTAU^{ProAggr}$ promeut son agrégation, ce qui est associé à des effets neuroprotecteurs. La construction $hTAU^{P301L}$ induit à la fois la formation d'agrégats solubles et matures, associée à un niveau intermédiaire de toxicité. Ces résultats supportent l'idée que les formes solubles oligomériques jouent un rôle crucial dans la pathologie associée à Tau.

Ces modèles rapides, obtenus après expression de Tau à des niveaux similaires, récapitulent donc la variabilité phénotypique observée dans les tauopathies humaines. Ils devraient servir dans le futur pour étudier les mécanismes sous-tendant la toxicité des différentes espèces de Tau. Ils pourraient aussi être utiles pour étudier la spécificité et la sélectivité de composés développés pour l'imagerie de Tau par tomographie par émission de positon.

Title : Characterizing the link between Tau aggregation and its toxicity in novel gene-transfer based rat models of pure tauopathy

Keywords : Rodent model, adeno-associated viruses, aggregation and tauopathies

Abstract: Tauopathies are neurodegenerative diseases characterized by the aggregation of Tau protein. Despite this common hallmark, tauopathies exhibit a wide variety of clinical and anatomo-pathological presentations, which may possibly result from different pathological mechanisms. One hypothesized common mechanism, however, implicates small oligo-meric aggregates as drivers of Tau-induced toxicity.

The aim of this project was to develop models of sporadic and genetic tauopathies, using adeno-associated viruses to mediate gene transfer of human Tau to the rat brain. Three different constructs were used, each giving rise to a specific phenotype. First, $hTAU^{WT}$ overexpression led to a strong hyperphosphorylation of the protein which was associated with neurotoxicity in absence of any significant aggregation. Its co-expression with the pro-aggregation peptide TauRD-ΔK280 in the $hTAU^{ProAggr}$ group strongly promoted its aggregation, with neuroprotective effects. $hTAU^{P301L}$ construct led to aggregation into soluble species as well as mature aggregates accompanied with an intermediate toxicity. Those results support the hypothesis that soluble oligo-meric species are key players of Tau-induced neurodegeneration.

Those fast developing models, obtained through similar overexpression of human Tau, thus recapitulated the phenotypic variability observed in human tauopathies. Those should prove useful in the future to study mechanisms underlying the toxicity of various Tau species. Those could also serve to study the specificity and selectivity of Tau-directed tracers for positon emission tomography imaging.